
THE UNIVERSITY *of* EDINBURGH

# Synthesis of the C(1)-C(9) Fragment of Disorazole $C_1$ and Novel Heterocyclic Analogues

**Helen S. Niblock**


A thesis submitted for the degree of
Doctor of Philosophy

University of Edinburgh

2012

# Contents

# Declaration

This thesis is submitted in part fulfilment of the requirements for the degree of Doctor of Philosophy at the University of Edinburgh. Unless otherwise stated the work described in this thesis is original and has not been submitted previously in whole or in part for any degree or other qualification at this, or any other university. In accordance with the regulations this thesis does not exceed 70,000 words in length.

Helen Sarah Niblock

# Acknowledgements

Firstly, I would like to thank Dr. Alison Hulme for her support and direction through this project; I know the last 3 years haven't been easy with twins in tow! I have developed my chemistry knowledge and attention to detail through your mentorship over the past 3 years.

Thank you to all of the support staff at the University of Edinburgh who keep the Chemistry department running. Especially thanks to Juraj Bella, Lorna Murray and Marika DeCremoux for running the NMR service and Alan Taylor and Paul Angus for running the mass spectrometry service over the past three years. Also, thank you to John Monaghan for some insightful mass spectrometry advice.

Thank you to Alison, Heather and Kevin for reading over parts of this manuscript.

Thanks to past members of the Hulme group, Phil Dorgan, Emiliano Gemma, Odile Meyer, Jill Hanna, Felicia Landi and Sarah Boys for their help, support and friendship through the early years. Thank you to the current members of the group, Nicolas Petitjean, Lore Troalen, Sarah Thomas, Kevin Ralston, Heather Johnston, Alex Saunders and Faye Cruickshank for entertaining social nights and I wish you all the best for the future. Special thanks to Heather Johnston for turning into the group social secretary and for being my running and climbing partner. A special mention to the Hulme girls Alison, Sarah T. and Heather for completing CRUK Race for Life 10 km in 2011, well done girls! Also thanks to members of the Lam group who I have become friends with over the years, and to everyone who has made the last 3 years in Edinburgh very enjoyable, even if it was hard work!

And thank you to my family for supporting me wherever I am!

Finally, thank you to Alex for always being there and supporting in me in whatever I do.

# Abstract

A highly convergent strategy for the synthesis of the antitubulin polyketide disorazole $C_1$ is proposed based around the alkyne precursor **I**, featuring a novel Evans-Tishchenko/ring closing alkyne metathesis approach. Due to the inherent symmetry of the molecule this retrosynthesis leads to two fragments: a β-hydroxyketone **II** and the oxazole C(1)-(9) fragment **III**.

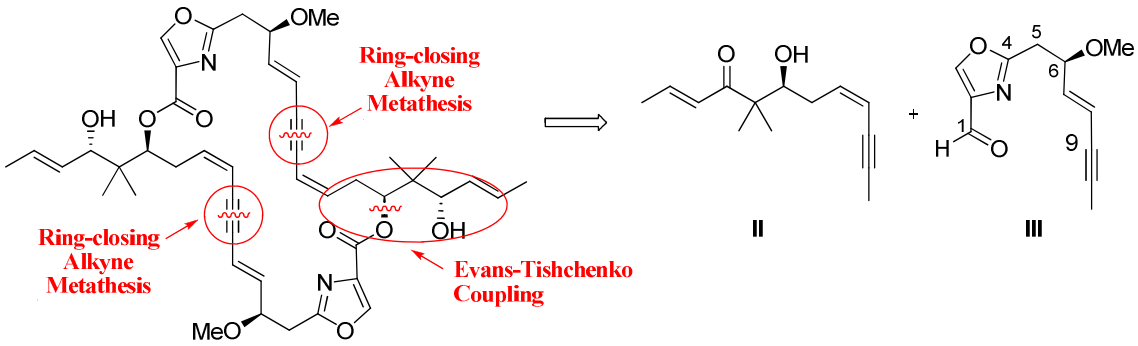


**I**

A review of previous syntheses of disorazole $C_1$ and established structure activity relationships (SARs) highlights a gap in current knowledge relating to the role of the oxazole in tubulin binding. Therefore, the focus of this research has been towards developing new routes for the synthesis of the C(1)-C(9) fragment that can be adapted to the synthesis of heterocyclic analogues to further establish the SAR of disorazole $C_1$.

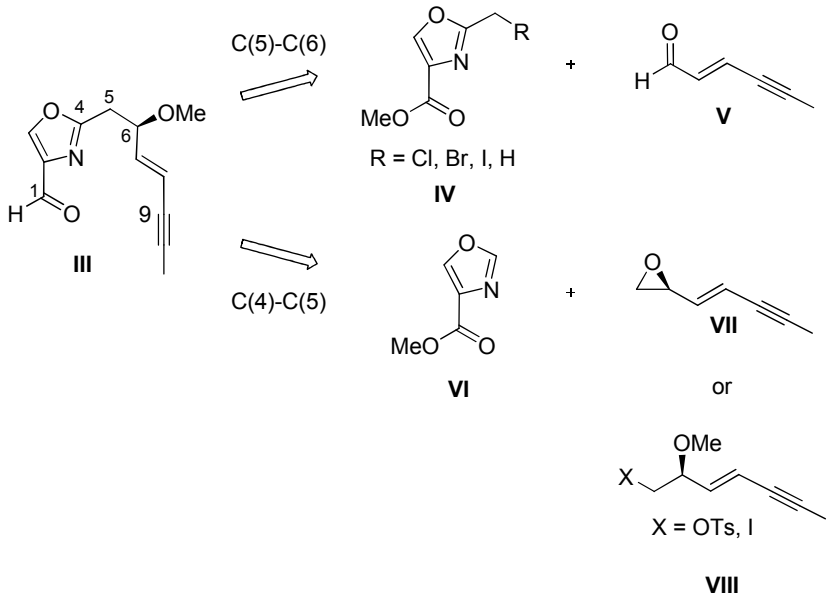

Chapter 2 focuses on a disconnection at the C(5)-C(6) bond and a novel synthesis of the racemic C(1)-C(9) fragment has been achieved *via* a lithiation of methyl 2-methyl-1,3-oxazole-4-carboxylate and coupling to aldehyde **V**. First generation asymmetric routes to the C(1)-C(9) fragment centred on i. a biomimetic amino acid condensation route *via* an oxazoline intermediate based on the precedent of Meyers *et al*. and ii. a C(4)-C(5) disconnection approach based around the epoxide **VII**; are discussed in chapter 3. A second generation C(4)-C(5) disconnection centred on the novel tosylate **VIII** is discussed in chapter 4. Attempts to synthesise the parent C(1)-C(9) oxazole fragment using the tosylate **VIII** *via* i. a palladium catalysed C-H activation of ethyl 4-oxazole carboxylate and ii. lithiation of oxazole are reported. Coupling of fragment **VIII** (X = OTs) with ethyl 1*H*-pyrazole-4-carboxylate and a CuAAC coupling of the azide derived from tosylate **VIII** with methyl propiolate has allowed the successful completion of the synthesis of pyrazole and triazole analogues of this fragment.

# 1 Chapter 1: Introduction

Natural products are an important source of anticancer agents and provide an excellent starting point to provide inspiration for developing new chemotherapy drugs. A review by Butler[1] highlights 79 natural products and natural product derived drugs that entered clinical trials to treat cancer between 2005 and 2007. An important mechanism of action of these natural products is an interaction with tubulin and 25% of the compounds discussed by Butler exhibit this mode of action. Disorazole $C_1$ is a natural product originating from a bacterial fermentation which has been proven to interact with tubulin and act as an anticancer agent. Further research into its biological activity, binding mode, mechanism of action and synthesis are ongoing in a number of research groups.

## 1.1 Isolation and Biosynthesis

Disorazole $C_1$ (**1**) was first isolated in 1994 by Höfle *et al*.[2] from the fermentation broth of the myxobacterium *Sorangium cellulosum* So ce12. The Höfle group were screening the bacteria for novel antibiotics and discovered sorangicin A and its structural variants. A series of antifungal co-metabolites, including the chivosazoles, sorangiolides and the disorazoles were also isolated. These metabolites were isolated by a series of solvent partitions and chromatographic techniques including reversed-phase medium pressure liquid chromatography (RP-MPLC), HPLC and column chromatography. Disorazole $C_1$ is a member of a family of 29 closely related macrocyclic polyketides, the most abundant of which are shown in figure **1**. Accounting for 71% of the mass of the isolated disorazoles, disorazole $A_1$ was the major component of the fermentation broth.

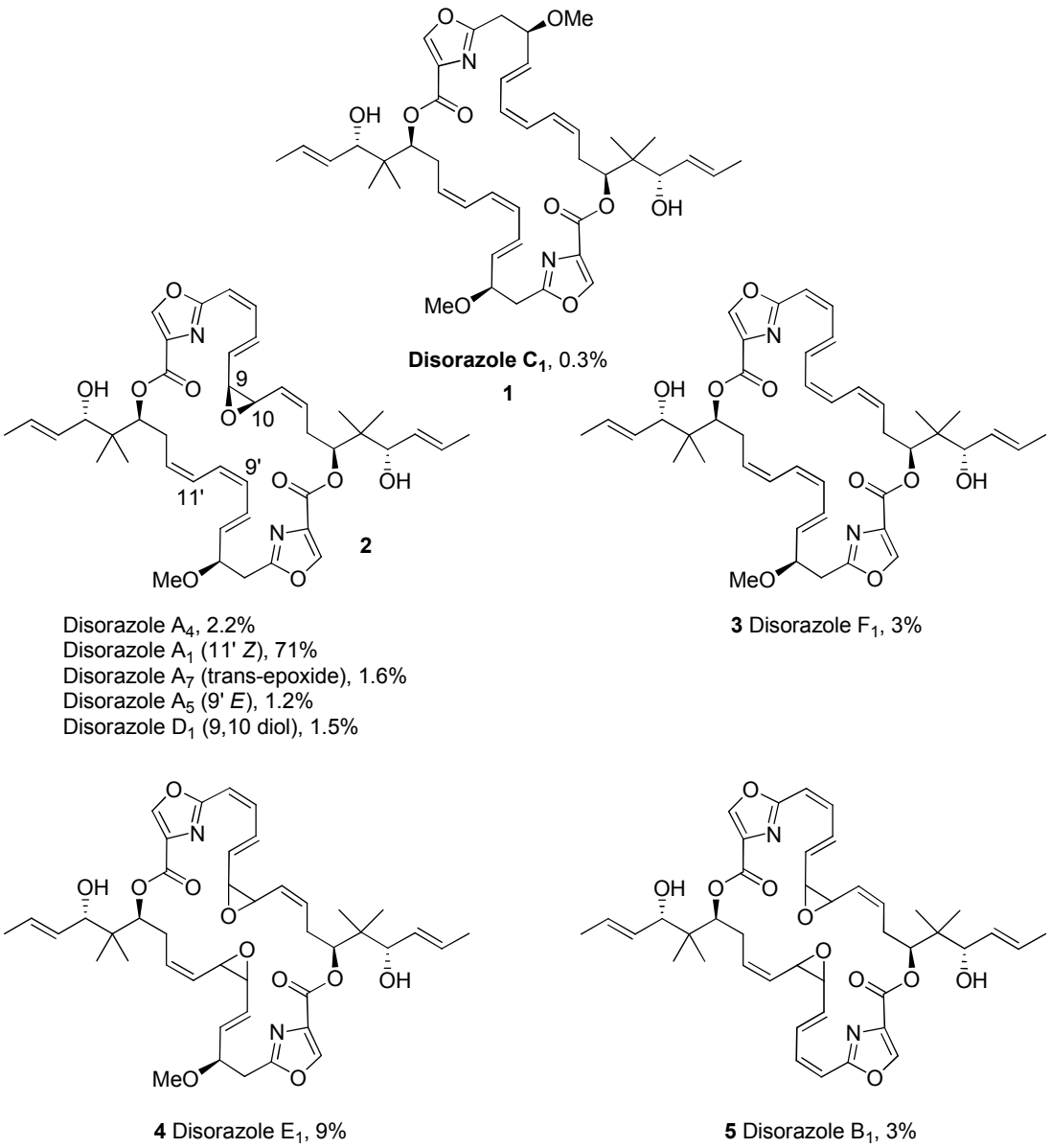


**Figure 1: Most abundant members of the disorazole family**

The structure elucidation of the disorazoles was based on disorazole $A_1$ due to its high abundance. The molecular formula was deduced using negative and positive FAB mass spectrometry, high resolution mass spectrometry and elemental analysis. The structural subunits were determined using 1D and 2D NMR spectroscopy techniques. The NMR spectra of disorazole $C_1$ were compared to those of disorazole $A_1$ and a symmetric macrodiolide structure was suggested based on the southern half of disorazole $A_1$. No stereochemical information was elucidated during this investigation.

The disorazoles possess potent biological activity and are therefore medicinally attractive targets; for that reason, synthetic or fermentation routes to these compounds are required. As shown in figure **1** disorazole $A_1$ is the most abundant of the family and the most efficient route to production of this compound would be through fermentation. Understanding the biosynthesis of the disorazoles would enable optimisation of the fermentation process; hence the gene cluster responsible for the biosynthesis of the disorazoles was identified and sequenced in 2005 (figure **2**).[3,4]

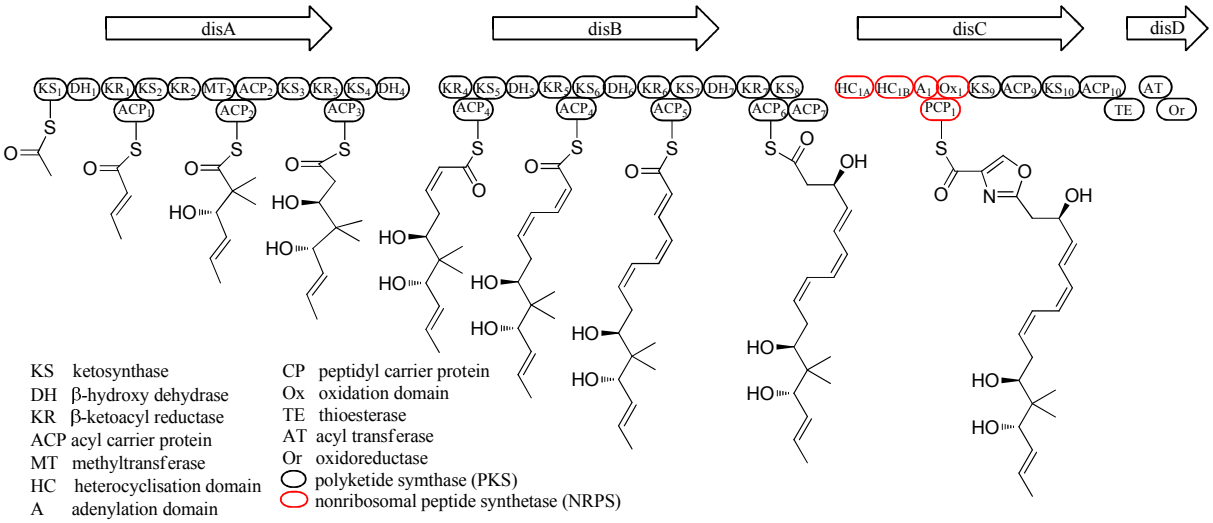


**Figure 2: Disorazole biosynthetic pathway**

The first gene in the disorazole cluster is disA, which codes for a polyketide synthase (PKS). Unusually, the PKS domain begins with a ketosynthase (KS) and not the common acyltransferase (AT) loading module. It is most likely that initiation of biosynthesis occurs *via* a direct transfer of an acetyl group from coenzyme A (CoA) onto the KS module. This acetate starter undergoes condensation with malonyl-S-ACP1; the subsequent reduction of the β-keto intermediate is catalysed by a ketoreductase (KR) and dehydratase (DH) to form the enone. Chain extension proceeds in module two by a KS and KR; a methyl transferase (MT) follows to insert both of the methyl groups directly at C15. $^{13}$C-labelled methionine feeding studies showed that the methyl groups are derived from *S*-adenosyl methionine; rather than through a classical macrolide biosynthetic pathway of condensation with isobutyrate.[2,5] The β-hydroxyl group is installed by the KS, KR and acyl carrier protein (ACP) domains of module two.

Modules four to six are located mainly on the DisB gene, where carbon chain extension continues through a series of KR, ACP, KS and DH domains resulting in the triene section of disorazole $C_1$. Interestingly, a mixture of *cis* and *trans* double bonds are formed in this section, this has been attributed to the presence or absence of a key aspartic acid residue in the KR amino acid sequence. It can be seen in figure **3** that modules 4 and 5 do not possess the key aspartic acid residue and this is where the *cis*-double bonds are formed; whereas, KR6 does feature this aspartic acid reside and a *trans*-double bond results.[3] This can be explained by the mechanism shown in scheme **1** where the β-ketoacyl chains enter the KR active site from opposite directions. The positions of the NADPH and lysine residue are fixed, resulting in the formation of opposite alcohol enantiomers **6a** and **6b**.[3,6,7] Dehydration of the β-hydroxyketones then results in the formation of the *cis*- and *trans*-alkenes **7a** and **7b** respectively.

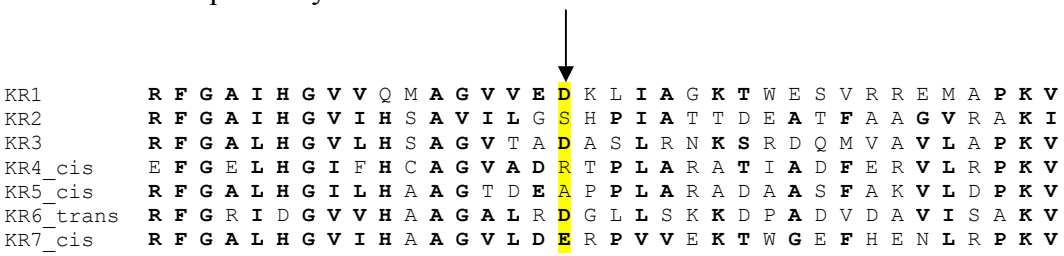


**Figure 3: Ketoreductase domain core region**

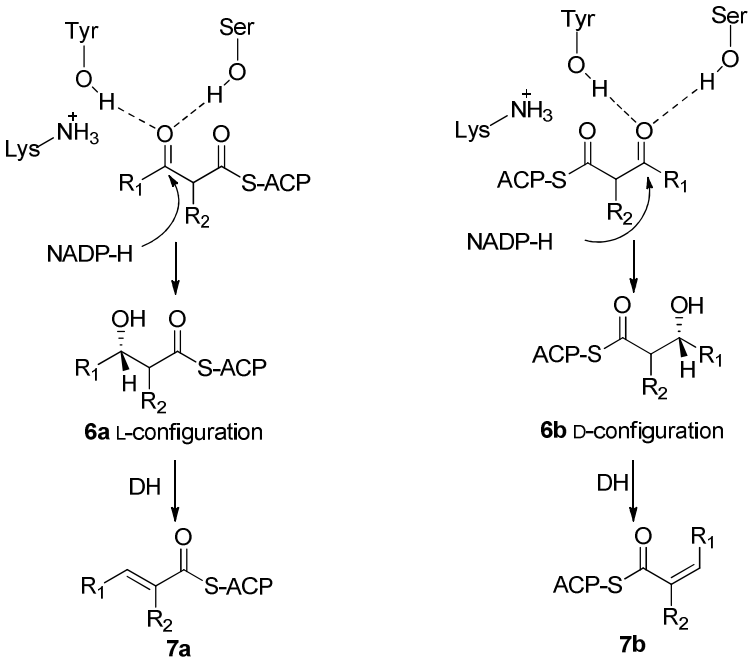


**Scheme 1: Alkene biosynthesis**

Module seven installs the hydroxyl group at C6 *via* a KS, DH, KR and ACP sequence. Oxazole formation follows on the NRPS module, encoded by the disC gene. Unusually, the disorazole gene contains two heterocyclisation domains; it is unknown whether both of these are involved in the oxazole formation. The first domain incorporates serine, and either this first domain, or the second one initiates cyclisation to the oxazoline; which is oxidised to the oxazole by the oxidation domain (Ox). The carbon backbone is now complete, and it is thought that modules nine and ten could be involved in the release and cyclisation of the macrocycle.[3]

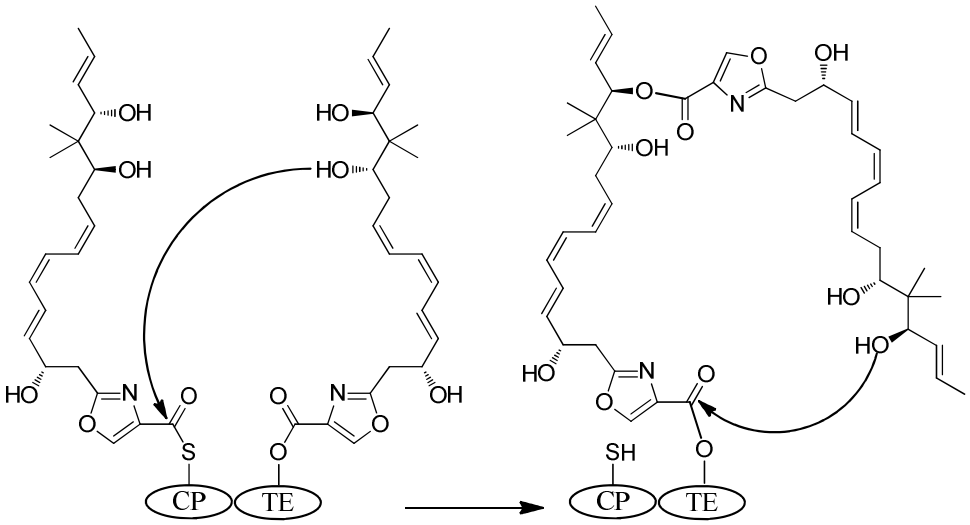


**Scheme 2: Disorazole biosynthetic cyclisation**

Thioesterases (TE) are the final modules of PKSs and they terminate the chain with a hydrolysis reaction. The release and cyclisation of the disorazoles is not fully understood, but one proposed mechanism is shown in scheme **2**. The first monomer synthesised is transferred to the TE and the hydroxyl at C(6) of this monomer can attack the thioester bond of the carrier protein which is carrying the second monomer. The hydroxyl group from the second monomer can form the cyclised dimer and release the molecule from the protein. As there is no MT present in module seven to methylate the hydroxyl at C6, this modification must take place once the molecule has been released from the PKS, by an enzyme not located within the Dis gene cluster. Also, epoxidation will take place post PKS to generate other members of the disorazole family, such as A, D and E.

## 1.2 Biological Activity

After the initial isolation of the disorazoles, preliminary biological tests were carried out on disorazole $A_1$, as it was the most abundant from the fermentation broth and therefore most readily accessible.[8] Disorazole $A_1$ showed activity against various filamentous fungi, with minimum inhibition concentration (MIC) values ranging from 0.1 to 1 µg/ml; but showed no activity against yeast or bacteria. Disorazole $A_1$ was proved to be extremely toxic against mammalian cells with a MIC of 0.003 ng/ml against mouse fibroblast L 929 cells and a MIC of 0.03 ng/ml against HeLa ATCC CCL 2 cells.

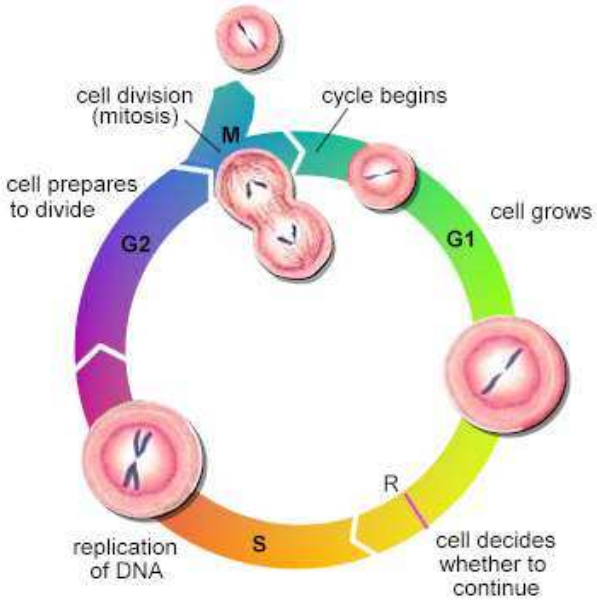


**Figure 4: The cell cycle**[9]

It was not until ten years after the discovery of the disorazoles that further biological evaluation and insight into the mode of action was published by Elnakady *et al.*[10] Disorazole $A_1$ was found to be a highly effective inhibitor of cell proliferation in an MTT assay with mouse fibroblast L929 cells, demonstrating an $IC_{50}$ of 3 pM. Disorazole $A_1$ exhibited greater potency than vinblastine and epothilone in a series of cell proliferation assays against a range of cell lines. For example, against cell line A-549 originating from a human lung carcinoma, disorazole $A_1$ exhibited an $IC_{50}$ of 0.0023 nM, epothilone B 0.26 nM and vinblastine 5.9 nM. This trend was evident through all cell lines tested from different cancer cells, including a multi-drug resistant cell line. The next investigation carried out by the group was to establish at which point in the cell cycle disorazole $A_1$

takes effect. Treatment of histiocytic lymphoma U-937 cells with disorazole $A_1$ and analysis by flow cytometry resulted in an accumulation of cells in the G2/M phase. Figure **4** shows a schematic diagram of the eukaryotic cell cycle; the G2/M phase is at the end of interphase, where the cell is preparing to divide and the beginning of mitosis, where the cell starts to divide into two cells.

A number of natural product chemotherapeutic agents interact with tubulin, for example the vinca alkaloids inhibit microtubule polymerisation, whereas taxanes promote it; both disrupt the cell cycle and result in cell death.[11,12] Microtubules are important structural elements essential for a number of cell processes, including mitosis, cytokinesis and vesicular transport.[11] Microtubules are polymers made up of the protein tubulin, which exists as a dimeric structure consisting of α and β subunits. The dimers assemble with an α unit adjacent to a β unit, resulting in a polarised microtubule structure (figure **5**).[13] The microtubules undergo a dynamic process of polymerisation from the (+)-end and depolymerisation from the (–)-end, as shown in figure **5**;[13] either of these mechanisms can be disrupted. The microtubules make up the mitotic spindle, which is essential for cell division and facilitates correct segregation of the chromosomes before the cell splits. Therefore, any disruption to the components of this process is detrimental to cell division.

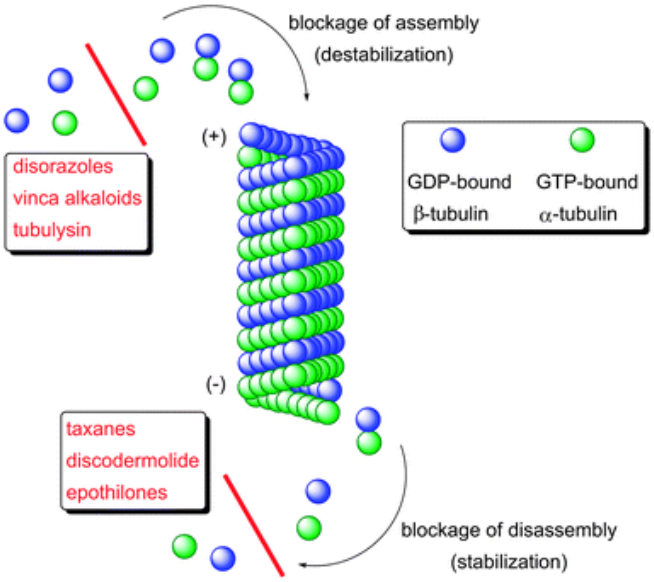


**Figure 5: Microtubule assembly**[13]

Microscopic investigations using immunofluorescence techniques confirmed that disorazole $A_1$ interferes with the microtubular structures in the cell and the effect is concentration dependent.[10] It was also established that disorazole $A_1$ interacts with tubulin to inhibit its polymerisation. In addition, the effect of binding to tubulin was found to be irreversible, which suggests a high binding affinity between disorazole $A_1$ and tubulin.

Due to the low natural abundance of disorazole $C_1$, biological studies were not carried out until the first total synthesis was completed by Wipf *et al.* in 2004.[14,15,16] Nanomolar concentrations of disorazole $C_1$ caused microtubule disorganisation and an increase in mitotic cells. Disorazole $C_1$ showed a comparable degree of mitotic arrest as the vinca alkaloid vincristine.[14] At high concentrations of disorazole $C_1$ the mass of tubulin in the cells was found to decrease, which is in contrast to paclitaxel, which causes microtubule stabilisation.[14,16] The $IC_{50}$ of disorazole $C_1$ was found to be less than 4 nM in 5 different cell lines; in comparison to the vinca alkaloids, vincristine showed an $IC_{50}$ of 5-22 nM and vinblastine 1-2 nM.[16] This therefore suggests that the disorazoles have a mode of action similar to the vinca alkaloids, which is different to paclitaxel. These results are encouraging, as it demonstrates that the chemically reactive vinyl oxirane and the tetraene moieties of disorazole $A_1$ are not essential to the mode of action. Competitive binding studies with tubulin showed that disorazole $C_1$ inhibited vinblastine binding in a non-competitive manner.[16] It was also discovered that disorazole $C_1$ exhibits non-competitive binding with dolastatin 10, which binds at the desipeptide binding site on tubulin, which overlaps the vinca alkaloid binding site. This therefore suggests that the disorazoles may interact *via* a novel binding site.

## 1.3 Structure Activity Relationship of the Disorazoles

### 1.3.1 Disorazole $A_1$

Disorazole $A_1$ is extremely toxic to cells and realistically is too potent to be useful as a chemotherapeutic drug, as it is highly likely to cause side effects. Vinblastine, which has been used in clinical oncology for nearly 50 years,[12] has an $IC_{50}$ against the lung cancer cell line A549 of 5.9 nM;[10] hence this is the target region of activity for an anticancer agent. Nevertheless, Disorazole $A_1$ is an important starting point in order to gain an understanding of the biological activity and SAR, due its ease of availability from the fermentation broth. There have been a limited number of disorazole analogues synthesised due to the long synthetic routes involved. The essential functional groups of the disorazoles need to be identified in order to develop better synthetic strategies and simpler analogues.

As disorazole $A_1$ is the most accessible of the family from the fermentation broth, a starting point to develop some SAR would be to directly modify the extracted compound. Methanolysis of disorazole $A_1$ was performed by Hearn *et al*[17] (table **1**), using dichloroacetic acid; during the reaction two methanol adduct products were observed in equal quantities (**8** and **9**). When stronger acids such as trifluroacetic acid, or methanesulfonic acid were used, only product **8** and dehydration products were observed. The structures of these products were elucidated using HRMS and $^1$H NMR spectroscopy as well as 2D NMR experiments such as COSY, HSQC, HMBC and TOCSY.[17]

The methanolysis products were tested against a range of cancer cell lines (table **1**) and showed equipotent inhibition of cell proliferation as disorazole $A_1$ against breast and lung cancer cell lines (table **1**, entries 1 and 3).[17] However **8** and **9** were less active in multi-drug resistant cell lines which overexpress the transporter protein P-glycoprotein 1 (pgp) (table **1**, entries 2 and 5).[17] Due to the high potency of these new analogues, it can be deduced that the epoxide in disorazole $A_1$ (**2**) is not necessary for activity. Therefore, more stable analogues lacking the epoxide can be investigated without compromising loss in activity.

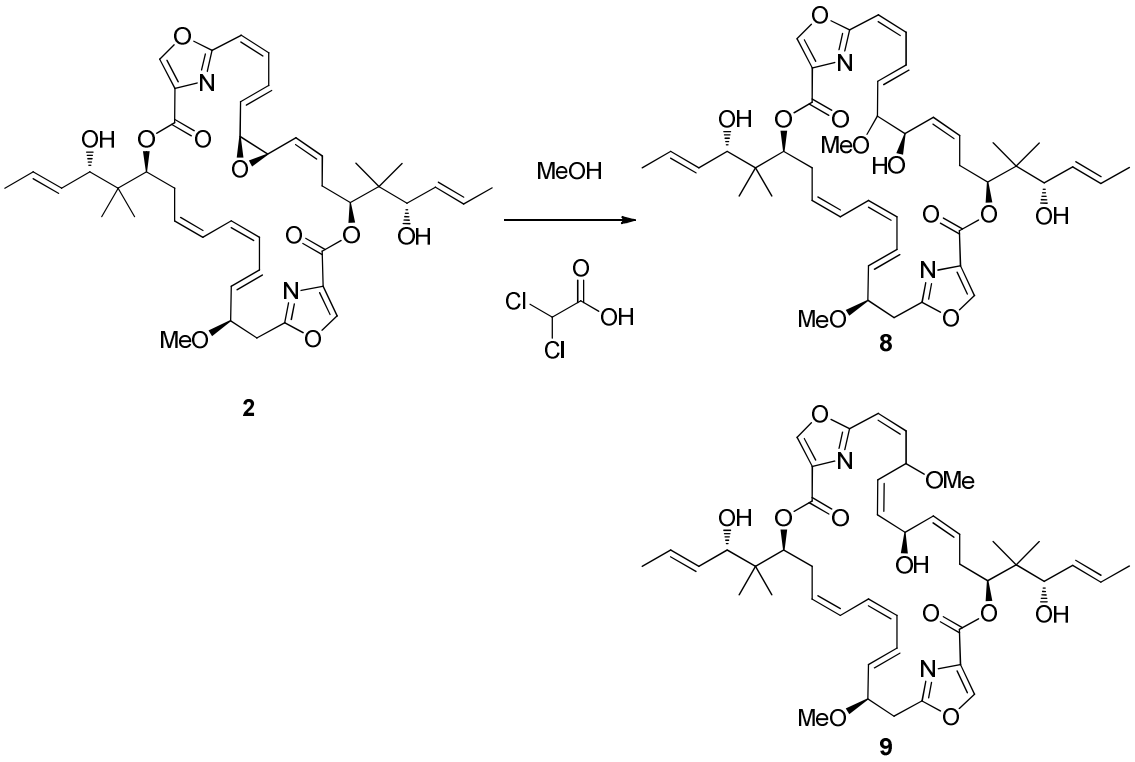


**Table 1: Disorazole $A_1$ methanolysis**

| | | | $IC_{50}$ (nM) | | |
|---|---|---|---|---|---|
| **Entry** | **Cell line** | **Tumour origin** | **Disorazole $A_1$** | **8** | **9** |
| 1 | MCF-7 | breast | 0.25 | 0.24 | 0.62 |
| 2 | NCI/ADR | breast, MDR | 0.52 | 2.80 | 28 |
| 3 | A549 | lung | 0.31 | 0.25 | 0.73 |
| 4 | CCRF-CEM | T-cell leukaemia | 0.070 | 0.11 | 0.33 |
| 5 | CCRF-CEM/PTX | T-cell leukaemia, MDR | 0.066 | 0.24 | 1.30 |

### 1.3.2 Disorazole $C_1$

The majority of the biological analysis of analogues of disorazole $C_1$ has been carried out by the Wipf group and collaborators. [13,14,16,18,19] This work includes rationally designed analogues, as well as synthetic intermediates from the total synthesis of disorazole $C_1$. The most noteworthy structures, synthetically, are the alkyne **10**[15] and the cyclopropyl analogue **11**;[20] these analogues display cytotoxic activity against cancer cell lines. A comparison of assays which have been carried out in equivalent cell lines for the

analogues, disorazole $C_1$, $A_1$ and vincristine is shown in table **2**. It can be seen that against the PC3 prostate cancer derived cell line, the alkyne analogue **10** is 3 orders of magnitude less potent than disorazole $C_1$.

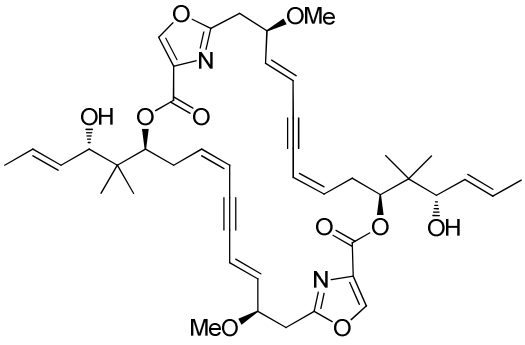


**10**

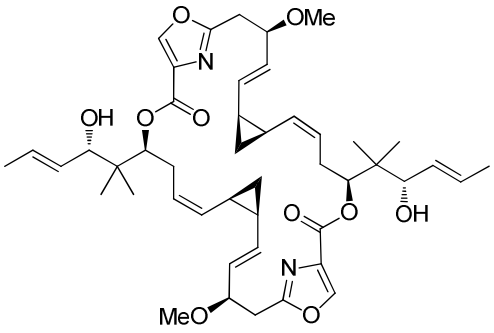


**11**

| | $IC_{50}$ (nm) | | | | |
|---|---|---|---|---|---|
| **Cell line** | **Disorazole $C_1$** | **Disorazole $A_1$** | **Vincristine** | **Alkyne precursor 10** | **Cyclopropyl 11** |
| PC3 | 1.57 | 0.0071 | 4.68 | 2640 | |
| HCT 116 | 1.09 | | 35.2 | | 28.3 |

**Table 2: Biological activity of disorazole $C_1$ analogues**

Interestingly, this large difference in activity between disorazole $C_1$ and the alkyne analogue **10** was not expected, as the alkyne analogue contains only a minor structural change. Molecular modelling studies were therefore carried out to determine the lowest energy conformation of disorazole $C_1$ and the alkyne analogue **10**.[14] A 10,000 step Monte Carlo conformational analysis was performed on the two molecules, with Macromodel 5.5,[21] using the chloroform solvation model and the MM2* force field.[14] The 3D structures obtained from these studies are shown in figure **6**.[14] It can be seen that disorazole $C_1$ forms a figure-of-eight-type shape (figure **6**, A), which is bought about by the conformation of the (*Z*)-alkenes. This figure-of-eight motif is not common in macrodiolides, however, this $C_2$-symmetric shape is apparent in this case and the folding brings the vinyl alcohol side chains into close proximity. In comparison, masking the C(9)-C(10) alkene of the triene as an alkyne greatly affects the 3D shape of the macrocycle and now a narrow bowl shape is

evident (figure **6**, B). The $C_2$-symmetry is now lost and the methoxy groups and vinyl alcohol side chains are further apart; consequently the solvent accessible surface is reduced. The results of the biological assays and the molecular modelling can be combined, to suggest that the 3D structure of the disorazoles is highly important for the activity and therefore must affect how the molecule interacts with tubulin protein.

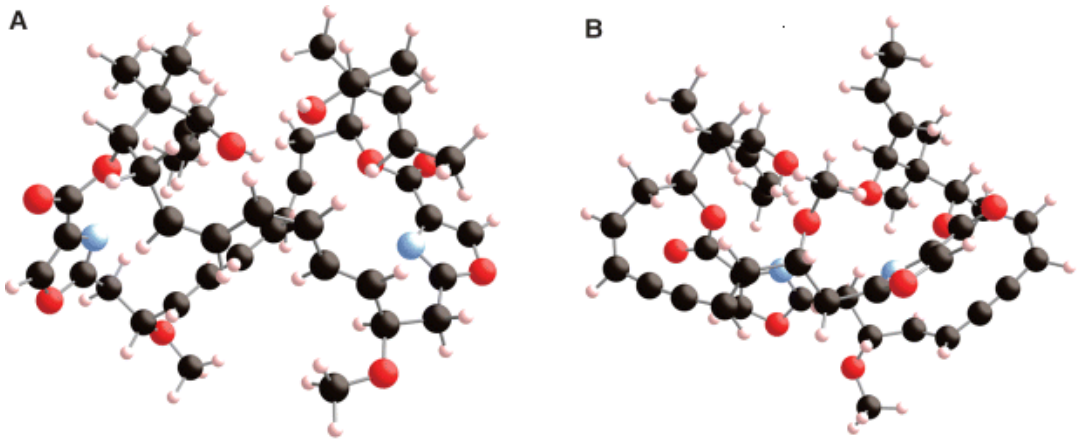


**Figure 6: Energy minimised structures of A-Disorazole $C_1$ and B-alkyne analogue**[14]

The other analogue featured in table **2** to show noticeable activity was the cyclopropyl analogue **11**, which can be compared to disorazole $C_1$ in colon cancer cell line HTC 116.[20] With an $IC_{50}$ of 28.3 nM the cyclopropyl analogue **11** is approximately 4-fold less active than disorazole $C_1$; nevertheless this analogue has comparable activity to vincristine. However, only preliminary results for this analogue have been published and there was not a sample of disorazole $C_1$ available for direct comparison in this recent assay; further investigations are on going. This cyclopropyl analogue shows potential for further development of SAR, to build on the fact that the highly labile triene moiety is not required for activity.

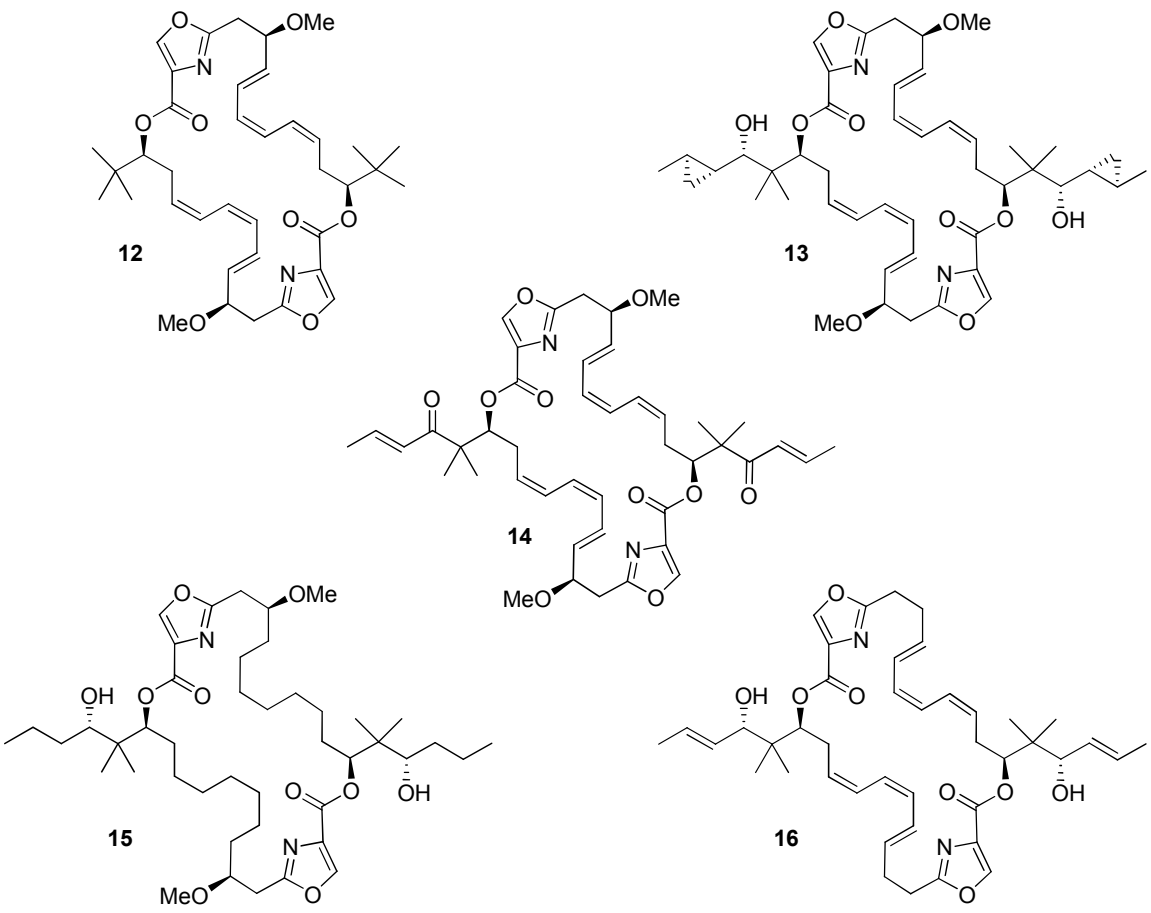


**Figure 7: Disorazole $C_1$ analogues**

Other significant analogues synthesised by the Wipf group are shown in figure **7**.[19] These molecules were rationally designed to establish further SAR around specific areas of the macrodiolide. Structures **12-14** were designed to investigate the importance of the allylic alcohol side chain. The *t*-butyl analogue **12** was the easiest way to simplify the side chain, thereby replacing the allylic alcohol with a methyl group. This analogue was found to be inactive, therefore demonstrating that the allylic alcohol is essential for the biological activity of the disorazoles.[14,19]

The next logical modification was to replace the C(17)-C(18) alkene with the isosteric cyclopropyl, thus probing the impact of the double bond on the binding, while theoretically maintaining the 3D shape of the molecule.[19] Analogue **13** was inactive at concentrations of less than 5 μM, again supporting the necessity of the allylic alcohol for biological activity and for preserving the 3D shape of the molecule.

A theory for the importance of the allylic alcohol is based on *in vivo* oxidation of the C(16) alcohol to an enone, which could undergo irreversible conjugate addition to an amino acid, resulting in a breakdown of protein activity and therefore cellular disruption. Based on this theory, the alcohol of disorazole $C_1$ was oxidised to the ketone **14**. However, the analogue was found to be inactive at concentrations of less than 5 μM, suggesting the importance of the allylic alcohol may be based on a different interaction.[19] The alkyne precursor to this enone analogue was also biologically tested, but it too proved to be inactive.[19] It can be deduced that the allylic alcohol is highly important to the activity of the disorazoles and it cannot be altered in order to attempt to enhance the cytotoxicity of the molecule.

Disorazole $C_1$ was hydrogenated to yield the saturated analogue **15**, which was also inactive in the range of cell lines tested.[14,19] It is understandable that this saturated analogue would hold a different energy minimised shape to disorazole $C_1$, which in turn would affect the binding to tubulin.

Another molecule inspired by the desire to simplify the structure of disorazole $C_1$ was the desmethoxy analogue **16**. The synthesis of this compound could not be completed due to poor recovery of intermediates, difficult purification and possible instability of the compounds, perhaps by destabilising the sensitive triene moiety.[19]

Late stage intermediates isolated during the total synthesis of disorazole $C_1$ and the aforementioned analogues were also screened for efficacy, along with monomeric cyclic by-products, but they were all proven to be inactive.[14,19]

### 1.3.3 Disorazole Z

Recently, a new member of the disorazole family was isolated and identified from the fermentation broth of *Sorangium cellulosum* and it was assigned the name disorazole Z **17**.[22] This latest disorazole was found to be highly toxic against the mouse fibrolast cell line L929, exhibiting an $IC_{50}$ of 30 pg/ml. This compound comprises of a smaller ring than disorazole $C_1$ and it lacks the C(6) methoxy group; it also contains a methyl ester substitution on the side chain, rather than a *gem*-dimethyl moiety. Kalesse *et al* were also interested in investigating the SAR of the disorazoles and they synthesised the 'simplified disorazole' **18**.[23] This molecule contains the same ring structure as disorazole Z, but the side chain now mirrors that of the other disorazoles and contains the *gem*-dimethyl substituents.

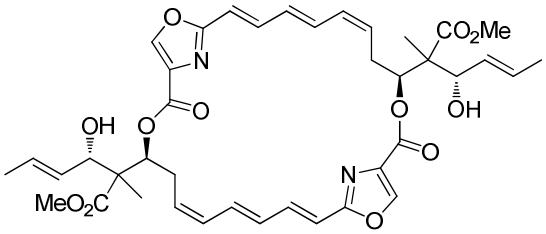


**17** disorazole Z

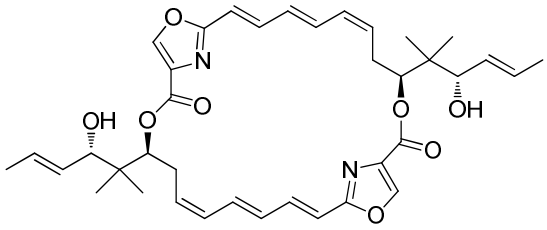


**18** simplified disorazole

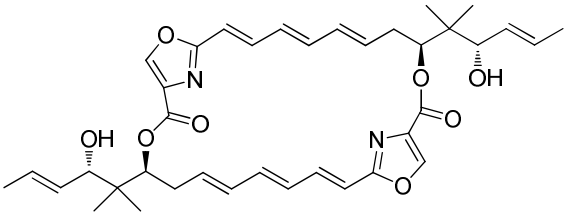


**19** (*E*,*E*,*E*)-analogue

**Table 3: Simplified disorazoles**

| | $IC_{50}$ (nm) | | | |
|---|---|---|---|---|
| **Cell line** | **Disorazole $C_1$** | **Disorazole $A_1$** | **(*Z*,*E*,*E*) 18** | **(*E*,*E*,*E*) 19** |
| PC3 | 1.57 | 0.0071 | 1.44 | 50 |

The simplified disorazole **18** was tested against a range of cancer cell lines, and table **3** highlights the prostate cancer cell line PC3, to enable the results to be compared to previous disorazoles tested in the same cell line. This simplified disorazole **18** showed comparable activity to disorazole $C_1$, with an $IC_{50}$ of 1.44 nM. This suggests that the methoxy group is not necessary for activity and a smaller ring is tolerated. However, the (*E*,*E*,*E*)-analogue **19**, which was readily available from the synthetic procedure, demonstrated approximately 50 times less activity than the (*Z*,*E*,*E*)-analogue **18** against all cancer cell lines. This minor structural alteration would affect the 3D shape of the molecule, therefore influencing the binding interaction with tubulin and in turn, decreasing the activity.

An *in vitro* tubulin polymerisation assay was conducted using purified microtubule protein from porcine brain. The results shown in figure **8**[23] illustrate the same trend as the cell assays, where disorazole $A_1$ is the most active by several orders of magnitude. The (*Z,E,E*)-analogue **18** showed intermediate activity, whereas, the (*E,E,E*)-analogue **19** is only slightly more active than the control. This suggests that it is the binding of the compounds to the protein tubulin that affects the $IC_{50}$ in cell assays, rather than any differences in cellular uptake.

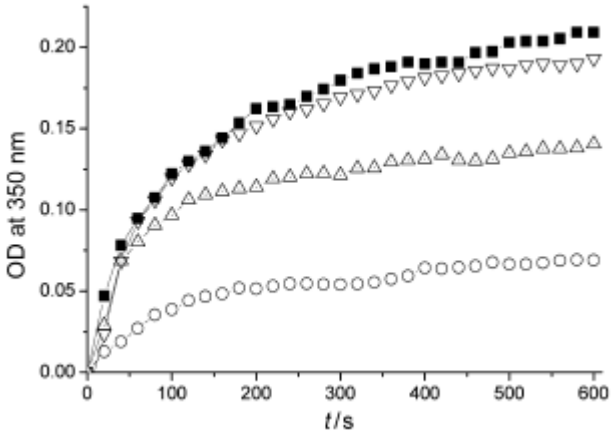


**Figure 8: Influence of compounds 18 and 19 on polymerization of purified porcine tubulin at 37 °C in comparison with disorazole $A_1$ (■ control; △ 18; ▽19; ○ disorazole $A_1$; microtubule protein 1 mg $mL^{-1}$; compound concentrations 5 µM $mL^{-1}$).[23]**

From all of the analogues published some SARs have been established and these findings are summarised in figure **9**. It can be concluded that the allylic alcohol side chain is essential for activity and cannot be modified. The desmethoxy analogue **16** could not be synthesised, yet the simplified disorazole **18** does not contain the methoxy group and it maintained activity against cancer cells. Modifications of the sensitive triene system are tolerated, such as the cyclopropyl **11** and alkyne **10** analogues, but activity is compromised. The overall conclusion to be drawn from the available data, is that small alterations to the structure of the disorazoles can greatly affect the activity. From computational studies it appears that small structural changes can have a great impact on the 3D conformation of the molecules, thereby influencing the binding to tubulin. Disorazole $C_1$ contains a number of functional groups and they are yet all to be explored to establish SAR. Furthermore, the binding and interaction with tubulin is still not fully understood and investigations are ongoing in a number of research groups. [13,14,18,19,20,23]

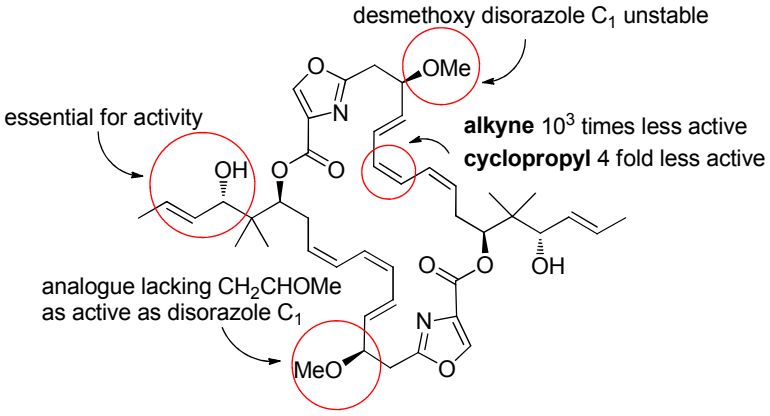


**Figure 9: SAR summary**

## 1.4 Synthesis of Disorazole $C_1$ and Analogues

### 1.4.1 Meyers Partial Synthesis of Disorazole $C_1$

The first efforts towards the synthesis of disorazole $C_1$ were published by the Meyers group in 2000,[24] which was prior to the relative or absolute stereochemistry of the disorazoles being determined. The initial efforts concentrated on forming what they assumed to be disorazole $C_1$ (**1b**) from its monomeric triene subunit **20** by a dilactonisation reaction (scheme **3**).[24] The triene subunit **20** could be formed by a Stille coupling between the vinylstannane moiety **23** and the oxazole-containing vinyl iodide **24**. However, it was found that the triene subunit was unstable and the synthesis of **1b** could not be completed using this route. Therefore, attention was then focused towards the dienyne monomer **22**, where the C(11)-C(12) alkene had been replaced by an alkyne.[25] This target can be reached by a Sonogashira coupling between the vinyl iodide **24** and the alkyne **25**.

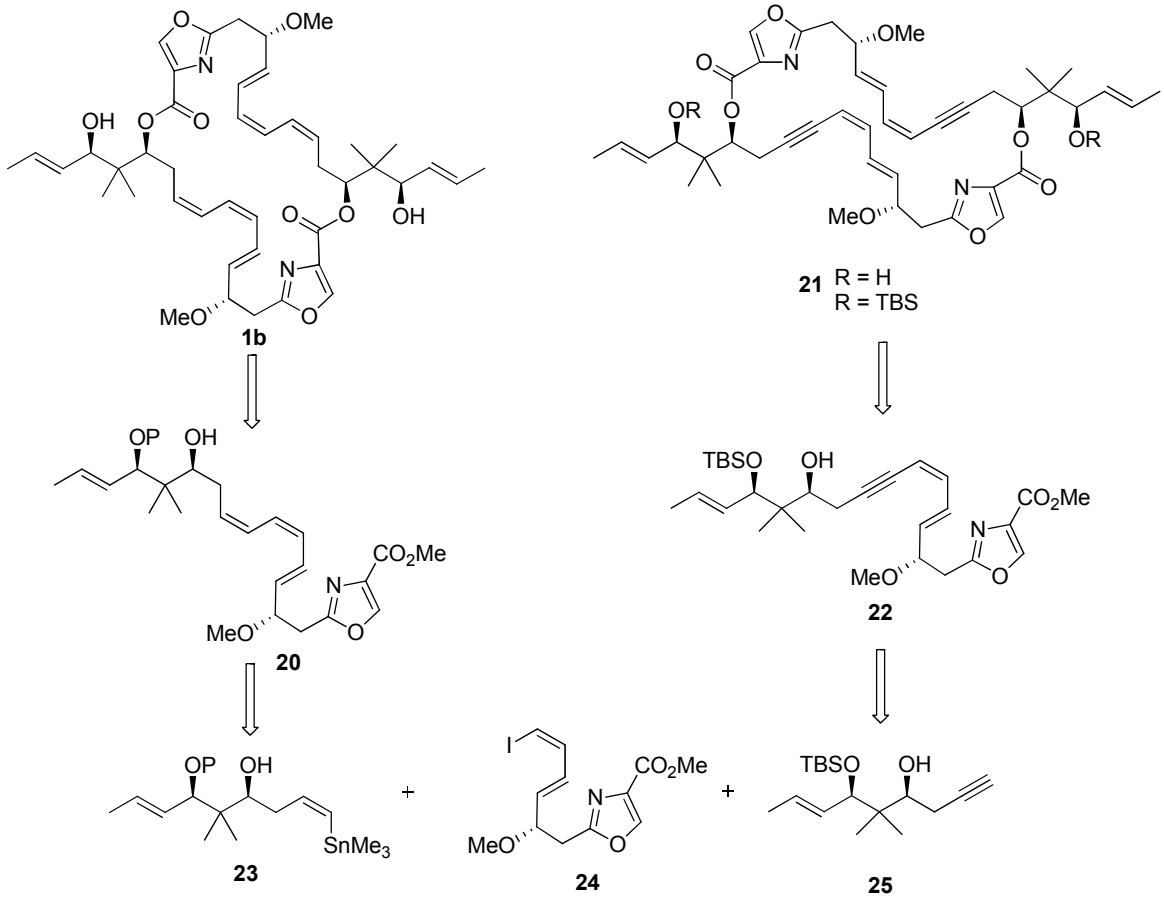


**Scheme 3: Meyers retrosynthesis of Disorazole $C_1$**

The synthesis of vinyl iodide **24** began from acid **26** (synthesised from L-malic acid), which was coupled with L-serine methyl ester hydrochloride to give amide **27** (scheme **4**). Cyclodehydration of **27** with DAST led to the oxazoline, which was oxidised with DBU and $BrCCl_3$ to the oxazole **28**; the acetonide of which was subsequently hydrolysed to the diol using Dowex-$H^+$. The primary alcohol was then selectively protected as the TIPS ether, the free secondary alcohol was methylated and TIPS deprotection led to alcohol **29** in 48% yield over the 4 steps. Alcohol **29** was subjected to Parikh-Doering oxidation[26] and the resulting aldehyde was used directly in a Wittig reaction with triphenylphosphoranylidine acetaldehyde, to produce the enal **30**. Aldehyde **30** was subjected to a Stork-Zhao[27] modified Wittig reaction to generate the dienyl iodide **24** in a reasonable 76% yield (*Z*:*E*, 8:1).

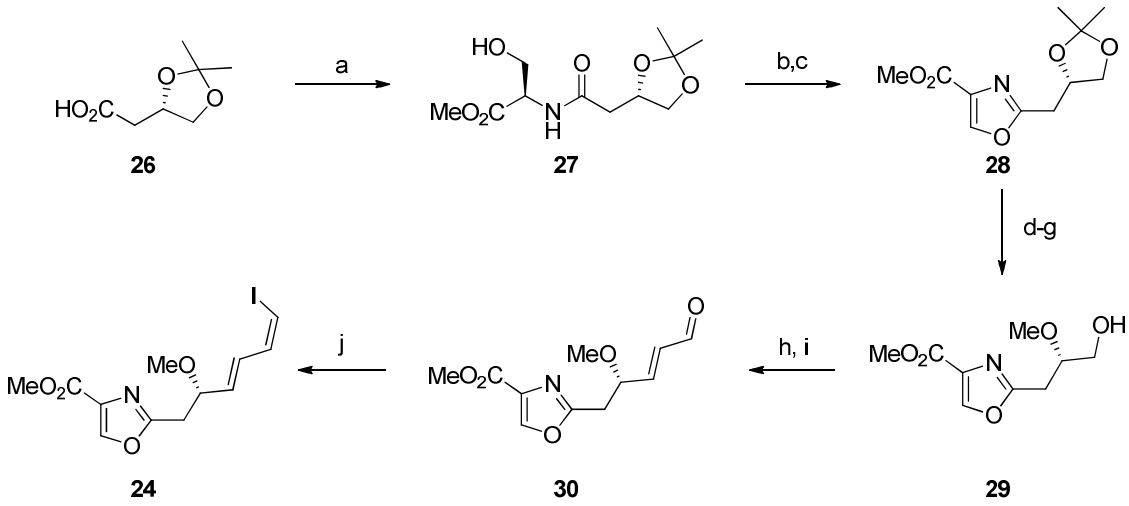


**Scheme 4: Meyers synthesis of dienyl iodide fragment**

(a) L-SerOMe•HCl, 1,1'-CDI, THF, 67%; (b) DAST, DCM, −78 °C; (c) DBU, $BrCCl_3$, DCM, 0 °C to rt, 79% over 2 steps; (d) Dowex-$H^+$, MeOH; (e) TIPSOTf, 2,6-lutidine, DCM, −78 °C; (f) MeI, $Ag_2O$, $CH_3CN$, Δ; (g) TBAF, THF, 48% over 4 steps; (h) $SO_3$·Pyr, DMSO, $Et_3N$, DCM; (i) $Ph_3P{=}CH_2CHO$, THF, 45% over 2 steps; (j) $I^-Ph_3P^+CH_2I$, NaHMDS, HMPA, −78 °C, 76%.

The first step towards the alkyne fragment **25** (scheme **5**) utilised a modified Mukaiyama aldol reaction between (*E*)-crotonaldehyde (**31**) and the *tert*-butyldimethylsilyl ketene acetal **32** to give alcohol **33** in 85% yield and 92% ee. It was found that α,β-unsaturated ester **34** could be formed in a one-pot reaction, where NaH would cause a 1,5-*O*→*O* silyl migration of **33** followed by ethoxy elimination

to form the intermediate aldehyde. Then, a Horner-Wadsworth-Emmons reaction occurred with triethylphosphonoacetate to give alkene **34**. The ester of **34** was reduced to the alcohol using DIBAL; Sharpless epoxidation of the alkene resulted in the epoxide **35** as the major product of a diastereomeric mixture (14:1). The mixture was selectively reduced to the 1,3-diol using Red-Al, and then protected as the PMB acetal **36**, which was formed as a single diastereomer. The acetal ring was regioselectively opened under reductive conditions using DIBAL and the primary alcohol was oxidised to the aldehyde **37** using Dess-Martin periodinane. The resulting aldehyde was subjected to a Stork-Zhao modified Wittig reaction and the PMB protecting group was removed with DDQ to give the vinyl iodide **38**. The vinyl iodide was treated with NaHMDS, resulting in elimination to the alkyne **25**.[25]

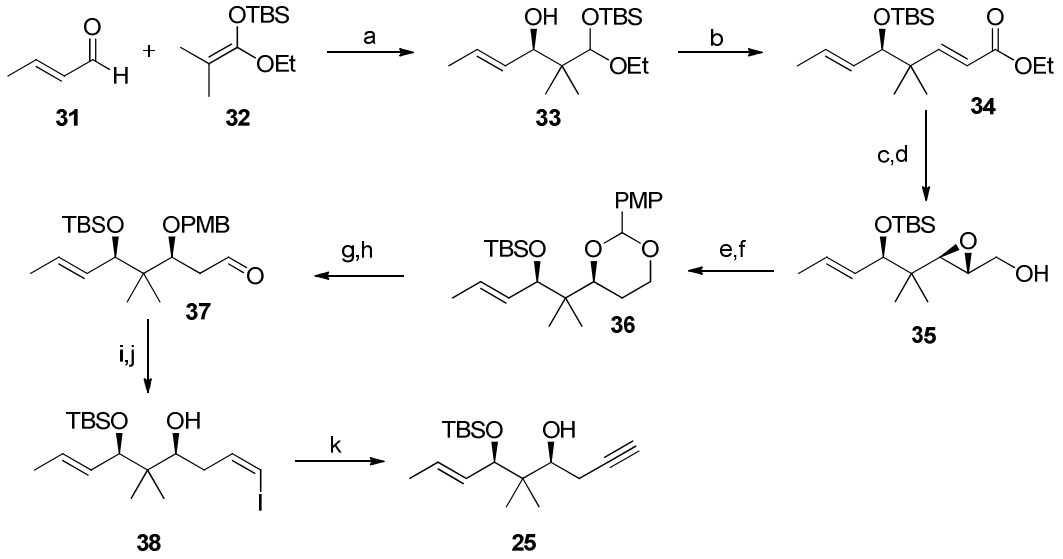


**Scheme 5: Meyers synthesis of alkyne fragment**

(a) $BH_3$•THF, *N*-Ts-L-valine, DCM, −78 °C, 85%; (b) $(EtO)_2P(O)CO_2CH_2Et$, NaH (2 equiv), THF, −78 °C to rt, 72%; (c) DIBAL, DCM, −78 °C; (d) D-(−)-DIPT, *t*-BuOOH, $Ti(O\text{-}i\text{-}Pr)_4$, DCM, −30 °C, 80% over 2 steps; (e) Red-Al, THF, −20 to 0 °C; (f) *p*-methoxybenzylidene dimethyl acetal, PPTS, DCM, 77% over 2 steps; (g) DIBAL, DCM, −78 °C; (h) DMP, pyridine, *t*-BuOH, DCM, 90% over 2 steps; (i) $I^-Ph_3P^+CH_2I$, NaHMDS, HMPA, −78 °C; (j) DDQ, DCM, $H_2O$, 67% over 2 steps; (k) NaHMDS (2 equiv), THF, −78 °C to rt, 67%.

Once the two key fragments had been synthesised, they could be coupled together using Sonogashira coupling to give the dienyne monomer **22** (scheme **6**). The cyclodimerisation was attempted firstly by hydrolysing the methyl ester of **22** to the acid, which was treated with DPTC and DMAP to effect lactonisation. Unfortunately, this procedure only resulted in the cyclic monomer **39**.[25]

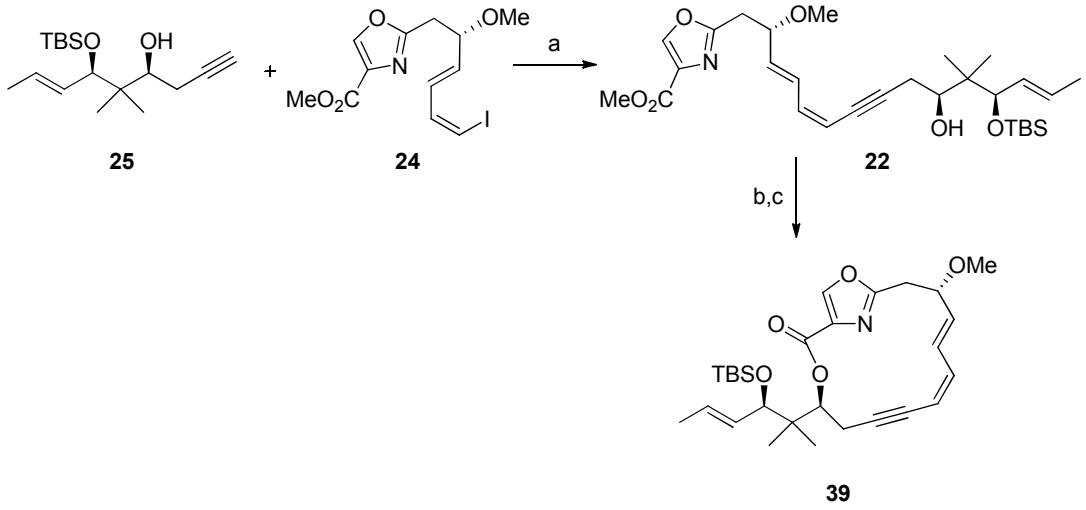


**Scheme 6:Meyers attempted cyclodimerisation**

(a) $PdCl_2(PPh_3)_2$, CuI, $Et_3N$, $CH_3CN$, –20 °C to rt, 87%; (b) 1 N LiOH, THF; (c) DPTC, DMAP, toluene, Δ, 46% over 2 steps.

A stepwise approach (scheme **7**) was then adopted to avoid monomer cyclisation. This involved protection of the alcohol of **22**, saponification of the ester and coupling to another equivalent of **22** with a free hydroxyl group to give **40**. Deprotection of the hydroxyl group and Yamaguchi lactonisation resulted in the desired cyclic dimer **21**. Attempts to remove the TBS protecting group resulted in a mixture of inseparable isomers and partial hydrogenation of the alkyne to provide the (*Z*)-alkene was unsuccessful; this synthesis of what was assumed to be disorazole $C_1$ was not completed.[25]

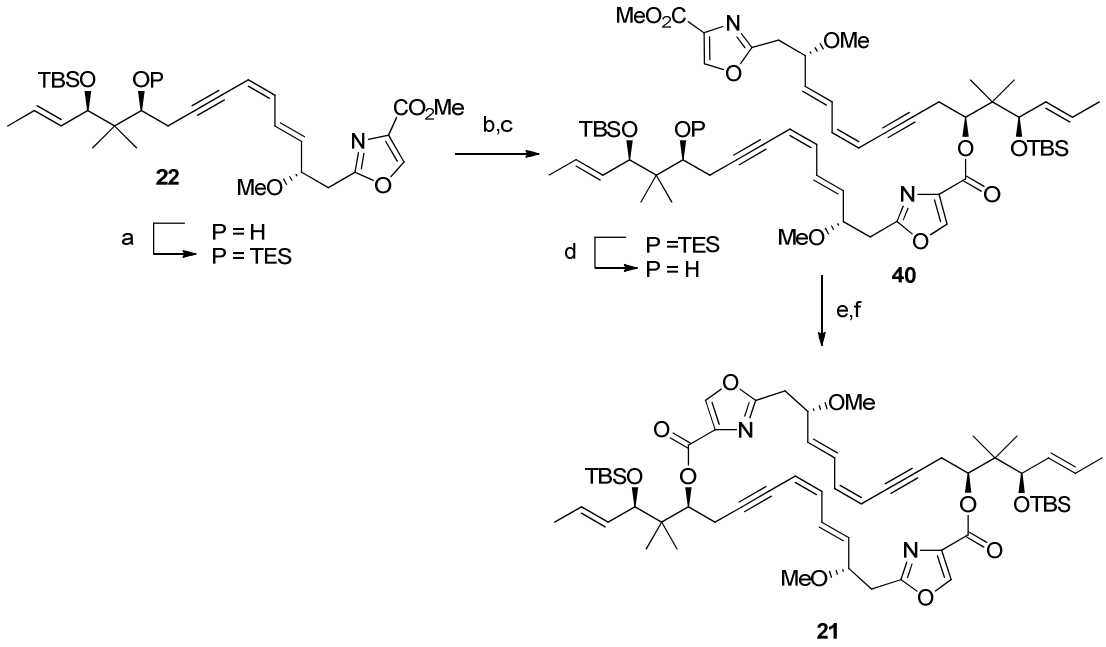


**Scheme 7: Meyers stepwise dimerisation**

(a) TESOTf, 2,6-lutidine, DCM, −78 °C, 69%; (b) 1 N LiOH, THF; (c) **22**, DPTC, DMAP, toluene, Δ, 65% over 2 steps; (d) TFA, $H_2O$, THF, 65%; (e) 1 N LiOH, THF; (f) 2,4,6-trichlorobenzoyl chloride, DMAP, toluene, rt, 24% over 2 steps.

## 1.4.2 Hoffmann Synthesis of Tetradehydro-Disorazole $C_1$

The absolute stereochemical configuration of disorazole $C_1$ was published in 2000[28] and with this information the Hoffmann group set about constructing the southern segment of disorazole $A_1$ and $C_1$. The Hoffmann group carried out initial computational studies to ascertain the best retrosynthetic strategy. The strategy was to avoid the problems encountered by the Meyers group, namely, the use of the sensitive triene fragment and the formation of the cyclic monomer. A Monte Carlo global minimum search was carried out using geometries minimised using the MMFF ForceField within MacroModel 7.2.[21] The results of these calculations are shown in figure **10**; it was concluded that placing the alkyne at the C(9)-C(10) position would lead to the most strained 15 membered macrocycle **42**, but the desired 30-membered macrocycle **10** would be less strained than the C(11)-C(12) alkyne equivalent **21b**.[29]

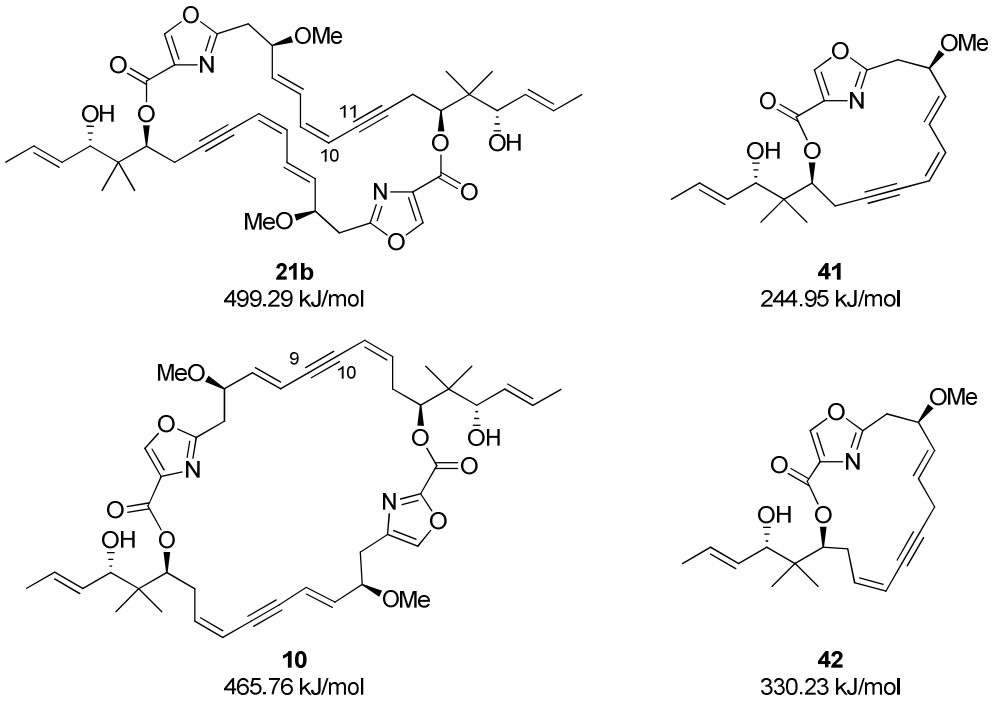


**Figure 10: Relative energies of 15- and 30-membered rings**

The retrosynthesis shown in scheme **8** is the second generation approach used for the Hoffmann group's total synthesis of disorazole $C_1$. The key fragments for this synthesis were the alkyne **44** and vinyl iodide **45**.[30]

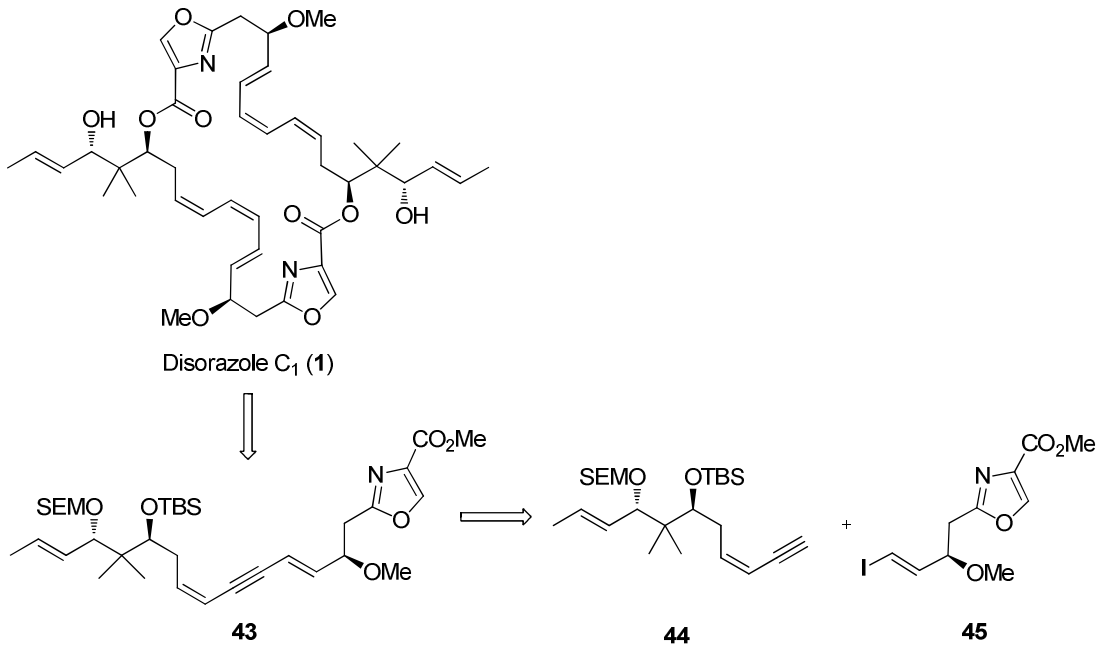


**Scheme 8: Hoffmann retrosynthetic analysis of disorazole $C_1$**

The first generation approach to the synthesis of the oxazole fragment **52** (scheme **9**) started with a Keck allylation of 2-benzyloxy acetaldehyde **46**, using (*R*)-BINOL and allyltributylstannane, generating the homoallylic alcohol **47** in 84% yield and >94% ee. *O*-Methylation followed by ozonolysis, then oxidation of the resulting aldehyde gave the carboxylic acid **48**. The oxazole was formed in three steps: an initial amide coupling between the acid **48** and serine methyl ester hydrochloride generated hydroxyamide **49**. Cyclodehydration using DAST and subsequent oxidation of the resulting oxazoline furnished oxazole **50**. The benzyl group was removed with hydrogen and carbon on palladium and the resulting alcohol was oxidised to the aldehyde **51**. This underwent a Wittig reaction with TMS-protected propargyl triphenylphosphonium bromide (2.5:1, *E*:*Z* selectivity) and the TMS group was removed to give the terminal alkyne **52**.[29]

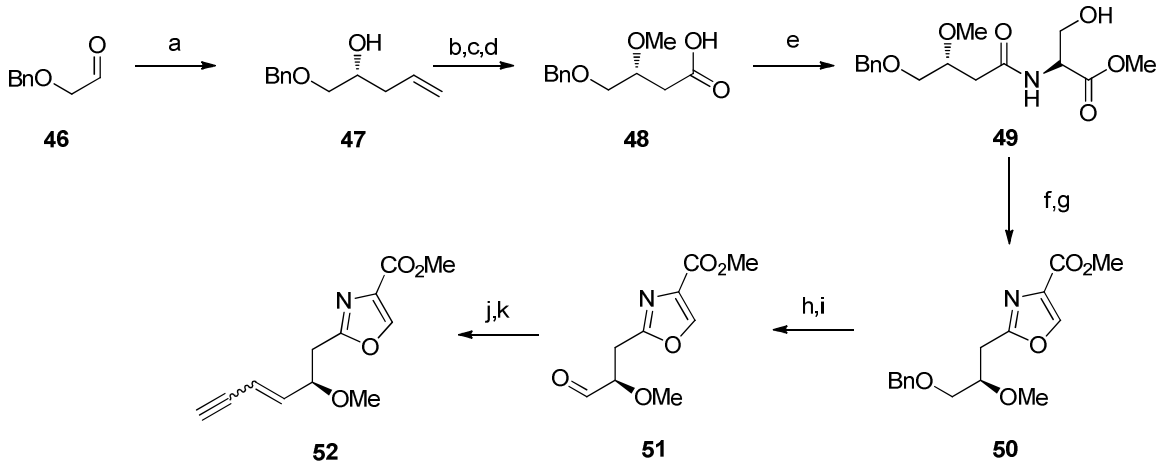


**Scheme 9: Hoffmann's oxazole synthesis**

(a) (*R*)-BINOL, $Ti(O^iPr)_4$, 4 Å MS, allyltributylstannane, DCM, −20 °C, 84%; (b) NaH, MeI, THF, rt, 94%; (c) $O_3$, DCM, −78 °C; $PPh_3$, rt, 86%; (d) $NaClO_2$, $KH_2PO_4$, $H_2O_2$, $CH_3CN$/MeOH/$H_2O$ (1:1:2), 10 °C, 98%; (e) L-SerOMe•HCl, IBCF, NMM, THF, −25 °C to rt, 71%; (f) DAST, $K_2CO_3$, DCM, −78 °C; (g) DBU, $BrCCl_3$, DCM, 0 °C to rt, 79% from **49**; (h) $H_2$, Pd/C, EtOH, rt, 97%; (i) $SO_3$•pyr, $Et_3N$, DCM:DMSO (4:1), 0 °C, 75%; (j) $Br^-Ph_3P^+CH_2C{\equiv}CTMS$, *n*-BuLi, THF, −78 to 0 °C, 49% (2.5:1, *E*:*Z*); (k) $K_2CO_3$, MeOH, rt, 77%.

The first generation synthesis used Sonogashira coupling to join the oxazole alkyne **52** with the vinyl iodide **62**.[29] Due to the selectivity problems encountered when constructing the C(7)-C(8) double bond (**52**) *via* a Wittig reaction, the Sonogashira coupling partners were reversed in the second generation synthesis.[30] Therefore the oxazole fragment required the vinyl iodide functional group which was synthesised as shown in scheme **10**. The alcohol **53** was oxidised to the aldehyde and then converted to the terminal alkyne **54** using the Ohira-Bestmann reagent (**A**). This alkyne was transformed selectively into the (*E*)-vinyl iodide **45** by hydrostannylation/metal-iodine exchange with good yield (88%).[30]

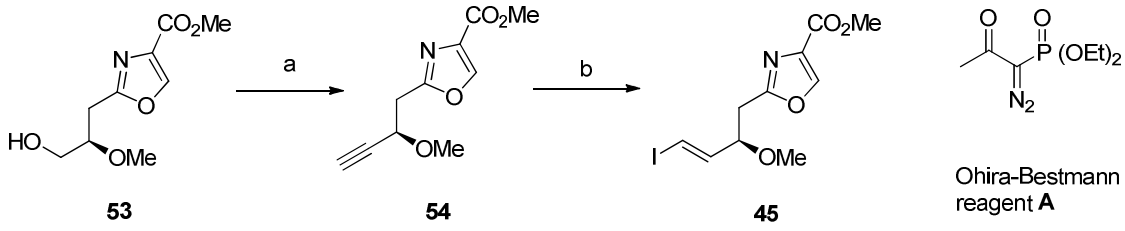


**53** **54** **45**

**Scheme 10: Hoffmann second generation oxazole fragment synthesis**

(a) i. $(ClCO)_2$, $Et_3N$, DMSO, DCM, –78 °C to –40 °C; ii. **A**, $K_2CO_3$, MeOH, 0 °C to rt, 75% from **53**; (b) $n$Bu$_3$SnH, Pd$(PPh_3)_4$, THF, then $I_2$, 88% (*E*-selective).

The first step towards the synthesis of the alkyne fragment **44** involved an asymmetric Mukaiyama-aldol addition of silyl ketene acetal **55** to the readily available aldehyde **56**, generating alcohol **57** in 96% yield and 88% ee. The secondary alcohol was protected as the TBS ether and the aldehyde was formed by reduction of the ester with DIBAL followed by Dess-Martin oxidation to give the aldehyde **58**. Addition of lithiated (*E*)-1-bromoprop-1-ene resulted in a mixture of *syn* and *anti* alcohols **59a** and **59b** (**59a**:**59b** = 1.1:1), but these could be separated by column chromatography and the desired diastereomer **59a** was carried through. The free alcohol was protected as the SEM ether **60** and then the primary alcohol was deprotected with DDQ, enabling Parikh-Doering oxidation to the aldehyde **61**. The aldehyde was converted to the vinyl iodide **62** using the Stork-Zhao procedure and this was coupled with (trimethylsilyl)acetylene in a Sonogashira coupling, resulting

in the terminal alkyne. Removal of the TBS group with TBAF concluded the sequence to provide enyne **44** in 95% yield.[30,29]

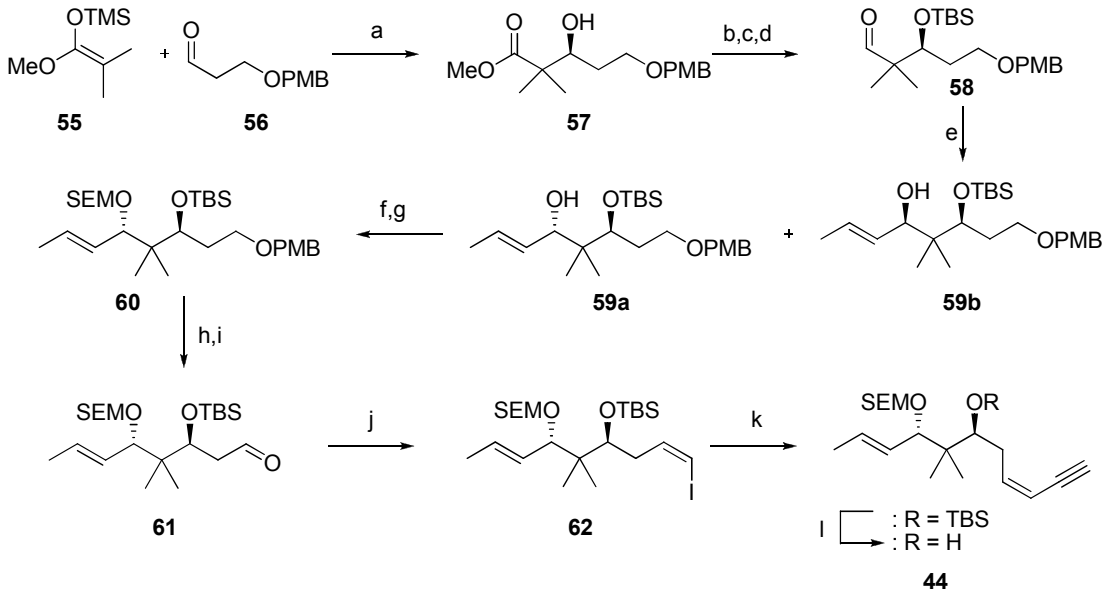


**Scheme 11: Hoffmann alkyne synthesis**

(a) i. *N*-Tos-D-valine, $BH_3$•THF, DCM, −78 °C; ii. $K_2CO_3$, MeOH, 96%; (b) TBSOTf, 2,6-lutidine, DMAP, DCM, rt, 99%; (c) DIBAL, toluene, −78 °C, 94%; (d) DMP, DCM, 0 °C to rt, 83%; (e) *trans*-1-bromopropene, *t*-BuLi, $Et_2O$/THF (1:1), −95 °C, 99% (**59a**:**59b**, 1.1:1); (f) separation of diastereomers; (g) SEMCl, $^{i}Pr_2NEt$, $Bu_4N^+I^-$, DCM; (h) DDQ, DCM/$H_2O$ (10:1), 0 °C, 98% from **59a**; (i) $SO_3$•pyr, $Et_3N$, DCM/DMSO (6:1), 0 °C, 80%; (j) $I^-Ph_3P^+CH_2I$, NaHMDS, THF/HMPA (10:1), −78 °C, 82%; (k) i. (trimethylsilyl)acetylene, $PdCl_2(PPh_3)_2$, CuI, $Et_3N$, $CH_3CN$, rt, 99%; ii. TBAF (1.1 equiv.), THF, 0 °C to rt, 81%; (l) TBAF (10.0 equiv.), THF, rt, 95%.

The route towards the total synthesis of disorazole $C_1$ is shown in scheme **12**; this involved a Sonogashira coupling between the alkyne **44** and the vinyl iodide **45**. Problems were encountered when removing the TBS group, so this was replaced by the more labile TES group and the ester of one half of the dimer was hydrolysed to the carboxylic acid **63**. An esterification between alcohol **43** and acid **63** provided **64** in a 35% yield; it was found this reaction was more efficient if the acid was activated portionwise resulting in an improved 60% yield. The final step involved selective saponification of the methyl ester, followed by Yamaguchi lactonisation to give **65**. The tetradehydro-analogue could be deprotected and the alkyne reduced to the (*Z*)-alkene under Lindlar conditions, but this step was not reported.[30]

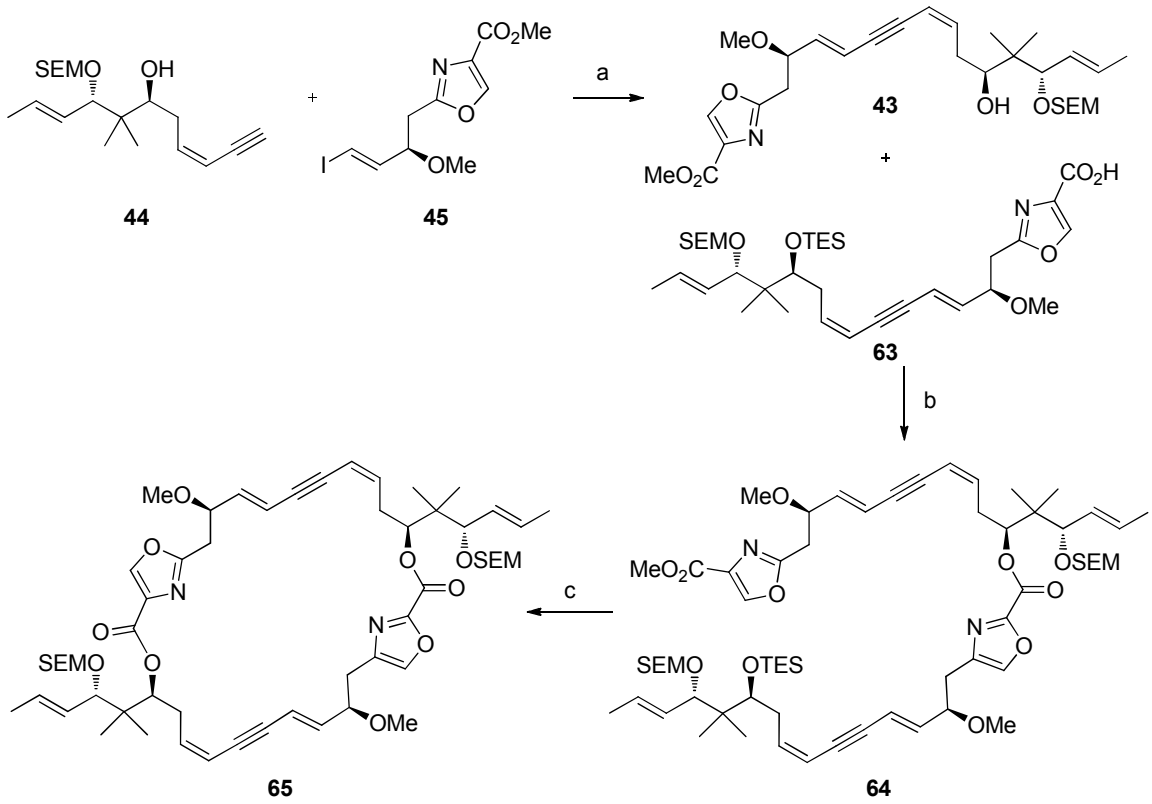


**Scheme 12: Hoffmann cyclisation**

(a) $PdCl_2(PPh_3)_2$, CuI, $Et_3N$, DMF, rt, 89%; (b) $Cl_3C_6H_2COCl$, $Et_3N$, DMAP, toluene, rt, 8 h, 34%; (c) i. TBAF, AcOH/ $H_2O$ (1:1), THF, rt, 86%; ii. $Ba(OH)_2$, $H_2O$, MeOH, THF, rt, quant; iii. $Cl_3C_6H_2COCl$, $Et_3N$, DMAP, toluene, rt, 35%.

## 1.4.3 Wipf Total Synthesis of Disorazole $C_1$

To date, there has only been one total synthesis of disorazole $C_1$, which was reported by Wipf and Graham in 2004.[15] The retrosynthetic analysis shown in scheme **13** proposed that disorazole $C_1$ could be synthesised from the masked alkene analogue **66** as based on the Hoffmann group studies. It was suggested that this cyclic diyne could be constructed from the alkyne **67** and the vinyl iodide **45**.

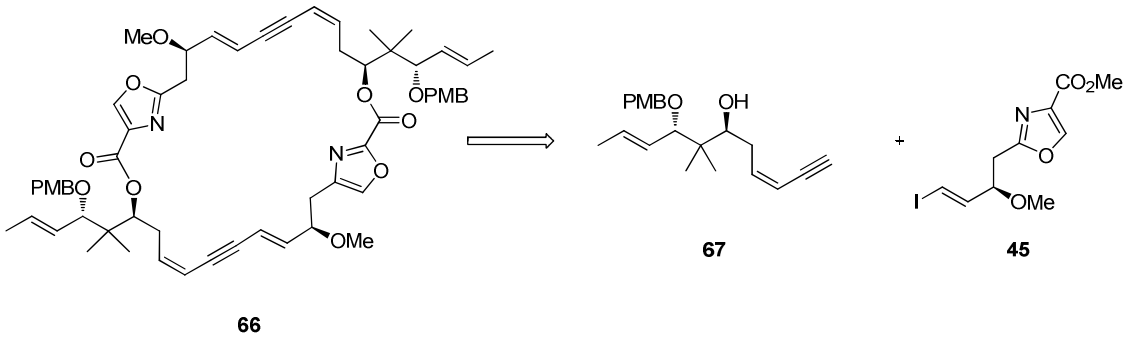


**Scheme 13: Wipf retrosynthesis**

The synthesis of the enyne **67** is shown in scheme **14**. The homoallylic alcohol **68** was synthesised using known methods[31] in 91% yield and 92% ee from naphthalene-2-carboxylic acid 2,2-dimethyl-3-oxo-propyl ester *via* a $TiF_4$/(S)-BINOL-catalysed allylation with allyltrimethylsilane. The terminal alkene of the homoallylic alcohol **68** was converted to the alcohol by ozonolysis, followed by reduction with $NaBH_4$; subsequent 1,3-diol protection and saponification led to alcohol **69**. Swern oxidation was utilised to give the corresponding aldehyde, which was reacted with 1-lithiopropyne to afford a ~1:1 mixture of alcohol diastereomers **70a** and **70b**, which were easily separable by column chromatography. The alkyne of the desired *anti*-diastereomer **70a** was reduced to the (*E*)-alkene using Red-Al. The resulting allylic alcohol was protected and the acetonide was removed to give the diol **71**. Protecting group manipulation of the alcohol groups and oxidation of the terminal alcohol under Swern conditions provided the aldehyde, which was in turn reacted with lithiated 1,3-bis(triisopropylsilyl)propyne. The protecting groups were removed to give the enyne **72** as a 1:8 mixture of double bond isomers (*E/Z*). Following separation of

these isomers by flash chromatography, desilylation of the alkyne **72a** gave the required enyne **67**.[15]

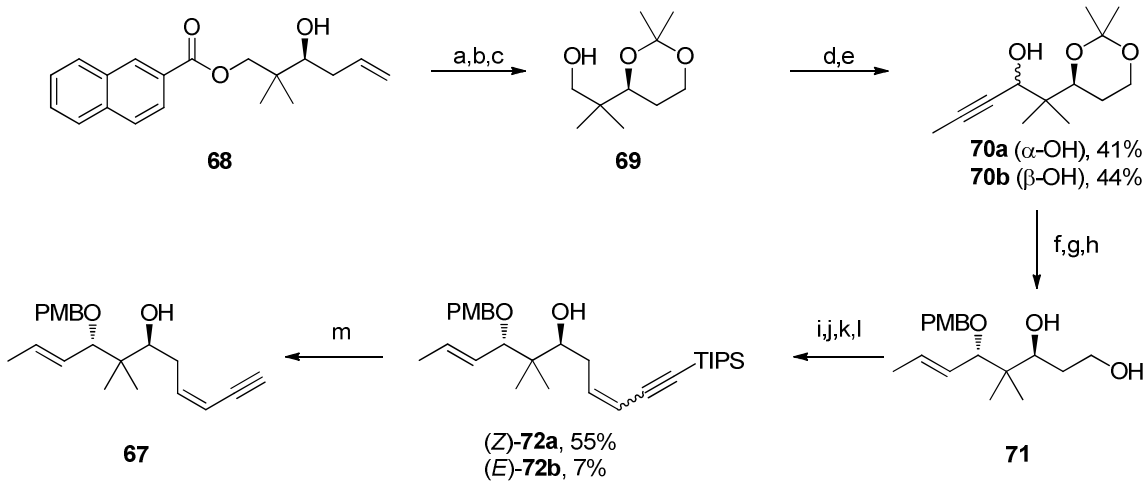


**Scheme 14: Wipf enyne synthesis**

(a) i. $O_3/O_2$, Sudan III, MeOH, DCM, −78 °C; ii. $NaBH_4$, −78 °C to rt, 88%; (b) 2,2-dimethoxypropane, PPTS, THF, 0 °C to rt, 36 h, 97%; (c) 1 M LiOH, THF, MeOH, 0 °C to rt, 20 h, 82%; (d) $(COCl)_2$, DMSO, $Et_3N$, −78 °C; (e) $CH_3C{\equiv}CLi$, −78 °C to 0 °C, 1.5 h (f) Red-Al, THF (degassed), reflux, 25 h, 83%; (g) PMB-Br, $Et_3N$, KHMDS, THF, −78 °C, 1 h then rt, 2 h; (h) AcOH/THF/$H_2O$ (4:1:1), 60 °C, 12 h, 84% (2 steps); (i) TESOTf, 2,6-lutidine, DCM, 0 °C, 30 min; (j) $(COCl)_2$, DMSO, $Et_3N$, DCM, 75% (2 steps); (k) $TIPSC{\equiv}CCH_2Li$, THF −78 °C, 30 min (l) chloroacetic acid, MeOH/DCM (3:1), rt, 14 h; (m) TBAF, THF, 0 °C to rt, 14 h, 94%.

The synthesis of the oxazole fragment (scheme **15**) started from silyl ether protection of hydroxynitrile **73**, followed by DIBAL reduction, resulting in the aldehyde **74**. The TMS-acetylene was added with control of absolute stereochemistry, using diethyl zinc, Ti(*i*-OPr)$_4$ and (*S*)-Binol, producing alcohol **75**. The enantiomeric excess was determined as 92% by converting the alcohol to the benzoate **76** and analysis by chiral HPLC. *O*-Methylation of **75** with dimethyl sulfate under phase transfer conditions resulted in concomitant loss of the TMS group. TIPS deprotection with HF, followed by oxidation of the resulting alcohol provided the carboxylic acid **77**. Coupling of serine methyl ester hydrochloride and acid **77**, followed by cyclodehydration of the resulting hydroxyamide and oxidation of the oxazoline resulted in the desired oxazole **78**, plus the bromide **79**. Formation of the bromide **79**

was unexpected**,** but it could rapidly be converted to the desired iodide **45** and then saponification of the methyl ester resulted in carboxylic acid **80**.[15]

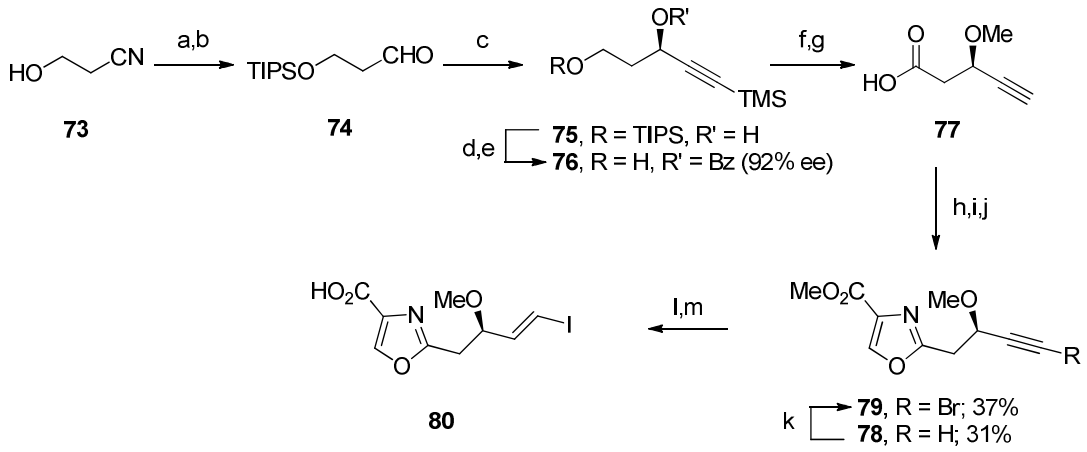


**Scheme 15: Wipf oxazole synthesis**

(a) TIPS-Cl, imid, DMF, rt, 16 h; (b) DIBAL, DCM, −10 °C, 50 min, 78% (2 steps); (c) i. TMS-acetylene, $Et_2Zn$, toluene, reflux, 1 h; ii. (*S*)-Binol, $Ti(O^iPr)_4$; iii. **74**, rt, 20 h, 66%; (d) PhCOCl, DMAP, pyridine, rt, 4 h, 100%; (e) HF (48% aq), $CH_3CN$, rt, 12 h, 93%; (f) Dimethyl sulfate, *n*-$Bu_4NHSO_4$, NaOH (50% aq, $^w/_w$), toluene, 0 °C to rt, 3.5 h, 95%; (g) i. HF, $CH_3CN$, rt, 24 h; ii. NaOCl, $NaClO_2$, TEMPO, $CH_3CN$, phosphate buffer (pH 6.7), 45 °C, 18 h, 99%; (h) SerOMe•HCl, EDC, HOBt, NMM, DCM, 0 °C to rt, 16 h, 55%; (i) i. DAST, DCM, −78 °C, 1 h; ii. $K_2CO_3$, −78 °C to rt, 40 min; (j) DBU, $BrCCl_3$, DCM, 0 °C to 4 °C, 20 h; (k) NBS, $AgNO_3$, acetone, rt, 1 h, 54%; (l) i. *n*-$Bu_3SnH$, $PdCl_2(PPh_3)_2$, THF, −78 °C to rt, 3 h; ii. $I_2$, 0 °C, 45 min, 92%; (m) LiOH, $H_2O$, THF, rt, 12 h, 97%.

Wipf *et al*. constructed Disorazole $C_1$ from the four segments as shown in scheme **16**; firstly coupling fragments **45** and **67** in a Sonogashira coupling to give alkyne **81**. Coupling the alcohol of **81** with the carboxylic acid **80** led to **82**, which was subjected to a further Sonogashira coupling with **67**, resulting in **83**. Selective mono-saponification of the methyl ester, followed by Yamaguchi lactonisation provided the macrocycle **66** in 79% yield. Finally, reduction of the alkyne with Lindlar's catalyst provided disorazole $C_1$ in 20 steps with an overall yield of 1.5%.[15]

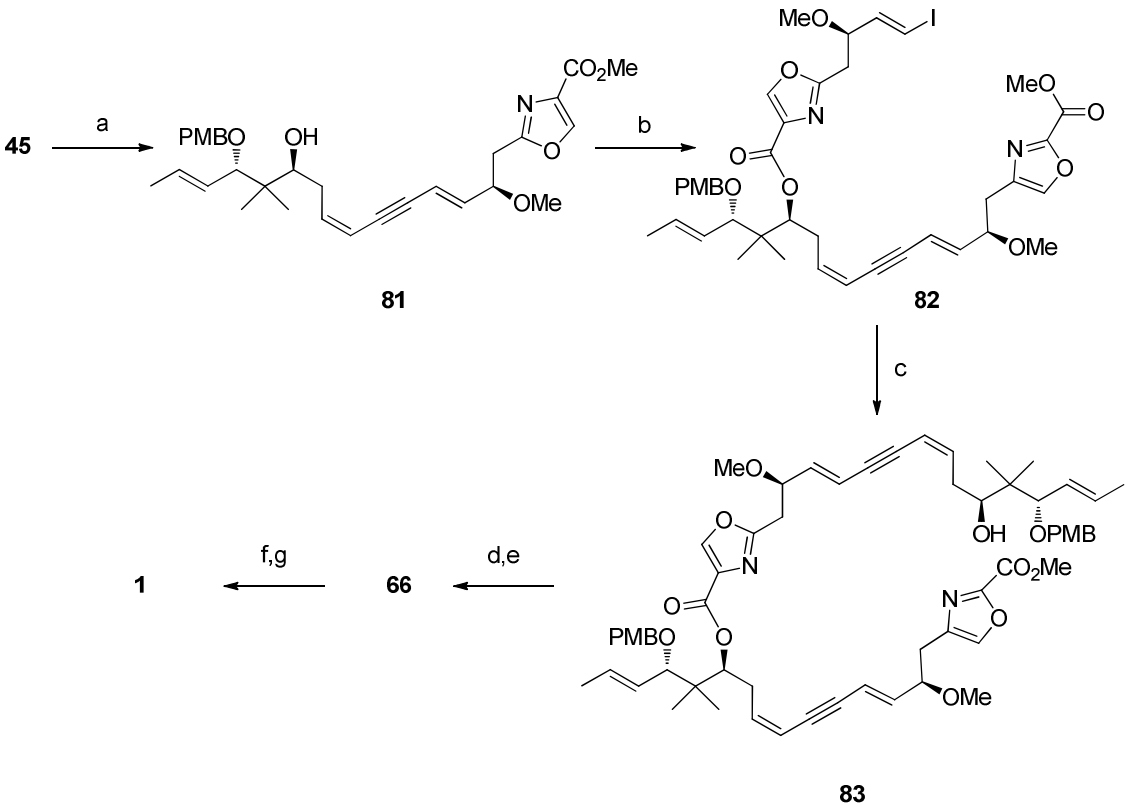


**Scheme 16: Wipf synthesis of disorazole $C_1$**

(a) **67**, $PdCl_2(PPh_3)_2$, CuI, $Et_3N$, $CH_3CN$, −20 °C to rt, 75 min, 94%; (b) **80**, DCC, DMAP, DCM, 0 °C to rt, 14 h, 80%; (c) **67**, $PdCl_2(PPh_3)_2$, CuI, $Et_3N$, $CH_3CN$, −20 °C to rt, 75 min, 94%; (d) LiOH, $H_2O$, THF, rt, 13.5 h, 98%; (e) 2,4,6-trichlorobenzoyl chloride, $Et_3N$, THF, rt, 2 h then DMAP, toluene, rt, 16 h, 79%; (f) DDQ, phosphate buffer, DCM, rt, 15 min, 61%; (g) $H_2$, Lindlar catalyst, quinoline, EtOAc, rt, 1 h, 57%.

## 1.5 Synthesis of Analogues

### 1.5.1 *t*-Butyl Analogue

The *t*-butyl analogue **12** synthesised by Graham[19] consisted of a simpler side chain than disorazole $C_1$, which was constructed in a similar way to the alkyne **67** required for the total synthesis (scheme **17**). An enantioselective allylation between pivaldehyde (**84**) and allyl trimethyl silane, followed by protection of the alcohol, resulted in the silyl ether **85** in a good yield (78%) over the two steps and 91% ee. Ozonolysis of the olefin, followed by a reductive workup, provided the aldehyde, which underwent condensation with 1,3-bis(triisopropylsilyl)propynyl lithium to yield the alkyne. Cleavage of the TBS group resulted in a mixture of enynes **86a** and **86b** (~1:4, *E*:*Z*) which were easily separable by column chromatography. The TIPS group was removed to reveal the terminal alkyne **87**, which was coupled to the vinyl iodide **45** *via* a Sonogashira reaction to provide the *t*-butyl monomer methyl ester **88** in 94% yield. The synthesis of the macrocycle was completed in an analogous manner to the total synthesis of disorazole $C_1$.[19]

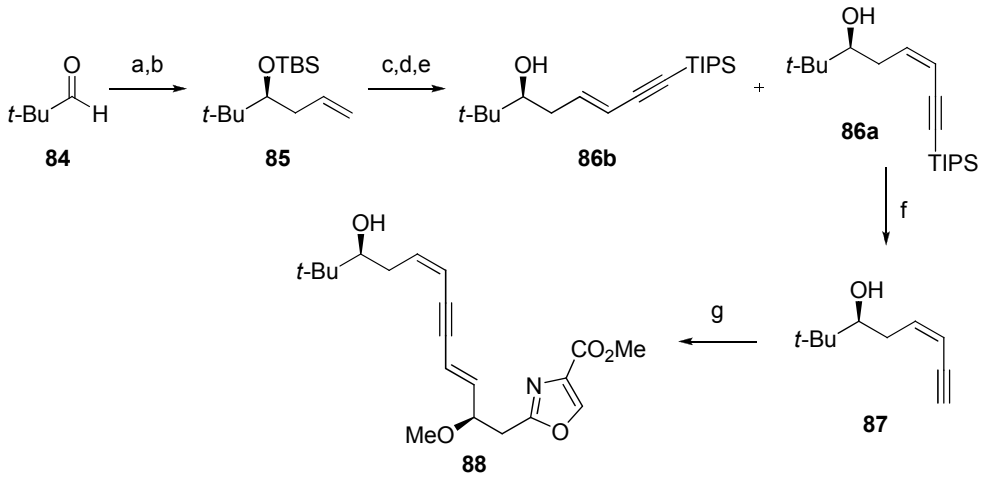


**Scheme 17: *t*-Butyl analogue synthesis**

(a) i. allyltrimethylsilane, (*S*)-BINOL, $TiF_4$, $CH_3CN$, DCM; ii. HF (48% aq), $CH_3CN$, 56%; (b) TBS-Cl, imid, DMF, 99%, 91% ee; (c) $O_3$, Sudan III, DCM, then $PPh_3$; (d) $TIPSC{\equiv}CCH_2Li$, THF –78 °C, 30 min; (e) aq HF, (*Z*)-**86a** 43% (3 steps), (*E*)-**86b** 10% (3 steps); (f) TBAF, AcOH, THF, 76%; (g) **45**, $PdCl_2(PPh_3)_2$, CuI, $Et_3N$, $CH_3CN$, 94%.

## 1.5.2 C(17)-C(18) Cyclopropyl Analogue

For the synthesis of the C(17)-C(18) cyclopropyl analogue **13**, again only the side chain required modification and the synthesis of this fragment is shown in scheme **18**.[19] The alkene of the allylic alcohol **89** was converted to the cyclopropane **90** *via* a Furukawa-modified Simmons-Smith cyclopropanation,[32] which displayed excellent diastereoselectivity (>9:1). The secondary alcohol was protected as the 3,4-dimethoxybenzyl ether and the acetonide group was removed using acidic conditions, providing the diol **91** in good yield (84%) over the two steps. The diol was protected as the bis-triethylsilylether and selective Swern oxidation followed, yielding the aldehyde **92**. Analogous to the previous side chain syntheses, the aldehyde underwent condensation with 1,3-bis(triisopropylsilyl)propynyl lithium to provide the alkyne. The triethylsilylether was removed and the desired (*Z*)-isomer **93a** was isolated in 32% yield over 4 steps. The sequence was completed with removal of the TIPS group to provide alkyne **94**, which could undergo Sonogashira coupling to the vinyl iodide **45**. This provided the required monomer to complete the analogue synthesis in an equivalent manner to the total synthesis of disorazole $C_1$.[19]

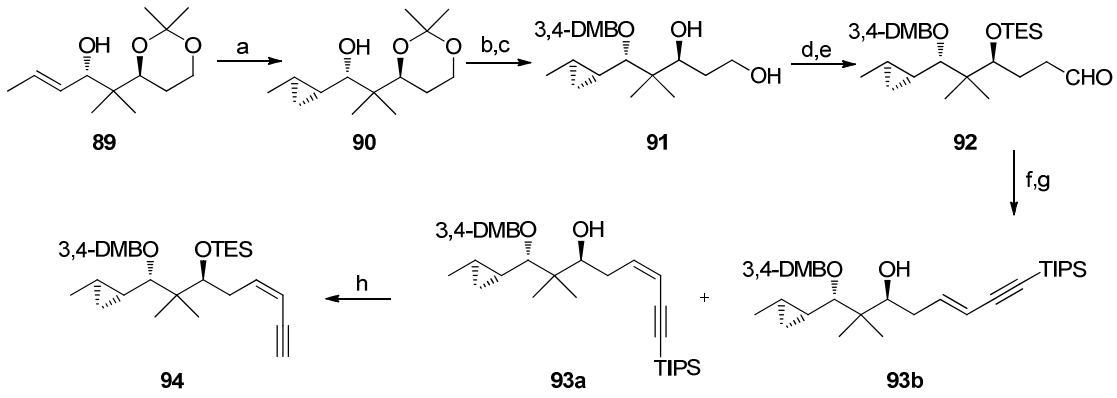


**Scheme 18: C(17)-C(18) Cyclopropyl analogue synthesis**

(a) $CH_2I_2$, $Et_2Zn$, DCM, 98%, dr>9:1; (b) 3,4-DMBBr, $Et_3N$, KHMDS, THF; (c) AcOH/THF/$H_2O$ (4:1:1), 84% over 2 steps; (d) TESOTf, 2,6-lutidine, DCM; (e) $(COCl)_2$, DMSO, then $Et_3N$, DCM; (f) TIPSC≡$CCH_2Li$, THF −78 ° C, 30 min; (g) chloroacetic acid, MeOH/DCM (3:1) (*Z*)-**93a** 32% (4 steps), (*E*)-**93b** 12% (4 steps); (h) TBAF, THF, 89%.

### 1.5.3 Attempted Synthesis of the C(6)-Desmethoxy Analogue

A modified oxazole fragment was required in order to synthesise the C(6)-desmethoxy analogue **16**.[19] This was constructed using a comparable route to that used for the total synthesis of disorazole $C_1$; but with the benefit of a shorter sequence, due to the lack of substitution at C(6), as shown in scheme **19**. The commercially available 4-pentynoic acid (**95**) was coupled to serine methyl ester hydrochloride to provide the hydroxyamide **96**. Cyclodehydration of the hydroxyamide **96** with DAST to the oxazoline and subsequent oxidation resulted in the oxazole. The terminal alkyne was subjected to bromination using NBS and silver nitrate, affording the bromoalkyne **97** in 51% yield over 3 steps. The bromoalkyne underwent a hydrostannylation-iodination to yield the vinyl iodide **98**, which in turn was coupled to the alkyne **67** in a Sonogashira reaction to give the alkyne **99**. Saponification of the ester followed by dimerisation under Yamaguchi conditions was attempted, but this resulted in low yields and this route was not completed. As a result, a stepwise approach was attempted (*cf.* scheme **16**: Wipf synthesis of disorazole $C_1$), but, unfortunately low yields were encountered through the route and the target compound **16** could not be isolated in acceptable yield or in a pure form. The problems faced could have been due to possible instability of the molecule.

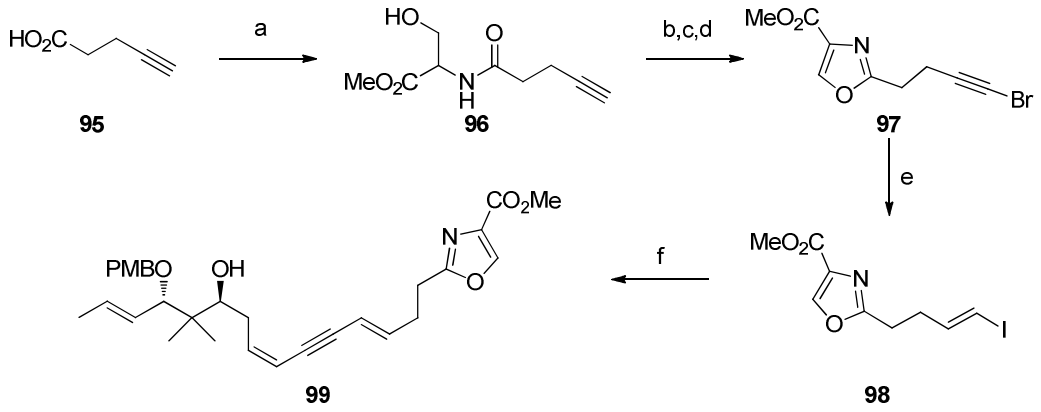


**Scheme 19: Attempted synthesis of the C(6)-desmethoxy analogue**

(a) SerOMe•HCl, EDC, HOBt, NMM, DCM, 34%; (b) DAST, DCM; (c) DBU, $BrCCl_3$, DCM; (d) NBS, $AgNO_3$, DMF 51% over 3 steps; (e) *n*-$Bu_3SnH$, $PdCl_2(PPh_3)_2$, THF, then $I_2$, 90%; (f) **67**, $PdCl_2(PPh_3)_2$, CuI, $Et_3N$, $CH_3CN$, 56%.

## 1.5.4 Hydrogenated Disorazole $C_1$

During the hydrogenation of the alkyne **10** to disorazole $C_1$ **1** (scheme **16**), a mixture of by-products were collected that had similar structures, perhaps originating from alkene isomerisation or saturation. This mixture was treated with hydrogen and palladium on carbon to provide a single saturated analogue (**15**) in 61% yield.[19]

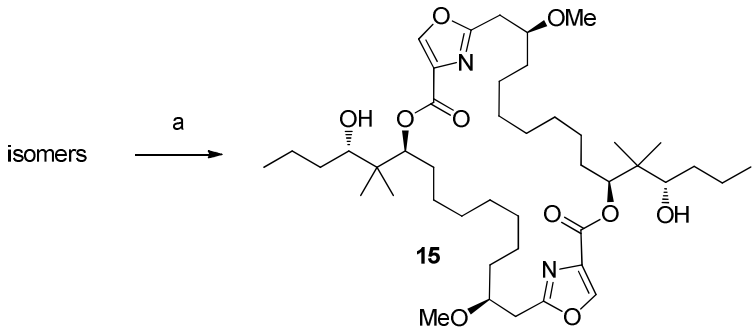


**Scheme 20: Hydrogenated disorazole $C_1$ synthesis**

(a) $H_2$, Pd/C, MeOH, rt, 2 h, 61%

## 1.5.5 C(16)-Ketone Analogue

The ketone analogue **14** was simply prepared *via* a Dess-Martin oxidation of disorazole $C_1$, affording the analogue in an excellent yield (91%).

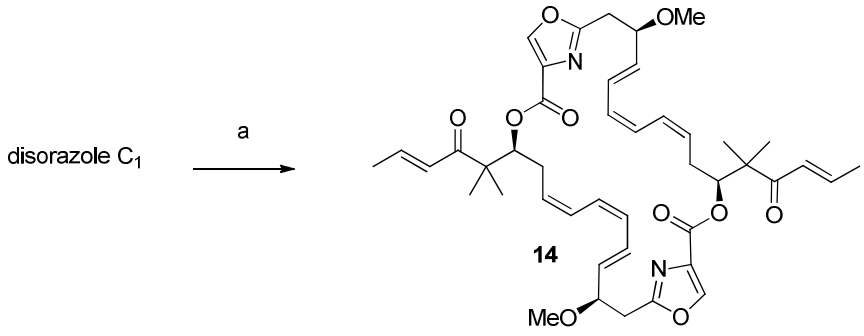


**Scheme 21: Ketone analogue synthesis**

(a) DMP, $NaHCO_3$, DCM (wet), 91%.

## 1.5.6 (–)-CP$_2$-Disorazole C$_1$

The most recent analogue to be published by the Wipf group is (–)-CP$_2$-disorazole C$_1$ (**11**), the retrosynthesis of which is shown in scheme **22**.[20] The key fragments required for this analogue synthesis were the phosphonium salt **100** and the protected alcohol **101**. In a forward sense the alcohol would be deprotected and oxidised to the aldehyde, in order to carry out a Wittig olefination.

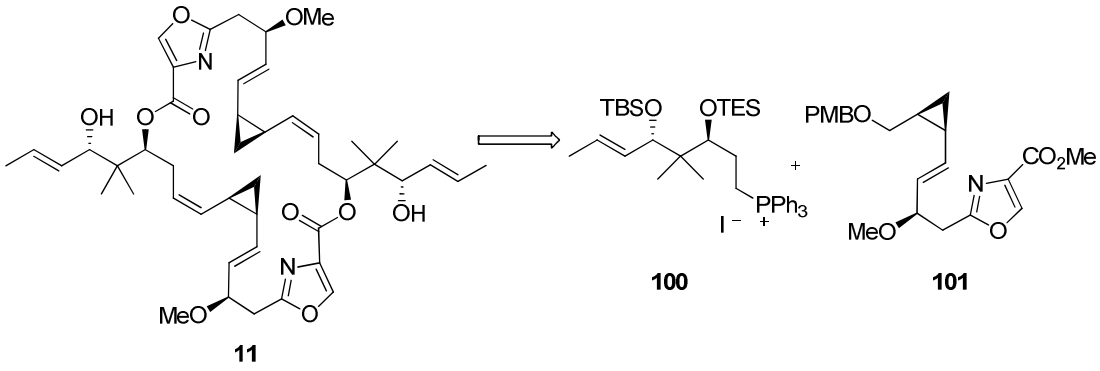


**Scheme 22: (–)-CP$_2$-Disorazole C$_1$ retrosynthesis**

The synthesis of the oxazole fragment **101** is shown in scheme **23**. The known alkyne[33] **102** was subjected to basic conditions to remove the TMS group and hydrogenation of the alkyne resulted in the alkene **103** in excellent yields. Cross metathesis of alkene **103** with alkene **105** (which had been prepared by means of a Wittig olefination of the known aldehyde **104**) resulted in an inseparable mixture of the *E*/*Z* isomers of alkene **106** (*E*/*Z* = 10:1), which was nonetheless carried forward.[34] *O*-Methylation, enzymatic ester hydrolysis and coupling of the resulting acid with serine methyl ester hydrochloride gave amide **107** in a good yield (65%). Cyclisation to the oxazoline and oxidation to the oxazole furnished **101** in good yields. The PMB group was removed and the liberated alcohol was oxidised to provide the aldehyde **108**.

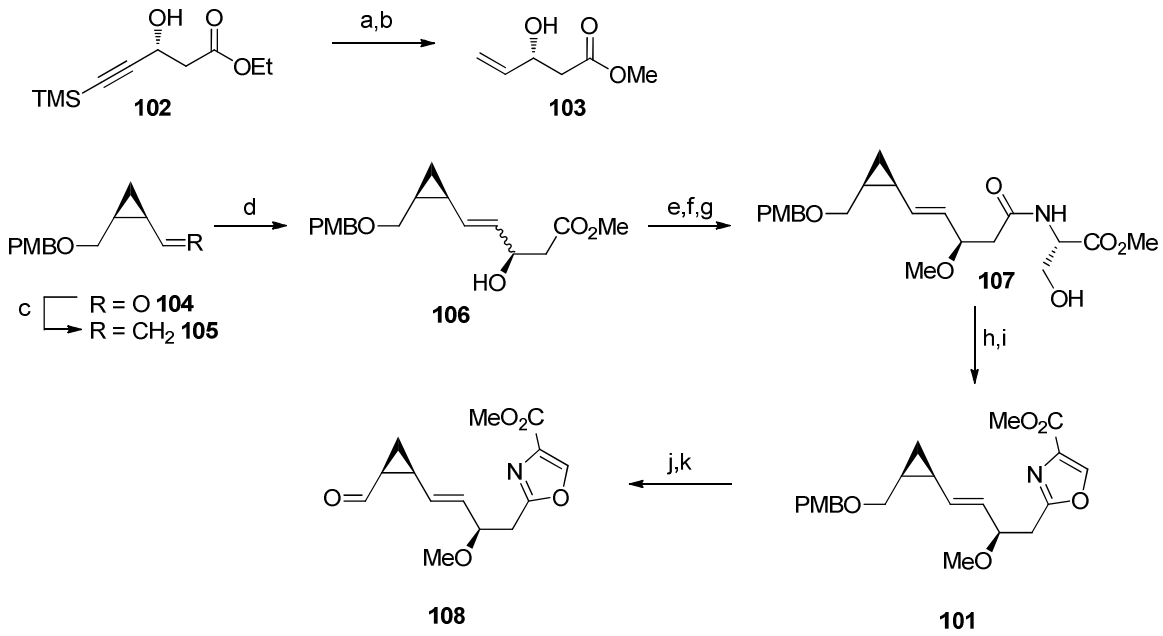


**Scheme 23: (–)-CP$_2$-Disorazole C$_1$ oxazole fragment synthesis**

(a) $K_2CO_3$, MeOH, 85%; (b) $H_2$, Lindlar cat., quinoline, EtOAc, 96%; (c) $I^-Ph_3P^+CH_3$, KHMDS, THF, −78 to 0 °C, 74%; (d) **103**, Grubbs II (5 mol%), DCM, 40 °C, 70% (*E*/*Z* = 10:1); (e) $Ag_2O$, MeI, $Et_2O$, 98%; (f) PLE, pH 7.0 phosphate buffer, EtOH, quant; (g) L-SerOMe•HCl, PyBOP, $^iPr_2NEt$, DMF, 65%; (h) DAST, DCM, −78 °C, then $K_2CO_3$, 69%; (i) $BrCCl_3$, DBU, 71%; (j) DDQ, DCM/$H_2O$, pH 7.0, 0 °C, 97%; (k) DMP, $NaHCO_3$, DCM, 0 °C, 98%.

The synthesis of the corresponding phosphonium salt fragment **100** commenced with an asymmetric Mukaiyama aldol reaction under Kiyooka's conditions[35] between the silyl ketene acetal **55** and crotonaldehyde (**32**), yielding the aldol product **109** in very good yield and 93% ee (scheme **24**). The alcohol was protected as a DMB ether, the ester was reduced and the resulting alcohol was oxidised to the aldehyde **110** under Swern conditions. Duthaler-Hafner allylation[36] conditions using the titanium catalyst **111** proved to be the most successful method of subsequent asymmetric allylation, forming the alcohol **112** in 87% yield and a 4.8:1.0 diastereomeric ratio, favouring the *anti*-configuration. The free secondary alcohol was protected as a TES ether and the DMB group was removed and exchanged for a TBS ether. This was to prevent formation of an unwanted tetrahydropyran by-product which was observed in the later stage formation of the alkyl iodide (step l) when the free allylic alcohol **112** was carried through the sequence. Oxidative cleavage of the alkene **113**, followed by $NaBH_4$ reduction of the resulting aldehyde afforded the alcohol **114** in a good yield

of 73% over the 3 steps. Iodination and generation of the phosphonium salt afforded **100**, which in turn was subjected to Wittig olefination conditions with the oxazole aldehyde fragment **108**, furnishing the (*Z*)-alkene selectively in 86% yield. Finally, the TES group was selectively removed with PPTS providing the desired cyclopropyl monomer **115**.[20]

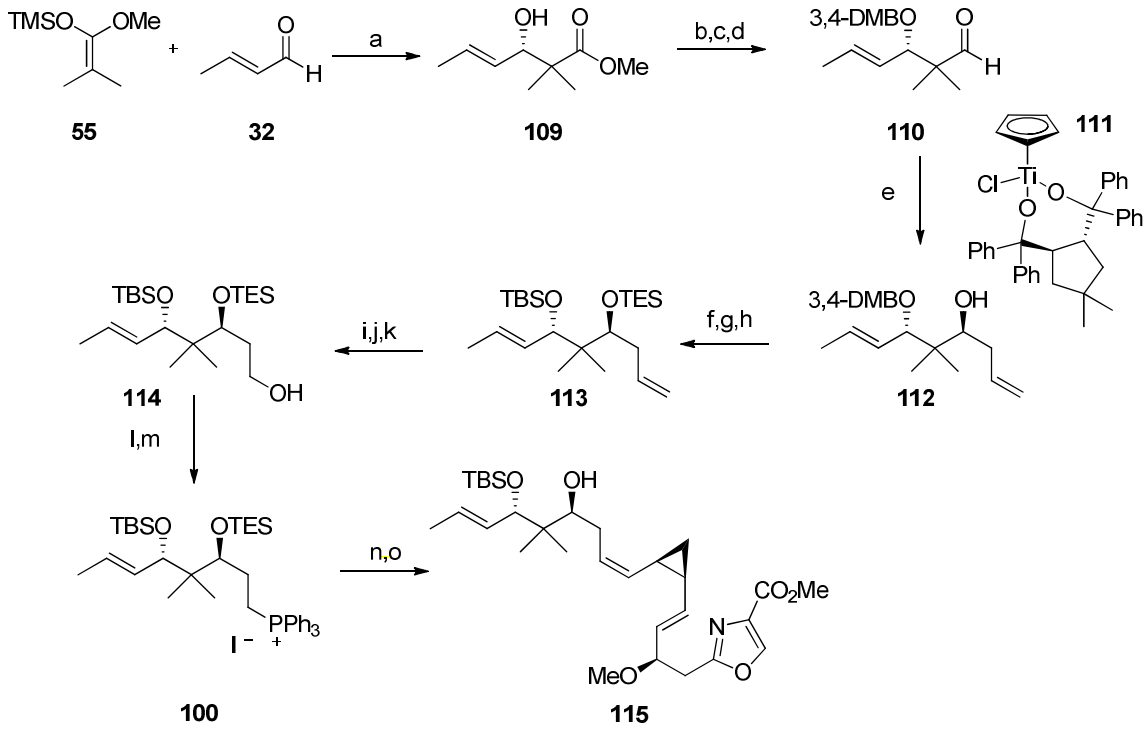


**Scheme 24: Synthesis of the phosphine and subsequent Wittig reaction**

(a) *N*-Ts-D-Val, $BH_3$•THF, DCM, −78 ºC, 79%, 93% ee; (b) 3,4-DMBBr, NaH, DMF, 75%; (c) $LiAlH_4$, $Et_2O$, −78 ºC, 91%; (d) $(COCl)_2$, DMSO, $Et_3N$, −78 °C, 94%; (e) allylmagnesium chloride, $Et_2O$, −78 ºC, 87% (dr = 4.8:1.0); (f) TESOTf, 2,6-lutidine, DCM, 0 ºC, 93%; (g) DDQ, pH 7.0, DCM/*t*-BuOH/$H_2O$ (2:1:1), 0 ºC, 85%; (h) TBSCl, Imid., DMF, 50 ºC, 84%; (i) $OsO_4$, NMO, *t*-BuOH/$H_2O$ (2:1), 0 ºC; (j) $NaIO_4$, dioxane/$H_2O$ (2:1), 0 ºC to rt; (k) $NaBH_4$, MeOH, 0 ºC, 73% over 3 steps; (l) $I_2$, $PPh_3$, imid., DCM, 0 ºC, 85%; (m) $PPh_3$, $^{i}Pr_2NEt$, toluene, 130 ºC, 92%; (n) **108**, KHMDS, THF, −78 ºC to 0 ºC, 86%; (o) PPTs, MeOH, 0 ºC, 65%.

Dimerisation of the acid of **115** was desired, however all attempts resulted in the 15-membered cyclic monomer. Therefore, a more stepwise approach was taken (scheme **25**), proceeding with the ester hydrolysis of **101** and coupling to the alcohol **115**, to afford ester **116**. The PMB group was removed revealing the primary alcohol, which was oxidised to the aldehyde under Dess-Martin conditions. The resulting aldehyde and phosphonium salt **100** underwent a Wittig reaction to afford the (*Z*)-alkene **117**

exclusively. The final steps towards the synthesis of the analogue involved selective deprotection of the more labile TES ether over the TBS ether, followed by saponification of the methyl ester with barium hydroxide. Shiina lactonisation[37] with 2-methyl-6-nitrobenzoic anhydride and DMAP was utilised to form the macrocycle. Removal of the TBS ether resulted in completion of the synthesis of (−)-$CP_2$-disorazole $C_1$ (**11**) in 23 steps and 1.1 % overall yield for the longest linear sequence.[20]

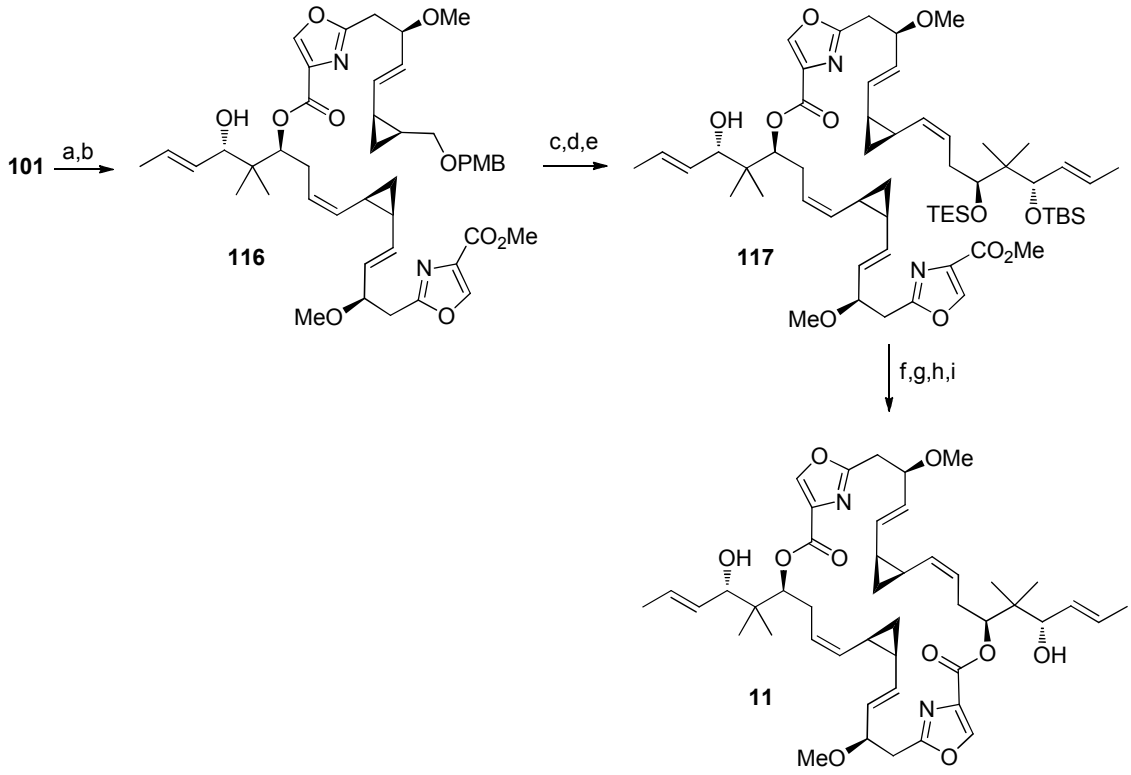


**Scheme 25: (–)-$CP_2$-Disorazole $C_1$ synthesis**

(a) LiOH, THF/$H_2O$; (b) **115**, DCC, DMAP, DCM, 0 ºC to rt, 89% (2 steps); (c) DDQ, DCM, $H_2O$, pH 7.0, 0 ºC, 81%; (d) DMP, $NaHCO_3$, DCM, 0 ºC, 99%; (e) **114**, KHMDS, THF, −78 ºC to 0 ºC, 74%; (f) PPTs, MeOH, 0 ºC, 63%; (g) $Ba(OH)_2$, THF/$H_2O$; (h) MNBA, DMAP, $Et_3N$, toluene, 55% (2 steps); (i) HF•Py, THF, 64%.

## 1.5.7 Synthesis of Simplified Disorazole 18

The retrosynthesis of the simplified disorazole **18**, designed by Kalesse and co-workers,[23] shown in scheme **26** also centred on a key Wittig reaction, requiring the phosphonium salt **118** and the aldehyde **119**.

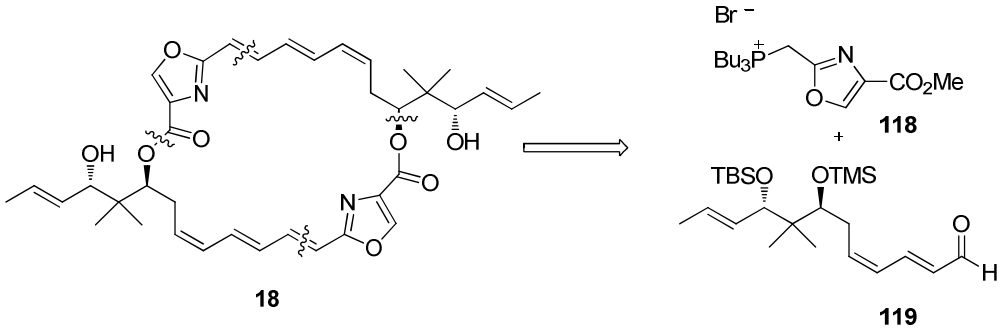


**Scheme 26: Simplified disorazole retrosynthesis**

The synthesis of the aldehyde fragment **119 (**scheme **27**) commenced with a Kiyooka aldol reaction,[35] generating the allylic alcohol **121** in 86% yield, 92% ee and 4:1 diastereoselectivity. Exposing the acetal **121** to NaHMDS resulted in migration of the TBS group to the secondary alcohol and concurrent generation of the aldehyde **122** in excellent yield. The desired (*Z*)-configured lactone **125** was obtained in 30% yield and a diastereoselectivity of 5:1, *via* an asymmetric vinylogous aldol reaction under Campagne's conditions[38] making use of Carreira's catalyst.[39] The undesired open chain (*E*)-isomer **124** was isolated in 25% yield, however this was not a great hindrance as this by-product could be incorporated into the synthesis at a later stage to create the (*E,E,E*)-analogue **19**. The lactone **125** was reduced to the lactol, which in turn was subjected to a Wittig-Horner reaction with triethyl phosphonoacetate, generating the *E*-alkene. Finally, protection of the secondary alcohol as the TMS ether, followed by reduction of the ethyl ester and oxidation to the aldehyde resulted in the target fragment **119**.

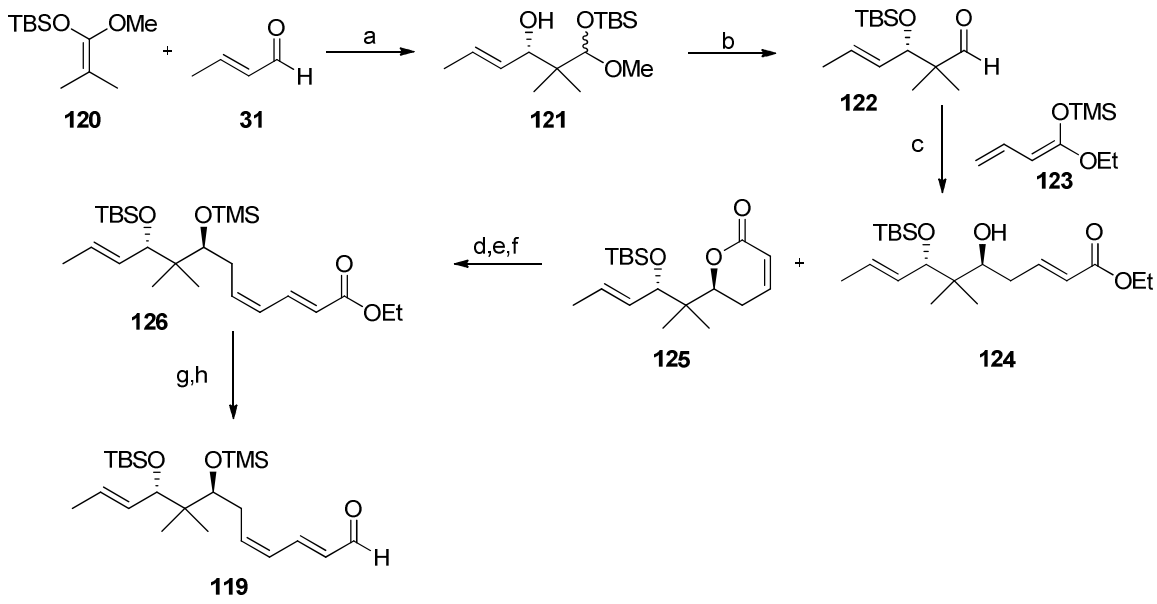


**Scheme 27: Simplified disorazole: aldehyde fragment**

(a) *N*-Ts-D-Val, $BH_3$•THF, DCM, −78 ºC, 86%, 92% ee, dr = 4:1; (b) NaHMDS, THF, −78 ºC to 0 ºC, 92%; (c) **123**, CuF•(*R*)-Tol-BINAP (10 mol%), THF, rt, **125** 30%, dr = 5:1, **124** 25%, dr = 3:1; (d) DIBAL, DCM, −78 ºC, 88%; (e) Triethyl phosphonoacetate, LiHMDS, THF, 0 ºC to rt, 87%; (f) TMSOTf, 2,6-lutidine, DCM, 0 ºC, 93%; (g) DIBAL, DCM, −78 ºC, 91%; (h) $MnO_2$, DCM, rt, 96%.

The synthesis of oxazole fragment **118** (scheme **28**) started with the condensation of serine methyl ester hydrochloride and methyl acetimidate hydrochloride (**127**), providing the oxazoline, which in turn was oxidised to the oxazole **128**. Radical bromination followed by displacement with $PBu_3$ afforded the required phosphonium salt **118**.

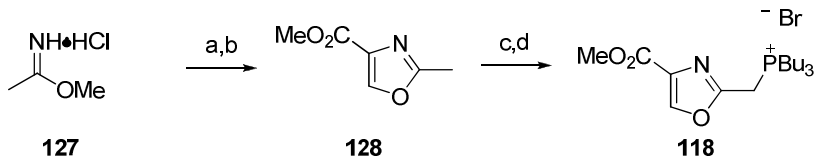


**Scheme 28: Simplified disorazole: oxazole fragment**

(a) DL-SerOMe•HCl $Et_3N$, DCM, 0 ºC to rt, 54%; (b) DBU, $BrCCl_3$, DCM, −10 ºC to rt, 50%; (c) NBS, AIBN, $CCl_4$, reflux, 50%; (d) $Bu_3P$, $CH_3CN$, rt, quant.

With the two key fragments **118** and **119** in hand, the synthesis was completed as shown in scheme **29**. A Wittig reaction between aldehyde **119** and phosphonium salt **118**, followed by selective cleavage of the TMS group and hydrolysis of the methyl ester resulted in the triene **129**. The conjugated triene proved to be difficult to handle, therefore all reactions including the ester hydrolysis and subsequent steps had to be performed in brown glassware and in the absence of light. Dimerisation was successfully executed using Shiina's lactonisation conditions,[40] providing the macrocycle in 26% yield. Finally, the TBS groups were cleaved to afford the novel simplified disorazole analogue **18**.

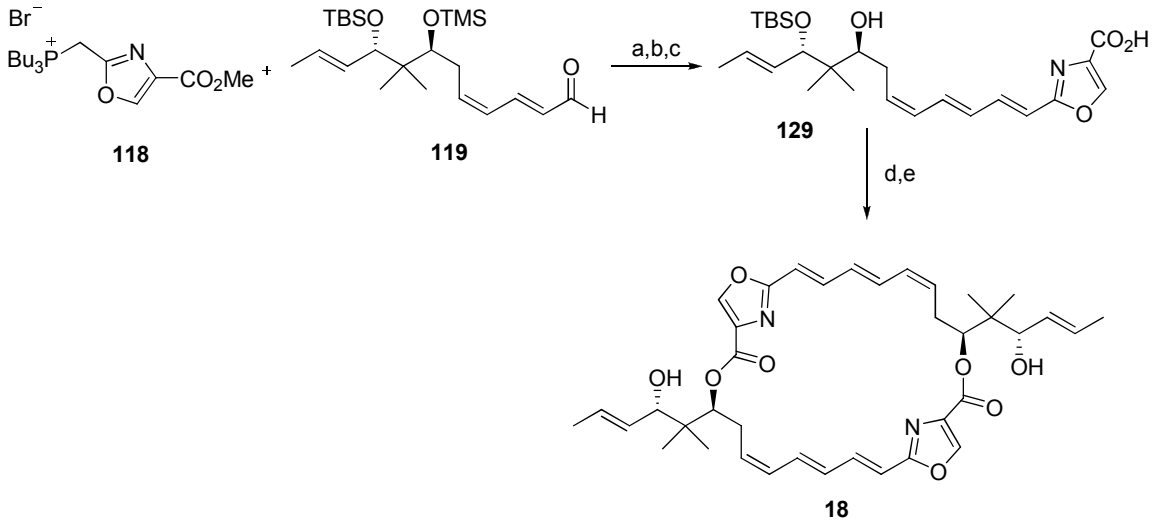


**Scheme 29: Completion of simplified disorazole**

(a) KO$^t$Bu, THF, −78 ºC to 0 ºC, 85%; (b) HF•Py, pyridine, THF, 0 ºC to rt, 75%; (c) exclusion of light, 1 M LiOH, THF, 0 ºC to rt, quant; (d) exclusion of light, MNBA, DMAP, toluene, rt, 26%; (e) exclusion of light, HF (aq), $CH_3CN$, −20 ºC, 22%.

## 1.6 Novel Disorazole $C_1$ Synthesis Utilising the Evans-Tishchenko Reaction and Ring Closing Alkyne Metathesis

All of the previous strategies towards disorazole $C_1$ and its analogues have featured macrolactonisation, which requires protecting group strategies and can be poor yielding; therefore a novel methodology towards the total synthesis as shown in scheme **30** was proposed. This strategy will exploit the C(9)-C(10) alkyne **10**, which has proven to be a successful precursor to disorazole $C_1$ by masking the unstable triene moiety. However, in this approach, the macrocycle will be constructed using alkyne metathesis, thus developing a highly convergent route. Ring closing alkyne metathesis (RCAM) was chosen over ring-closing metathesis (RCM) due to the fact that the (*Z*)-alkene geometry can be controlled *via* hydrogenation with Lindlar's catalyst, whereas the geometrical outcome of RCM cannot always be predicted. The proposed diyne can be disconnected to the β-hydroxyketone **130** and the aldehyde **131**, which in a forward sense would be joined *via* an Evans-Tishchenko (ET) reaction.[41] The ET reaction is regioselective and proceeds with excellent diastereoselectivity, as demonstrated by the Hulme synthesis of octalactin,[42] which successfully applied an Evans-Tishchenko/RCM approach to this medium ring lactone. This approach also holds the benefits of avoiding the need for protecting groups on the allylic alcohol side chain, which have to be chosen carefully to avoid problems late on in the synthesis as exemplified by the Meyers' synthesis of disorazole $C_1$ (section **1.4.1**). As highlighted by the SAR summary in figure **10**, generating heterocyclic analogues of disorazole $C_1$ is a novel area of research, and it is an area in which this highly convergent original strategy can be applied. Herein, novel approaches to the synthesis of the C(1)-C(9) fragment and heterocyclic analogues will be discussed.

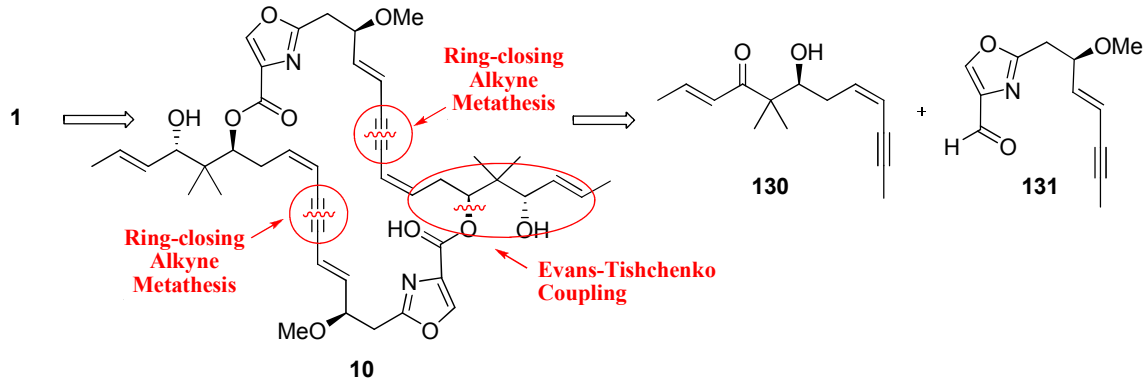


**Scheme 30: Novel retrosynthesis of disorazole $C_1$**

# 2 Chapter 2: Racemic Fragment Synthesis

## 2.1 Oxazole Natural Products

Oxazoles are a common functionality in natural products, where they are derived from enzymatic post-translational modifications of peptidic precursors. This is exemplified in the biosynthesis of disorazole $C_1$ (section **1.1**), where the oxazole is incorporated at a late stage in the process by a non-ribosomal peptide synthetase (NRPS). The exact role and involvement in oxazole formation of each domain sequenced on the disC gene is unknown; however, a general mechanism for oxazole biosynthesis has been established as shown in scheme **31**.[43] The hydroxyl of amide **132**, derived from serine, undergoes a heterocyclisation onto the preceding carbonyl to form **133**. This is followed by a dehydration to form the oxazoline **134**; finally a two-electron oxidation generates the oxazole **135**.

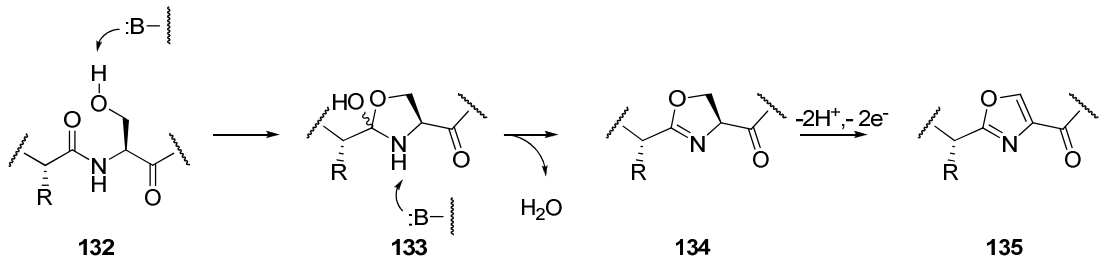


**Scheme 31: Oxazole biosynthesis**

Oxazole-containing natural products, such as those shown in figure **11**, possess a range of valuable biological activities. For example, hennoxazole A **136** exhibits potent activity against the herpes virus ($IC_{50}$ = 0.6 μg $mL^{-1}$).[44] Virginiamycin $M_2$ **137** and related compounds form a family of streptogramin antibiotics.[45] The phorboxazoles A and B (**138a** and **138b**) display potent antifungal activity, as well as anticancer activity.[46]

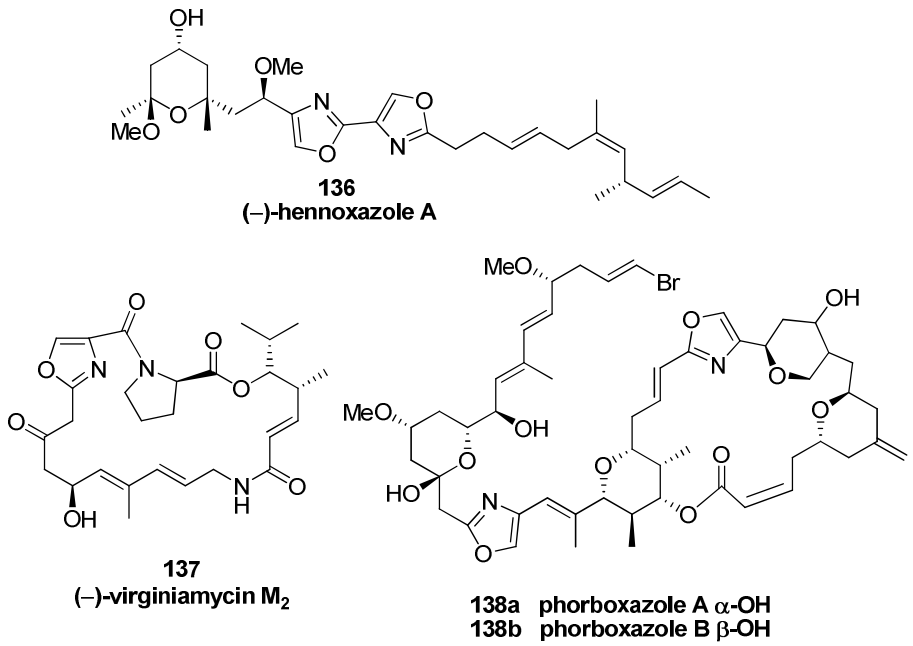


**Figure 11: Examples of oxazole containing natural products**

## 2.2 Disorazole $C_1$ C(1)-C(9) Fragment Retrosynthesis

As discussed in Chapter **1**, the previous syntheses of the oxazole fragment of disorazole $C_1$ have been long and linear; in contrast to this, a novel convergent route that can be adapted towards heterocyclic analogues was desired. Taking this into consideration, the initial retrosynthesis developed is shown in scheme **32**, where the disconnection is made at the C(5)-C(6) bond. In a forward sense both routes require the aldehyde **140**: route A will involve a metal-halogen exchange of the halomethyloxazole **139**, whereas route B will require a lateral lithiation of methyl oxazole **141**.

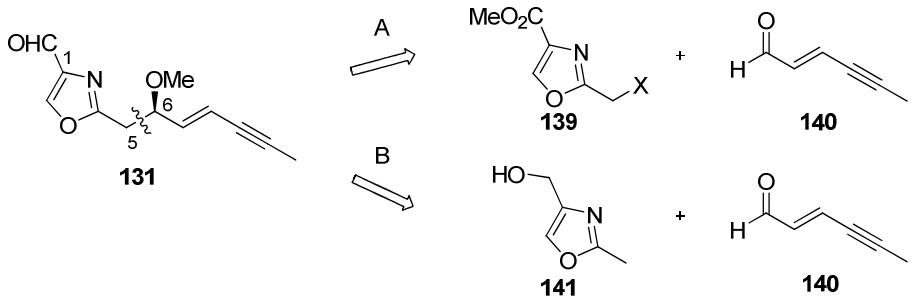


**Scheme 32: C(1)-C(9) fragment retrosynthesis: disconnection at C(5)-C(6)**

## 2.3 C(1)-C(5) Oxazole Syntheses

### 2.3.1 Halomethyloxazole Syntheses

In order to examine the metal-halogen exchange reaction (route A scheme **32**), the chloro-, bromo- and iodomethyloxazoles were synthesised, as at this stage the reactivity of these oxazoles towards the C(6)-C(9) aldehyde was not known. The chloromethyloxazole **139a** was synthesised following a literature procedure,[47] in a 2-step process. This sequence commenced with condensation of dichloroacetonitrile **142** and serine methyl ester hydrochloride *via* an imidate intermediate to give the oxazoline **143**. Subsequent DIPEA mediated elimination of HCl afforded the chloromethyloxazole **139a** in very good yield (83%).

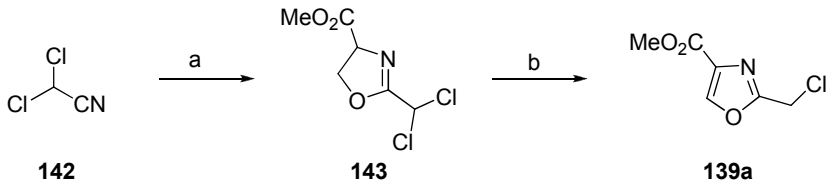


**Scheme 33: Chloromethyloxazole synthesis**

(a) NaOMe, MeOH, DCM, 0 ºC then DL-SerOMe•HCl, DCM, rt, 24 h, 84%; (b) $^{i}Pr_2NEt$, DCM, 50 ºC, 6 h then rt, 18 h, 83%.

Analysis of the literature suggested that the most successful syntheses of the desired bromomethyloxazole **139b** have been *via* the route shown in scheme **34**.[48,49] This involves the nucleophilic attack of ethyl diazoacetate (**144**) onto Vilsmeier's reagent[50] to form ethyl 2-diazo-3-oxopropanoate (**145**) and ethyl chloroacetate (**146**). Treatment of ethyl 2-diazo-3-oxopropanoate (**145**) with catalytic rhodium acetate forms the corresponding carbene, which reacts with bromoacetonitrile to form the oxazole **147**. This reaction was attempted and appeared to be moderately successful by NMR spectroscopy analysis; however, product (**147**) of acceptable purity was not obtained following the purification steps. Other drawbacks to this route include the use of an expensive rhodium catalyst and the requirement of having to handle a sensitive aldehyde intermediate. As a result, this route was not investigated further and an alternative method was sought.

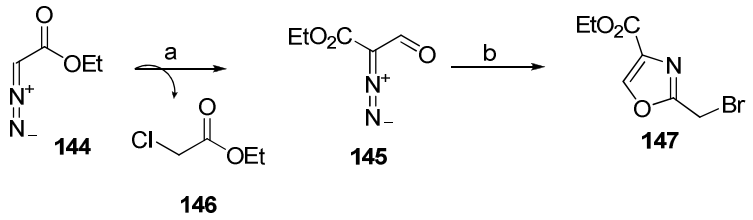


**Scheme 34: Attempted bromomethyloxazole synthesis**

(a) *N,N*-Dimethylformiminium chloride, $CHCl_3$, 10 ºC to rt, 1 h; (b) bromoacetonitrile, $Rh_2(OAc)_4$, 70 ºC, 6 h.

Following the success of using dichloroacetonitrile and serine methyl ester hydrochloride to synthesise the chloromethyloxazole **139a**, it was envisaged that this method could be adapted towards the synthesis of the desired bromomethyloxazole **139b**. This was a novel route towards the bromomethyloxazole; pleasingly, the synthesis of the required dibromoacetonitrile (**149**) from cyanoacetic acid (**148**) and NBS was rapid (5 minutes) and high yielding (96%).[51] Subsequently, the analogous sequence of reactions that were used for the synthesis of chloromethyloxazole was followed. That is, condensation with serine methyl ester hydrochloride, followed by base promoted elimination to afford the bromomethyloxazole **139b** in moderate to good yields.

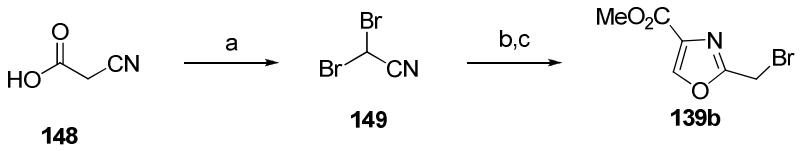


148 149 139b

**Scheme 35: Bromomethyloxazole synthesis**

(a) NBS, $H_2O$, rt, 5 min, 96%; (b) NaOMe, MeOH, DCM, 0 ºC then DL-SerOMe•HCl, DCM, rt, 24 h, 64%; (c) DBU, DCM, 0 ºC, 1 min, 79%.

With the chloromethyloxazole **139a** in hand, a simple transformation to the iodomethyloxazole **139c** *via* a halogen-exchange reaction with sodium iodide in THF was effected,[47] thus concluding the synthesis of the required halomethyloxazoles (**139a-c**). Attention was then focused towards the synthesis of the methyl oxazole **128** for subsequent aldehyde coupling following the lateral lithiation approach.

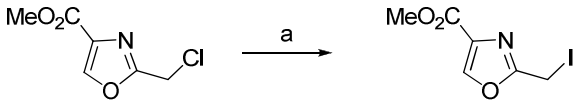


139a 139c

**Scheme 36: Iodomethyloxazole synthesis**

(a) NaI, THF, rt, 20 min, 79%.

## 2.3.2 Methyloxazole Synthesis

The preferred route to the desired methyloxazole **128** was a synthesis which had been optimised by an industrial process group[52] and consequently the route has been used to produce the oxazole in bulk quantities (scheme **37**). The route was also analogous to the successful routes used towards the halomethyloxazoles **139**. The first step of the reaction involved formation of an imidate, originating from the treatment of chloroacetonitrile (**150**) with sodium methoxide. This was followed by condensation of the imidate with serine methyl ester hydrochloride to form the oxazoline **151**. Treatment of the crude oxazoline with DBU resulted in elimination of HCl to produce the desired methyl oxazole **128**, which precipitated out as a colourless solid.

Preliminary investigations into this route provided the oxazole **128** in low yields of approximately 25%, however, recrystallisation of serine methyl ester from anhydrous ethanol and the use of dry solvents increased the yield to a more acceptable 65% overall from chloroacetonitrile.

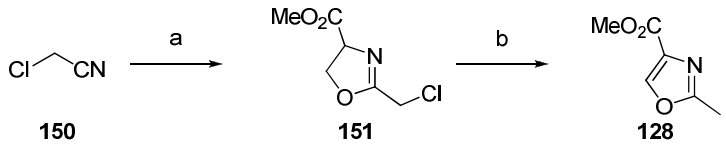


**150** **151** **128**

**Scheme 37: Methyloxazole synthesis**

(a) NaOMe, MeOH, DCM, 0 ºC then DL-SerOMe•HCl, DCM, rt, 24 h; (b) DBU, DCM, 30 ºC, 30 min, 65% over 2 steps.

After initial difficulties in generating the methyloxazole **128** in a good yield, other routes to the oxazole were probed. One alternative route involved the reaction of ethyl acetimidate hydrochloride **152** and serine methyl ester hydrochloride, to provide the oxazoline **153**, which was oxidised to the oxazole **128** with copper (II) bromide (scheme **38**).[53] Overall, the yield was lower than the original route and purification was not as simple; therefore this synthesis was not progressed any further.

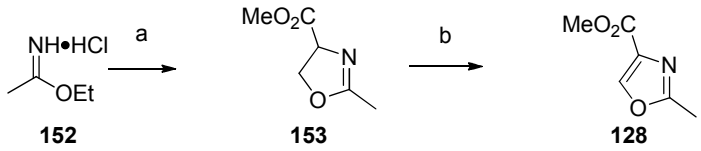


**152** **153** **128**

**Scheme 38: Alternative methyloxazole synthesis**

(a) DL-SerOMe•HCl, $Et_3N$, DCM, rt, 18 h; (b) i. $CuBr_2$, DBU, HMTA, 20 min, 0 ºC; ii. **153**, THF, 3 h, rt, 52% over 2 steps.

Another alternative option was a modified literature procedure,[54] involving the reaction between acetamide **154** and ethyl bromopyruvate, generating the oxazoline **155**; and elimination of water provides the oxazole **156** (scheme **39**). Unfortunately, the desired product could not be isolated, however, the conditions for the first route (scheme **37**) had been now been optimised and no further investigations were required towards this route.

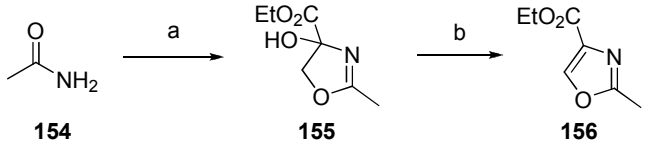


**154** **155** **156**

**Scheme 39: Ethyl bromopyruvate based methyloxazole synthesis**

(a) Ethyl bromopyruvate, $NaHCO_3$, THF, reflux, 24 h; (b) TFAA, 2,6-lutidine, THF, 0 ºC, 1 h.

Once the synthesis of the methyloxazole **128** was satisfactorily optimised, the methyl ester was reduced to the alcohol **141** in good yield (70%), using lithium aluminium hydride following the procedure of Carey *et al*.[52] With syntheses towards the halomethyloxazoles and the methyloxazole established, attention was now focused towards the aldehyde required for both coupling strategies.

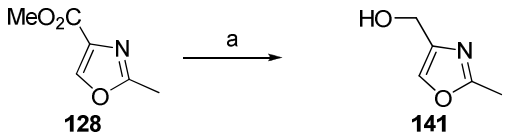


**128** **141**

**Scheme 40: Methyl ester reduction**

(a) $LiAlH_4$, $Et_2O$, −5 ºC, 1 h, 79%.

## 2.4 C(6)-C(9) Aldehyde Synthesis

The synthesis of the required enyne side chain was based on the synthesis of the related TMS protected alkyne **160** published by Trost and *et al.*[55] (scheme **41**). Ethyl propiolate (**157**) was regio- and stereoselectively hydroiodinated to the (*Z*)-alkene **158** with sodium iodide in acetic acid. Literature procedures for this reaction reported reaction times of over 12 hours; however, by TLC monitoring the reaction was found to be complete in 3 hours and the (*Z*)-alkene **158** was obtained in excellent yield (91%). Formation of the (*Z*)-alkene was confirmed by a *J*-coupling value of 9.0 Hz in the proton NMR spectrum. Isomerisation with hydroiodic acid afforded the (*E*)-alkene **159** in 92% yield, confirmed by a *J*-coupling value of 14.8 Hz.

In order to develop a highly convergent synthesis towards the C(1)-C(9) fragment, a Negishi coupling[56] with propynylmagnesium bromide was anticipated to be the most suitable coupling strategy; rather than attempting a Sonogashira reaction with gaseous propyne. The Negishi coupling between the vinyl iodide **159** and propynyl magnesium bromide proceeded smoothly, and generated the enyne **161** in an excellent 90% yield. The best yields for the Negishi coupling were obtained when solid zinc chloride was dried under vacuum with a heat gun (~400 ºC) and a fresh slurry in THF was prepared, rather than using a commercial solution. Further optimisation of the reaction indicated $Pd(PPh_3)_2Cl_2$ to be the optimum catalyst over $Pd(PPh_3)_4$.[57]

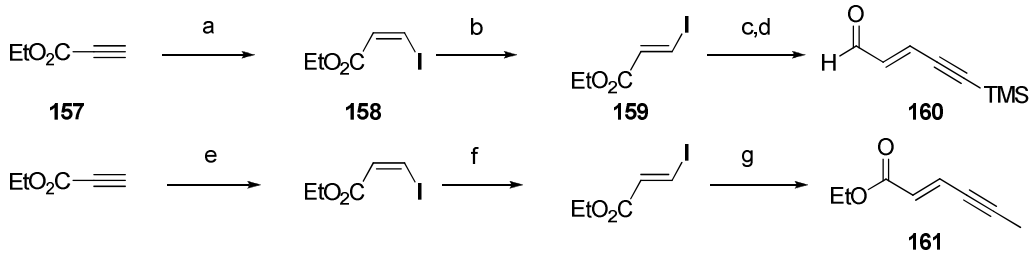


**Scheme 41: (*E*)-Vinyl iodide synthesis**

(a) NaI, AcOH, 70 °C, 13 h, 95%; (b) HI (aq), benzene, 80 °C, 8 h, 95% (*E*:*Z* 16:1); (c) trimethylsilylacetylene, CuI, $Pd(PPh_3)_2Cl_2$, $Et_3N$, 50 °C, 13 h, 89%; (d) DIBAL, toluene, –95 °C, 1 h, 70%;[55](e) NaI, AcOH, 70 ºC, 3 h, 91%; (f) HI (57% aq), toluene, 80 ºC, 8 h, 92 % (20:1, *E*:*Z*); (g) i. $ZnCl_2$, propynylmagnesium bromide, THF, 0 ºC, 15 min; ii. **159**, $Pd(PPh_3)_2Cl_2$, rt, 18 h, 90 %.

Attempts were made to reduce the ethyl ester **161** directly to the aldehyde **140** with DIBAL, but unfortunately, either incomplete conversion, or over reduction to the alcohol were observed. As a result, a two-step approach involving total reduction to the alcohol **162** with DIBAL, followed by partial oxidation to the aldehyde was adopted. Since the aldehyde **140** is volatile and unstable (boiling point = 56 ºC[58]), a suitable oxidation procedure had to be established which was mild and required little, or no purification. Oxidations with IBX in either DMSO,[59] or hot ethyl acetate resulted in poor yields and the product was contaminated with IBX by-products. Manganese dioxide has been shown to be effective at oxidising similar allylic alcohols,[58,60] and taking this into consideration, the aldehyde **140** was successfully generated from alcohol **162** using manganese dioxide, in sufficient purity to be used directly in the next step without further purification. It is worthwhile to note that a cleaner oxidation was observed when the activated manganese dioxide was sonicated in diethyl ether prior to the addition of the alcohol. Now with all of the required coupling partners in hand, the coupling strategies could be examined, starting with the halomethyloxazoles and aldehyde *via* route A.

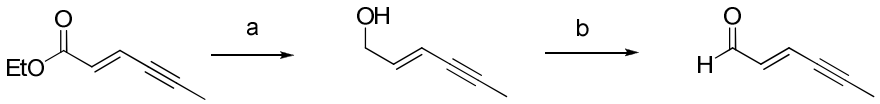


**161** **162** **140**

**Scheme 42: Enyne aldehyde synthesis**

(a) DIBAL, DCM, −78 ºC, 2 h, 73%; (b) $MnO_2$, $Et_2O$, rt, 18 h, assumed quant.

## 2.5 Halomethyloxazole and Aldehyde Coupling-Route A

Within the last 20 years, the use of Barbier-type reactions for the synthesis of oxazole-containing natural products has increased and it was envisaged that this approach could be applied to the synthesis of the C(1)-C(9) fragment of disorazole $C_1$. The Barbier reaction is a one-pot, metal-mediated addition between an alkyl halide and a carbonyl group thereby generating an alcohol product. A number of different metals have been used in this type of reaction, including zinc,[61] samarium,[62] indium,[63] chromium,[64] tin[65] and cadmium.[66] The proposed Barbier coupling between the halomethyloxazoles **139a-c** and C(6)-C(9) aldehyde **140** is shown in scheme **43**. Literature examples of Barbier reaction involving halomethyloxazoles will now be reviewed, followed by results obtained when these methods were applied to our system.

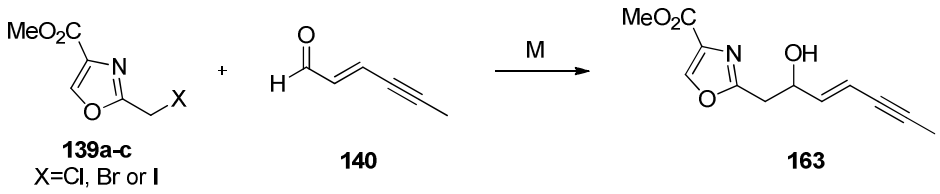


**Scheme 43: Proposed Barbier coupling between halomethyloxazole and C(6)-C(9) Aldehyde**

## 2.5.1 Oxazole Zinc Barbier-Type Coupling

Helquist *et al.* realised that the bromomethyloxazole could be used to generate an organometallic reagent. Hence, a simple zinc-promoted Barbier reaction with bromomethyloxazole **147** was developed and the scope of the reaction was investigated.[67] The reaction proved to be versatile, affording moderate to excellent yields of the alcohol products **164** with aliphatic, aromatic and conjugated aldehydes (table **4**, entries 1-6). The reaction also proceeded successfully with ketones (table **4**, entries 7-10) and no Michael addition products were observed with α,β-unsaturated ketones (table **4**, entries 11 and 12). The group proceeded to use this methodology to develop a synthesis of the C(9)-C(23) fragment of virginiamycin $M_2$ and madumycin I.[68] A zinc Barbier reaction was also utilised in Schlessinger's total synthesis of virginiamycin $M_2$.[69]

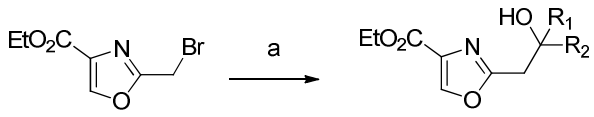


**147** **164**

(a) i. Zn, THF, 0 ºC; ii. Carbonyl compound.

**Table 4: Helquist Zinc Barbier reaction substrate screen**

| Entry | Substrate | Yield % |
|---|---|---|
| 1 | hexanal | 92 |
| 2 | benzaldehyde | 96 |
| 3 | PhCH=CHCHO | 97 |
| 4 | $(Me)_2C$=CHCHO | 62 |
| 5 | 2,4-hexadienal | 40 |
| 6 | TBDMSO$(CH_2)_3$CHO | 62 |
| 7 | $Me_2CH(CH_2)_2C$(O)Me | 39 |
| 8 | cyclohexanone | 49 |
| 9 | PhC(O)Me | 47 |
| 10 | cyclopentenone | 90 |
| 11 | PhCH=CHC(O)Me | 93 |
| 12 | $H_2C$=CHC(O)Me | 52 |

A zinc Barbier reaction was found to be the optimum coupling strategy for a key step in the synthesis of siphonazole (scheme **44**). The coupling between iodomethyloxazole **166** and aldehyde **165** provided the required alcohol product **167** in 73% yield.[70] In this case, the zinc was activated with 1,2-dibromoethane, trimethylsilyl chloride and the Lewis acid boron trifluoride diethyletherate. In addition, it was established that the iodomethyloxazole was essential for reactivity; a result notably in contrast to the successful bromomethyloxazole method developed by Helquist.

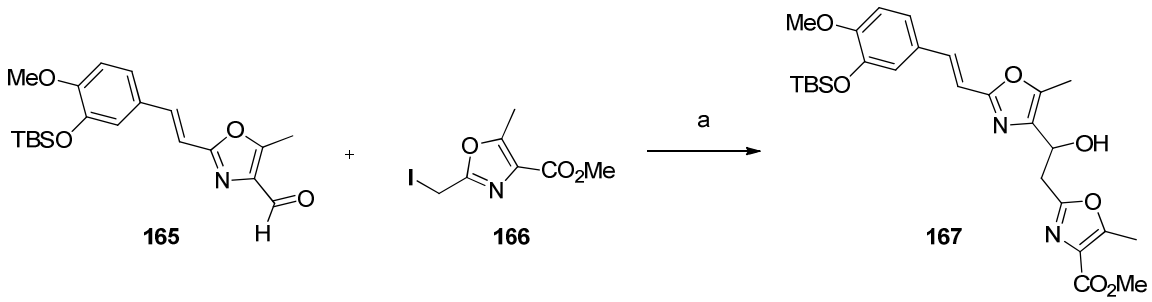


**Scheme 44**

(a) Zn, 1,2-dibromoethane, $Me_3SiCl$, $BF_3$•$OEt_2$, 73%.

## 2.5.2 Oxazole Samarium Barbier-type coupling

The importance of samarium diiodide in organic synthesis was highlighted by Kagan and it is now a widely used reagent for a number of transformations.[71] Kagan demonstrated its use in deoxygenation reactions, reductions of double bonds, reduction of halides and tosylates, as well as alkylations of ketones by organic halides or organic sulfonates.[71] $SmI_2$ has proven to be superior to other metals commonly used in the Barbier reaction, by promoting otherwise sluggish reactions. For example, in Williams and co workers' synthesis of phorboxazole A (scheme **45**), the organozinc oxazole derivative of iodomethyloxazole **169** was found to have long reaction times when coupling to aldehyde **168** and only low yields of the alcohol

product **170** were obtained. However, when $SmI_2$ was utilised, extremely rapid reaction times and excellent yields of up to 92% were observed.[72]

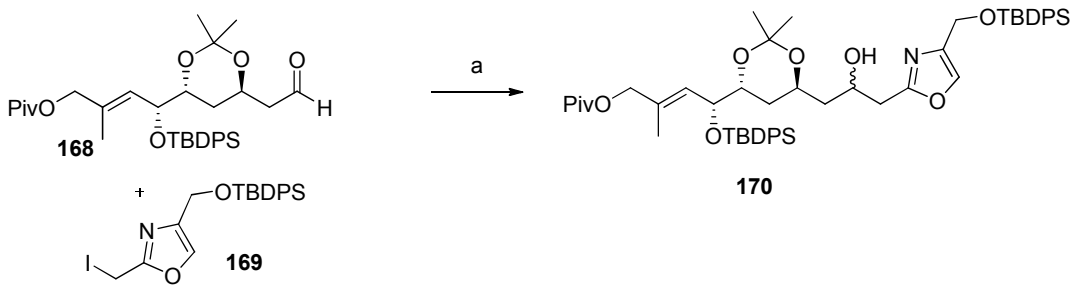


**Scheme 45: Sm Barbier reaction towards the synthesis of phorboxazole A**

(a) $SmI_2$, THF, rt, 92% (1:1 dr) from preceding alcohol.

Following on from the total synthesis of phorboxazole A, the Williams group further investigated the scope of the samarium Barbier reaction with iodomethyloxazoles, benzoxazoles and thiazoles with aliphatic aldehydes.[47] The studies with 2,4-substituted oxazoles **171** are highlighted in table **5**. It was found that aromatic aldehydes could not be used in this reaction, as they gave rise to competing pinacol coupled products. However, 3-phenylpropanal and 3-(benzyloxy)propanal generated the desired alcohol products **172** in moderate yields (table **5**, entries 1 and 2). Isobutyraldehyde provided the most successful results in the samarium-mediated Barbier coupling, generating the alcohol product in 98% yield (table **5**, entry 3). Conversely, α-benzyloxyacetaldehyde showed diminished yields of only 40% (table **5**, entry 4), owing to competing side reactions, including carbonyl reduction and reductive elimination.

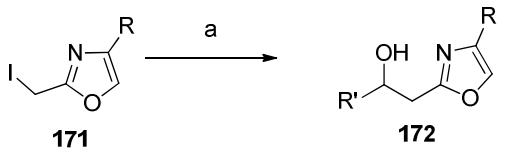


**171** **172**

(a) $SmI_2$, aldehyde, THF, rt.

**Table 5: Scope of $SmI_2$ Barbier reaction**

| Entry | Oxazole | Aldehyde | Product | Yield (%) |
|---|---|---|---|---|
| 1 | 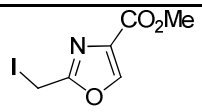 | 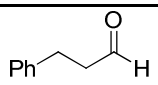 | 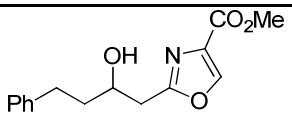 | 60 |
| 2 | 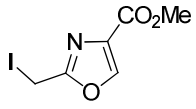 | 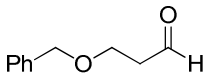 | 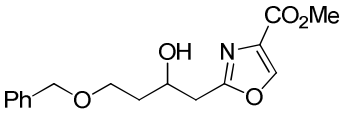 | 55 |
| 3 | 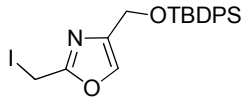 | 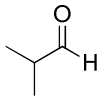 | 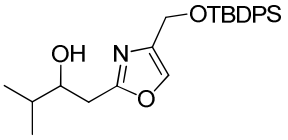 | 98 |
| 4 | 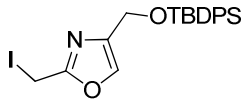 | 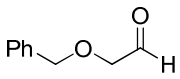 | 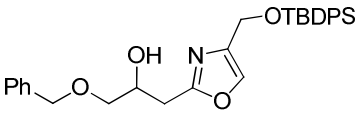 | 40 |

In contrast to Schlessinger's synthesis of virginiamycin $M_2$ which utilised a zinc Barbier reaction,[69] Panek *et al.* opted for a samarium based approach and the Barbier reaction was used to close the macrocyclic ring (scheme **46**).[73] Interestingly, when THF was used as the solvent, low yields of the macrocycle **173** were obtained (~10%); however, the yield was increased to 42% when the reaction was carried out in benzene. Benzene was required as the solvent to limit a competitive dehalogenation, which occurred when the oxazole benzylic radical abstracted a hydrogen from THF, which in turn prevented the formation of the organosamarium intermediate. It is also noteworthy, that in this case, the chloromethyloxazole and iodomethyloxazole demonstrated similar reactivities, providing the macrocycle **174** in comparable yields of 40 and 42% respectively.

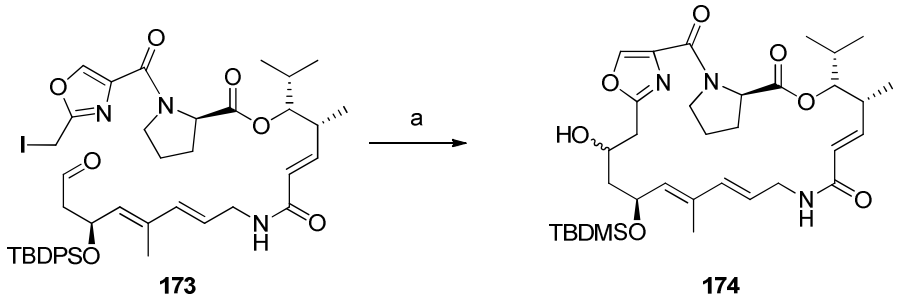


**173** **174**

**Scheme 46: Intramolecular Sm Barbier reaction**

(a) $SmI_2$, benzene, 42%.

## 2.5.3 Use of Other Metals in Oxazole Centred Barbier Reactions

Other metals have also been used in studies towards the synthesis of oxazole-containing natural products. For example, Uguen's synthesis of virginiamycin $M_2$ featured a building block similar to the one utilised by Panek (scheme **46**); however, in this case the macrocycle was constructed using a Takai coupling, which generated an organochromium species *in situ* using $LiAlH_4$ and $CrCl_3$.[74] This reaction was not as successful as Panek's samarium-mediated coupling and afforded the macrocycle in 23% yield. It was postulated that the low yield could be due to restricted rotation around the peptide bond, resulting in an unfavourable conformation for the organochromium and aldehyde to react.

After considerable experimentation, the Smith group found a Grignard exchange reaction most successful towards their synthesis of (+)-phorboxazole A (scheme **47**).[75] This reaction presumably occurred through a Grignard exchange of the bromomethyloxazole, to generate the metallooxazole, which in turn attacked the lactone **175**, to generate the alcohol **176** as a single stereoisomer. This stereoselectivity was thought to be due to the anomeric effect.

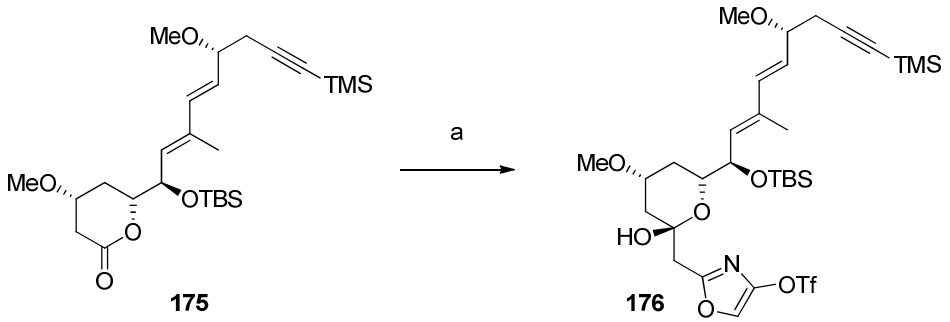


**Scheme 47**

(a) 2-(bromomethyl)oxazol-4-yl trifluoromethanesulfonate, $^{i}$PrMgCl, −78 to −15 ºC, 76%.

## 2.5.4 Route A: Attempted Synthesis of C(1)-C(9) fragment

Based on the review of the literature regarding halomethyloxazole Barbier reactions, zinc and samarium Barbier conditions were attempted, in order to develop a route towards the C(1)-C(9) fragment of disorazole $C_1$. Model studies were performed using commercially available crotonaldehyde (**31**), which was deemed a suitable substitute for the unstable and volatile C(6)-C(9) aldehyde **140**.

The simple zinc Barbier conditions developed by Helquist *et al.*[67] were applied to the model system, but unfortunately their successes could not be repeated. The chloromethyloxazole **139a** appeared to be less reactive than the bromomethyloxazole **139b**, yet both reactions with HCl-activated zinc (table **6**, entries 1 and 2) generated the methyl oxazole **128**. In 3 hours 12% of the chloromethyloxazole **139a** had been

converted to the methyloxazole **128**, compared to the majority of the bromomethyloxazole **139b** being converted to the methyloxazole **128** in the same amount of time. In addition, traces of the desired product **177** could be seen in the NMR spectrum of the bromomethyloxazole crude reaction mixture. The use of diethylaluminium chloride[69] as an activating agent (table **6**, entry 3), again resulted in the majority of the bromomethyloxazole **139b** being converted to the methyloxazole **128**, with traces of starting material and product visible in the NMR spectrum. No reaction was observed when the zinc Barbier reaction was carried out in the presence of ammonium chloride[76] (table **6**, entry 4). Submitting the HCl-activated zinc and bromomethyloxazole **139b** to ultrasonic vibration prior to the addition of aldehyde **31** and leaving the reaction for an extended time of 40 hours, also resulted in conversion to the methyloxazole **128** (table **6**, entry 5). The conversion to the methyloxazole suggests that the bromozinc species was formed, but was subsequently reduced after picking up a proton, perhaps from residual water in the reaction mixture.

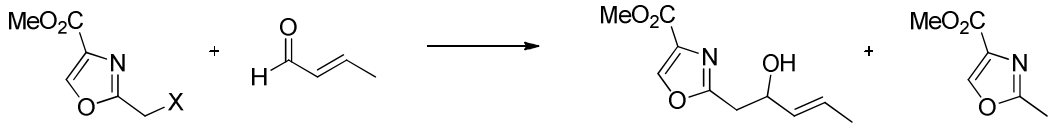


**139** **31** **177** **128**

**Table 6: Attempted Barbier reactions**

| Entry | X | Conditions | 139[a] (%) | 177[a] (%) | 128[a] (%) |
|---|---|---|---|---|---|
| 1 | Cl **139a** | HCl activated Zn (1.5 equiv), THF, 0 ˚C, 3 h | 88 | 0 | 12 |
| 2 | Br **139b** | HCl activated Zn (1.5 equiv), THF, 0 ˚C, 3 h | trace | trace | 99 |
| 3 | Br **139b** | Zn (2.4 equiv), $Et_2AlCl_3$ (1 equiv) THF, 30 ˚C, 1 h | trace | trace | 99 |
| 4 | Br **139b** | Zn, aq $NH_4Cl$:THF (1:1), rt, 18 h | 100 | 0 | 0 |
| 5 | Br **139b** | HCl activated Zn (1.5 equiv), sonication, THF, rt, 40 h | 48 | 0 | 52 |
| 6 | I **139c** | $SmI_2$ (2.5 equiv), THF, rt, 30 min | 100 | 0 | 0 |

[a] NMR analysis of reaction mixture.

Williams' samarium Barbier conditions[47] were also attempted, this time utilising the iodomethyloxazole **139c**, but again, no desired alcohol product **177** could be isolated (table **6**, entry 6). The samarium diiodide was successfully formed after sonication of samarium metal and iodine in THF, in the absence of light. The formation was confirmed by the colour change of the mixture from orange to the dark blue of the Sm(II). Following the literature precedent, it is unknown why the reaction between the halomethyloxazoles **139** and crotonaldehyde failed, especially when taking into consideration that in Helquist's investigations, 3-methylcrotonaldehyde afforded the alcohol product in 62% yield (table **4**, entry 4). The difficulties could have been due to the known air and moisture sensitivities of metal-halogen species; especially the $SmI_2$. In addition, previous publications have reported difficulties in reproducing or adapting known Barbier reactions.[47]

After unsuccessful attempts at applying the common methods of Barbier reactions for halomethyloxazoles, new reagents and methods were sought. The halomethyl group can be considered as a heteroaromatic benzylic moiety, therefore more general reagents to activate benzylic halides were investigated. The Knochel group are currently at the forefront of organometallic research and recent publications[77,78,79] appeared to be applicable to the oxazole coupling. It is reported that LiCl facilitates the insertion of zinc into the carbon-chlorine bond; a particularly interesting example featured the coupling of ethyl 3-(chloromethyl)benzoate **178** and 4-bromobenzaldehyde to generate the secondary alcohol **179** in 91% yield (scheme **48**).[78] Accordingly, these conditions were applied to the chloro- and bromomethyloxazoles (**139a** and **b**) and crotonaldehyde (**31**) model system (scheme **48**); but unfortunately, no reaction was observed. Again, the problems could have arisen in the metal activation step; 1,2-dibromoethane and TMSCl were used as activating reagents, and consequently it is possible that acidic impurities in the TMSCl could have quenched the organometallic species. However, after premixing the TMSCl with triethylamine to eliminate acidic impurities, none of the desired alcohol **177** could be identified by NMR spectroscopy and in fact, formation of methyloxazole **128** was now observed.

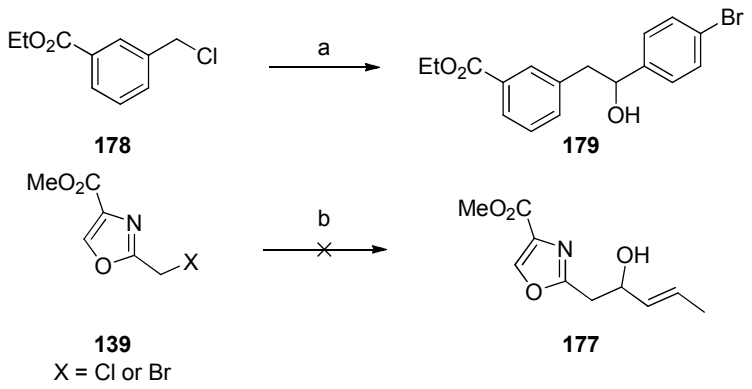


**Scheme 48: Lithium/zinc halogen exchange**

(a) i. LiCl, Zn; ii. 4-bromobenzaldehyde, THF, 0 ºC to rt, 4 h, 91%;[78](b) i. LiCl, Zn; ii. crotonaldehyde, THF, 0 ºC to rt, 2 h.

A subsequent publication by the Knochel group reported an improved formation of benzylic zinc chlorides.[79] This reaction is promoted by a rapid formation of a magnesium chloride species, followed by *in situ* transmetallation with zinc chloride, to generate the benzylic zinc chloride species. The zinc chloride species was successfully reacted with electrophiles, such as, acyl chlorides and aldehydes. For example, the reaction between chloride **180** and 4-bromobenzaldehyde as shown in scheme **49** generated the alcohol **181** in 82% yield. Once more, these conditions could not be transferred to our model system and no desired alcohol product **177** could be identified by TLC, or from the crude NMR spectrum. With this metallation approach proving to yield no results towards the desired product, attention was turned toward alternative routes including, a Fukuyama coupling and the aforementioned lateral lithiation approach.

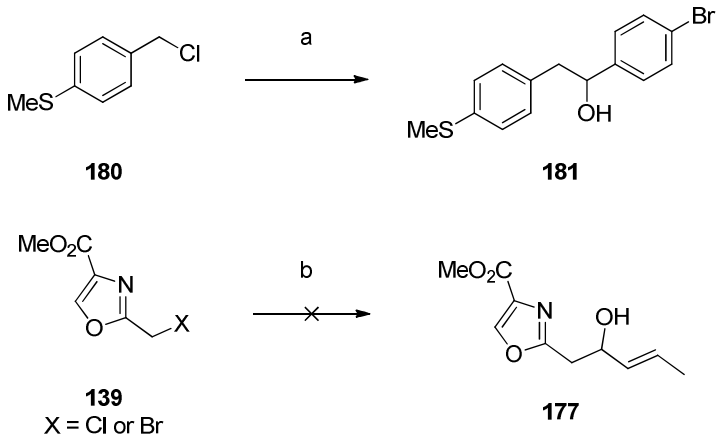


**Scheme 49: Mg/LiCl/$ZnCl_2$ halogen exchange**

(a) i. Mg, LiCl, THF, 1.5 h, 0 ºC to rt; ii. $ZnCl_2$; iii. 4-bromobenzaldehyde, THF, 2 h, 82 %;[79](b) i. Mg, LiCl, THF, 2.5 h, 0 ºC to rt; ii. $ZnCl_2$; iii. crotonaldehyde, THF, 2 h.

## 2.5.5 Fukuyama Coupling

An alternative line of investigation towards the C(1)-C(9) fragment of disorazole $C_1$ involved forming the ketone **183**, which could then be stereoselectively reduced to the required alcohol **163**. From the bromomethyloxazole **139b** and ester **161** it was envisaged that a Fukuyama coupling could be established. The Fukuyama coupling involves the formation of a bromo- or iodozinc species followed by a palladium catalysed reaction with a thioester.[80] The thioester **182** was effectively generated in a quantitative yield from the ethyl ester **161**, *via* a displacement with (ethylthio)trimethylsilane and aluminiumtrichloride.[81] The Fukuyama coupling failed when applied to the bromomethyl ester **139b** and enyne thioester **182** (scheme **50**), probably due to zinc activation issues, as previously discussed (section **2.5.4**). In addition, there is no record of this type of coupling with similar substrates in the literature; therefore, the failure of the reaction could have been due to poor reactivity of one, or both of the coupling partners. However, no further screening was performed to investigate the problematic substrates, as progress was being made through the lateral lithiation approach, which is to be discussed in the next section.

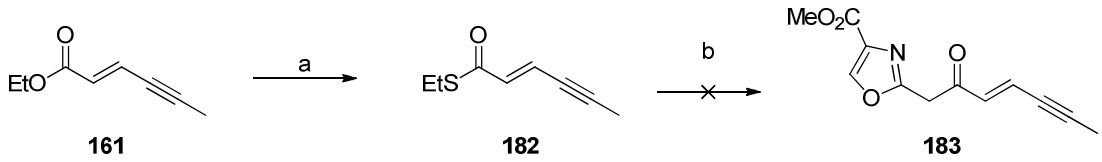


**161** **182** **183**

**Scheme 50: Attempted Fukuyama coupling**

(a) $Me_3SiSEt$, $AlCl_3$, THF, 70 ºC, 3 h, quant; (b) i. **139b**, Zn, THF, 70 ºC, 2 h; ii. $Pd(PPh_3)_2Cl_2$, **182**, THF, rt, 30 min.

## 2.6 Methyloxazole and Aldehyde Coupling - Route B

With established routes to the methyl oxazole **141** and aldehyde **140** it was believed that a lateral lithiation of the methyloxazole to generate the anion, followed by nucleophilic addition to the aldehyde would provide a highly convergent route towards the C(1)-C(9) fragment of disorazole $C_1$.

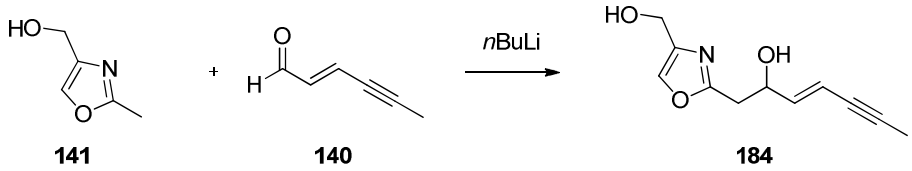


**141** **140** **184**

**Scheme 51: Proposed lithiation approach towards C(1)-C(9) fragment**

### 2.6.1 Oxazole Lateral Lithiation Background

One of the first examples of lateral lithiation on a 2-methyloxazole was published by Lipshutz.[82] Following lithiation of the trimethyloxazole **185** with LDA, the resulting lithium species was reacted with a variety of electrophiles, including ketones, epoxides, alkyl halides and, of particular interest towards our investigations, aldehydes were successfully coupled to provide secondary alcohols. An example of this is the reaction between the trimethyloxazole **185** and benzaldehyde (**186**) to afford the alcohol **187** in 89% yield (scheme **52**). Only lithiation at the C-2 methyl group was observed and, interestingly, when the first product (**187**) was subjected to a further lithiation, electrophilic addition once more occurred at the C-2 methyl position.

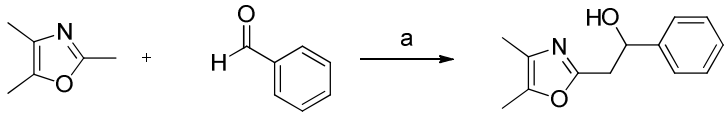


**185** **186** **187**

**Scheme 52: Lithiation of trimethyl oxazole**

(a) LDA, THF, –78 ºC, 89%.

The higher reactivity of C-2 methyl groups over the other positions of the oxazole can be attributed to the resonance stabilisation of the ionic intermediate, as shown in scheme **53**, where the negative charge can be delocalised into the C=N π system (**189**).[83]

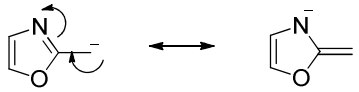


**188** **189**

**Scheme 53: Methyl oxazole resonance**

Although 2,4-substituted oxazoles are a common structural feature of natural products, it was not until 15 years after Lipshutz first published the lithiation of methyl oxazoles that this methodology was applied to natural product synthesis. Two examples of the application of lithiation of oxazoles to natural product synthesis are shown in scheme **54**. During the synthesis of phenoxan, Peña's group observed a selective alkylation with allyl bromide **190** at the C-2 methyl of (2-methyl-1,3-oxazol-4-yl)methanol (**141**) using LDA, thereby generating the oxazole **191** in 50% yield.[84] Pattenden's synthesis of virginiamycin also centres around the (2-methyl-1,3-oxazol-4-yl)methanol (**141**) and featured a deprotonation with *n*BuLi, followed by nucleophilic attack of the resulting anion on to the aldehyde **192**.[85] The desired alcohol **193** was obtained in a 34% yield.

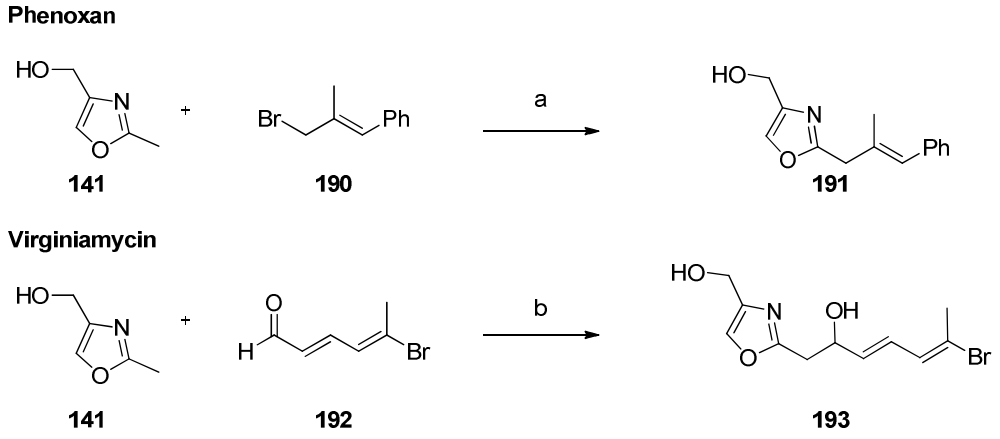


**141** **190** **191**

**141** **192** **193**

**Scheme 54: (2-Methyl-1,3-oxazol-4-yl)methanol lithiation examples in natural product synthesis**

(a) i. LDA (2 equiv), THF; ii. **190**, 50%; (b) i. *n*BuLi (2 equiv), THF; ii. **192**, 34%.

### 2.6.2 Results: Initial Investigation into (2-Methyl-1,3-oxazol-4-yl)methanol Lithiation

Encouraged by the regioselectivity demonstrated by Peña and Pattenden's lithiations of (2-methyl-1,3-oxazol-4-yl)methanol, lithiations with *n*BuLi and LDA formed the starting point for our investigations towards the synthesis of the C(1)-C(9) fragment of disorazole $C_1$ (table **7**). Once again, the crotonaldehyde model system was applied to initial studies, with the intention of optimising and developing the reaction conditions in preparation for application to the enyne aldehyde **140**. When oxazole **141** was treated with *n*BuLi at −78 °C, followed by addition of crotonaldehyde (**32**), two products were observed (table **7**, entry 1). An inseparable mixture (~1.5:1 **194**:**195**) of the desired alcohol **194** and the alcohol **195** was obtained, where deprotonation had occurred at the C-5 position. The identity of the by-product **195** was determined from the NMR spectrum by the disappearance of the C-5 oxazole proton and the continued presence of the C-2 methyl group. Contrary to Peña's group's reports that a selective lithiation occurs with LDA, a ~1:1.7 mixture of desired product **194** and by-product **195** was observed when deprotonation with LDA was applied to the crotonaldehyde model system (table **7**, entry 2).

The unexpected formation of the by-product (**195**) led to further investigations into the lithiation reaction and a range of bases were screened as highlighted in table **7**. Hamana and Sugasawa demonstrated the use of 9-BBN triflate and diisopropylethylamine to selectively deprotonate 2-methyl-4-phenyl-1,3-oxazole at the C-2 methyl group, and upon reaction with benzaldehyde they successfully generated the alcohol product in 70% yield.[86] Unfortunately, when the reported conditions were applied to our model system, no alcohol product could be identified by NMR spectroscopy (table **7**, entry 3). It should be noted that Hamana and Sugasawa only observed reactions with benzaldehyde derivatives and attempts to apply these conditions to aliphatic aldehydes and ketones failed. Deprotonation with LHMDS also failed to provide any of the desired alcohol **194** (table **7**, entry 4). Conditions developed by the Evans group involving *n*BuLi and diethylamine[87] provided the most promising results, whereby no by-product **195** was observed, but unfortunately only 44% of the oxazole starting material **141** was converted into the

desired product **194** (table **7**, entry 5). Inspired by these promising results and with the knowledge that the base can affect the regioselectivity of the reaction, the use of sparteine as a chiral directing agent, as well as an additive base was investigated (table **7**, entry 5). Unfortunately, this reaction did not proceed to completion and in addition, the reaction was not regioselective, with 26% desired product (**194**) and 21% by-product (**195**) observed in the crude NMR spectrum.

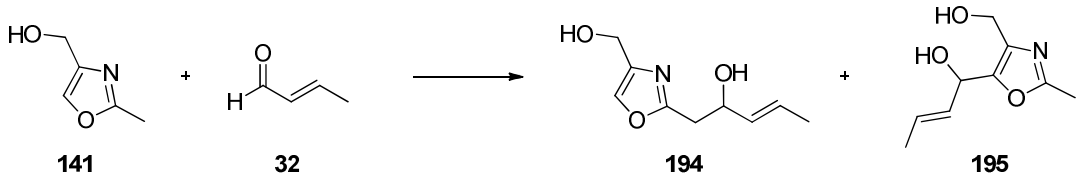


**141** **32** **194** **195**

**Table 7: Initial investigations into lithiation of (2-methyl-1,3-oxazol-4-yl)methanol**

| Entry | Base (equiv.) | Aldehyde equiv. | Amine (equiv.) | Time (h) | 141 (%)[a] | 194 (%)[a] | 195 (%)[a] |
|---|---|---|---|---|---|---|---|
| 1 | *n*BuLi (2) | 1 | | 1.5 | 8 | 57 | 35 |
| 2 | LDA (2.1) | 1 | | 1 | 3 | 36 | 64 |
| 3 | 9-BBN triflate (1) | 1 | $^{i}$PrNEt(1.2) | 18 | 100 | 0 | 0 |
| 4 | LHMDS (2) | 1.1 | | 2 | 100 | 0 | 0 |
| 5 | *n*BuLi (2) | 1.2 | $NHEt_2$ (3) | 0.75 | 56 | 44 | 0 |
| 6 | *n*BuLi (5) | 2 | sparteine (6) | 0.75 | 53 | 26 | 21 |

[a] NMR analysis of crude reaction mixture after work up

## 2.6.3 Evans Group Investigation into Base Effect

The influence of diethylamine on the regioselectivity of the lithiation of methyloxazoles was discovered by the Evans group, through the development of routes towards the total synthesis of the phorboxazoles.[87] Table **8** highlights some of the results obtained by the Evans group that are relevant to our studies and understanding of the mechanism of this reaction. The initial studies featured a range of functional groups at the C-4 position of oxazole and of particular interest were the investigations with (2-methyl-1,3-oxazol-4-yl)methanol (table **8**, entries 1-3). These results are comparable to the results obtained in our crotonaldehyde model system; that is, approximately 50:50 ratio of product and by-product when *n*BuLi or LDA are utilised, but regioselectivity is observed when lithium diethylamine is employed as the base. Two equivalents of *n*BuLi were required for this reaction, as the alcohol proton is first removed, followed by deprotonation of the C-2 methyl group. A

greater excess of diethylamine was also required for reactions with (2-methyl-1,3-oxazol-4-yl)methanol compared to other C-4 substituents, where there was no free alcohol present.

More detailed mechanistic investigations were carried out by the Evans group with a methyloxazole featuring an (*E*)-alkene side chain (**196**), as a model study towards the synthesis of the phorboxazoles.[87] It was found that increasing the temperature of the reaction from −78 to −50 ºC favoured the formation of the desired C-2 methyl substituted product **197**. This effect was more pronounced when the amine base used was diisopropylamine, rather than TMP (table **8**, entry 8). Furthermore, regioselectivity could be achieved with diisopropylamine by increasing the reaction time to 60 minutes, as well as performing the reaction at −50 ºC (table **8**, entry 9). Interestingly, when the temperature of the *n*BuLi mediated reaction was increased to −50 ºC, the ratio of product **197** to by-product **198** was not significantly affected, but a small amount of decomposition was observed (table **8**, entry 10). It is also noteworthy to mention that the Evans group experienced incomplete consumption of starting materials; however most reactions proceeded with ≥93% conversion.

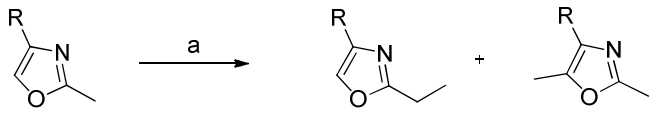


**197** **198**

(a) i. see table, THF (amine); ii. MeOTf.

**Table 8: Evans investigation into base effect on lithiation regioselectivity**

| Entry | R | Base | Amine | Temp (ºC) | Time (min) | **197**: **198** |
|---|---|---|---|---|---|---|
| 1 | $CH_2OH$ (**141**) | *n*BuLi | | −78 | 20 | 55:45 |
| 2 | | LDA | | −78 | 20 | 50:50 |
| 3 | | $LiNEt_2$ | | −78 | 20 | >95:5 |
| 4 | 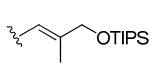 (**196**) | *n*BuLi | | −78 | 20 | 61:39 |
| 5 | | *n*BuLi | $Et_2NH$ | −78 | 10 | >95:5 |
| 6 | | *n*BuLi | $^iPr_2NH$ | −78 | 10 | 66:34 |
| 7 | | *n*BuLi | TMP | −78 | 10 | 64:36 |
| 8 | | *n*BuLi | $^iPr_2NH$ | −50 | 10 | 82:18 |
| 9 | | *n*BuLi | $^iPr_2NH$ | −50 | 60 | >95:5 |
| 10 | | *n*BuLi | | −50 | 60 | 55:45 |

## 2.6.4 Proposed Lithiation Mechanism

Based on the experimental results obtained by the Evans group, a mechanism for the lithiation reaction has been proposed. As increasing the temperature of *n*BuLi reaction had no effect on the ratio of the products, it can be assumed that during this reaction a kinetic mixture of the products **197** and **198** is formed and there is no interconversion between the two lithiated species **205** and **206** (scheme **56**). After a series of crossover experiments at −78 ºC (scheme **55**), Knaus and Meyers also drew the conclusion that lithiated 2,4-dimethylthiazole does not interconvert between the two lithium intermediates **199** and **202**.[88] For example, when the lithiated methylthiazole **199** was exposed to 2-methyl-4-phenylthiazole **200**, followed by quenching with iodomethane, only the ethylthiazole **201** was isolated. The corresponding experiment where the C-5 lithiated species **202** was exposed to 2,4-dimethylthiazole **203**, followed by quenching with iodomethane resulted in only the trisubstituted thiazole **204**. This suggests that no lithium-proton exchange takes place at −78 ºC, as there was no evidence of the crossover products. Knaus and Meyers have suggested that at −78 ºC the kinetic acidities of the C-2 methyl proton and the C-5 proton are similar. However, a +I effect (for example $CH_2OH$ or methyl) can increase the electron density at C-5, making the proton less acidic and therefore, the C-2 methyl proton is more likely to be removed by a base. This idea is reflected in the observed results obtained by Evans, where the 55:45 ratio of product **197** to by-product **198** slightly favours 2-methyl lithiation when *n*BuLi is used as a base.

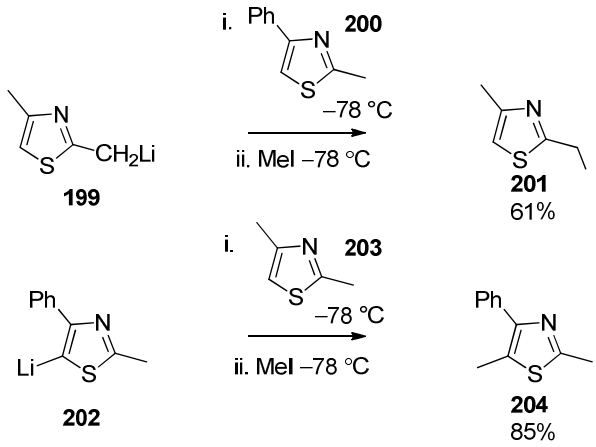


**Scheme 55: Meyers methylthiazole crossover experiments**

Evans *et al.* have proposed that once an amine is introduced into the lithiation reaction, interconversion between the lithiated regioisomers (**205** and **206**) can occur *via* a reversible pathway, which is now available (scheme **56**). *Via* this pathway, the 5-lithiated species **206** converts to the more thermodynamically stable 2-methyl lithiated species **205**, which goes on to react with the electrophile, therefore providing the ethyl oxazole **197** as the major product. Evidence of the two lithiated intermediates (**205** and **206**) and their equilibration to C-2 methyl intermediate **205** has been observed by NMR experiments.[87] It can be observed from the results in table **8** that the steric bulk of the amine affects the kinetics of this equilibrium, with diethylamine proving to be the quickest and TMP the slowest. Moreover, increasing the reaction time gave a longer duration for interconversion to the more thermodynamically stable product **205**. Based on these findings, it was suggested that the regioselectivity encountered when $LiNEt_2$ was used as a base resulted from the equilibrium promoted by diethylamine liberated *in situ* from the lithium base.

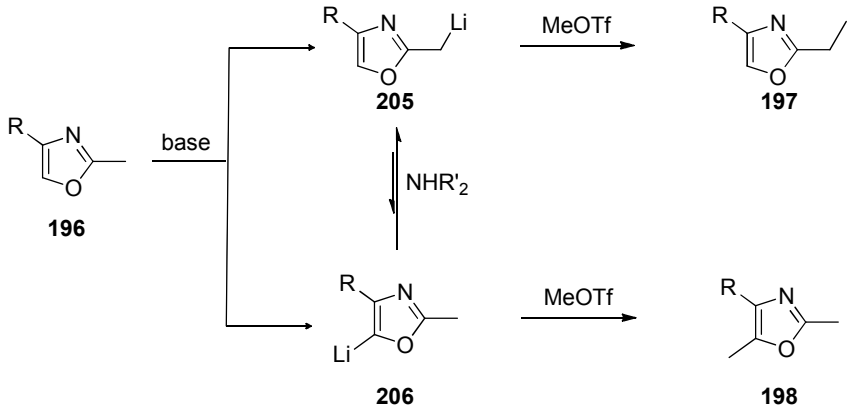


**Scheme 56: Evans proposed oxazole lithiation mechanism**

Encouraged by the results obtained while working with the Evans group, Smith went on to further investigate the factors controlling this equilibrium pathway in detail.[89] It was established that other lithium dialkylamides facilitate the equilibrium between the two lithiated oxazole species. The effectiveness of the lithium base centres on the $pK_a$ of the conjugate acid lying between the $pK_a$s of the C-5 ring proton and the C-2 methyl proton. When the base satisfies this $pK_a$ condition, the conjugate acid of the lithium amide base can act as a proton shuttle between the two lithiated oxazole species. The base investigation was performed on the phenylmethyloxazole **207** and table **9** highlights the lithium amide bases that were screened, in increasing order of size. As $pK_a$ and amine size parallel each other, an increase in $pK_a$ can also be assumed on descending the table. Excellent regioselectivity and good conversion was observed for LiNEtMe, $LiNEt_2$, $LiN^iPr_2$ and $LiNEt^iPr$ (table **9**, entries 2-5). Therefore, it can be assumed that these bases are an appropriate size and posses the correct $pK_a$ range to initiate the equilibrium pathway between the lithio-intermediates. Conversely, regioselectivity and conversion declined when the stronger and larger bases $LiN^nBu_2$ and $LiN^iPr_2$ were employed (table **9**, entries 6 and 7); furthermore, dialkylation was also observed. $LiN(SiMe_3)_2$ demonstrated high regioselectivity (table **9**, entry 1), but only moderate conversion was observed and significant amounts of double alkylated products were detected; a result that could possibly be ascribed to the lower basicity of this lithium amide.

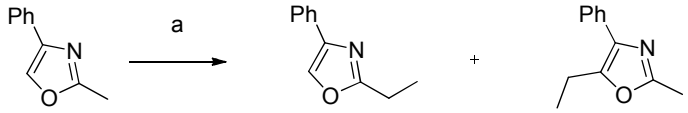


**207** **208** **209**

(a) i. base, THF, −78 ºC, 30 min; ii. MeI, −78 ºC, 3 h.

**Table 9: Smith further investigation into the effect of base on the lithiation reaction**

| Entry | Base | $pK_a$ of conjugate acid | 208:209 | Conversion (%) |
|---|---|---|---|---|
| 1 | $LiN(SiMe_3)_2$ | 29.5 | 95:5 | 59 |
| 2 | LiNEtMe | 30.9 | >99:1 | >99 |
| 3 | $LiNEt_2$ | 31.7 | >99:1 | 89 |
| 4 | $LiN^nPr_2$ | | >99:1 | 97 |
| 5 | $LiNEt^iPr$ | | 99:1 | 79 |
| 6 | $LiN^nBu_2$ | | 53:47 | 67 |
| 7 | $LiN^iPr_2$ | 34.4 | 23:77 | 72 |

Another factor that could influence the regioselectivity of this reaction is the nature of the electrophile. Smith's group found that as the reactivity of the electrophile decreased, there was in increase in regioselectivity towards the C-2 methyl product **210** (table **10**).[89] However, this trend was only apparent when *n*BuLi or LDA was used as the base. Consistent with previous results, high regioselectivity for the C-2 methyl product **210** was observed with all electrophiles when $LiNEt_2$ was used as the base.

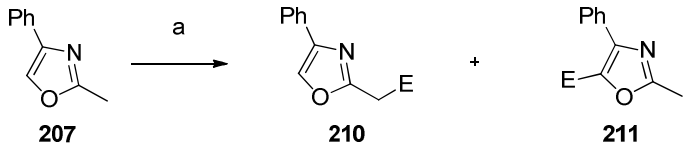


**207** **210** **211**

(a) i. base, THF, −78 ºC, 30 min; ii. Electrophile, −78 ºC, 3 h.

**Table 10: Smith investigation into the effect of electrophiles with methyloxazole**

| | | ***n*BuLi** | | **LiN$^i$Pr$_2$** | | **LiNEt$_2$** | |
|---|---|---|---|---|---|---|---|
| **Entry** | **Electrophile** | **(210:211)** | **Conversion (%)** | **(210:211)** | **Conversion (%)** | **(210:211)** | **Conversion (%)** |
| 1 | benzaldehyde | <1:99 | >99 | <1:99 | >99 | 98:2 | 86 |
| 2 | TMSCl | 4:96 | 97 | 1:99 | 78 | >99:1 | 92 |
| 3 | MeOTf | 9:91 | ≥90 | 9:91 | ≥90 | 99:1 | ≥90 |
| 4 | MeI | 14:86 | 83 | 37:63 | 78 | 99:1 | 89 |
| 5 | acetone | 20:80 | 78 | 58:42 | 61 | 96:4 | 88 |

The differences in product ratio and conversion rate on descending table **10** has been attributed to a difference in nucleophilicity of the two lithium intermediates (**205** and **206**) resulting in different rates of reaction with the electrophiles. A reactive electrophile such as benzaldehyde (table **10**, entry 1) will result in a product ratio reflecting the kinetic ratio of the lithio-intermediates. However, if a less reactive electrophile such as acetone (table **10**, entry 5) is used the more nucleophilic C-2 methyl anion reacts preferentially and this is reflected in the observed product ratio. A decrease in starting material conversion is also observed as electrophilicity decreases.

## 2.6.5 Results: Base Optimisation

With the *n*BuLi and diethylamine reaction being the only conditions to promote a C-2 methyl regioselective lithiation onto oxazole **141**, attempts were made to optimise the reaction and to facilitate consumption of the oxazole starting material **141**. It was found that increasing the reaction time from 45 minutes to one hour had little effect on the outcome of the reaction. It could even be considered to be detrimental, with a 37% conversion to the desired product **194** in one hour, compared to a 44% conversion observed in the 45 minute reaction (table **11**, entry 1 and table **7**, entry 5). In addition, increasing the quantity of *n*BuLi did not seem to affect the product (**194**) to starting material (**141**) ratio; 82-84% conversion was observed when the molar ratio of *n*BuLi was increased from 2.8 to 5 equivalents (table **11**, entries, 2-4). Interestingly, it was the increase in quantity of diethylamine (from 3.3 equivalents to 6 equivalents) that had the greatest influence on the conversion of starting material to product, with this modification to the reaction conditions providing an 85% yield of alcohol **194** (table **11**, entry 3). However, this could not be improved upon, and increasing the excess of crotonaldehyde to 3 equivalents resulted in a slightly diminished yield and the appearance of the unwanted by-product **195** (table **11**, entry 5).

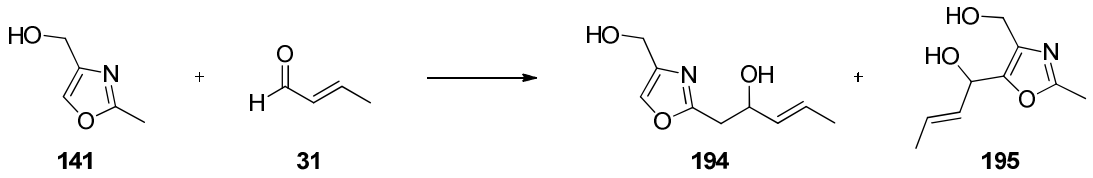


**141** **31** **194** **195**

**Table 11: Optimisation of $NHEt_2$ promoted lithiation**

| Entry | Base (equiv.) | Aldehyde equiv. | $NHEt_2$ (equiv.) | Time (h) | 141 (%)[a] | 194 (%)[a] | 195 (%)[a] |
|---|---|---|---|---|---|---|---|
| 1 | *n*BuLi (2.2) | 2 | 3.3 | 1 | 63 | 37 | 0 |
| 2 | *n*BuLi (2.8) | 2 | 6 | 0.5 | 18 | 82 | 0 |
| 3 | *n*BuLi (4) | 2 | 6 | 0.5 | 14 | 86 | 0 |
| 4 | *n*BuLi (5) | 2 | 6 | 0.75 | 16 | 84 | 0 |
| 5 | *n*BuLi (4) | 3 | 6 | 0.5 | 14 | 78 | 8 |

[a] NMR analysis of crude reaction mixture after work up

## 2.6.6 Alcohol Protecting Group Effect

The best results obtained from the model studies with (2-methyl-1,3-oxazol-4-yl)methanol (**141**) and crotonaldehyde (**32**) are comparable with those published by Evans,[87] whereby excellent C-2 methyl regioselectivity was achieved. However, the reaction did not proceed to completion; this is also consistent with literature reports. Unfortunately, a further problem became apparent in that, in this case, the product **195** could not be separated from the unreacted starting material **141**, despite numerous attempts at optimising solvent conditions for column chromatography. Based on the proposed mechanism by Evans and Smith,[87] we wanted to investigate the effect of protecting groups on the alcohol, specifically to see if larger groups might block lithiation at the C-5 position. In addition, it was envisaged that a protecting group could aid the purification step of separating product from unreacted starting material. A range of different sized protecting groups and groups containing different functionalities were investigated. As shown in scheme **57**, TBDMS, MOM and SEM ethers (**212a-c**) were readily synthesised in good yields.

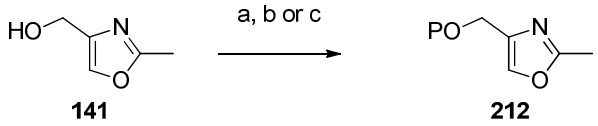


**141** **212**

**Scheme 57**

P = TBDMS **212a** (a) TBDMSOTf, 2,6-lutidine, DCM, 0 ºC, 1 h, 89 %; P = SEM **212b** (b) i. NaH; ii. SEMCl, THF, 0 ºC to rt, 3 h, 68 %; P = MOM **212c** (c) i. NaH; ii. MOMCl, THF, 0 ºC to rt, 3 h, 73 %.

The protected alcohol oxazoles **212** were subjected to the optimised conditions for the oxazole lithiation with crotonaldehyde (**32**), however, fewer equivalents of *n*BuLi (two rather than four) were required as initial deprotonation of the alcohol did not have to be considered in these reactions. Highly interesting was the reaction with the TBDMS protected oxazole **212a**, as no reaction was observed over several attempts (table **12**, entry 2). This could have been because the TBDMS group is sterically bulky and may be hindering access of the *n*BuLi to the C-5 proton. Therefore, the C-

5 lithio-species is not generated and the diethylamine cannot act as a proton shuttle to convert to the C-2 methyl lithiated intermediate.

Pleasingly, the reactions with the SEM (**212b**) and MOM (**212c**) protected oxazoles were highly regioselective, with no addition at C-5 observed. Also, the reactions showed a greater conversion of starting material **212** to product **213** than the corresponding free alcohol (table **12**, entries 3 and 4). These protecting groups are longer chained and more flexible than the TBDMS group; it is therefore postulated that the *n*BuLi is required to first deprotonate at C-5 and subsequently the interconversion to the C-2 methyl lithio-species is facilitated by diethylamine. Unfortunately, the SEM protected product **213b** could not be separated from the unreacted oxazole starting material **212** by column chromatography. Nevertheless, the MOM protected oxazole **212c** demonstrated the highest conversion rate and separation of the desired product and starting material was possible. However, the purification process required the mixture to be passed through two silica gel columns, run at a slow rate with 2% methanol in DCM; even then there was some co-elution of the two components **212** and **213**. In the interest of maximising purity, these were discarded to give a satisfactory isolated yield of the desired product **213** (50%). To this end, a satisfactorily optimised lateral lithiation of methyloxazole had been established using a model system and this could now be applied to the synthesis of the C(1)-C(9) fragment of disorazole $C_1$.

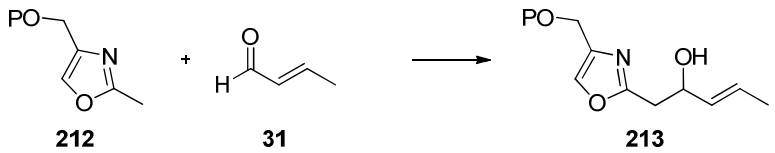


**212** **31** **213**

(a) i. *n*BuLi, THF, –78 C; ii. $NHEt_2$; iii. Crotonaldehyde.

**Table 12: Investigation into effect on alcohol protecting group**

| Entry | P | **212** (% by NMR) | **213** (% by NMR) | **213 isolated yield (%)** |
|---|---|---|---|---|
| 1 | H | 14 | 86 | |
| 2 | TBDMS | 100 | 0 | |
| 3 | SEM | 8 | 92 | |
| 4 | MOM | 4 | 96 | 50 |

## 2.7 Completion of the Racemic C(1)-C(9) Fragment of Disorazole $C_1$

With the required methyl oxazole **212c** and aldehyde **140** in hand, the optimised conditions for the lateral lithiation could be applied to these key substrates (scheme **58**). As with the model system, the coupling reaction did not proceed to completion, and unexpectedly, there was approximately 80% conversion of starting material **212c**, as determined by NMR spectroscopy which was less than that observed for the model system. This could have been due to the change of aldehyde; the enyne aldehyde **140** is volatile and unstable and the exact quantity added to the reaction was unknown, as it was used in crude form directly from the previous oxidation step. Nevertheless, alcohol product **214** was obtained in a 40% yield based on the starting material **212c** recovered from the silica column.

The final steps to the desired fragment involved sodium hydride-mediated *O*-methylation of **214** with iodomethane, which generated the methyl ether **215** in a low yield of 29%. This was followed by deprotection of the MOM group under acidic conditions and finally, Dess-Martin oxidation[90] of the resulting primary alcohol to the aldehyde **(±)-131** in 43% yield. Some of these reactions were low yielding; however, no attempt was made to optimise these steps as alternative routes towards the fragment synthesis were now being investigated. Overall, the desired C(1)-C(9) fragment of disorazole $C_1$ **(±)-131** was synthesised in a racemic manner, with the longest linear route being 9 steps and an overall yield of 1.6 %.

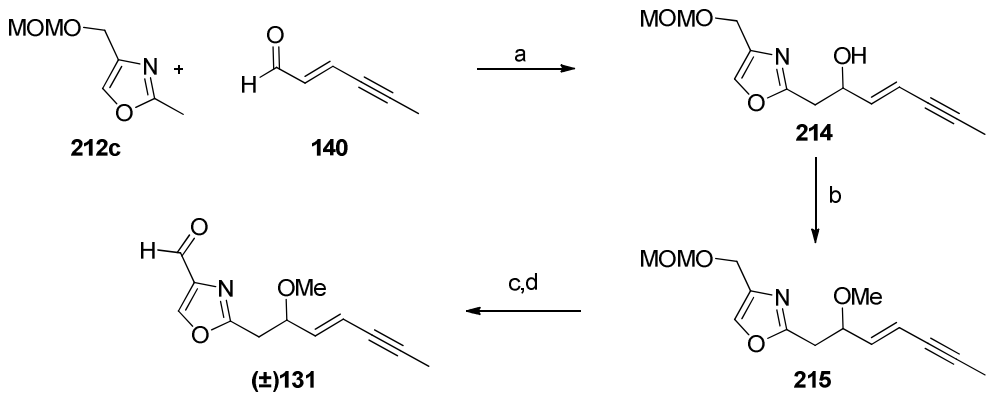


**Scheme 58: Completion of the racemic C(1)-C(9) fragment of disorazole $C_1$**

(a) i. *n*BuLi, THF, −78 ºC, 45 min; ii. $NHEt_2$, 45 min; iii. **140,** 45 min, 40%; (b) i. NaH, THF, 0 ºC; ii. MeI, 0 ºC to rt, 18 h, 29 %; (c) HCl, MeOH, rt, 18 h, 74%; (d) DMP, $NaHCO_3$, DCM, 0 ºC, 2 h, 43%.

## 2.8 Summary

Two routes towards the C(1)-C(9) fragment of disorazole $C_1$ have been attempted following a C(5)-C(6) disconnection. Zinc or samarium promoted metal-halogen exchange with halomethyloxazoles, followed by nucleophilic attack of crotonaldehyde proved to be unsuccessful. Investigations into lateral lithiation of (2-methyl-1,3-oxazol-4-yl)methanol provided some interesting results and changing the protecting group of the "benzylic" alcohol had an effect on the regioselectivity of the reaction and ease of purification of the product. Following optimisation of this route the coupling between the methyl oxazole and the enyne aldehyde was successfully completed, albeit in low yield. Consequently, the racemic synthesis of the C(1)-C(9) fragment was completed. It was initially anticipated that the desired enantiomer could be separated from the racemic mixture, for example using a lipase catalysed kinetic resolution. However, ultimately this lithiation route resulted in some low yielding steps and in order to complete the total synthesis of disorazole $C_1$ it was deemed not to be an optimum synthetic route. Alternative disconnections were therefore investigated which might allow greater flexibility for analogue synthesis and easier generation of the stereogenic centre.

# 3 Chapter 3: Enantiospecific Fragment Synthesis I

## 3.1 Adaptation of Previous Disorazole $C_1$ Syntheses

After the successful synthesis of the racemic fragment, focus was now towards an asymmetric synthesis that could provide rapid access to the C(1)-C(9) fragment and possibly be adapted towards heterocyclic analogues. Inspiration was drawn from the previous syntheses of disorazole $C_1$ and these routes will now be discussed.

### 3.1.1 Meyers Based Approach

After examining the other previous syntheses of disorazole $C_1$ (section **1.4**), it appeared that the Meyers synthesis,[25] featuring a condensation between the acid **26b** and serine methyl ester **216**, would be the shortest route and it could be adapted to provide the desired C(1)-C(9) fragment. There was also the added advantage that the required alcohol starting material **220** containing the stereogenic centre is commercially available. Another attractive feature of the Meyers based approach is that it could be adapted towards heterocyclic analogues, such as the triazole **217**, as highlighted by the retrosynthesis shown in scheme **59**. The triazole could be constructed from methyl propiolate **218** and the azide **219** *via* a copper catalyzed azide-alkyne cycloaddition (CuAAC) reaction. This route towards the triazole was investigated by the Hulme group; however, some difficulties were encountered and an improved route was later discovered which will be discussed in Chapter **4**.

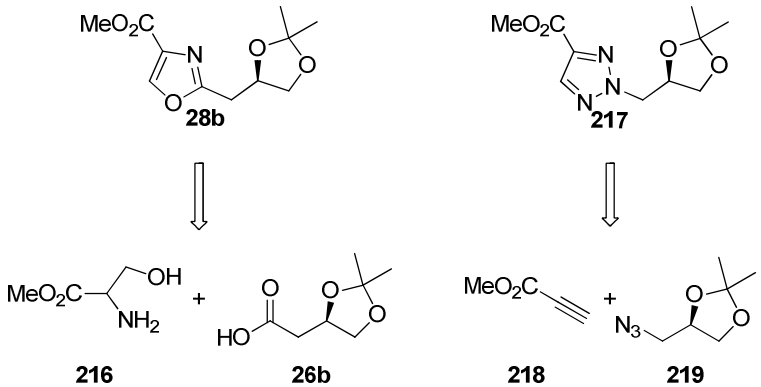


**Scheme 59: Meyers based retrosynthesis of oxazole and triazole analogue**

When the Meyers group commenced the total synthesis of disorazole $C_1$ the stereochemistry of the molecule had not been assigned. It was later confirmed[28] that that the Meyers group had synthesised the incorrect stereoisomer at the C(6) centre; this incorrect assignment therefore had to be taken into consideration when following this route.

Direct routes for the oxidation of the commercially available alcohol **220** to the carboxylic acid **26b** were investigated, as shown in table **13**. Oxidation with $NaIO_4/RuCl_3$ (table **13**, entry 1) resulted in loss of the acetonide group, which was unexpected, as oxidation under these conditions had successfully been performed on a molecule containing an acetonide group.[91] Oxidation with PDC[92] (table **13**, entry 2) resulted in complete conversion of the alcohol to the acid by NMR spectroscopy, however purification and isolation was difficult, resulting in a low isolated yield of the acid **26b**. A milder oxidation involving $TEMPO/NaClO_2/NaOCl$ (table **13**, entry 3) only resulted in 40% conversion of the alcohol **220** to the acid **26b**.[93] It was therefore decided to adopt a two-step oxidation of the alcohol **220** to the acid *via* the aldehyde **221**.

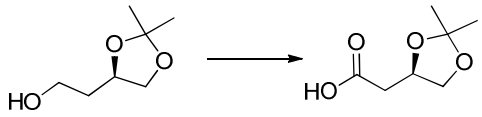


**220** **26b**

**Table 13: Attempted oxidation of alcohol to acid**

| Entry | Reagents | Result |
|---|---|---|
| 1 | $RuCl_3$, $NaIO_4$ | No desired product isolated, removal of acetonide observed |
| 2 | PDC | 100% conversion, but difficult isolation |
| 3 | TEMPO,$NaClO_2$, NaOCl | 40% conversion of alcohol to acid |

A Swern oxidation,[94] followed by oxidation with sodium chlorite and hydrogen peroxide[95] proved to be most successful, providing the acid **26b** in 76% yield over the two steps (scheme **60**). However, both the acid **26b** and aldehyde **221** were found to be unstable, and they were therefore used directly in subsequent steps without purification.

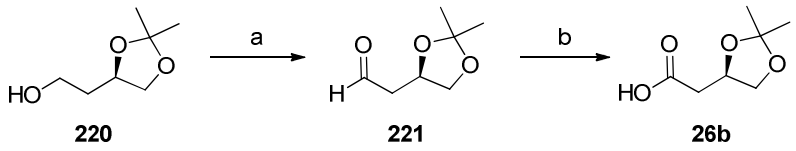


**Scheme 60: Carboxylic acid synthesis**

(a) $(COCl)_2$, DMSO, $Et_3N$, DCM, −78 °C, 2 h, assume quant; (b) $NaClO_2$, $H_2O_2$, *t*BuOH/$H_2O$, rt, 18 h, 76 % over 2 steps.

The succeeding steps shown in scheme **61** followed the Meyers synthesis (section **1.4.1**),[25] commencing with an amide coupling between serine methyl ester hydrochloride and the acid **26b** to provide the amide **27b** in 47% yield. This low yield was unexpected, as the Meyers group reported a yield of 67%.[25] All attempts to improve the yield were unsuccessful and isolation and purification of the amide **27b** proved difficult, due to the high polarity of the molecule; hence, some of the product could have been lost during aqueous work-up and column chromatography. Diminished yields were also encountered when the oxidation (scheme **60**) and amide coupling reactions (scheme **61**) were performed on larger scales, therefore these reactions had to be performed in batches of approximately 5 g of the starting alcohol **220**. Cyclodehydration of the amide **27b** to the oxazoline with DAST, followed by oxidation with DBU and $BrCCl_3$ resulted in the oxazole **28b** in 68% yield over the two steps. A by-product was also isolated after column chromatography of the oxazole; analysis of the by-product by NMR spectroscopy suggested the compound to be alkene **222**; this could have resulted from direct dehydration of the alcohol **27b**.

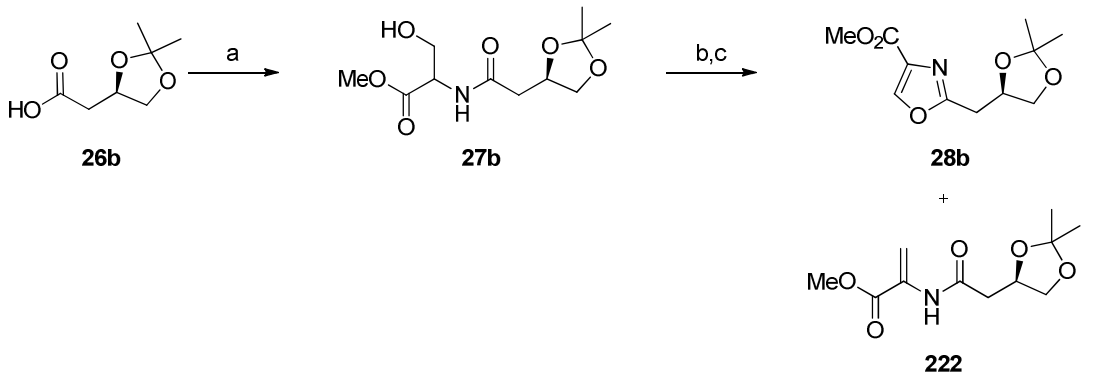


**Scheme 61: Oxazole formation**

(a) HCl•L-SerOMe, 1,1'-CDI, THF, 0 ºC to rt, 18 h, 47%; (b) DAST, $K_2CO_3$, DCM, −78 °C to rt, 2 h; (c) DBU, $BrCCl_3$, DCM, 0 °C to rt, 18 h, 66% over 2 steps.

The subsequent four steps (scheme **62**) revolved around alcohol protecting group manipulations, starting with the deprotection of the acetonide **28b** using acidic DOWEX resin. This allowed for simple isolation of the product following removal of the resin by filtration, providing the diol (quantitative yield) of suitable purity to advance to the next step. The primary alcohol was selectively protected with a TIPS group providing **223** in 78% yield, allowing for methylation of the secondary alcohol (63% yield). This was followed by TIPS deprotection with TBAF, furnishing the key primary alcohol **53** in 73% yield.

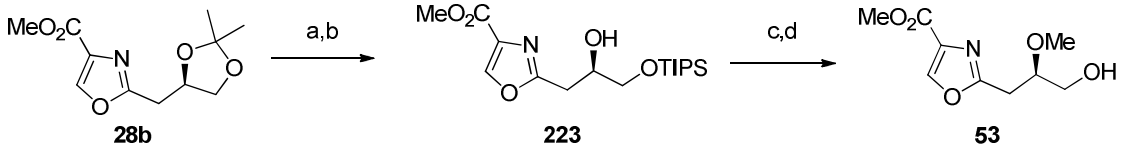


**Scheme 62: Formation of alcohol**

(a) Dowex-$H^+$, MeOH, rt, 18 h, quant; (b) TIPSOTf, 2,6-lutidine, DCM, −78 °C to rt, 2 h, 78%; (c) MeI, $Ag_2O$, $CH_3CN$, 60 °C, 18 h, 63%; (d) TBAF, THF, 0 °C to rt, 18 h, 73%.

Alcohol **53** and its enantiomer **24** were key intermediates in both the Meyers synthesis[25] and the Hoffmann synthesis[30] of disorazole $C_1$ and both syntheses involved the oxidation to the unstable aldehyde **224**. As described in Section **1.4.2**, the Hoffmann synthesis went on to form the vinyl iodide **45** through a reaction with

the Ohira-Bestmann reagent, followed by hydrostannylation/metal–iodine exchange. However, in order to shorten the route it was realised that a Takai olefination[96] could convert the aldehyde **224** directly to the vinyl iodide **45**. Taking into consideration the unstable nature of the aldehyde, an oxidation method with a straightforward purification was required. Therefore, a Parikh-Doering oxidation,[26] as used by Meyers, was utilised and the aldehyde was immediately subjected to Takai olefination conditions (scheme **63**). Unfortunately, only small amounts of the vinyl iodide **45** could be isolated. A Dess-Martin oxidation[90] was also attempted as an alternative oxidation method, but no improvement could be made to the yield of the vinyl iodide **45**. A trial Negishi reaction, to complete the fragment synthesis, was attempted on 2 mg of the vinyl iodide **45**. Analysis of the crude reaction mixture by NMR spectrometry showed evidence of the alkyne $CH_3$ coupled to one of the alkene protons with a doublet at 1.96 ppm, demonstrating the synthesis of desired product **225**. Sadly, the final fragment **225** could not be isolated due to the small scale of the reaction. The Meyers route was not as easily reproducible as expected and, in particular, difficulties were encountered in performing the initial steps towards the oxazole formation. Therefore, this route was abandoned in favour of the development of more convergent syntheses and those which could be more readily adapted to heterocyclic analogues.

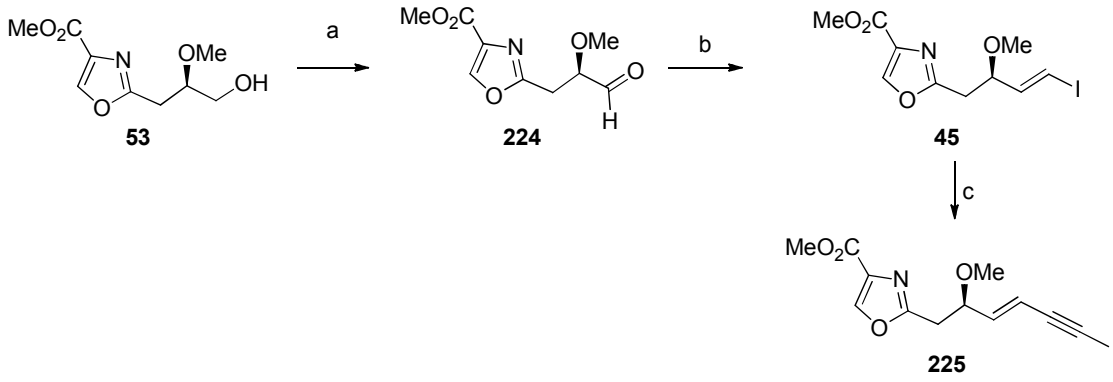


**Scheme 63: Attempted synthesis of C(1)-C(9) fragment**

(a) $SO_3$•Pyr, DMSO, $Et_3N$, DCM or DMP, $NaHCO_3$, DCM; (b) $CrCl_2$, $CHI_3$, THF/dioxane (1:6), rt, 18 h; (c) i. propynylmagnesium bromide, $ZnCl_2$, toluene, rt, 15 min; ii. $Pd(PPh_3)_2Cl_2$, **45**, rt, 18 h.

## 3.1.2 Wipf Based Approach

Another previous synthesis of disorazole $C_1$ which looked adaptable towards our fragment synthesis was the Wipf strategy (Section **1.4.3**).[15] The Wipf group's synthesis featured alkyne **77,** which was coupled to serine methyl ester hydrochloride and cyclised to form the oxazole **78**.

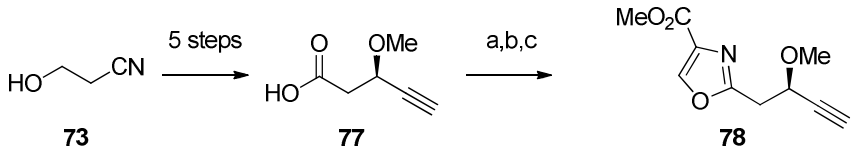


**73** **77** **78**

**Scheme 64: Wipf oxazole synthesis**

(a) SerOMe•HCl, EDC, HOBt, NMM, DCM, 0 °C to rt, 16 h, 55%; (b) i. DAST, DCM, −78 °C, 1 h; ii. $K_2CO_3$, −78 °C to rt, 40 min; (c) DBU, $BrCCl_3$, DCM, 0 °C to 4 °C, 20 h.

The Wipf synthesis consisted of 8 steps to generate the oxazole **78**, however a concise route to the TMS protected alkyne **102** was published in 2008 (scheme **65**);[33] it was thought this new route would provide rapid access to our desired oxazole fragment. With a desire to shorten the route further, we commenced the synthesis using ethyl propiolate **157**, rather than the TMS protected alkyne **226**. Condensation of the lithium enolate of ethyl acetate with ethyl propiolate generated the β-ketoester **228**. The product could be identified by proton NMR spectroscopy, but the presence of keto-enol tautomers complicated the spectrum. Unfortunately, the β-ketoester **228** appeared to be unstable, as low yields of product were isolated and decomposition was observed over a few days. Nevertheless, the crude mixture obtained from the reaction was advanced to the next step involving an enantioselective reduction of the ketone **228** in the presence of *Saccharomyces cerevisiae*. However, none of the desired alcohol **229** could be isolated.

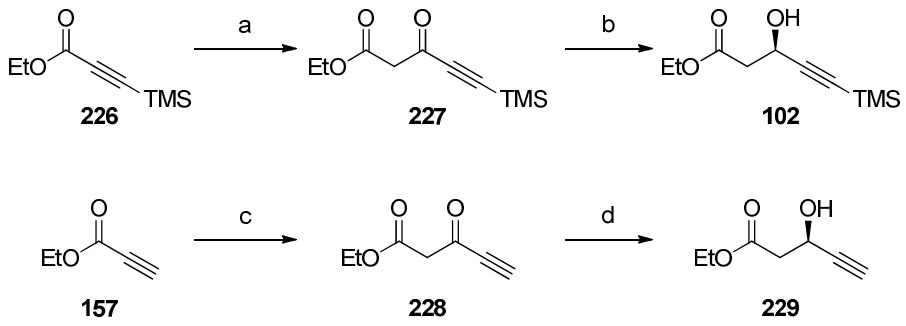


**Scheme 65: Attempted synthesis of alkyne alcohol**

(a) i. *i*PrNH, *n*BuLi, −78 ºC, THF; ii. EtOAc, 1 h; iii. AcOH, 91%; (b) *S. cerevisiae*, glucose, $H_2O$, EtOH, 30 °C, 18 h, 72%, 92% ee; (c) i. *i*PrNH, *n*BuLi, −78 ºC, THF; ii. EtOAc, 1 h; iii. AcOH; (d) *S. cerevisiae*, glucose, $H_2O$, EtOH, 30 °C, 18 h.

After our unsuccessful attempts at the synthesis of the alkyne **229**, the Wipf group published the synthesis of (−)-$CP_2$-disorazole which featured the Meyer and Cossy[33] route towards alkyne **102** (Section **1.5.6** and scheme **66**).[20] However, no yield or enantiomeric excess were reported by the Wipf group for their synthesis of the alkyne after reproducing the literature procedures. The TMS protecting group was cleaved under mild basic conditions and the alkyne was reduced to the alkene **103** using Lindlar's catalyst. Alkene cross metathesis between the alkenes **103** and **105** resulted in alkene **106**, which was later transformed into the oxazole segment. It would appear that the TMS group is necessary for the stability of the β-ketoester **227**, however, our attention was now focused on alternative more convergent routes towards the C(1)-C(9) fragment and the synthesis of the TMS protected alkyne **102** was not attempted.

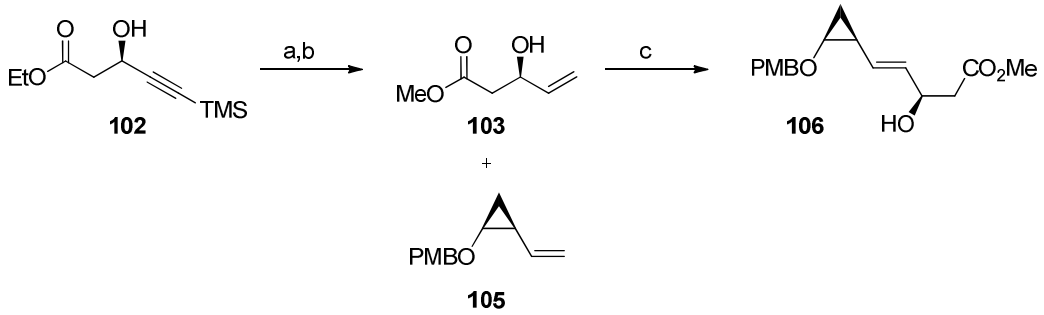


**Scheme 66: Wipf use of alkyne 102 in (–)-CP$_2$-disorazole C$_1$ synthesis**

(a) $K_2CO_3$, MeOH, 85%; (b) $H_2$, Lindlar cat., quinoline, EtOAc, 96%; (c) Grubbs II (5 mol%), DCM, 40 °C, 70% (*E*/*Z* = 10:1).

### 3.1.3 Summary

Investigations into adapting the previous syntheses of the oxazole section of disorazole $C_1$ proved to be more difficult than expected and a number of problems were encountered. The initial steps of the Meyers based route from the alcohol to the oxazole, involved unstable intermediates and synthesis of these intermediates on a large scale resulted in poor yields. This in turn limited options for optimising later stage reactions. Overall, this was a long linear sequence involving unstable intermediates and low yielding steps and adequate amounts of late stage intermediates could not be isolated. The Wipf based route also involved handling unstable intermediates and this synthesis could not be progressed. A convergent, adaptable route towards the C(1)-C(9) fragment was always desired, therefore focus was now turned to a disconnection at the C(4)-C(5) bond.

## 3.2 C(4)-C(5) Disconnection Approach

### 3.2.1 C(1)-C(9) Fragment Retrosynthesis

After investigating a C(5)-C(6) disconnection (as outlined in Chapter **2**) and encountering difficulties with designing an enantioselective route based around this, or the literature precedented routes to the disorazoles (section **3.1**) it was decided that a different disconnection approach was required. Therefore, the next disconnection we chose to investigate was at the C(4)-C(5) bond (scheme **67**). This would still generate a convergent synthesis towards the desired fragment and heterocyclic analogues, with the advantage now being that the stereogenic centre would be set into the epoxide fragment **231** prior to the key coupling to the oxazole. The retrosynthesis shown in scheme **67** is akin to the retrosynthesis discussed in Chapter **2**, where the epoxide **231** could either be coupled to a halooxazole **230** *via* a metal-halogen exchange (route A) or through a direct lithiation of the oxazole **232** (route B).

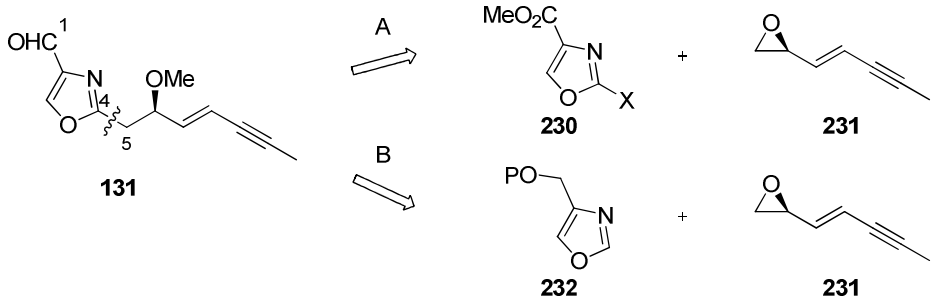


**Scheme 67: C(4)-C(5) disconnection of the $C_1$ C(1)-C(9) fragment**

There is no literature precedent for the formation of C-2 substituted oxazoles *via* a coupling with epoxides, there are however examples of opening epoxides to produce secondary alcohols with aromatics such as bromobenzene, 2-(bromomethyl)thiophene and furan. As demonstrated by Carnell and Allan (scheme **68**, reaction A),[97] a simple bromine-lithium exchange on arylbromides **233a-c** facilitated the regioselective opening of propylene oxide to generate 1-phenyl propan-2-ol **234a**, 1-thienyl propan-2-ol **234b** and 1-furyl propan-2-ol **234c**, all in

good yields. Newman *et al.*[98] (scheme **68**, reaction B) generated the Grignard reagent phenylmagnesium bromide from bromobenzene **235**, which in turn was used in a regioselective nucleophilic opening of (*S*)-epichlorohydrin, catalysed by copper iodide, to generate the secondary alcohol **236** in a very good yield (85%). An example of direct lithiation of a heterocycle, followed by epoxide opening was published by Lipshutz (scheme **68**, reaction C).[99] The C-2 lithiated furan was generated, which in turn was converted to a cuprate. The Lewis acid boron trifluoride diethyletherate was required to promote the nucleophilic, regioselective ring opening of the epoxide by this cuprate and the secondary alcohol **238** was generated in a high yield of 81%. Based on these high yielding, regioselective examples of generating secondary alcohols from epoxides and aryl rings, the retrosynthesis of the C(1)-C(9) fragment outlined in scheme **68** appeared to be a viable, convergent route and the synthesis of the required oxazoles and epoxide was commenced.

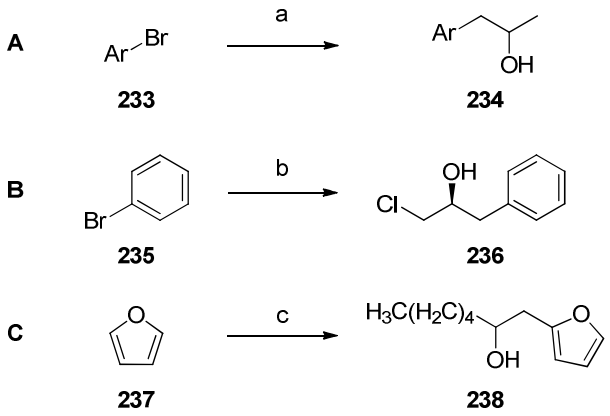


**Scheme 68: Examples of epoxide opening**

(a) i. *n*BuLi, THF, −30 ºC to rt, 30 min; ii. −30 ºC to rt, 1 h, propylene oxide, Ar = 1-phenyl propan-2-ol **234a** 68%, 1-thienyl propan-2-ol **234b** 61%, 1-furyl propan-2-ol **234c** 77%; (b) i. Mg, $I_2$, THF, reflux, 30 min; ii. (*S*)-epichlorohydrin, CuI, THF, −60 ºC to rt, 1 h, 85%; (c) i. *n*BuLi, THF, −30 ºC to rt, 1 h; ii. CuCN, −30 ºC to 15 ºC; iii. 2-pentyloxirane, $BF_3$•$Et_2O$, −78 ºC, 2 h, 81%.

## 3.2.2 C(1)-C(4) Oxazole Synthesis

### 3.2.2.1 Halooxazoles

Hodgetts and Kershaw pioneered the synthesis of ethyl 2-chlorooxazole-4-carboxylate **230a** to create a simple building block which could be elaborated to aid the synthesis of the common 2,4-disubstituted oxazole motif.[100] Their method was repeated, commencing with the condensation of ethyl bromopyruvate (**239**) and urea to provide the HCl salt of aminooxazole **240** in 73% yield (scheme **69**). This was followed by conversion of the aminooxazole **240** into the chlorooxazole **230a** by treatment with *tert*-butyl nitrite and copper (II) chloride. Despite other published reproductions of this transformation,[101,102] in our hands only low yields of the desired chlorooxazole **230a** product could be isolated, with the greatest yield being 27%. Monitoring the consumption of the aminooxazole **240** was difficult by TLC due to the highly polar nature of the compound. Formation of the product **230a** could be observed by TLC; however analysis of the reaction mixture by mass spectrometry did show some starting material remaining. The isolated yield of the desired product **230a** could not be improved by increasing the reaction time.

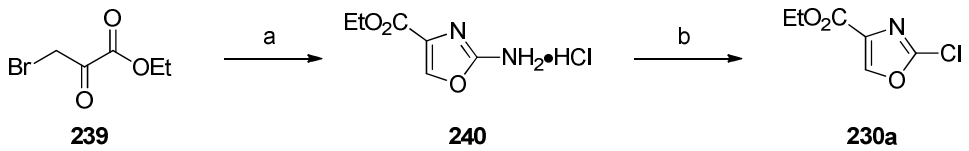


**239** **240** **230a**

**Scheme 69: Synthesis of chlorooxazole**

(a) Urea, EtOH, 85 ºC, 2 h, 73%; (b) *t*BuO-NO, $CuCl_2$, $CH_3CN$, 60-80 ºC, 2 h, 27%.

The analogous bromooxazole **230b** would also be a desirable intermediate; however when this synthesis was attempted by Hodgetts and Kershaw the desired monobromooxazole **230b** was generated in only 21% yield; in addition, the dibromooxazole **241** was isolated in 16% yield (scheme **70**).[100] Attempts by Hodgetts and Kershaw to optimise this reaction were unsuccessful, the yield could not be improved and selectivity for one product over the other could not be established.[100]

Following our disappointing results towards the synthesis of the chlorooxazole **230a**, and considering the limited published routes towards the bromooxazole **230b**, it was decided not to pursue the synthesis of the bromooxazole **230b**. Reported yields of the synthesis of the corresponding iodooxazole are also low (28%),[103] therefore, attention was turned to the synthesis of ethyl 1,3-oxazole-4-carboxylate.

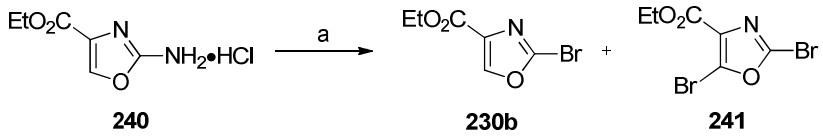


**240** **230b** **241**

**Scheme 70: Literature synthesis of bromooxazole**

*(a) t*BuO-NO, $CuCl_2$, $CH_3CN$, 60-80 ºC, 2 h, **230b** 21%, **241** 16%.

## 3.2.2.2 Synthesis of 1,3-Oxazol-4-ylmethanol

Known compound ethyl 1,3-oxazole-4-carboxylate **244** was synthesised following a literature procedure *via* a condensation between formic acid (**242**) activated by 1,1'-carbonyldiimdazole and ethyl isocyanoacetate (**243**), as shown in scheme **71**.[104] Ethyl 1,3-oxazole-4-carboxylate **244** was readily generated on a large scale of up to 6 grams and in very good yield of 80%.

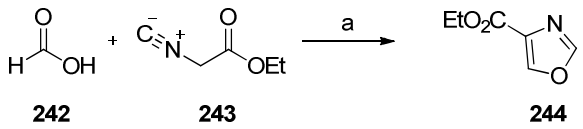


**242** **243** **244**

**Scheme 71: Synthesis of ethyl 1,3-oxazole-4-carboxylate**

(a) 1,1'-CDI, $NEt_3$, THF, rt to 80 ºC, 24 h, 80%.

The simple reduction of the ethyl ester **244** to the primary alcohol **245** proved to be more difficult than anticipated. Reductions with common agents, such as sodium borohydride,[105] lithium aluminium hydride,[106] lithium triethylborohydride[107] and DIBAL showed complete consumption of the ethyl ester **244**; formation of the product alcohol **245** was confirmed by proton NMR spectroscopy. However, isolated

yields of **245** were very poor and the alcohol proved to be volatile and therefore difficult to handle. The alcohol **245** was required for a multi-step synthesis and hence large quantities of this intermediate were desired; however, due to the volatile nature of the alcohol these requirements could not be met. Following on from the discoveries of chapter **2**, where the protecting group was shown to affect the regioselectivity of the lithiation of the 2-methyl oxazole, it was thought that a protecting group could also affect lithiation reactions with 1,3-oxazol-4-ylmethanol. Therefore attempts were made to immediately protect alcohol **245** with a TBDMS group (simultaneously increasing the weight of the molecule and decreasing the volatility). Unfortunately, the desired product **246** could not be isolated in reasonable yields, most likely due to loss of the intermediate alcohol during work-up and isolation.

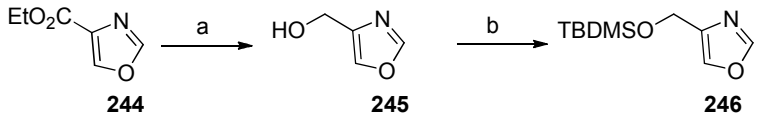


**244** **245** **246**

**Scheme 72: Ester reduction to alcohol**

(a) $H^-$; (b) TBDMSOTf, 2,6-lutidine, DCM, 0 ºC, 1 h.

Despite promising literature precedent for the synthesis of the chlorooxazole **230a** and oxazole **245** the procedures could not reliably be reproduced. The alcohol **245** proved difficult to handle due to volatility and attempts to ease handling by adding a TBDMS group failed. Investigations into the synthesis of the epoxide were being carried out in parallel and these results will now be discussed.

### 3.2.3 C(5)-C(9) Epoxide Retrosynthesis

The desired epoxide **231** can be disconnected at the C(7)-C(8) double bond to the alkene **247** and enyne 2**48**, which in a forward sense would be coupled by an alkene cross metathesis (Scheme **73**, route A). An alternative would be route B (scheme **73**), where the alkene can be constructed from the aldehyde **249** and phosphine salt **250** by a Wittig reaction.

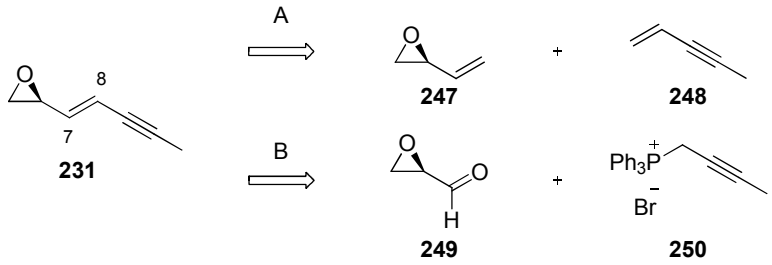


**Scheme 73: C(7)-C(8) alkene disconnection**

### 3.2.4 C(7)-C(8) Alkene Bond Formation *via* Cross Metathesis - Route A

#### 3.2.4.1 Alkene Cross Metathesis Background

It was envisaged that the epoxide enyne **231** could be synthesised *via* a cross metathesis reaction between (*S*)-2-vinyloxirane **247** and pent-1-en-3-yne **248**. Metathesis reactions are now commonly used in organic synthesis and the development of new catalysts and reaction conditions is on going. Cross metathesis (CM) reactions hold the caveat of limited selectivity of the CM product over the homometathesis products. The CM between 2-vinyloxirane **247** and pent-1-en-3-yne **248** has not been reported and their respective reactivities were unknown, therefore investigations into this coupling were carried out.

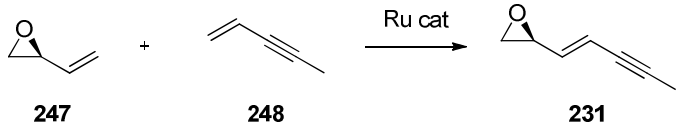


**Scheme 74: Proposed cross metathesis reaction**

Examples of the use of 2-vinyloxirane **247** in olefin cross metathesis (CM) have shown formation of the (*E*)-isomer as the major product. For example, when exploring the scope of a new catalyst **251**, the Grubbs group showed CM between 2-vinyloxirane and the alkene **249** to be sucessful.[108] The CM product **250** was isolated in 55% yield and an *E*:*Z* ratio of 5:1.[108] The yield of the CM product was greatest when the 2-vinyloxirane was added slowly over 12 hours, rather than all in one portion; homodimerisation of the starting materials was also observed. In their synthetic studies towards (+)-strictifolione, Kumar *et al.* investigated a CM route between (*S*)-2-vinyloxirane and the alkene **252** catalysed by Grubbs' II catalyst.[109] The desired product **253** was isolated in a low 16% yield (6:1, *E*:*Z*) and homodimerisation products from both starting materials were observed. The yields from both of these CM reaction with 2-vinyloxirane were low; however, the (*E*)-isomer was the major product, which was encouraging for our own investigations into CM with 2-vinyloxirane.

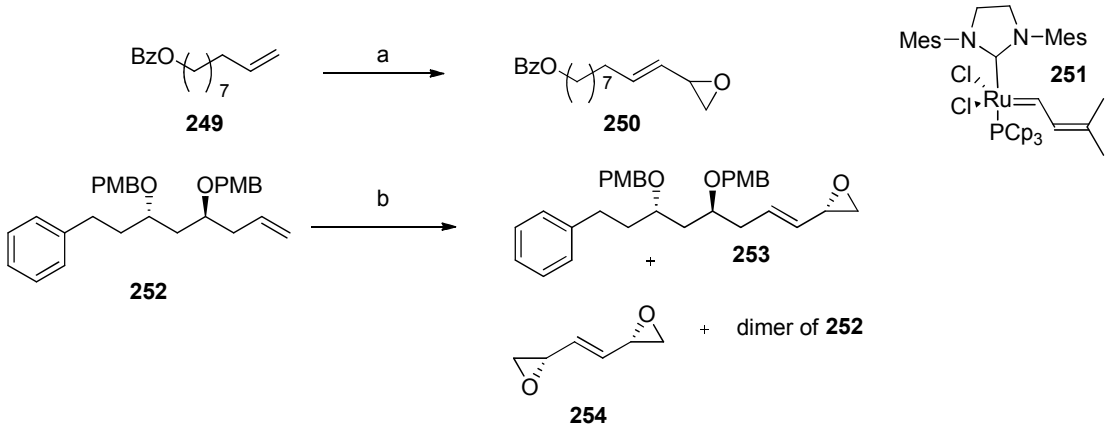


**Scheme 75: Literature examples of CM with 2-vinyloxirane**

(a) 2-vinyloxirane, catalyst **251** (5 mol%), DCM, reflux, 12 h, 55% (5:1, *E*:*Z*);[108](b) (*S*)-2-vinyloxirane, Grubbs II (10 mol%), DCM, reflux, 18 h, **253** 16% (6:1, *E*:*Z*).[109]

The first investigations into CM with conjugated enynes were published in 2003 by Chang *et al.*[110] CM reactions with 4-phenyl-1-buten-3-yne (**255**), catalysed by Grubbs I or Grubbs II failed and the starting material (**255**) was recovered in quantitative yield. It is thought that the alkyne triple bond binds to the ruthenium centre of the catalyst, therefore rendering it inactive.[110] The binding of the enyne to the catalyst was monitored by IR spectroscopy, where the peak of the alkyne shifted from 2217 to 2151 $cm^{-1}$, representing a weakened triple bond due to binding to a metal. When a new catalyst **257**, developed by the Grubbs group,[111] was employed in CM reactions with enynes, the desired CM products were isolated in acceptable yields. For example, the CM reaction between 4-phenyl-1-buten-3-yne (**255**) and allyltrimethylsilane catalysed by **257** resulted in the alkene product **256** in 60% yield; surprisingly, an *E*:*Z* ratio of 1:3.1 was observed (scheme **76**). Conversely, Hansen and Lee reported successful CM reactions with various conjugated enynes catalysed by Grubbs II catalyst.[112] They found that yields were not greatly improved by the use of catalyst **257**; but interestingly, the (*Z*)-isomer was once again the major product.[112]

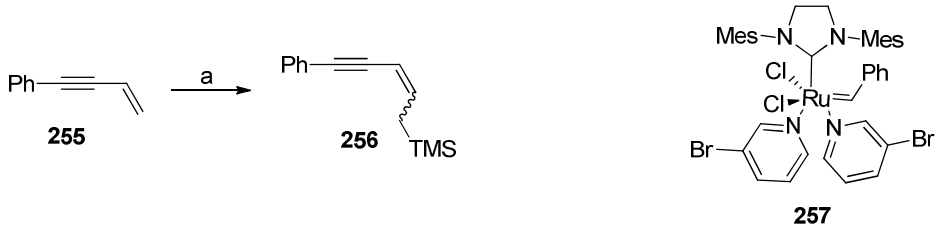


**Scheme 76: Example of CM with enyne**

(a) Allyltrimethylsilane, catalyst **257** (10 mol%), toluene, reflux, 12 h, 60% (1:3.1, *E*:*Z*).

Olefin CM reactions commonly generate the (*E*)-isomer as the major product, as it is the most thermodynamically stable isomer. Consequently, the results observed with the enynes reported by Chang and Hansen and Lee were unexpected. The generation of the (*Z*)-isomer as the major product was repeatedly observed across a range of enyne substrates and alkene coupling partners. Examining the metallacyclobutane intermediate of the CM mechanism (scheme **77**), it can be seen that the *N*-heterocyclic carbene ligand blocks one face of the metallacyclobutane **258**. This would force the two alkene substrates to approach from the same side, because if the

substrates approached from different sides it would result in unfavourable steric hindrance as shown in intermediate **260**. In addition, it has been suggested that the enynes do not participate in the reversible metathesis cycles,[113] therefore it is the kinetic ratio of products that is isolated, with the (Z)-isomer **259** being the predominant species.

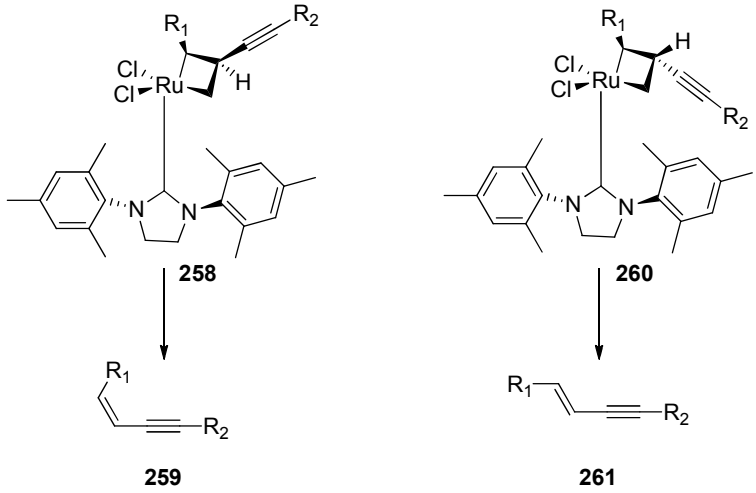


**Scheme 77: Enyne CM metallacyclobutane intermediates**

## 3.2.4.2 C(7)-C(9) Enyne Synthesis

Inspired by the successful synthesis of the enyne ester **161** in Chapter **2 (**scheme **41)**, Negishi conditions were applied to 1-propynylmagnesium bromide (**262**) and vinyl bromide in an attempt to synthesise the enyne **248** (scheme **78**). The enyne **248** is reported to have a boiling point of 60 ºC;[114] therefore care had to be taken during work-up and purification. After work-up and extraction with diethyl ether, the crude mixture was distilled to isolate the desired product. A proton NMR spectrum of the distillate showed small amounts of the desired enyne **248**, however THF from the solutions of 1-propynylmagnesium bromide and vinyl bromide had co-distilled and was the major component of the distillate.

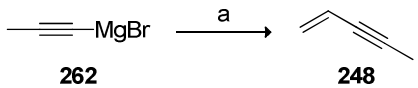


**Scheme 78: Negishi reaction to generate enyne**

(a) i. $ZnCl_2$, toluene, rt, 15 min; ii. $Pd(PPh_3)_2Cl_2$, vinyl bromide (1 M in THF), rt, 18 h.

Eglington and Whiting reported the conversion of β,γ-acetylenic tosylates to vinylacetylenes under alkaline conditions.[115] To this end, the alcohol **263** was treated with tosylchloride in pyridine to provide the tosylate **264** in excellent yield (scheme **79**). The tosylate **264** was subsequently heated with potassium hydroxide in ethanol and water at 120 ºC; a few drops of detergent were also added as Eglington and Whiting reported cleaner reactions and higher yield when a trace of "Teepol" was added to the reaction mixture.[115] The enyne **248** was evolved as a gas and to aid purification, the product was collected by passage through a fractionating column and condenser. The liquid collected was highly volatile and identification of the product **248** was confirmed through proton NMR spectroscopy. Some co-distillation of ethanol was observed, as evidenced by the NMR spectrum, however the liquid collected was mainly composed of the enyne **248**, which was used immediately in the next step.

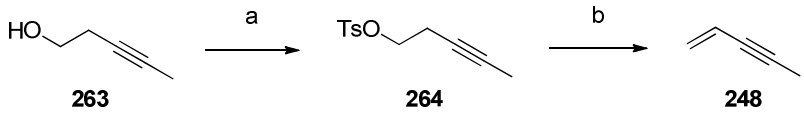


**Scheme 79: Enyne synthesis**

(a) TsCl, pyridine, 0 ºC to rt, 18 h, 92%; (b) KOH, EtOH, $H_2O$, 120 ºC, assume quant.

### 3.2.4.3 Attempted Cross Metathesis

Based on the published results, it seemed likely that the (*Z*)-alkene would be the major isomer for our system. However, CM conditions have not been applied to these exact substrates, therefore investigations were carried out. The enyne **248** was used immediately after distillation from the previous step, it was treated with 2-vinyloxirane **247** and Grubbs II catalyst in DCM (scheme **80**). After heating at reflux for 5 hours more catalyst was added and the reaction mixture was stirred overnight. Following purification by silica column chromatography, the only isolable product was the homodimer of 2-vinyloxirane (**254**). The identification of **254** was based on the observations of Kumar *et al*.,[109] and comparison of NMR data to the literature.[116]

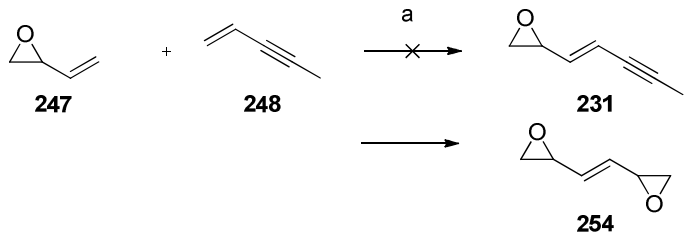


**Scheme 80: Attempted cross metathesis between 2-vinyloxirane and pent-1-en-3-yne**

(a) Grubbs II (20 mol%), DCM, 40 ºC, 24 h.

The enyne **248** is highly volatile and proved difficult to handle, and it is also likely that the (*Z*)-isomer would be the major product in the CM reaction. Therefore, further investigations into cross metathesis were terminated and attention was turned to the Wittig reaction.

### 3.2.5 C(7)-C(8) Alkene Bond Formation *via* Wittig Reaction - Route B

It was envisaged that the desired epoxide **231** could be constructed *via* a Wittig reaction between the epoxide aldehyde **249** and the phosphorus ylide **250**. Considering stabilised ylides favour the formation of the (*E*)-alkene in the Wittig reaction, the butyne section was chosen to contain the ylide, as it is more stabilised than the epoxide half. In addition, there is literature precedent for using this ylide **250** and aldehyde **249** independently in Wittig reactions, however not for coupling them together.

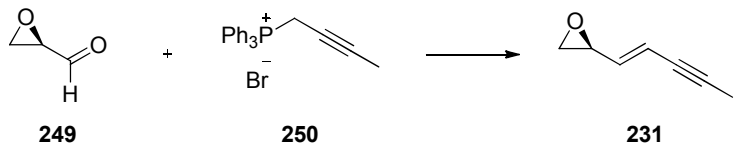


**Scheme 81: Proposed Wittig reaction**

Examples of the use of these the aldehyde **249** and ylide **250** are shown in scheme **82**. But-2-ynyltriphenylphosphonium bromide **250** was utilised in a Wittig reaction with aldehyde **265** in the synthesis of pheromone dodeca-8*E*,10*E*-dien-1-ol. Despite the low yield of the product **266**, the (*E*)-isomer was generated as the major isomer with an *E*:*Z* ratio of 7:3.[117] An example of the use of an *in situ* oxidation of glycidol

**267**, followed by a Wittig reaction is also shown in scheme **82**; the (*E*)-isomer of **268** was generated in 70% yield as the major isomer, though no *E*:*Z* ratio was reported.[118]

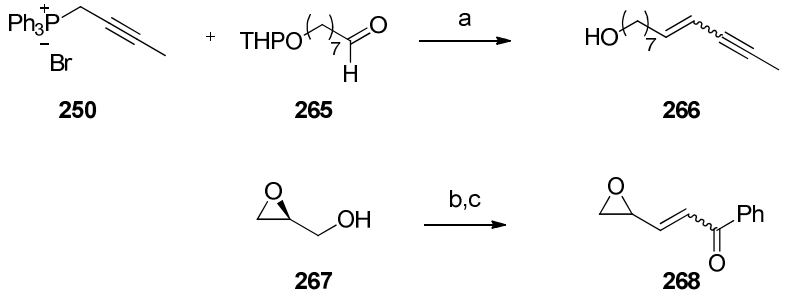


**Scheme 82: Examples of Wittig reaction with alkyne 250 and epoxide 267**

(a) i. *n*BuLi, THF, −78 ºC, 30 min; ii. **265**, −78 to −40 ºC, 1 h; iii. $H^+$, 37% (7:3, *E*:*Z*); (b) DMSO, $(COCl)_2$, $Et_3N$, DCM, −78 ºC, 1 h; (c) $Ph_3PCHCOPh$, rt, 20 h, 70% over 2 steps.

The phosphine salt required for the Wittig reaction, shown in scheme **83**, was readily synthesised from 1-bromo-2-butyne **269** and triphenyl phosphine;[119,120] the phosphorus ylide **250** was generated after exposure to potassium *tert*-butoxide. Glycidol (**267**) was oxidised to the aldehyde **249**, using BAIB and TEMPO,[121] and it was used immediately in the next step (as it was predicted to be unstable and volatile). After work-up and purification of the Wittig reaction, no alkene product **231** could be isolated and the triphenyl phosphine oxide (**270**) by-product was difficult to separate. It is likely that the enyne epoxide **231** is volatile, therefore a simple purification procedure was required. Therefore, the use of polymer supported triphenylphosphine was investigated, as this has proven to be advantageous in other Wittig reactions involving volatile and unstable products.[122]

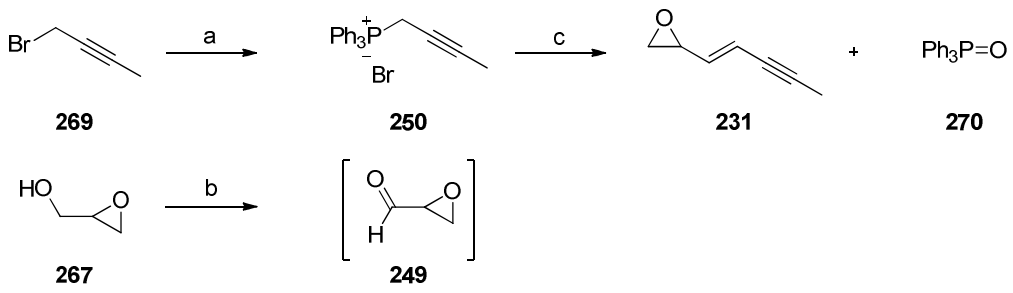


**Scheme 83: Attempted Wittig reaction**

(a) $PPh_3$, rt, 16 h, 72%; (b) BAIB, TEMPO, DCM, rt, 4 h, assume quant; (c) i. *t*BuOK, DCM, rt, 1 h; ii. **249**, rt, 18 h.

A polymer supported phosphorus ylide would enable the triphenyl phosphine oxide to be removed by filtration, thereby simplifying the purification and isolation of the desired product. The polymer supported phosphine salt was synthesised by heating 1-bromo-2-butyne **269** and polymer supported triphenylphosphine in DMF for 48 hours (scheme **84**). This time, the aldehyde **249** was synthesised by a Dess-Martin[90] oxidation of glycidol (**267**); the phosphorus ylide generated after treatment of salt **271** with potassium *tert*-butoxide was added directly into the oxidation reaction. After filtration of the polymer support, aqueous work-up of the crude mixture and column chromatography, none of the desired enyne epoxide **231** could be isolated. This reaction was attempted a number of times, and the base to form the phosphorus ylide was altered to *n*BuLi, but to no avail.

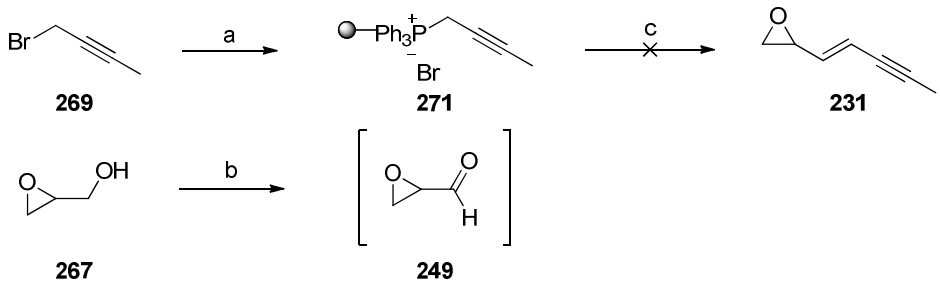


**Scheme 84: Polymer supported Wittig reaction**

(a) polymer supported $PPh_3$, DMF, 70 ºC, 48 h, quant; (b) DMP, $NaHCO_3$, DCM, 0 ºC to rt, 2 h, assume quant; (c) i. *t*BuOK, DCM, rt, 1 h; ii. **249**, rt, 18 h.

Intriguingly, each time the reaction was performed the only compound isolated was an unidentified by-product. This by-product was only isolated in small amounts, for example 50 mg was isolated when the reaction was performed on 1.74 mmol of phosphorus ylide. With a desire to identify this by-product full characterisation was carried out. The main distinguishing peaks in the NMR spectrum included an ethyl group and a doublet at 6.74 ppm, representing a proton on a trisubstituted alkene next to a CH. After further analysis of the proton and carbon NMR spectra, the remaining peaks appeared to correspond to an epoxide. It can be seen from the HSQC-TOCSY spectrum (figure **12**), that the ethyl group is contained in a separate spin-system from the rest of the molecule.

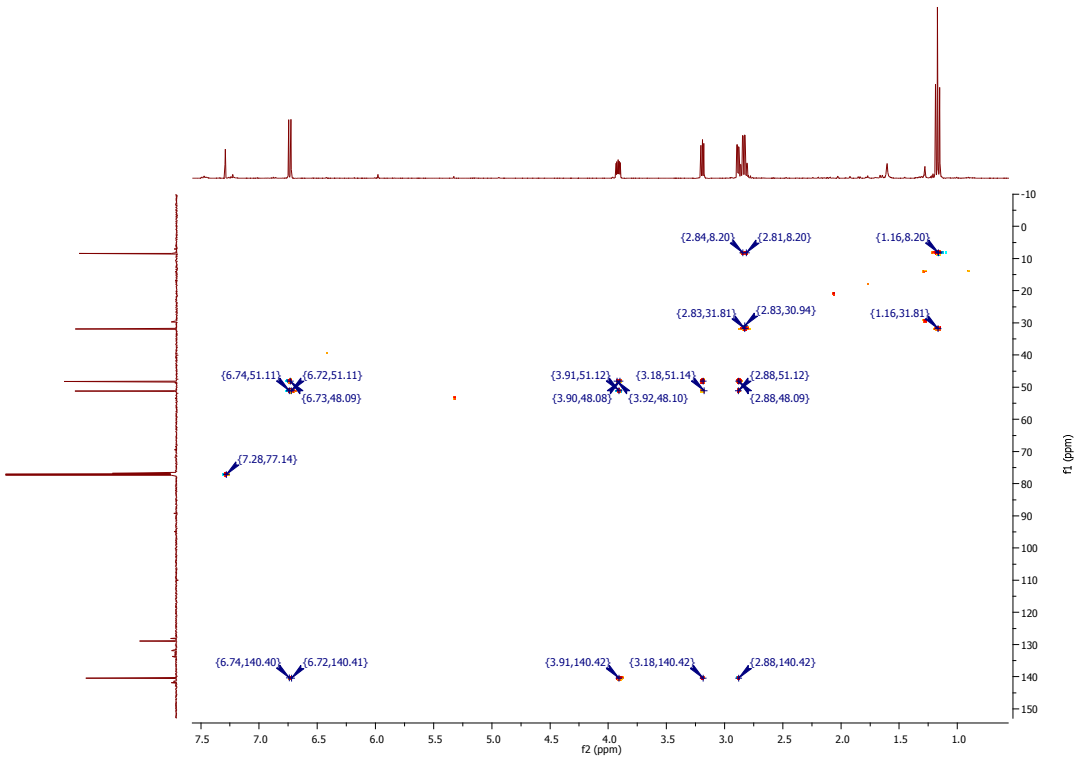


**Figure 12: HSQC-TOCSY NMR spectrum of the unknown by-product**

A distinctive carbonyl peak was visible in the IR spectrum at 1693 $cm^{-1}$, which represents a conjugated carbonyl group. The total number of carbon and hydrogen atoms could be deduced from the NMR spectra, which corresponded to 7 and 9 respectively. Interestingly, an unexpected characteristic bromine isotope pattern was observed in the mass spectrum of the isolated product and after piecing together the data already collected, the main peaks in the mass spectrum did not correspond to the expected mass. Taking into consideration the data collected the mass expected to be seen in the EI spectrum was 203/205 ($C_7H_9BrO_2$), however the highest mass peak was observed at 174/176. This difference of 29 mass units could be attributed to the loss of an ethyl group; however it is more likely to be due to the fragmentation of an epoxide and loss of formaldehyde. Epoxides are relatively unstable and fragmentation is highly likely, especially by the harsh conditions of EI mass spectrometry, thereby explaining the absence of the predicted mass peaks at 203/205. A mechanism for epoxide fragmentation is shown in scheme **85**; initially a rearrangement tales place to provide aldehyde **273**, which undergoes loss of formaldehyde, generating the cation **274**, which is observed in the mass spectrum.[123]

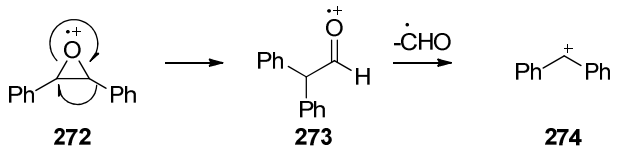


**Scheme 85: Epoxide fragmentation under EI mass spectrometry conditions**[123]

Upon mass spectrometry analysis of the commercial 1-bromo-2-butyne (**269**) a small amount of 1,1-dibromobut-2-yne was evident. Based on this observation, and after combining the available data, the structure **277** was proposed. A plausible mechanism is shown in scheme **86**: ylide **275** could have been formed from 1,1-dibromobut-2-yne and a subsequent Wittig reaction with aldehyde **249** could have resulted in enyne **276**. Hydrolysis of the alkyne **276** would generate the enone **277**. Alternatively, the alkyne on the ylide could have been hydrolysed to generate **278** and this could have undergone a Wittig reaction to generate the enone **276**. It is thought that this was the only compound isolated from the reaction mixture as it was likely to be the most stable compound.

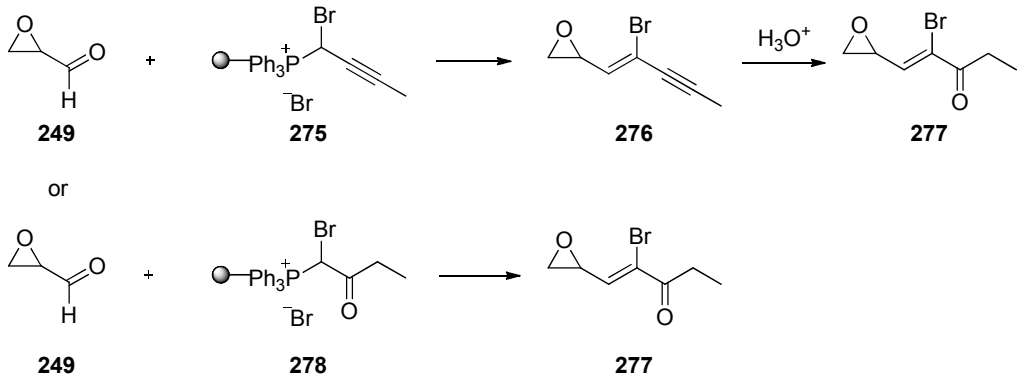


**Scheme 86: Possible routes to Wittig reaction by-product**

As the desired epoxide enyne **231** could not be obtained through the cross-metathesis or Wittig reaction, alternative routes including the HWE reaction and epoxidation of an aldehyde were briefly investigated

## 3.2.6 Horner-Wadsworth-Emmons Reaction

HWE reactions have the advantage over Wittig reactions of the dialkylphosphate salt by-product being water soluble and therefore it can be more easily removed from the reaction mixture. An example of the synthesis of an enyne by the HWE reaction is shown in scheme **87**. The phosphonate ester **279** was exposed to KHMDS and the reaction with acetaldehyde resulted in the enyne **280** in 66% yield, however no *E*:*Z* ratio was reported.[124]

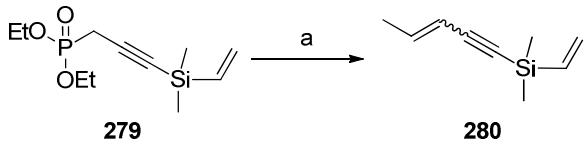


**Scheme 87: HWE enyne synthesis**

(a) KHMDS, acetaldehyde, THF, −78 ºC, 66%

The required phosphonate ester **281** was readily synthesised from 1-bromo-2-butyne (**269**) in quantitative yield. The phosphonate ester was subsequently subjected to similar conditions used in the Wittig reaction described above. Unfortunately, no desired product **231** could be identified in a proton NMR spectrum of the crude reaction mixture. Despite the literature precedent for the synthesis of enynes with the HWE reaction, the phosphonate ester **281** is not as stabilised as common HWE reagents. Also, the alkyne is not a strong electron withdrawing group, which would decrease the reactivity of the phosphonate salt and decrease the likelihood of the reaction proceeding to give the desired alkene product **231**.

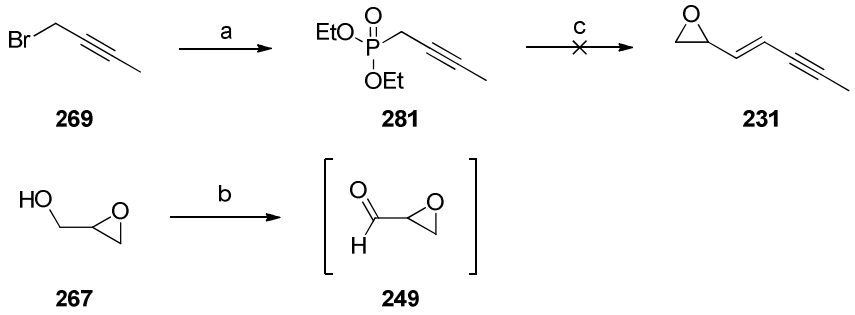


**Scheme 88: Attempted HWE reaction**

(a) $P(OEt)_3$, 160 ºC, 3 h, quant; (b) DMP, $NaHCO_3$, DCM, 0 ºC to rt, 2 h, assume quant; (c) i. *n*BuLi, DCM, 1 h, rt; ii. **249**, rt, 18 h.

## 3.2.7 Epoxidation of C(6)-C(9) Aldehyde

The cross metathesis and Wittig reaction routes both hold the disadvantage that the formation of the alkene bond tends not to be stereoselective, resulting in *E*/*Z* isomer mixtures. It would therefore be advantageous to develop a route with greater alkene stereoselectivity, hence a brief investigation was carried out into a Corey-Chaykovsky epoxidation[125] of the C(6)-C(9) aldehyde **140**, which had been previously synthesised (Section **2.4**). The viability of this reaction was initially tested on a racemic system. Purpura and Krause, reported the epoxidation of enyne aldehyde **282** following treatment with trimethylsulfonium bromide and base to provide the enyne epoxide **283** in 80% yield (scheme **89**).[126] These conditions were applied to the aldehyde **140**, however no desired product **231** could be identified in the crude reaction mixture. The conditions of the epoxidation were tested on a more stable aldehyde, namely 4-bromobenzaldehyde (**284**) and the epoxide **285** was successfully synthesised in 78% yield.[127] This result would suggest the aldehyde **140** is not a good substrate for this epoxidation, or the epoxide product was too unstable, or volatile to be isolated. Chiral sulfur ylides can be used to establish asymmetric syntheses of epoxides,[128,129] however this methodology has only been used to create non-terminal epoxides. Taking this into consideration, this route was not investigated any further; as the development of an enantioenriched fragment would most likely require a kinetic resolution of a racemic mixture of product which would be difficult on this volatile, unstable intermediate.

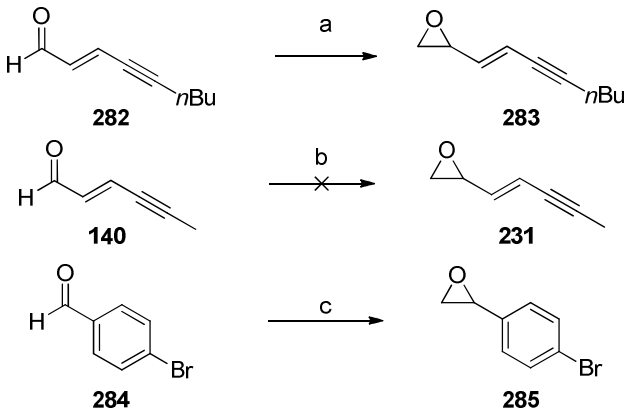


**Scheme 89: Aldehyde epoxidation**

(a) $Me_3S^+Br^-$, KOH, $H_2O$, MeCN, 60 ºC, 2 h, 80%;[126](b) $Me_3S^+I^-$, KOH, $H_2O$, MeCN, 60 ºC, 2 h; (c) $Me_3S^+I^-$, KOH, $H_2O$, MeCN, 60 ºC, 2 h, 78%.

### 3.2.8 Summary

Despite promising literature precedent for this novel epoxide based route, the C(4)-C(5) disconnection approach involved many small, unstable, volatile intermediates that were difficult to handle. The problem of generating the chiral centre at C(6) was solved by using commercially available chiral starting materials, however with this route there was now the issue of stereoselectively generating the (*E*)-alkene. Progression of this epoxide based approach was difficult and it would not be a suitable route to generate the C(1)-C(9) fragment of disorazole $C_1$. The C(4)-C(5) disconnection led to a highly convergent route and we were encouraged by the potential of the chemistry introduced in section **3.1.1** (Meyers based approach), therefore, a new route was developed and this will be discussed in Chapter **4**.

# 4 Chapter 4: Enantiospecific Synthesis II and Heterocyclic Analogues

## 4.1 Retrosynthesis of C(1)-C(9) Fragment and Heterocyclic Analogues

A new approach towards the synthesis of the C(1)-C(9) fragment was desired and a convergent synthesis which could be adapted to analogue syntheses was the main priority. The C(4)-C(5) disconnection, as discussed in Chapter **3**, was still attractive as a convergent route, however alternative synthons were required. To overcome the earlier difficulties encountered with generating the epoxide, it was anticipated that a large leaving group (*e.g.* OTs or I) would reduce the volatility of the intermediate and increase ease of handling. The C(4)-C(5) retrosynthesis of **286,** shown in scheme **90**, would therefore lead to the heterocyclic ester **287** and the enyne **288**.


**Scheme 90: C(4)-C(5) disconnection of fragment and heterocyclic analogues**

## 4.2 Synthesis of C(5)-C(9) Tosylate

A strategy inspired by chemistry developed in the Meyers based approach (section **3.1.1**) was adopted towards the synthesis of the desired tosylate fragment, due to the commercial availability of the chiral alcohol **289**. The initial steps involved a straightforward tosylation of the alcohol **289** with tosyl chloride in pyridine, providing the tosylate **290** in quantitative yield. This was followed by deprotection of the acetonide group with acidic DOWEX resin, resulting in the diol **293** in an excellent yield (87%).

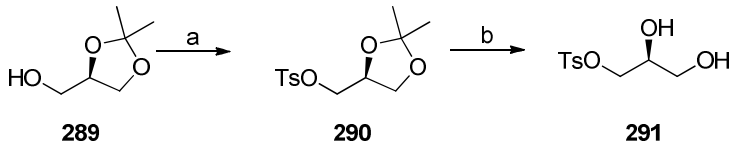


289 290 291

**Scheme 91: Synthesis of diol**

(a) TsCl, pyridine, 0 ºC to rt, 18 h, quant; (b) DOWEX, MeOH, rt, 18 h, 87%.

In order to shorten the synthesis and avoid the use of alcohol protecting groups, attempts were made to selectively oxidise the primary alcohol of **291** over the secondary alcohol. It was predicted that the aldehyde **292** would be unstable, therefore, it was used immediately in the Takai olefination step without isolation. Mild oxidation with sodium hypochlorite, potassium bromide, and TEMPO looked promising with the aldehyde visible by TLC;[130] however, only on one occasion was the resulting vinyl iodide **293** isolated and in a very poor yield (scheme **92**). It was therefore decided that alcohol protecting group strategies would enable progression though this route.

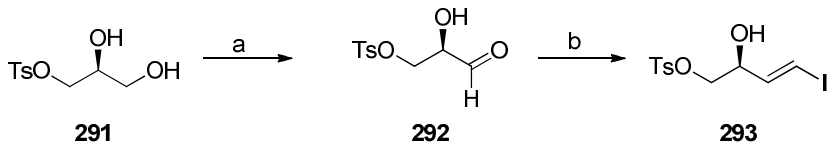


291 292 293

**Scheme 92: Attempted selective oxidation of primary alcohol followed by Takai olefination**

(a) NaOCl, KBr, TEMPO, $NaHCO_3$, DCM/$H_2O$ (9:1), 0 ºC, 10 min, assume quant; (b) $CrCl_2$, $CHI_3$, THF:dioxane (1:6), rt, 18 h, 10 % over 2 steps.

As the TIPS protection had proved to be successful in the Meyers based approach (section **3.1.1**), the primary alcohol was protected as a TIPS ether and *O*-methylation of the secondary alcohol provided the methyl ether **294** in 55% yield (scheme **93**). However, deprotection of the TIPS group with TBAF resulted in a mixture of products (including compounds where the tosylate group had been removed) and the desired product **295** could not be isolated in an acceptable yield.

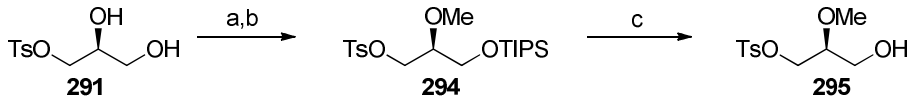


291 294 295

**Scheme 93: TIPS protection**

(a) TIPSOTf, 2,6-lutidine, DCM, −78 °C to rt, 2 h, quant; (b) MeI, $Ag_2O$, $CH_3CN$, 60 °C, 18 h, 55%; (c) TBAF, THF, 0 °C to rt, 18 h.

Reducing agents, such as DIBAL, can promote reductive cleavage of the PMB acetals of 1,2-diols to generate primary alcohols.[131] It was therefore anticipated that a PMB acetal could be reductively cleaved to give the protected secondary alcohol, enabling further manipulations of the primary alcohol. Treatment of the diol **291** with *p*-methoxy benzaldehyde dimethyl acetal and *p*-toluenesulfonic acid in DMF afforded the PMB acetal **296** in 80% yield (scheme **94**). The acetal precipitated out as a colourless solid, thus some product may have been lost during filtration, or lost in solution. When DIBAL cleavage of the acetal was performed at 0 ºC a mixture of the desired alcohol **297** and a by-product was obtained, in approximately 3:2 ratio. From analysis of the NMR spectrum the by-product was found to be alcohol **298**. Loss of the tosyl group could have occurred through a substitution of hydride for the tosylate generating **298**; this is feasible as there were 3 equivalents of DIBAL in the reaction mixture.

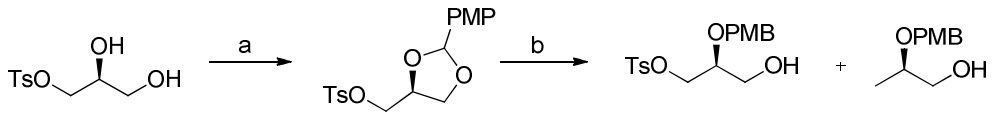


291 296 297 298

**Scheme 94: PMB acetal formation and ring opening**

(a) TsOH•$H_2O$, *p*-methoxy benzaldehyde dimethyl acetal, DMF, rt, 18 h, 80%; (b) DIBAL, DCM, 0 ºC, 1 h.

Pleasingly, when the reaction temperature was reduced to −78 ºC the by-product **298** could not be detected. Also, the amount of DIBAL could be reduced to 2.3 equivalents without detrimental effect to the yield and the alcohol was isolated in quantitative yield. The presumed product was the primary alcohol **297**, however upon oxidation under Swern[94] or Dess-Martin[90] conditions the expected aldehyde

was not observed (scheme **95**). In the proton NMR spectrum two singlets of integration 2H were visible at 4.79 and 4.17 ppm, thereby indicating that the ketone **300** had been generated and the product from the DIBAL cleavage was in fact the secondary alcohol **399**.

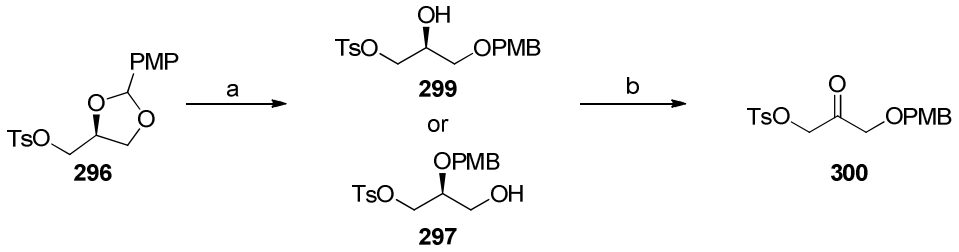


**Scheme 95: PMB acetal opening**

(a) DIBAL, DCM, −78 ºC, 1 h, quant; (b) Swern or Dess-Martin oxidation.

The generation of the secondary alcohol can be explained by the mechanism shown in scheme **96**. DIBAL can co-ordinate to the oxygen of the tosylate (**301**) and cleavage of the acetal results in the PMB protection of the primary alcohol (**302**).[131] Even though the protected primary alcohol **297** would have been preferred, the synthesis of the secondary alcohol **299** was straightforward. All steps to the secondary alcohol **299** were relatively high yielding; therefore this route was used as the basis to develop the desired enyne fragment.

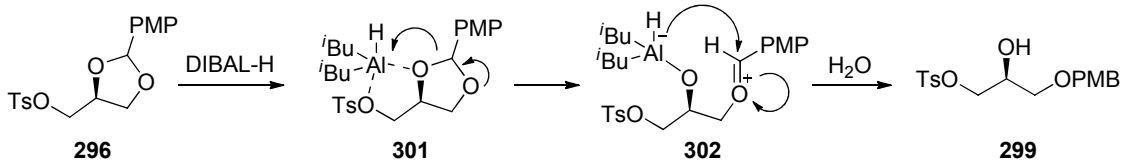


**Scheme 96: DIBAL opening of PMB acetal to generate secondary alcohol**

Methylation of the secondary alcohol furnished the methyl ether **303** in a high yield of 85% (scheme **97**), however a by-product (~10% yield) was routinely isolated after column chromatography. Comparison to literature data[132] indicated the epoxide **304** had been formed, where the alcohol had undergone an intra-molecular cyclisation and elimination of the tosyl group followed. Further optimisation of this reaction could be carried out in the future to eliminate this by-product. Oxidative cleavage of the PMB group with DDQ provided the key alcohol **295** in 79% yield.

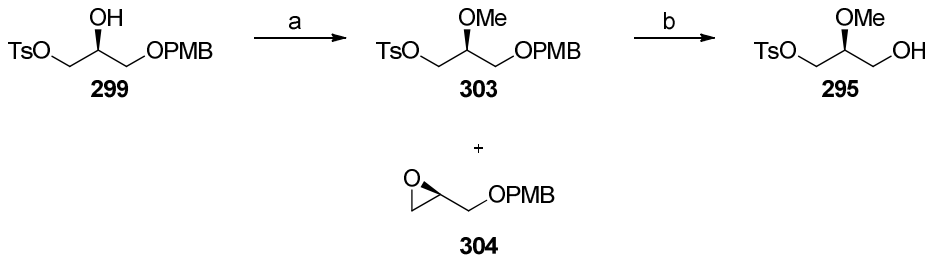


**Scheme 97: *O*-Methylation and PMB deprotection**

(a) MeI, $Ag_2O$, $CH_3CN$, 60 ºC, 18 h, 85%; (b) DDQ, DCM:$H_2O$ (10:1), 30 min, rt, 79%.

With a route to the key alcohol **295** developed (6 steps, 47% overall yield), investigations towards the synthesis of the vinyl iodide **305** were commenced. Based on the results obtained towards the Meyers synthesis of the oxazole fragment (Section **3.1.1**), it was predicted that the intermediate aldehyde would be unstable, therefore the aldehyde was carried straight through to the Takai olefination step.[96] Swern and Dess-Martin oxidations followed by Takai olefination were carried out in parallel and the Dess-Martin oxidation resulted in the greatest yield of the desired vinyl iodide **305** (scheme **98**). Evans *et al.* discovered that there is a solvent effect on the stereoselectivity of the Takai olefination, with a mixture of THF/dioxane providing the highest *E*/*Z* ratio.[133] In our investigations the highest yield of the vinyl iodide **305** obtained was 45%; with *E*/*Z* ratio of 5:1, as determined by NMR spectroscopy. These results were not always reproducible, the reaction is unreliable and the desired product could not be isolated every time the reaction was performed. It is likely that the intermediate aldehyde is unstable, and in addition, chromium (II) chloride is extremely hygroscopic and water sensitive. Steps taken to keep the chromium (II) chloride dry included, drying it under vacuum with a heat gun (~400 ºC) before use and oven dried glassware was used; in addition the reaction was carried out under an inert atmosphere of nitrogen or argon. Carrying out the reaction in a glove bag under nitrogen made no improvement to the yield. Nevertheless, adequate amounts of the vinyl iodide **305** were isolated in order to carry out subsequent reactions. Further optimisation of the oxidation and conversion to the vinyl iodide should be able to improve the yield. The Negishi reaction conditions

developed in Section **2.4** were successfully applied to the vinyl iodide **305** to provide the desired enyne fragment **306** in 86% yield.

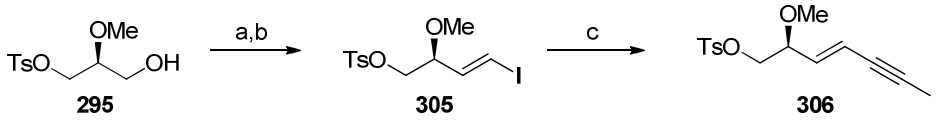


**Scheme 98: Completion of enyne**

(a) DMP, $NaHCO_3$, DCM, rt, 2 h, assume quant; (b) $CrCl_2$, $CHI_3$, THF:dioxane (1:6), rt, 18 h, 45% (5:1, *E*:*Z*); (c) i. propynylmagnesium bromide, $ZnCl_2$, toluene, rt, 15 min; ii. $Pd(PPh_3)_2Cl_2$, **305**, rt, 18 h, 86%.

## 4.3 Investigations into Oxazole C(1)-C(4) and Tosylate Coupling

### 4.3.1 Oxazole C-H Activation

Direct palladium catalysed C-H activation of (hetero)aromatic rings is a highly active area of current research in organic synthesis and its applications to the synthesis of C-2 substituted oxazoles is a recent development.[134] Based on recent advances in the palladium C-H activation of oxazole, a route towards the C(1)-C(9) fragment of disorazole $C_1$ was proposed as shown in scheme **99**. This involved the coupling between ethyl 4-oxazole carboxylate **244** and the tosylate **306**.

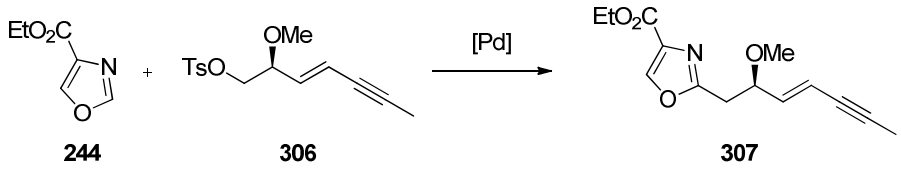


**Scheme 99: Proposed palladium C-H activation of oxazole**

### 4.3.1.1 Oxazole C-H Activation Background

Hoarau *et al*. realised the importance of the development of a methodology to regioselectively synthesise 2,4-substituted oxazoles, due to their occurrence in natural products. A model system investigating the coupling between ethyl 4-oxazole carboxylate **244** and phenyliodide was used as a basis to investigate reaction conditions to develop a C-2 regiospecific arylation of oxazoles (scheme **100**).[135] After screening a range of palladium catalysts, ligands and solvents, the optimum conditions to direct a C-2 arylation of oxazole **244** were found to be Pd(OAc) (5%), $Cs_2CO_3$ (2 equiv) and P(*o*-Tol)$_3$ in toluene. With these conditions, the oxazole **308** was generated in 86% yield with no C-5 substituted product or di-substituted product observed.

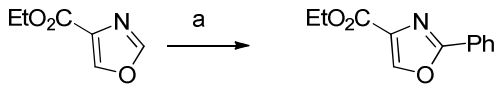


**244** **308**

**Scheme 100: Hoarau optimised Pd catalysed arylation conditions**

(a) PhI (1 equiv), Pd(OAc) (5%), $Cs_2CO_3$ (2 equiv), toluene, P(*o*-Tol)$_3$, 110 ºC, 86%.

During the optimisation studies Hoarau *et al*. discovered that the solvent and ligand can have an effect on the regioselectivity of the reaction. However, it was found that ligand/catalyst concentration did not have an effect on the reaction outcome.[135] Copper iodide has been shown to promote arylation at acidic sites of heterocycles,[136] however, applying a copper iodide co-catalyst to the reaction conditions with ethyl 4-oxazole carboxylate **244** failed. This therefore suggests that the reaction does not go by the cross-coupling mechanism shown by other heterocycles (scheme **101**, route A). An aromatic electrophilic substitution mechanism (scheme **101**, route B) has therefore been proposed. At this stage, the regioselectivity of the reaction was attributed to the steric bulk of the phosphine ligand, with the largest ligands selectively generating the C-2 phenyl product.

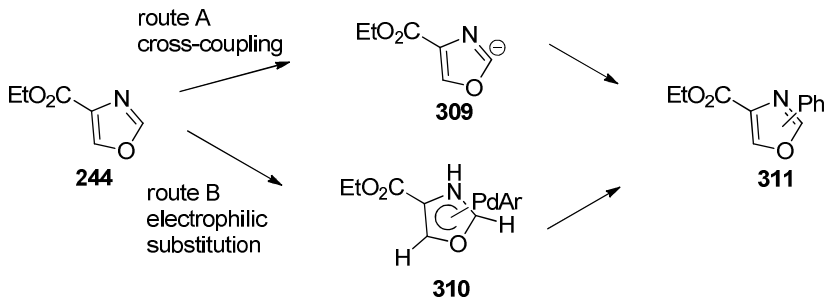


**Scheme 101: C-H activation mechanism**

Further developments have been made towards C-2 arylations of oxazoles, however of particular interest to our investigations were the C-2 alkylations of oxazoles. The first examples of alkylations of oxazoles by palladium catalysed C-H activation were published by the Hoarau group in 2009.[134] Ligand screening was carried out based on the reaction between oxazole **244** and 1-bromo-2-methylpropene. The optimum conditions were found to be palladium acetate, 2-(dicyclohexylphosphino)-biphenyl ligand (**313**), caesium carbonate and dioxane; which provided exclusively the C-2 alkenylated product **312a** in 92% yield (table **14**, entry 1). With these optimised conditions, the substrate scope of the reaction was investigated with alkenyl-, benzyl- and alkyl halides, the most interesting examples are highlighted in table **14**. The initial reaction between the oxazole **244** and butylbromide (1 equiv, table **14**, entry 2) resulted in an isolated yield of the product **312b** of 32%; but this was increased to 60% through the use of 2 equivalents of the bromide (table **14**, entry 3). Butylchloride (table **14**, entry 4) was inactive under these reaction conditions and screening of ligands could not generate the desired product **312b**. Reactions with the sterically hindered *t*-butylbromide also failed (table **14**, entry 5). Methylation with iodomethane successfully generated the methyloxazole **312d** (table **14**, entry 6) in 41% yield, however there was incomplete conversion of the starting material.

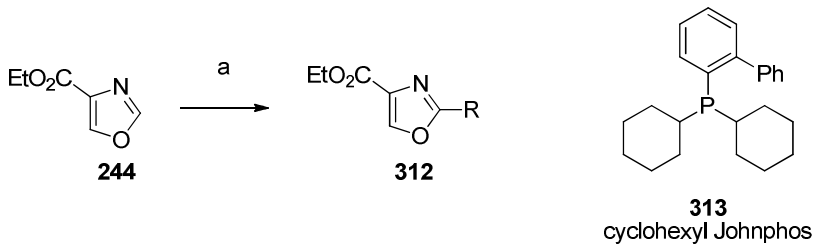


**244** **312** **313**
cyclohexyl Johnphos

(a) X–R, $Pd(OAc)_2$ (5 mol%), **313** (10 mol%), $Cs_2CO_3$ (2 equiv), 1,4-dioxane, 110 ºC, 18 h.

**Table 14: Hoarau Pd catalysed oxazole alkenylations and alkylations**

| Entry | Halide | X | Equiv | Product | Yield % |
|---|---|---|---|---|---|
| 1 |  | Br | 1 | 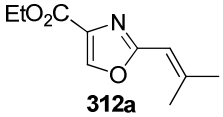 **312a** | 92 |
| 2 | 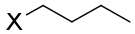 | Br | 1 | 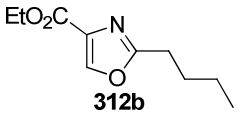 **312b** | 32 |
| 3 | | Br | 2 | | 60 |
| 4 | | Cl | 2 | | n.r. |
| 5 |  | Br | 2 | 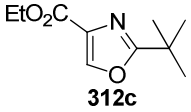 **312c** | n.r. |
| 6 |  | I | 2 | 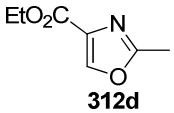 **312d** | 41 |

Miura *et al* have recently carried out a more detailed investigation into the palladium catalysed alkylation of benzoxazoles and oxazoles.[137] Catalysts and ligands were screened in order to optimise the reaction between benzoxazole and bromohexane. The optimal conditions were found to be [{$PdCl(\eta^3\text{-}C_3H_5)\}_2$] (3.75 mol%), P(*n*Bu)$_3$ (30 mol%) and LiO-*t*Bu (3 equivalents) in diglyme, heated at 120 °C for 4 hours. Application of the optimised conditions to oxazoles was also successful, as shown by the examples in figure **13**. An acetal protecting group was tolerated providing the product **314** in 67% yield from the alkyl chloride. In these examples with unfunctionalised alkyl halides the alkyl chloride provided higher yield (**315**, 60%) than the alkyl bromide (**316**, 44%). The majority of the published examples were

performed on 5-substituted oxazoles, however, one reaction was carried out on oxazole itself and the 2-subsituted product **317** was generated exclusively, albeit in a low yield of 25%.

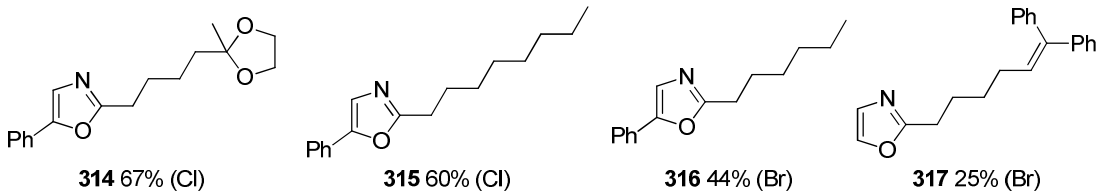


**314** 67% (Cl) **315** 60% (Cl) **316** 44% (Br) **317** 25% (Br)

**Figure 13: Miura [{PdCl($\eta^3$-$C_3H_5$)}$_2$] catalysed C-2 alkylation of oxazoles**

(a) 5-phenyl-1,3-oxazole or oxazole, X-R, [{PdCl($\eta^3$-$C_3H_5$)}$_2$] (3.75 mol%), P(*n*Bu)$_3$ (30 mol%), LiO-*t*Bu (3 equiv), diglyme, 120 °C, 4 h.

Nickel catalysis has also proved to be successful in alkylation of oxazoles, as demonstrated by Hu and co-workers (table **15**).[138] In these examples, alkyl iodides were just as successful as the bromides, with the octyl product **319a** being generated in 86% yield (table **15**, entry 1). The ether functionality was tolerated (table **15**, entry 2) and, surprisingly, the more sterically hindered (bromomethyl)cyclohexane also afforded the desired product **319c** in high yield (table **15**, entry 3). It is, however, noteworthy that reactions between benzoxazole and secondary alkyl halides such as cyclohexyl iodide and cycloheptyl bromide failed.

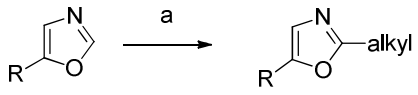


**318** **319**

(a) X-R, [(MeNN$_2$)NiCl] (5 mol%), CuI (5 mol%), LiO-*t*Bu (1.4 equiv), dioxane, 140 °C, 16 h.

**Table 15: Hu Nickel catalysed C-2 alkylation of 5-substitued oxazoles.**

| Entry | R | Halide | Yield % |
|---|---|---|---|
| 1 | 4-OMe-($C_6H_5$) | 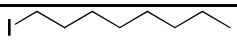 | 86 (**319a**) |
| 2 | 4-OMe-($C_6H_5$) | 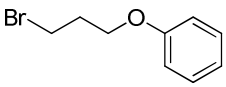 | 81 (**319b**) |
| 3 | 4-Br-($C_6H_5$) | 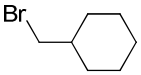 | 76 (**319c**) |

### 4.3.1.2 Oxazole C-H Activation Results

Investigations were carried out into coupling ethyl 4-oxazole carboxylate (**244**) and readily available compounds to act as model substrates for the C(5)-C(9) tosylate **306** or bromide. The optimised conditions developed by Hoarau[134] were chosen for this investigation. Ethyl 4-oxazole carboxylate **244** was stirred at 110 ºC with the coupling partner, palladium acetate, cyclohexyl Johnphos (**313**) and caesium carbonate in dioxane overnight, the reaction mixture was filtered through celite and the crude reaction mixtures were analysed by NMR spectroscopy (table **16**).

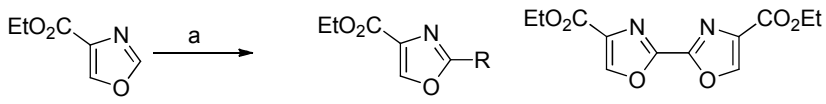


**244** **312** **320**

(a) X-R, $Pd(OAc)_2$ (5 mol%), cyclohexyl Johnphos **313** (10 mol%), $Cs_2CO_3$ (2 equiv), 1,4-dioxane, 110 ºC, 18 h.

**Table 16: Attempted Pd catalysed alkylation of ethyl 4-oxazole carboxylate with model substrates**

| Entry | X-R | X | Result |
|---|---|---|---|
| 1 | 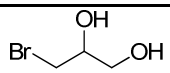 | | Trace **312** and **320** [a] |
| 2 | 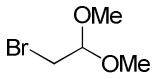 | | Isolated **320** |
| 3 | 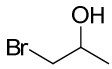 | | No reaction [a] |
| 4 | 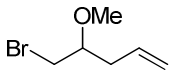 | | No reaction [a] |
| 5 | 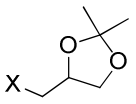 | Cl | Isolated **320** |
| 6 | | Br | Isolated **320** |
| 7 | | I | No reaction [a] |
| 8 | | OTs **290** | Isolated **320 a**nd unidentified by-product |
| 9 | 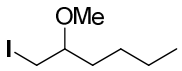 **322** | | Trace **312** by NMR and mass spectrometry |
| 10 | 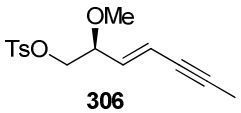 **306** | | Trace product **307** |
| 11 | 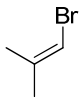 | | 95% yield of **312a** isolated |

[a] from analysis of crude proton NMR spectrum

In all reactions, the major component of the crude reaction mixture was the oxazole starting material **244**. No product **312** could be isolated from reactions with alkyl bromides featuring a β-alcohol or methyl ether (table **16**, entries 1-4). In some cases, a trace of product **312** could be identified in the NMR spectrum, however after attempted isolation only homo-coupled oxazole **320** could be isolated. Comparisons

between the chloro-, bromo-, iodo- and tosyl- substrates (table **16**, entries 5-8) proved inconclusive and only homo-coupled oxazole **320** could be isolated. In the case of the tosylate (table **16**, entry 8), a by-product was isolated where the tosyl group was present. However, it appeared that the ethyl ester had been displaced; but this product was not fully characterised and identified. It would appear that the oxazole **244** is more reactive than the halides, thereby generating the homo-coupled oxazole **320** and reducing the availability of the oxazole to couple to the halide.

1-Iodo-2-methoxyhexane (which was deemed a better model substrate) **322** was readily synthesised *via* a methanolysis and iodination of 1-hexene **321** (scheme **102**). Following the reaction with 1-iodo-2-methoxyhexane (table **16**, entry 9), traces of the desired product **312** could be seen in the proton NMR spectrum, and in addition, a peak at *m/z* 262 representing $[M+Na]^+$ was visible in an LC-MS of the crude mixture; but unfortunately, the product could not be isolated.

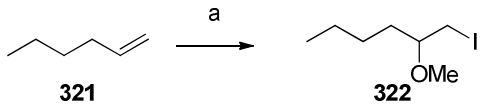


**Scheme 102: Synthesis of 1-iodo-2-methoxyhexane**

(a) $I_2$, $Ag_2O$, MeOH, 0 ºC, 6 h, 90%.

Since the reaction of iodoalkane **322** in entry 9 showed potential, further investigations towards optimisation for this substrate were pursued. The literature reaction with 1-bromo-2-methylpropene (table **16**, entry 11)[134] was shown to be reproducible in our hands, affording the alkenylated product **312a** in 95% yield. This result indicated that perhaps, a slight variation of conditions was required to enable the reaction of iodoalkane **322** to proceed in greater yield. Screening common palladium catalysts including $Pd(dba)_2$, $Pd(PPh_3)_4$ and $Pd(PPh_3)_2Cl_2$ and alteration of the solvent to THF failed to improve the yield and the two starting materials (**244** and 1-iodo-2-methoxyhexane **322**) were the main components of the crude mixture. Once the tosylate **306** had been synthesised, a palladium coupling was attempted with ethyl 4-oxazole carboxylate **244** (table **16**, entry 10). Unfortunately, only traces of product could be seen in the NMR spectrum and column chromatography only resulted in the starting material oxazole **244** being recovered.

Hu had shown that the hindered substrate (bromomethyl)cyclohexane can be successfully coupled with a 5-substituted oxazole[138] under nickel/copper catalysis, and we wanted to see if these conditions could be applied to ethyl 4-oxazole carboxylate **244**. Applying Hu's reaction conditions[138] and substituting the oxazole substrate for ethyl 4-oxazole carboxylate **244** generated inconclusive results (scheme **103**). The major component of the crude NMR spectrum was the oxazole starting material **244**, but a singlet was apparent in the proton NMR spectrum of the crude mixture at 8.22 ppm. While this is representative of the C-5 proton of a 2,4-substituted oxazole, the desired product **323** could not be isolated. Given that the high yields reported by Hu could not be repeated on ethyl 4-oxazole carboxylate (**244**), no further investigations with other substrates were carried out regarding this nickel/copper catalyst and our focus was now towards the lithiation approach.

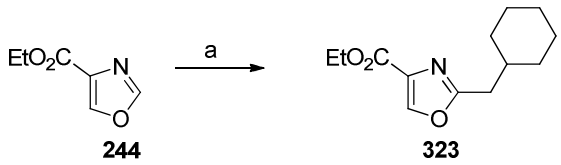


**244** **323**

**Scheme 103: Attempted Ni catalysed alkylation of ethyl 4-oxazole carboxylate with (bromomethyl)cyclohexane**

(a) (bromomethyl)cyclohexane, [($MeNN_2$)NiCl] (5 mol%), CuI (5 mol%), LiO-*t*Bu (1.4 equiv), dioxane, 140 °C, 16 h.

## 4.3.2 Oxazole Lithiation

C-2 lithiation of oxazole is a developed methodology,[139] and with the tosylate **306** in hand, it was proposed that the C(1)-C(9) fragment **324** could be constructed *via* a regioselective C-2 lithiation of the protected alcohol oxazole **232** as shown in scheme **104**.

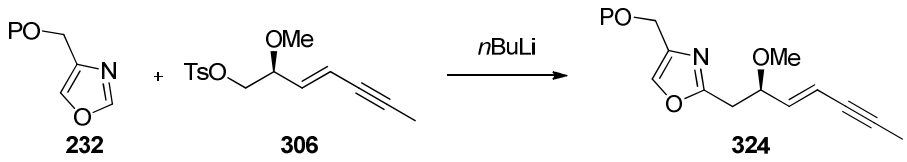


**Scheme 104: Proposed oxazole lithiation strategy**

### 4.3.2.1 Oxazole Lithiation Background

The C-2 proton of oxazole (**325**) has been shown to be the most acidic,[140] however investigations by Hodges *et al.* into the lithiation of oxazole (**325**) lead to some unexpected results. Lithiation of oxazole (**325**) with *n*BuLi at −75 ºC (scheme **105**), followed by exposure to benzaldehyde resulted in only 2% yield of the expected product **328** and 20% yield of the C-4 substituted product **331** (plus 20% benzyl alcohol isolated).[141] This observation can be explained by the aldehyde reacting with the ring open enolate **327** form of the oxazole, faster than it reacts with the lithium species **326**. A series of temperature controlled experiments demonstrated that the C-2 substituted product **328** was not formed at temperatures below 0 ºC. Following the lithiation of oxazole **325** with *n*BuLi a range of electrophiles were investigated, and it was found that aldehydes predominantly afforded the C-5 substituted products. However, reactions with iodobutane and benzylbromide were unsuccessful, even after prolonged reaction times at higher temperature

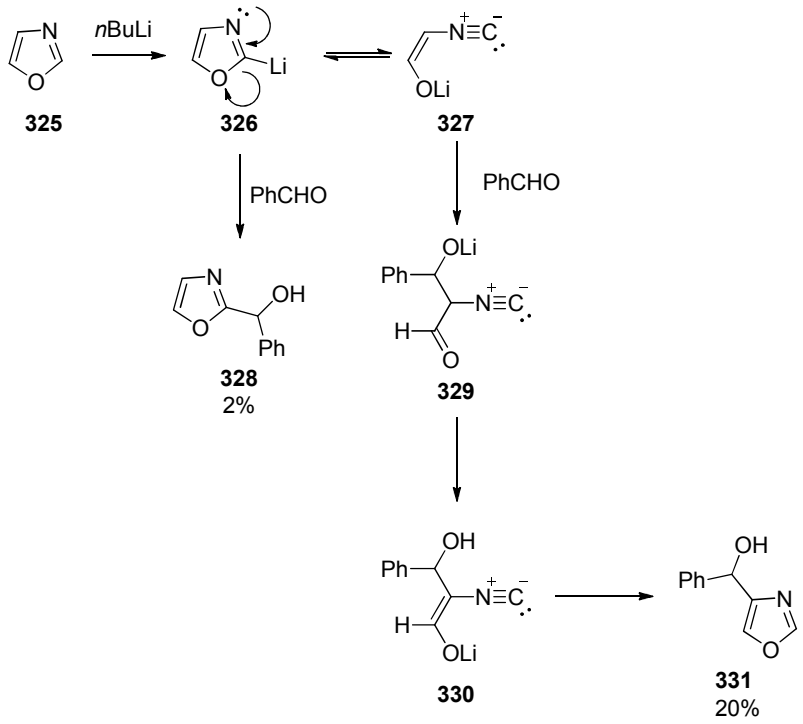


**Scheme 105: 2-Lithiooxazole ring opening mechanism**

Jacobi *et al.* carried out studies into the alkylation of the disubstituted oxazole **332**, and in all cases, only the formation of the ring opened products **333** was observed (table **17**).[142] These results contrast those published by Hodges, where no reaction was observed with alkyl halides. It is postulated that these differences in the observed results could be due to the different substituents of the oxazoles **325** and **332** resulting in different enolate stabilities. In the case of the results observed by Jabobi, the enolate could be stabilised by lithium co-ordination between the oxygens of the ethyl ether and the oxazole, therefore the ring opening of **332** is a fast process and the alkyl halides can go on to react with the enolate.

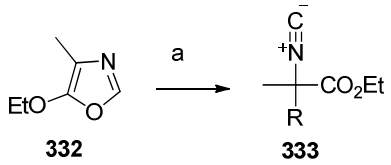


**332** **333**

(a) i. *n*BuLi, –78 ºC; ii. R-X.

**Table 17: Jacobi observation of ring opened products after attempted C-2 alkylation**

| Entry | R-X | Yield % (isolated/GC) |
|---|---|---|
| 1 | MeI | 81/93 |
| 2 | *n*BuI | 76/99 |
| 3 | Benzyl bromide | 77/86 |

Vedejs and Monahan sought to solve the problem of the ring opening of oxazole in order to devise a regioselective, reliable method for the synthesis of 2-substituted oxazoles.[143] They proposed that a Lewis acid could be used to complex to the nitrogen lone pair (**335**) and therefore prevent the ring opening; this complexation was also predicted to activate the C-2 proton for metallation.[143] Pleasingly, this hypothesis was true and only C-2 substituted products (**336**) were observed and no ring opened products were formed after electrophiles were reacted with **334** following lithiation (table **18**). Reactions with iodomethane and an alkyltriflate successfully generated the 2-substitued products **336** in good yields of 74% and 65% respectively (table **18**, entries 1 and 2). The reaction between the alkyltriflate and unsubstituted oxazole (**325**) also exclusively formed the 2-substituted product (76% yield).

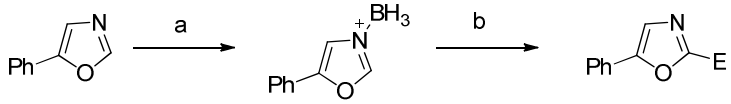


**334** **335** **336**

i. $BH_3$•THF, –78 ºC; ii. *n*BuLi; iii. $E^+$, –20 ºC.

**Table 18: Vedejs alkylation examples of C-2 oxazole lithiation mediated by $BH_3$•THF coordination**

| Entry | $E^+$ | Yield % |
|---|---|---|
| 1 | MeI | 74 |
| 2 | $PhCH_2CH_2OTf$ | 65 |

An example of lithiation of a C-4 protected alcohol oxazole is featured in Shioiri and co-workers' studies towards the synthesis of bengazoles.[144] Lithiation of **246** and **337** with *n*BuLi, followed by addition of 5-formyloxazole resulted in the secondary alcohols **339a** and **339b** in moderate yields (scheme **106**). The protecting group appears to have an effect on yield; the TBS product **339a** was isolated in 35% yield and the TBDPS product **339b** was isolated in 50% yield. The reaction took 3 days and resulted in moderate yields; moreover, attempts to improve the yield by altering the base, solvent and by the addition of a Lewis acid all failed.[144]

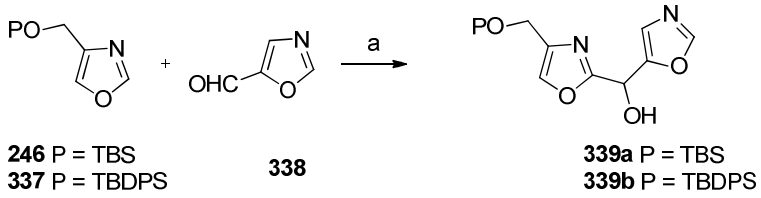


**246** P = TBS
**337** P = TBDPS

**338**

**339a** P = TBS
**339b** P = TBDPS

**Scheme 106: C-2 lithiation of 2-substituted oxazole**

(a) *n*BuLi, $Et_2O$, −75 ºC to 0 ºC, 3 days, **339a** 35%, **339b** 50%.

## 4.3.2.2 Oxazole Lithiation Results

Previous attempts at synthesising the alcohol **245** (Section **3.2.2.2**) had failed due to the volatility of the compound and the consequential difficulty in handling. However, we were able to purchase 500 mg of alcohol **245** to try out a few small scale reactions to attempt to complete the chiral synthesis of the C(1)-C(9) fragment of disorazole $C_1$. The alcohol was protected with a MOM group (**340**), based upon results obtained towards the synthesis of the racemic fragment (Section **2.6.6**), and a TBDMS group (**246**) based upon the results observed by Shioiri *et al.* (scheme **107**). Synthesis of the TBDPS protected alcohol **337** using TBDPSCl and imidazole in DMF was also attempted; however it could not be obtained in sufficient purity (possibly due to contamination with TBDPS alcohol) to advance to the next step. It was hoped that protection of the alcohol would ease the handling of the oxazole and it was thought that the protecting group could have an effect on the regioselectivity of the reaction.

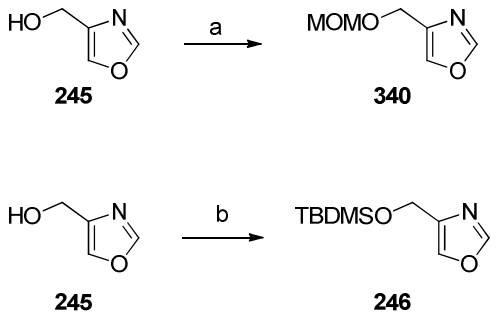


**Scheme 107: Alcohol protection**

(a) i. NaH, THF, 0 ºC, 10 min; ii. MOMCl, 3 h, rt, 73%; (b) 2,6-lutidine, TBDMSOTf, DCM, 0 ºC, 1 h, 85%.

Based on the literature, our desired reaction appeared feasible and conditions using borane and *n*BuLi were adopted in order to direct C-2 lithiation. Shioiri *et al* reported exclusive formation of the C-2 substituted product without the use of borane;[144] however, the electrophile in their case was an aldehyde, and the tosylate **306** or iodide **341** to be used in our synthesis were predicted to be less reactive. Therefore, the addition of borane was more likely to be beneficial than detrimental. The reaction with MOM protected oxazol-4-ylmethanol (**340**) and iodomethane showed promising results as product **212c** was isolated, albeit in a low yield (table **19**, entry 1). However, the reaction with the tosylate **306** failed and only the two starting materials (**306** and **340**) were visible in the crude NMR spectrum (table **19**, entry 2). Conversion of the tosylate **306** to the more reactive iodide **341** appeared to have no effect and no product could be seen in the NMR spectrum of this reaction (table **19**, entry 3). The lithiation of oxazoles is a temperature dependent reaction, but unfortunately, even after leaving the tosylate and iodide reactions for 3 days at room temperature, none of the product **215** could be detected. The reaction with the TBS protected alcohol **246** and iodomethane (table **19**, entry 4) was more successful than with the MOM protected oxazole. The desired product **212a** was the main component of the crude reaction mixture, demonstrating a 4:1 ratio of product **212a** to starting material **246** by proton NMR analysis. Furthermore, this reaction was cleaner than the reaction with iodomethane and MOM protected alcohol **340**. To further test the lithiation with the TBS protected alcohol, a reaction with 1-iodo-2-methoxyhexane (**322**) was performed and traces of the desired product could be observed in the proton NMR spectrum. In addition, a peak observed at *m/z* 326 in the

negative ESI mass spectrum is representative of $[M–H]^-$. A large scale, reliable synthesis of the TBS (or TBDPS) protected alcohol **246** is required in order for optimisation and further investigation into this lithiation reaction.

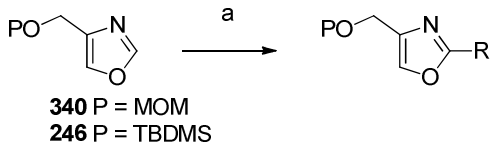


**340** P = MOM
**246** P = TBDMS

(a) i. $BH_3$•THF, rt; ii. *n*BuLi, −78 ºC; iii. X-R, −78 ºC to rt.

**Table 19: Investigations into lithiation of TBS and MOM protected alcohol oxazole**

| Entry | P | Substrate | Result |
|---|---|---|---|
| 1 | MOM | MeI | 10% yield **212c** (P = MOM, R = Me) |
| 2 | MOM | 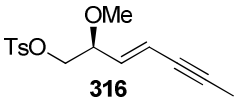 **316** | No reaction |
| 3 | MOM | 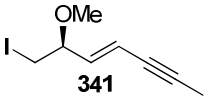 **341** | No reaction |
| 4 | TBS | MeI | 4:1 (**212a**:**246**) unseparable mixture 70% overall yield |
| 5 | TBS | 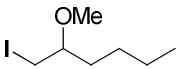 **322** | Trace product in NMR and identified in mass spectrum |

## 4.3.3 Summary

Investigations were carried out into the palladium catalysed C-H activation of ethyl 4-oxazole carboxylate, followed by alkylation with a number of model substrates. Traces of product could be identified by NMR spectroscopy and mass spectrometry, however further studies and optimisation will be required in order for the C(1)-C(9) fragment to be synthesised using this route.

Based on the literature evidence and our preliminary results with the TBS protected oxazole, the lithiation strategy coupled with the tosylate or iodide appears to be the most practical route towards the synthesis of the C(1)-C(9) fragment of disorazole

$C_1$. Unfortunately, at this time only small amounts of the oxazole and tosylate were available and optimisation and extensive studies into this reaction were not possible. Further investigations towards a reliable synthesis of the alcohol **245** are required, as well as optimisation of the Takai olefination (or alternative routes from the alcohol **295** to enyne **306**). The application of novel tosylate **306** towards heterocyclic analogues will be discussed in the next section.

## 4.4 Heterocyclic Analogues

As highlighted in the discussion of disorazole SAR in section **1.3**, to our knowledge, no investigations have been carried out regarding heterocyclic analogues of disorazole $C_1$. Centred around our desire to construct the ester linkage at C(1) of disorazole $C_1$ *via* an Evans-Tishchenko (ET) reaction, the Hulme group recently reported the first examples of the use of heteroaryl aldehydes in the ET reaction.[145] The Evans-Tishchenko reaction was modelled using the β-hydroxyketone **349** and the results showed it to be a promising reaction for generating the required ester in disorazole $C_1$, particularly with electron-poor heteroaryl aldehydes.

Application of the optimised ET conditions of $SmI_2$ (2.0 equiv), benzaldehyde (2.0 equiv), heteroaryl aldehyde (4.0 equiv), **342** (1.0 equiv), resulted in excellent yields and high diastereoselectivity of the products **346** using furancarboxaldehydes and thiophenecarboxaldehydes (table **20**, entries 1-4).[145,146] Substituted furans and thiophenes were also tolerated (table **20**, entries 5-8), particularly electron withdrawing substituents such as a nitro group (table **20**, entry 6). Bicyclic systems such as benzo[*b*]thiophene-3-carboxaldehyde and *N*-Boc-indole-3-carboxaldehyde were also successful (table **20**, entries 9 and 10).

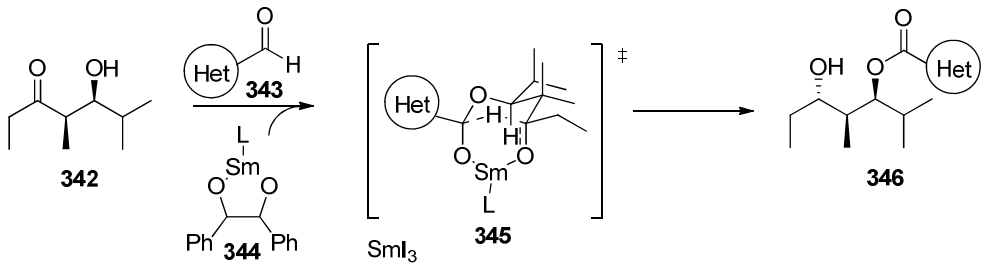


i. $SmI_2$ (2.0 equiv), PhCHO (2.0 equiv), THF, rt, 30 min; ii. HetCHO (4.0 equiv), **342** (1.0 equiv), THF, −15 ºC, 1 h.

**Table 20: Scope of heteroaryl aldehyde ET reaction**

| Entry | Aldehyde | Yield % | dr |
|---|---|---|---|
| 1 | 3-furancarboxaldehyde | 98 | >95:5 |
| 2 | 2-furancarboxaldehyde | 99 | 91:09 |
| 3 | 3-thiophenecarboxaldehyde | 99 | >95:5 |
| 4 | 2-thiophenecarboxaldehyde | 99 | 91:09 |
| 5 | 5-phenylfuran-2-carboxaldehyde | 92 | >95:5 |
| 6 | 5-nitrofuran-2-carboxaldehyde | 93 | >95:5 |
| 7 | 5-bromofuran-2-carboxaldehyde | 90 | 94:6 |
| 8 | 5-bromothiophene-2-carboxaldehyde | 99 | >95:5 |
| 9 | benzo[*b*]thiophene-3-carboxaldehyde | 95 | 92:8 |
| 10 | *N*-Boc-indole-3-carboxaldehyde | 90 | 90:10 |

*N*-Boc-indole-3-carboxaldehyde (**349**) performed well in the ET reaction (table **20**, entry 10), however no reaction was observed with the unprotected indole **347**.[146] It is possible that complexation with samarium results in delocalisation around the indole, which would lead to the stable enolate species **348**, rendering hemi-acetal formation with the alcohol of the β-hydroxyketone unfavourable (scheme **108**). However, Lewis-acid activation of the aldehyde is favoured in the Boc-protected species **350** and the ET reaction proceeds with excellent yield.

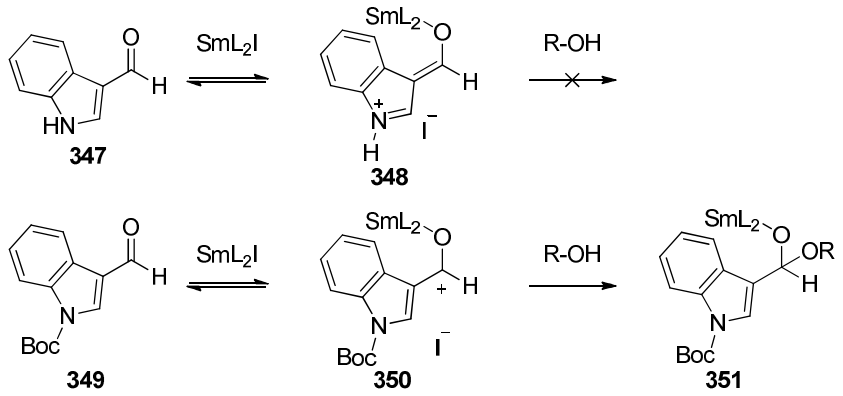


**Scheme 108: Possible enolate formation of Sm intermediate with indole**

Interestingly, it appears that a nitrogen at the 2-position relative to the aldehyde has a detrimental effect in the ET reaction. Examples of heteroaryl aldehydes which have failed in the ET reaction (figure **14**) include 2-methyl-oxazole-4-carbaldehyde **352**, 2-pyridine-carboxaldehyde **353**, 2-pyrrole carboxaldehyde **354** and *N*-methyl-2-pyrrole carboxaldehyde **355**. This observation could be due to the nitrogen being in a favourable position to co-ordinate to the samarium (**356**) and thereby rendering the samarium intermediate inactive. A brief investigation was carried out in the Hulme group with 2-pyridine-carboxaldehyde (**353**) to attempt to overcome the issue of nitrogen co-ordination. Attempts at methods such as 'capping' the samarium with cyclen, tetraglyme or BINAP, thus disabling the nitrogen co-ordination, gave only poor yields of product in the ET reaction.[146] Co-ordination of the lone pair of the nitrogen into a quarternised salt also failed to improve the yield of the reaction; however, low solubility of the salt could have been a factor in this low yield.[146] Further investigations into the ET reaction with heteroaryl aldehydes are required and in particular with the oxazole.

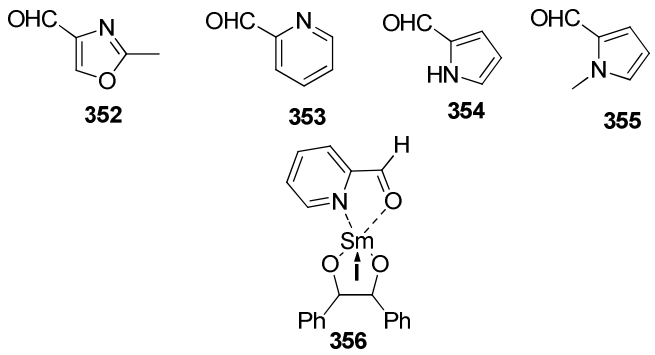


**Figure 14: Heterocycles which failed in preliminary ET reaction studies**

In view of the previous results obtained with heteroaryl aldehydes in the ET reaction, novel heterocyclic analogues were designed that could readily be synthesised by coupling to the tosylate **306** (figure **15**). A rapid route towards such analogues could be *via* an *N*-alkylation, therefore the pyrrole **357,** pyrazole **358** and indole **360** analogues were designed. These analogues do not have a nitrogen in the 2-position relative to the aldehyde and the nitrogen is alkylated, which will prevent resonance structures, such as the postulated enolate intermediate **348**. The triazole analogue **359** does possess a nitrogen in the 2-position relative to the aldehyde, however this heterocycle has not yet been subjected to the ET reaction. The triazole can be readily synthesised from the tosylate **306** and synthesis of this analogue would allow SAR development through comparison of the heterocycles containing 1, 2 and 3 nitrogen atoms. Taking into consideration the published analogues of disorazole $C_1$, preservation of the five membered heterocyclic shape was desired to prevent an alteration of the overall 3D structure of disorazole $C_1$. However, *N*-Boc-indole-3-carboxaldehyde (**349**) had performed well in the preliminary ET studies and we had an accessible route to this analogue through *N*-alkylation.

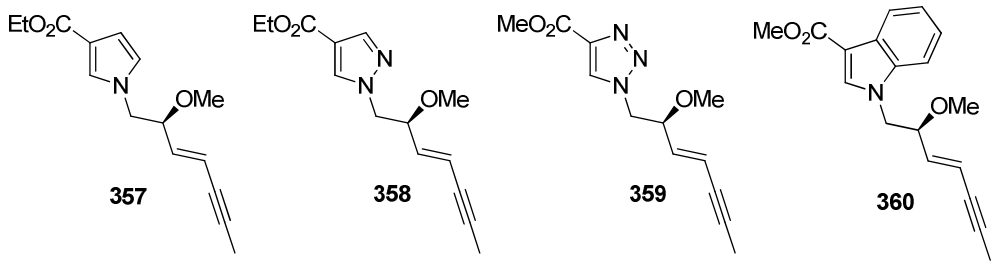


**Figure 15: Designed heterocyclic analogues**

The pyrazole analogue **358** was synthesised *via* an *N*-alkylation of commercially available ethyl 1*H*-pyrazole-4-carboxylate (**361**) with potassium carbonate and tosylate **306** (scheme **109**). The reaction was stirred at room temperature for 48 hours, yet the reaction did not go to completion and upon work-up and purification by column chromatography the pyrazole analogue **358** was obtained in 58% yield.

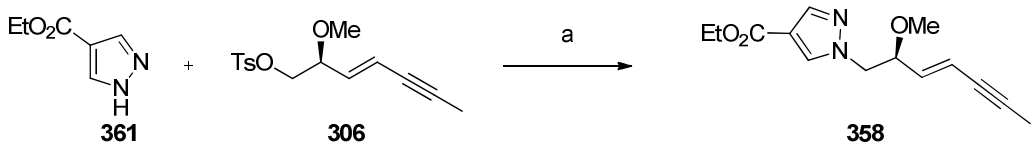


**Scheme 109: Pyrazole analogue synthesis**

(a) $K_2CO_3$, DMF, rt, 48 h, 58%.

The pyrrole **364** was synthesised in 43% yield following literature procedures,[147] *via* the van Leusen method,[148] from TosMIC (**362**) and ethylacrylate (**363**). This moderate yield is comparable to the literature procedure and a by-product was observed, possibly formed by a Michael addition of the pyrrole to ethyl acrylate. Under the alkylation conditions used for the synthesis of the pyrazole analogue, with potassium carbonate no reaction was observed between the pyrrole **364** and tosylate **306** after 72 h. The use of the stronger base sodium hydride did not improve the reaction. A trace of product **357** could be seen by proton NMR spectroscopy after using potassium hydroxide as the base, but unfortunately the product **357** could not be isolated.

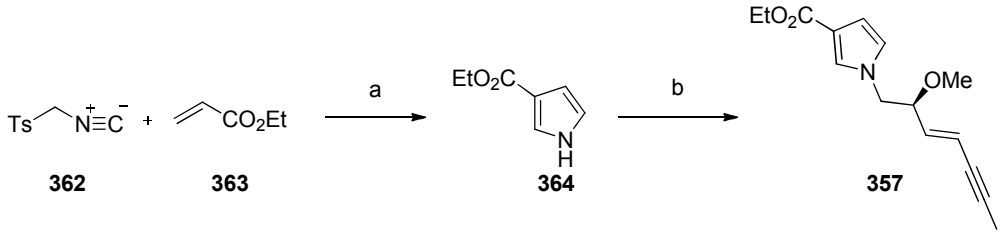


**Scheme 110: Pyrrole analogue synthesis**

(a) NaH, $Et_2O$/DMSO (2:1), rt, 3 h, 43%; (b) **306**, KOH, DMSO, rt, 18 h.

Poor conversion was also observed for the alkylation of the indole **365** (scheme **111**). The alkylation was attempted with sodium hydride at room temperature for up to 72 hours and at an elevated temperature of 80 ºC, however the conversion could not be

increased and only traces of the desired product **360** were observed by proton NMR spectroscopy. Model studies with tosylates are currently ongoing within the Hulme group to optimise the *N*-alkylations of these heterocycles.

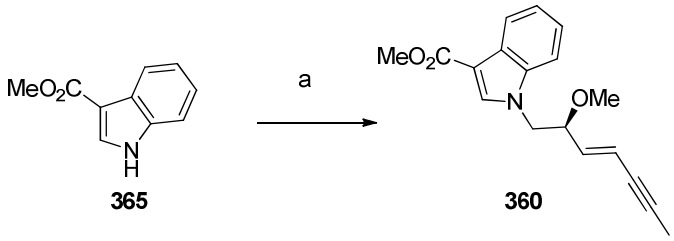


**Scheme 111: Attempted indole analogue synthesis**

(a) **306**, NaH, DMF, rt, 72 h.

The tosylate **306** was readily converted to the azide *via* a displacement with sodium azide in quantitative yield (scheme **112**). A copper catalysed azide-alkyne cycloaddition reaction[149] between the azide and methyl propiolate resulted in the triazole analogue **359** in 58% yield. The "click" reaction is usually very high yielding and this observed moderate yield can be attributed to the high volatility of the azide, which meant the exact amount of azide used in the reaction was unknown.

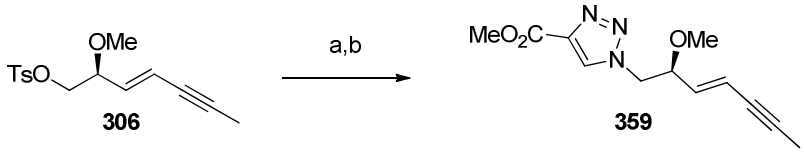


**Scheme 112: Triazole analogue synthesis**

(a) $NaN_3$, DMSO, reflux, 2 h, quant; (b) methyl propiolate (1.1 equiv), $CuSO_4$ (10 mol %), sodium ascorbate (20 mol %), $H_2O$:*t*BuOH (1:2), TBTA (10 mol %), rt, 18 h, 58%.

## 4.5 Summary

A novel route towards the synthesis of the C(1)-C(9) fragment and heterocyclic analogues of disorazole $C_1$ has been developed. The tosyl enyne side chain is a novel route towards the synthesis of the C(1)-C(9) fragment of disorazole $C_1$, this side chain also enables a highly convergent synthesis of the fragment and heterocyclic analogues. Optimisation of the route from the alcohol **295** to the vinyl iodide **305** is required.

The successful synthesis of the stable tosyl enyne side chain **306** opened up the possibility of palladium C-H activation of the oxazole. Alkylation of oxazoles under palladium catalysis is a new and emerging area of research and further exploration of catalysts, ligands and solvents is required to find the optimum conditions for the coupling of the oxazole and tosylate (or iodide) fragments. Lithiation of oxazole was attempted and appears to be the most promising route towards the synthesis of the C(1)-C(9) fragment of disorazole $C_1$, however a reliable synthesis of the TBS (or TBDPS) protected oxazole alcohol is first required in order for further investigations to be carried out.

Two fragment analogues have successfully been synthesised, namely the pyrazole and triazole. Once these are incorporated into the total synthesis of disorazole $C_1$ SAR can be developed to gain insight into the role of the oxazole in the binding of disorazole $C_1$ to tubulin.

# 5 Future work

## 5.1 Completion of C(1)-C(9) Fragment

The immediate future work for this project will revolve around optimisation of the synthesis of the vinyl iodide **305** from the alcohol **295** (scheme **113**). This will be achieved either through optimisation of the Takai olefination; or alternative routes such as conversion to the alkyne with the Ohira-Bestmann reagent, followed by hydrostannylation/metal-iodine exchange to the (*E*)-vinyl iodide, based on Hoffmann's synthesis of disorazole $C_1$.[30]

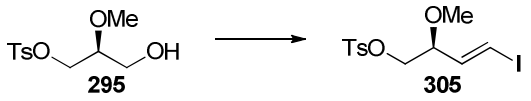


**Scheme 113: Synthesis of vinyl iodide**

Another possible option which would further shorten the synthesis of the enyne **306** would be a Wittig reaction between the aldehyde **366** and phosphorus ylide **250** (scheme **114**). There is literature precedent for Wittig reactions performed in the presence of tosylates[150] and the literature discussed in section **3.2.5** suggests that the (*E*)-isomer would be the major product following a Wittig reaction with **250**.

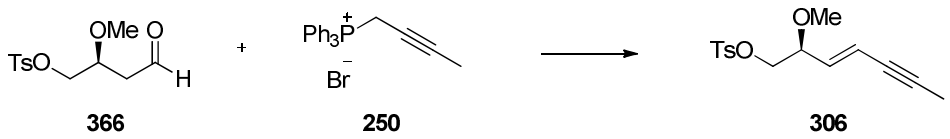


**Scheme 114: Proposed Wittig reaction**

Based on encouraging preliminary results, once a reliable route to the tosylate **306** has been established, further investigations into the palladium catalysed C-H activation and lithiation of the oxazole can be performed. C-H activation of oxazoles followed by alkylation is dependent on a number of factors, therefore screening to establish the optimum combination of ligand, catalyst, solvent and substrate (X = OTs, OTf, I, Br or Cl) will be required. Based on our limited oxazole lithiation

investigations, lithiation of the TBDMS protected oxazole showed the most promise, however a robust synthesis of the required oxazole **246** (or the TBDPS protected oxazole) needs to be established.

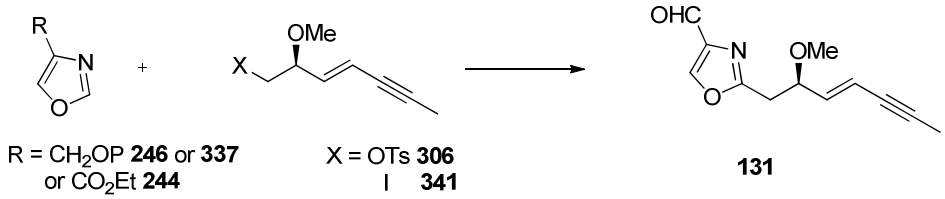


**Scheme 115: Completion of C(1)-C(9) fragment**

## 5.2 Heterocyclic Analogues

In order to develop a detailed SAR of disorazole $C_1$ a range of heterocyclic analogues of the C(1)-C(9) fragment are required. It is anticipated that the heterocyclic analogues shown in figure **16** could be synthesised after further development of the C-H activation and lithiation methodology. Possible heterocyclic analogues include furan **367**, thiophene **368**, thiazole **369**, isoxazole **370** and a 2,5-substituted oxazole **371**. Without greatly altering the 3D-shape of disorazole $C_1$ these analogues could provide insight into the role of the heteroatoms in the binding of disorazole $C_1$ to tubulin. To complete the initial studies detailed in this thesis, model studies are currently ongoing in the Hulme group to optimise the *N*-alkylation of pyrrole and indole with tosylates and a simple change of base to $Cs_2CO_3$ appears to provide alkylated products in high yield.[151]

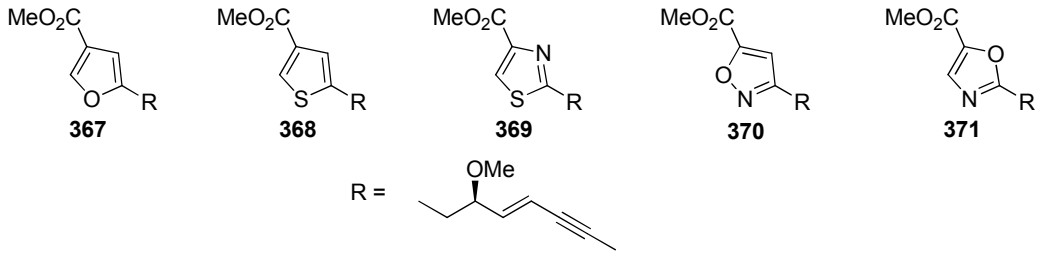


**Figure 16: Possible heterocyclic analogues**

## 5.3 Evans-Tishchenko Coupling

Further heterocyclic Evans-Tishchenko reaction model studies are underway, and particular attention is required regarding the reaction of the oxazole with the β-hydroxyketone. It is anticipated that, based on previous results, the pyrrole, pyrazole, indole, thiophene and furan analogues would be successful substrates for the Evans-Tishchenko reaction.[145,146] If however, a method for the Evans-Tishchenko reaction with the oxazole cannot be established, an alternative route towards the desired fragment **374** would be to construct the ester linkage *via* a standard esterification between the alcohol **372** and carboxylic acid **373** (scheme **116**). The required alcohol could be synthesised from the β-hydroxyketone **130** *via* an ET reaction with a sacrificial aldehyde such as benzaldehyde to generate the ester. The free alcohol formed would need to be protected and hydrolysis of the benzyl ester would yield the required alcohol **372**.

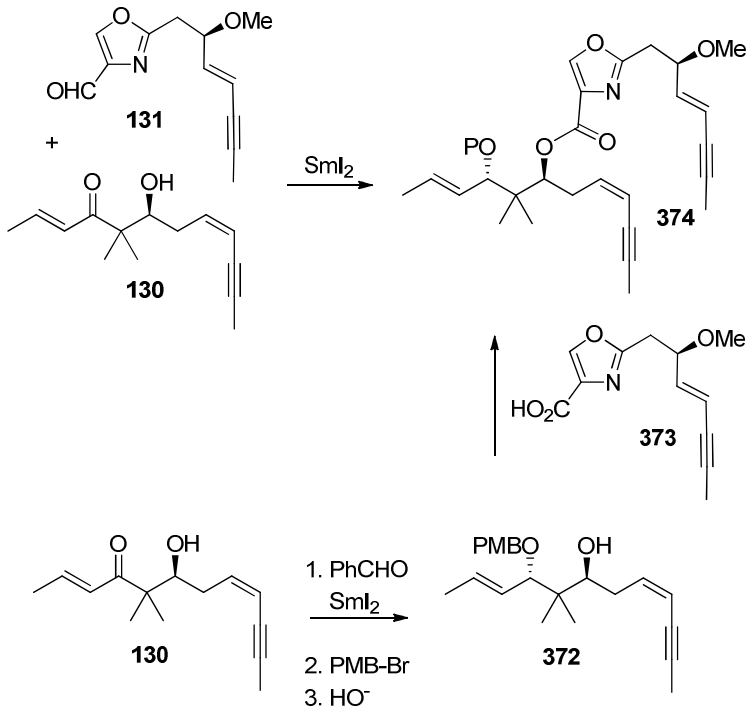


**Scheme 116: Desired Evans-Tishchenko reaction and esterification back-up**

## 5.4 Alkyne Metathesis

Alkyne metathesis, and particularly ring-closing alkyne metathesis (RCAM), is a relatively new field of research and has recently been applied to the total synthesis of natural products including epothilone A and C[152] and amphidinolide.[153] RCAM is a reliable method for the construction of cyclic alkynes, and in turn, stereoselective alkenes *via* partial hydrogenation. There are however, limited examples of the synthesis of cyclic diynes *via* a dimeric alkyne cross metathesis followed by RCAM.

In studies directed towards the synthesis of epothilones A and C the Fürstner group have investigated the use of new RCAM catalysts and have reported an example of the formation of a cyclic diyne.[152] After treating the diyne **375** with the catalyst [Mo{(*t*Bu)(3,5-dimethylphenyl)N}$_3$] **378** the cyclic monomer **376** was isolated in 45% yield and in addition the cyclic diyne **377** was isolated in 40% yield. This unexpected result was attributed to the high ring-strain experienced in the 11-membered monomer **376**.

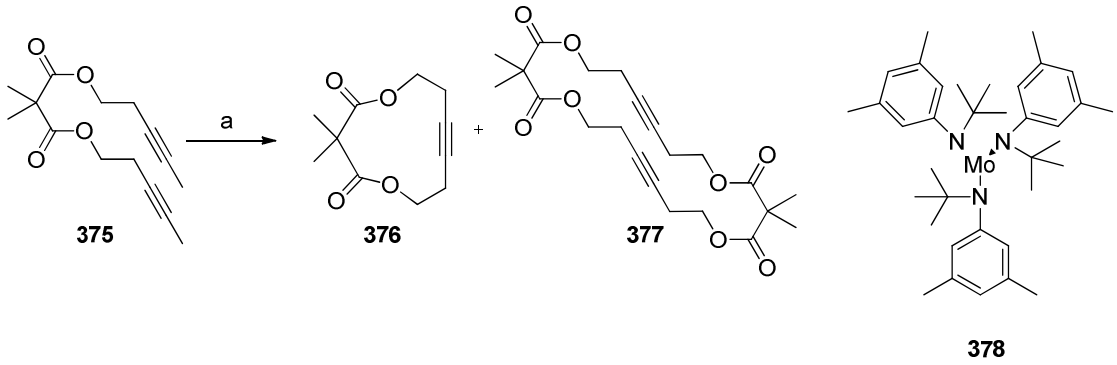


**Scheme 117: Observed cyclic diyne**

(a) **378** activated with DCM, toluene, 80 ºC, 20 h, **376** 45%, **377** 40%.

In efforts to expand on Fürtsner's results, with the aim of synthesising cyclic diynes, Gleiter *et al.* performed alkyne metathesis reactions on a range of diynes (**379**) of varying chain lengths using the Mortreux[154] system (due to its ease of preparation).[155] The results indicated in table **21** show that the optimum ring size for the formation of the cyclic diynes **381** is 16-26. Only the cyclic alkyne **380** was isolated when $n$ = 12 (table **21**, entry 1) and RCAM of the alkyne **379** was favourable. The yield of the cyclic diynes **381** also dropped off as the ring size decreases.

**Table 21: Investigation into cyclic diyne ring size**

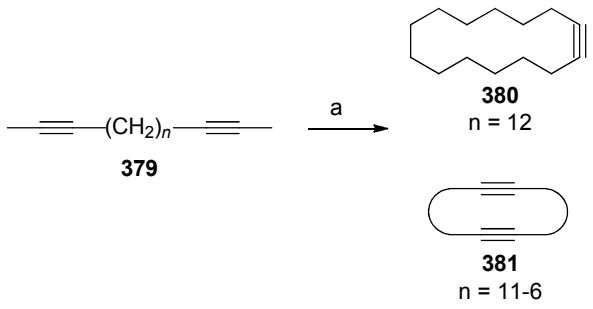


| Product | Yield |
|---|---|
| Cyclotetradecyne | 21% |
| Cyclohexacosa-1,14-diyne | 22% |
| Cyclotetracosa-1,13-diyne | 65% |
| Cyclodocosa-1,12-diyne | 42% |
| Cycloeicosa-1,11-diyne | 28% |
| Cyclooctadeca-1,10-diyne | 72% |
| Cyclohexadeca-1,9-diyne | 15% |

(a) $Mo(CO)_6$/trifluoromethyl phenol, toluene, 110 ºC.

Following on from the development of a new tungsten-based alkyne metathesis catalyst **385,**[156] the Tamm group investigated the effect of the substitution pattern around a phenyl ring on RCAM.[157] The results in table **22** show that the *meta*-substituted ring favoured monomer RCAM to **383**, however the *para*-substituted ring favoured the formation of the 28-membered cyclic diyne **384**. Interestingly, the more constrained *ortho*-substituted ring generated a mixture of **383** and **384**, favouring the diyne ring **384**. It was proposed that an equilibrium exits between **383** and **384** *via* a reversible ring-opening and ring-closing metathesis (RORCM). Following DTF calculations, the standard Gibbs free energy ($\Delta G^o$) of the equilibrium between **383** and **384** for the *meta*-substituted alkyne was found to be +4.00 kcal $mol^{-1}$ and the *para*-substituted alkyne –9.66 kcal $mol^{-1}$, this shows that for the *para*-substituted system the cyclic diyne **384** is the thermodynamically favoured product. The $\Delta G^o$ for the *ortho*-substituted alkyne was calculated to be –2.78 kcal $mol^{-1}$, therefore suggesting that the cyclic diyne **384** is the thermodynamically favoured product, as indicated by the experimental ratio. These results signify that the orientation of substitution has an effect on the outcome of the RCAM reaction. The most important factor determining the outcome of the alkyne metathesis is whether the cyclic monomer is highly strained and therefore, the cyclic diyne would be the thermodynamic product.

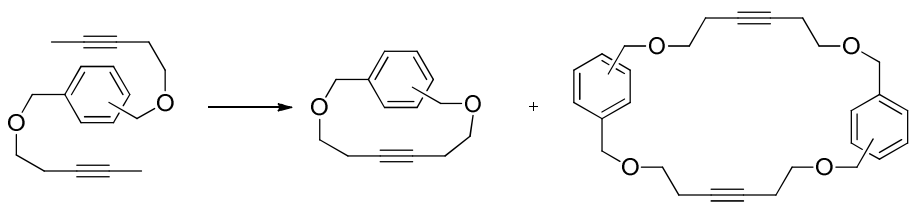

382 383 384

**Table 22: Effect of substitution on RCAM outcome**

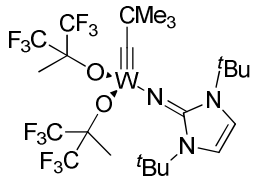

385

| Isomer | 383 | 384 |
|---|---|---|
| *o*-**382** | 24 | 76 |
| *m*-**382** | 100 | 0 |
| *p*-**382** | 0 | 100 |

## 5.4.1 Application to Disorazole $C_1$ Synthesis

The proposed alkyne metathesis end-game of disorazole $C_1$ is shown in scheme **118**. A cross metathesis of **374** to **386**, followed by ring closing alkyne metathesis is anticipated based on the results of Hoffmann's studies (Section **1.4.2**) which showed that placement of the alkyne at the C(9)-C(10) bond favoured the 30-membered dimer **10**, rather than the 15-membered monomer.[29] Taking into account published reports of cyclic diyne synthesis, it is possible that the desired ACM followed by RCAM will occur. Head-to-tail dimerisation of alkenes *via* alkene cross-metathesis has been reported by Smith during the total synthesis of (−)-cylindrocyclophanes A and F.[158] No tail-to-tail product was obsererved in this example, it was thought that the desired product was the most thermodynamically stable and the reversible nature of alkene cross-metathesis drove the reaction to the favoured product. However, the outcome of our proposed alkyne metathesis cannot be predicted as it is unknown how the oxazole substitution pattern, functional groups and branching of the disorazole fragment will affect the bias towards one ring size over the other. The published cyclic diyne examples all featured symmetrical linear alkynes and it is unknown whether the unsymmetrical disorazole monomers will undergo cross-metathesis in

the desired orientation. Therefore, computational studies are underway in the Hulme group to investigate the thermodynamic energies of alkyne metathesis of potential heterocyclic analogues. It could also be possible to use a templated alkyne metathesis strategy using a metal such as gold or platinum to co-ordinate to the oxazole nitrogen, therefore holding the monomers in the correct orientation for cross metathesis followed by RCAM.

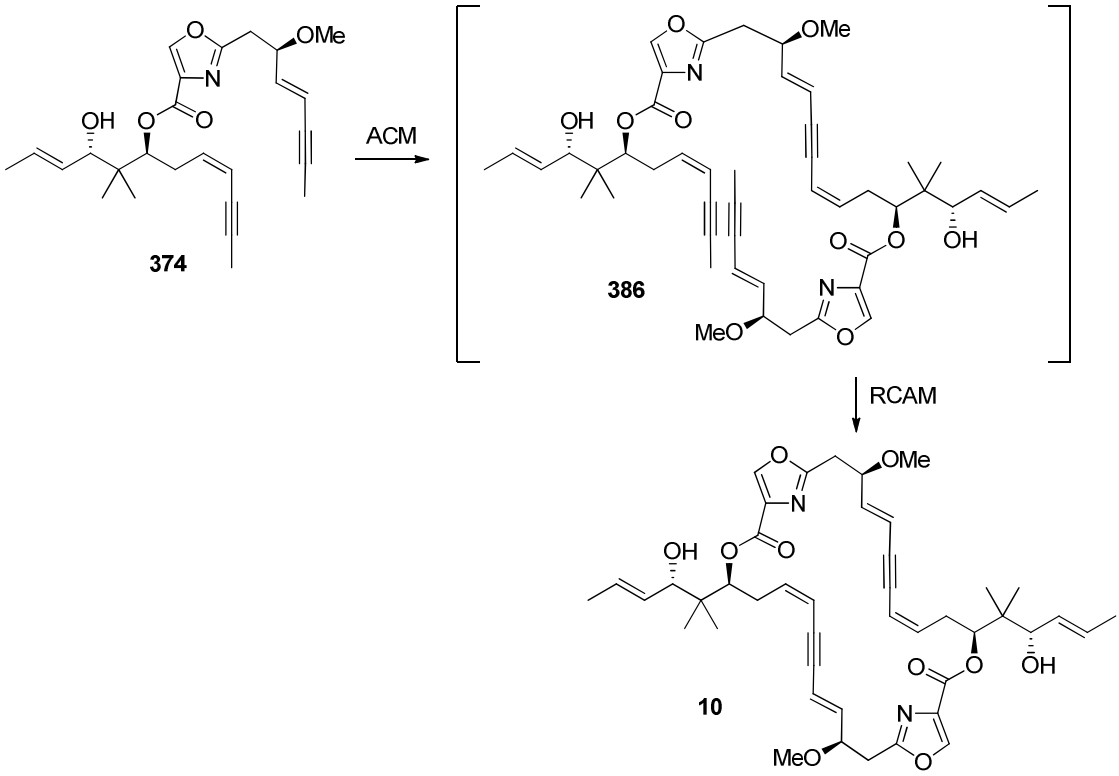


**Scheme 118: Proposed alkyne metathesis strategy**

## 5.5 Sonogashira option

If however, the cross-metathesis strategy is proving to be problematic, the C(1)-C(9) and C(10)-C(19) fragments could readily be transformed into Sonogashira reaction substrates **387** and **388** to facilitate the coupling (scheme **119**) as demonstrated by Hoffmann and Wipf's syntheses of the disorazole $C_1$ macrocycle. This process would

result in a more step-wise synthesis; however it could be more reliable than the unpredictable alkyne cross-metathesis which would precede the RCAM.

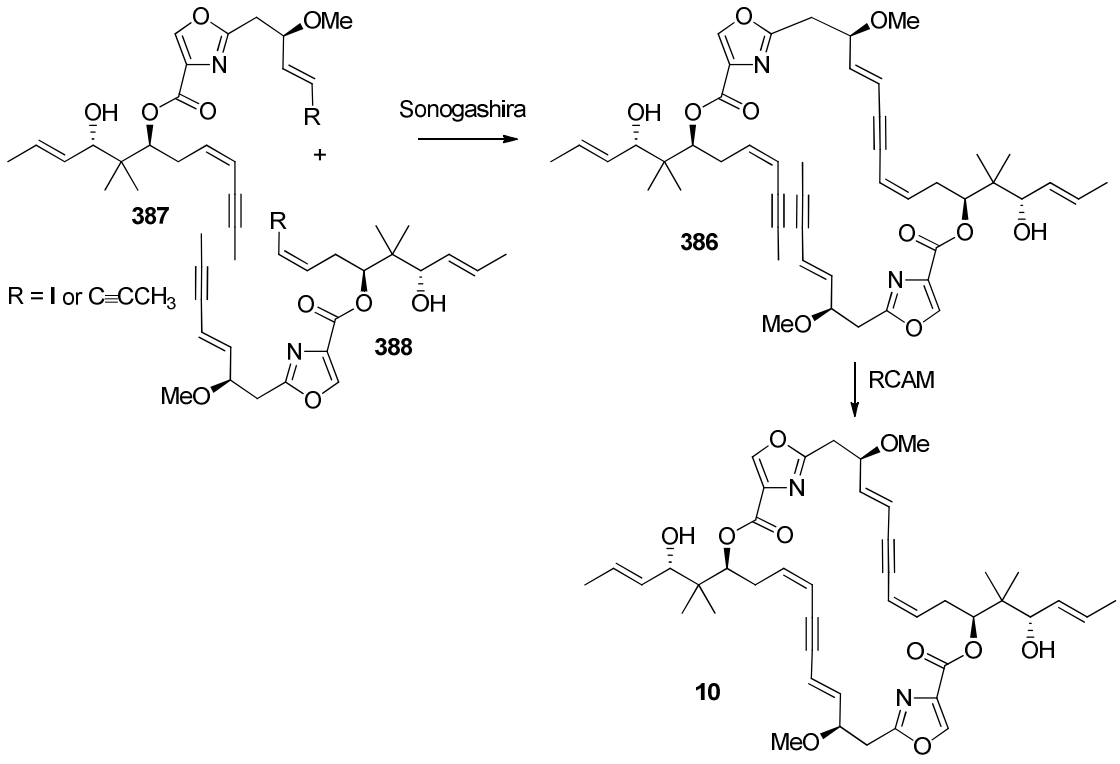


**Scheme 119: Sonogashira back-up strategy**

To conclude, novel routes towards the C(1)-C(9) fragment of disorazole $C_1$ have been developed and progress towards optimisation and scale up of the fragment are underway. A route towards the C(10)-C(19) fragment has been developed in the Hulme group, and further investigations into the Evans-Tishchenko reaction are on-going. As detailed in this chapter, there is an end-game strategy in place based on ET/RCAM and a back-up approach has been considered if it will be required. With a convergent route towards the C(1)-C(9) fragment developed this will allow rapid access to heterocyclic analogues of disorazole $C_1$. Biological evaluation of these novel analogues will take place in Edinburgh in due course.

# 6 Chapter 6: Experimental

## 6.1 General Experimental

$^{1}$H NMR spectra were recorded at ambient temperature (unless otherwise stated) on Bruker ARX250 (250 MHz), DPX360 (360 MHz), AVA400 (400 MHz), Open400 (400 MHz) and AVA500 (500 MHz) Fourier Transform instruments. The data is presented as follows: chemical shift (in ppm on the δ scale relative to $\delta_{TMS}$ = 0), integration, multiplicity (s = singlet, d = doublet, t = triplet, q = quartet, m = multiplet, br s = broad singlet), coupling constants (in Hertz, Hz) and interpretation. $^{13}$C NMR spectra were recorded at ambient temperature (unless otherwise stated) on Bruker ARX250 (62.9 MHz), DPX360 (90.6 MHz) AVA400 (101 MHz), Open400 (101 MHz) and AVA500 (126 MHz) Fourier Transform instruments and were referenced to the solvent carbon peak. The data is presented as follows: chemical shift (in ppm on the δ scale) and assignment; and were confirmed by DEPT90 and DEPT135.

Infra-red spectra were recorded on a Perkin Elmer Paragon 100 FT-IR using 5mm sodium chloride plates or a Shimadzu IRAffinity-1 machine as thin films unless otherwise stated. The wavelengths of maximum absorbance ($\upsilon_{max}$) are quoted in $cm^{-1}$.

Melting points were determined on a Gallenkamp Electrothermal melting point apparatus and are uncorrected.

Fast Atom Bombardment (FAB) mass spectra were obtained using a Kratos MS50TC mass spectrometer, Electrospray ionisation (ESI) mass spectra were recorded on a Finnigan LCQ instrument, Electron Ionisation (EI) mass spectra were recorded on a Finnigan 4500 or a MAT 900 XP mass spectrometer. The parent ion or relevant fragment is quoted, followed by significant fragments and their percentages.

Optical rotations were measured on an AA-1000 polarimeter with a path length of 1.0 dm at the sodium D line (589 nm) and are reported as follows: $[\ ]_D$, concentration

(c in g/ 100 $cm^3$), and solvent. All optical rotations were measured at room temperature.

TLC was performed on Merck $60F_{245}$ (0.25 mm) aluminium plates and visualised by ultraviolet light, potassium permanganate stain, ammonium molybdate stain or anisaldehyde stain. Flash column chromatography was carried out using silica gel (Fisher Scientific 60Å particle size 35-70 micron)

All non-aqueous reactions were performed under an inert atmosphere of nitrogen and under anhydrous conditions using oven- or flame-dried glassware cooled in a desiccator prior to use and anhydrous solvents were used (unless otherwise stated). Solvent were dried and purified by passage through activated alumina columns using a solvent purification system from www.glasscontoursolventsystems.com.

Organic layers were dried using magnesium sulfate unless otherwise stated. All reagents were used as supplied except where otherwise stated in the experimental text. Saturated aqueous solutions of inorganic salts are represented as (volume; sat. aq). Serine methyl ester hydrochloride was recrystallised from anhydrous ethanol. Oxalyl chloride and crotonaldehyde were distilled over $CaCl_2$. Triethylamine and diethylamine were distilled over CaH.

## 6.2 Experimental for Chapter 2

**Methyl 2-chloromethyl-1,3-oxazole-4-carboxylate 139a**

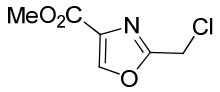


Sodium methoxide (4.0 μL, 25 % $^{w}/_{w}$ solution in methanol, 0.064 mmol) was added to a solution of methanol (2 mL) in DCM (15 mL) at 0 °C under nitrogen. After 5 min, dichloroacetonitrile (0.52 mL, 6.40 mmol) was added, and the solution was stirred at 0 °C for 1 h. Serine methyl ester hydrochloride (1.00 g, 6.40 mmol, recrystallised from ethanol) was added at 0 °C, and the resulting slurry was allowed to warm to rt and stirred for 18 h. The reaction mixture was diluted with DCM (10 mL) and water (20 mL) and the aqueous phase was extracted with DCM (2 × 15 mL). The organic extracts were combined, dried, filtered and concentrated *in vacuo* to give the intermediate methyl 2-(dichloromethyl)-4,5-dihydro-1,3-oxazole-4-carboxylate **143** as a brown gum (1.1 g, 84 %), which was used without further purification.

**$^{1}$H NMR** δ (360 MHz, $CDCl_3$) 6.28 (1H, s, C*H*$Cl_2$), 4.90 (1H, dd, *J* = 10.8, 8.2 Hz C$H_A$$H_B$O), 4.68 (1H, dd, *J* = 8.8, 8.2 Hz, C*H*N), 4.59 (1H, dd, 10.8, 8.8 Hz, $CH_A$$H_B$O), 3.82 (3H, s, C$H_3$).

To a solution of the crude oxazoline **143** (1.12 g, 5.28 mmol) in DCM (10 mL) was added DIPEA (1.38 mL, 7.92 mmol), the resulting mixture was stirred at 50 °C for 6 h, then at rt for ~18 h. The reaction mixture was diluted with DCM (30 mL) and water (20 mL), the aqueous phase was extracted with DCM (2 × 15 mL). The organic extracts were combined, dried, filtered and concentrated *in vacuo* and the crude residue was recrystallised from diethyl ether and hexane to give the oxazole **139a** as pale pink needles (776 mg, 69 %).

**$R_f$** (Hexane:EtOAc, 1:1) = 0.41; **Mp** = 73-74 °C, lit[74] 73-74 °C; **IR** (neat, $cm^{-1}$) 1715 (C=O), 1580 (C=C); **$^{1}$H NMR** δ (360 MHz, $CDCl_3$) 8.24 (1H, s, Ar*H*), 4.62 (2H, s, C$H_2$), 3.91 (3H, s, C$H_3$); **$^{13}$C NMR** δ (62.9 MHz, $CDCl_3$) 160.87 (C), 159.72 (C), 144.91 (CH), 133.55 (C), 52.14 ($CH_3$), 35.12 ($CH_2$); ***m/z*** (ESI+, MeOH) 373 ($[2M+Na]^+$, 75 %), 198 ($[M+Na]^+$, 100), 176 ($[M+H]^+$, 41).

Spectroscopic data are in good agreement with the literature.[74]

**Dibromoacetonitrile 149**

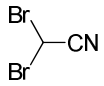

Cyanoacetic acid (8.00 g, 94.0 mmol) and *N*-bromosuccinimide (33.9 g, 188 mmol) were stirred in cold water (100 mL). Within 5 min, the solution clouded and a slightly exothermic reaction commenced with evolution of carbon dioxide. After another 5 min the mixture went clear and was allowed to settle into two layers. The bottom dibromoacetonitrile phase was removed and the top aqueous phase was extracted with ether (3 × 5 mL). The organic extracts were combined, washed with water (100 mL), dried and filtered. The ether was removed *in vacuo* and the residual dibromoacetonitrile dried under high vacuum giving the nitrile **149** as a pale brown oil (10.75 g, 96 %).

**$R_f$** (Hexane:EtOAc, 9:1) = 0.26; **IR** (neat, $cm^{-1}$) 1703 (C≡N); **$^1$H NMR** δ (250 MHz, $CDCl_3$) 5.82 (1H, s); **$^{13}$C NMR** δ (62.9 MHz, $CDCl_3$) 113.87 (C), 5.31 (C); ***m/z*** (CI, *i*-butane) 219 ($[^{81}Br^{81}BrM+H_2O]^+$, 45 %), 217 ($[^{81}Br^{79}Br+H_2O]^+$, 100), 215 ($[^{79}Br^{79}Br+H_2O]^+$, 46).

Spectroscopic data are in good agreement with the literature.[51]

**Methyl 2-bromomethyl-1,3-oxazole-4-carboxylate 139b**

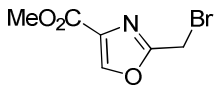


Sodium methoxide (4.0 μL, 25 % $^{w}/_{w}$ solution in methanol, 0.064 mmol) was added to a solution of methanol (2 mL) in DCM (15 mL) at 0 °C under nitrogen. After 5 min, dibromoacetonitrile (0.33 mL, 6.4 mmol) was added, and the solution was stirred at 0 °C for 1 h. Serine methyl ester hydrochloride (1.00 g, 6.40 mmol) was added at 0 °C, and the resulting slurry was allowed to warm to rt and stirred for ~18 h. The reaction mixture was diluted with DCM (10 mL) and water (20 mL) and the aqueous phase was extracted with DCM (2 × 15 mL). The organic extracts were combined, dried, filtered and concentrated *in vacuo* to give methyl 2-(dibromomethyl)-4,5-dihydro-1,3-oxazole-4-carboxylate as a pink oil (1.23 g, 64 %), which was used without further purification.

**$^{1}$H NMR** δ (360 MHz, $CDCl_3$) 6.13 (1H, s, C*H*$Br_2$), 4.84 (1H, dd, *J* = 10.7, 8.1 Hz, C$H_A$$H_B$O), 4.68 (1H, t, *J* = 8.6 Hz, C*H*N), 4.62 (1H, dd, *J* = 10.7, 8.8 Hz, $CH_A$$H_B$O), 3.82 (3H, s, C$H_3$).

The crude oxazoline (1.23 g, 4.09 mmol) was dissolved in DCM (25 mL) and the resulting solution cooled to 0 °C. DBU (0.709 mL, 4.75 mmol) was then introduced in one portion. After one minute, the reaction was diluted with diethyl ether (75 mL) and washed with $NH_4Cl$ (40 mL, sat aq), water (40 mL), brine (40 mL), dried, filtered and concentrated *in vacuo* to provide the oxazole **139b** as a brown solid (711 mg, 79 %).

**$R_f$** (Hexane:EtOAc, 3:1) = 0.36; **Mp** = 54 °C, lit[23] 49-51 °C; **IR** (neat, $cm^{-1}$) 1738 (C=O), 1579 (C=C); **$^{1}$H NMR** δ (360 MHz, $CDCl_3$) 8.26 (1H, s, Ar*H*), 4.47 (2H, s, C$H_2$), 3.93 (3H, s, C$H_3$); **$^{13}$C NMR** δ (62.9 MHz, $CDCl_3$) 160.85 (C), 159.90 (C), 144.80 (CH), 133.71 (C), 52.14 ($CH_3$), 19.22 ($CH_2$); ***m/z*** (EI) 221 ([$^{81}$BrM]$^{+}$, 7 %), 219 ([$^{79}$BrM]$^{+}$, 7 %), 190 (6), 188 (6), 140 (100).

Spectroscopic data are in good agreement with the literature.[23]

**Methyl 2-iodomethyl-1,3-oxazole-4-carboxylate 139c**

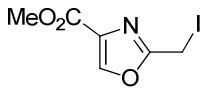


Methyl 2-chloromethyl-1,3-oxazole-4-carboxylate **139a** (0.20 g, 1.10 mmol) and NaI (0.82 g, 5.50 mmol) were dissolved in THF (5 mL) and stirred for 20 min at rt. The solution was diluted with EtOAc (20 mL) and washed with water (2 × 10 mL), $NaHSO_3$ (15 mL, sat aq) and brine (20 mL), dried, filtered and concentrated *in vacuo* to give oxazole **139c** as a brown oil. The crude product was crystallised from diethyl ether and hexane (1:4) to give a colourless solid (0.24 g, 79 %).

**$R_f$** (Hexane:EtOAc, 1:1) = 0.47; **Mp** = 68-69 °C, lit[74] 67 °C; **IR** (neat, $cm^{-1}$) 1749 (C=N), 1738 (C=O), 1579 (C=C); **$^1$H NMR** δ (360 MHz, $CDCl_3$) 8.22 (1H, s, Ar*H*), 4.39 (2H, s, C$H_2$), 3.92 (3H, s, C$H_3$); **$^{13}$C NMR** δ (62.9 MHz, $CDCl_3$) 161.43 (C), 161.17 (C), 144.46 (CH), 134.17 (C), 52.33 ($CH_3$), -12.55 ($CH_2$); ***m/z*** (CI, *i*-butane) 268 ($[M+H]^+$, 100 %), 142 (7).

Spectroscopic data are in good agreement with the literature.[74]

**Methyl 2-methyl-1,3-oxazole-4-carboxylate 128**

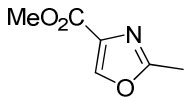


Method A[52]

Sodium methoxide (32 μL, 25 % $^{w}/_{w}$ solution in methanol, 0.14 mmol) was added to a solution of methanol (1 mL) in DCM (9 mL) at 0-5 °C. After 5 min, chloroacetonitrile (1.00 mL, 15.8 mmol) was added, and the solution was stirred at 0-5 °C for 1.5 h. Serine methyl ester hydrochloride (1.99 g, 12.8 mmol) was added at 0-5 °C, and the resulting slurry was allowed to warm to room temperature and stirred for ~18 h. Water (10 mL) was added, the mixture stirred for 10 min, and then the aqueous and organic layers were separated. The organic layer was washed with water (20 mL), dried, filtered and then concentrated *in vacuo* to leave a residual volume of ~5 mL. Fresh DCM (10 mL) was added, and the solution was warmed to 30 °C. DBU (1.89 mL, 12.6 mmol) was added dropwise over 30 min while maintaining the reaction temperature at 30 °C, during addition of DBU the solution turned from colourless to dark red/brown. Upon completion of the addition the reaction mixture was cooled to rt, and HCl (8 mL, 1 M aq) was added and the layers separated. Then the organic layer was washed with water (10 mL). The organic layer was concentrated *in vacuo* to leave a residual volume of ~6 mL. Hexane (8 mL) was added, and the solution was concentrated *in vacuo* to leave a residual volume of ~6 mL. More hexane (2 mL) was added, the solution was cooled to 0-5 °C and for 1.5 h and a colourless precipitate formed. The slurry was filtered, and the filtercake was washed with cold hexane and then dried to give methyl ester **128** as a colourless solid (1.18 g, 65 %).

Method B[53]

To a stirred suspension of ethyl acetimidate hydrochloride (1.00 g, 8.09 mmol) and serine methyl ester hydrochloride (1.26 g, 8.09 mmol) in DCM (16 mL) was added dropwise over 20 min a solution of triethylamine (2.44 mL, 17.5 mmol) in DCM (6 mL). The resulting solution was stirred at rt for ~18 h, after which the solids were removed by filtration and washed with ether. The filtrate was concentrated *in vacuo*,

and the resulting solid residue was taken into water (20 mL) and washed with ether (4 × 20 mL). The combined organic extracts were dried, filtered and concentrated *in vacuo* to give crude 4,5-dihydro-2-methyloxazole-4-carboxylic acid methyl ester **153**.

Hexamethylenetetramine (2.83 g, 20.2 mmol) and DBU (3.02 mL, 20.0 mmol) were added to a stirred suspension of $CuBr_2$ (4.51 g, 20.2 mmol) at 0 °C. After 20 min, the crude oxazoline **153** was added in THF (10 mL), and the reaction mixture was stirred at rt for 3 h. The solvent was removed *in vacuo*, and the residue was partitioned between EtOAc (30 mL) and a 1:1 mixture of $NH_4Cl$ (10 mL, sat aq) and $NH_4OH$ (10 mL, sat aq). The aqueous layer was extracted with EtOAc (30 mL), and the combined organic layers were washed with a 1:1 mixture of $NH_4Cl$ (10 mL, sat aq) and $NH_4OH$ (10 mL, sat aq), citric acid (20 mL, 10 % aq), $NaHCO_3$ (20 mL, sat aq), and brine (20 mL), then dried, filtered and evaporated *in vacuo* to give the crude oxazole **128** as a brown oil (0.6 g, 52 %).

**$R_f$** (Hexane:EtOAc, 1:1) = 0.34; **Mp** = 50 °C, lit[52] 48 °C; **IR** (neat, $cm^{-1}$) 1736 (C=O), 1592 (C=C); **$^1$H NMR** δ (250 MHz, $CDCl_3$) 8.12 (1H, s, Ar*H*), 3.89 (3H, s, O$CH_3$), 2.50 (3H, s, $CH_3$); **$^{13}$C NMR** δ (62.9 MHz, $CDCl_3$) 162.21 (C), 161.48 (C), 143.60 (CH), 132.98 (C), 51.86 ($CH_3$), 13.60 ($CH_3$); ***m/z*** (EI) 141 ($[M]^+$, 84 %), 110 (100), 100 (95).

Spectroscopic data are in good agreement with the literature.[52]

**(2-Methyl-1,3-oxazol-4-yl)methanol 141**

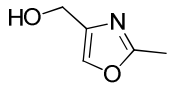


Methyl ester **128** (2.82 g, 20.0 mmol) was suspended in diethyl ether (30 mL) and cooled to −5 °C. Lithium aluminium hydride solution (18.0 mL, 1.0 M in THF, 18.0 mmol) was added while maintaining the temperature at −5 °C. After 1 h water (1 mL) was added, followed by NaOH (1 mL, 15 % $^{w}/_{v}$ aq) and further water (1.5 mL). Sodium sulfate (15 g) was added, and the resulting suspension was allowed to warm to rt. The slurry was filtered and the filtercake was washed with DCM (3 × 30 mL). The filtrate and washes were combined and then concentrated *in vacuo* to afford alcohol **141** as a brown solid (1.59 g, 70 %).

**$R_f$** (MeOH:DCM, 1:9) = 0.47; **Mp** = 42-43 °C, lit[52] 40-41 °C; **IR** (neat, $cm^{-1}$) 3387 (OH), 1645 (C=N), 1580 (C=C); **$^{1}$H NMR** δ (250 MHz, $CDCl_3$) 7.47 (1H, s, Ar*H*), 4.54 (2H, s, C$H_2$OH), 2.44 (3H, s, C$H_3$); **$^{13}$C NMR** δ (62.9 MHz, $CDCl_3$) 162.03 (C), 140.18 (C), 134.78 (CH), 55.58 ($CH_2$), 13.58 ($CH_3$); ***m/z*** (EI) 113 ($[M]^+$, 100%), 96 (15).

Spectroscopic data are in good agreement with the literature.[52]

**Ethyl (2*Z*)-3-iodoprop-2-enoate 158**

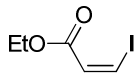

A stirred suspension of sodium iodide (10.0 g, 66.8 mmol, dried for ~18 h at 140 ºC) and acetic acid (20 mL) was heated to 70 ºC until all of the solid material was dissolved. To this yellow solution was added ethyl propiolate (4.50 mL, 44.4 mmol) and the mixture was stirred for 3 h at 70 ºC. The dark brown solution was cooled to rt and diethyl ether (50 mL) and water (50 mL) were added. The organic layer was separated and the aqueous phase was extracted with diethyl ether (3 × 50 mL) until the aqueous layer is colourless. The combined organic layers were adjusted to pH 7 with KOH (3 M, aq), and the organic layer was washed with $Na_2S_2O_3$ (50 mL, 10 % aq) and brine (50 mL). The clear colourless solution was dried, filtered and concentrated *in vacuo* to afford (*Z*)-alkene **158** as a brown oil (9.12 g, 91 %).

**$R_f$** (Hexane:EtOAc, 1:1) = 0.65; **IR** (neat, $cm^{-1}$) 1725 (C=O), 1600 (C=C); **$^1$H NMR** δ (250 MHz, $CDCl_3$) 7.44 (1H, d, *J* = 9.0 Hz, C*H*), 6.89 (1H, d, *J* = 9.0 Hz, C*H*), 4.24 (2H, q, *J* = 7.0 Hz, C$H_2$CH$_3$), 1.32 (3H, t, *J* = 7.0 Hz, CH$_2$C$H_3$); **$^{13}$C NMR** δ (62.9 MHz, $CDCl_3$) 164.48 (C), 129.81 (CH), 94.62 (CH), 60.71 ($CH_2$), 14.11 ($CH_3$); (ESI+, MeOH) 264 ($[M+K]^+$, 100 %), 239 (36), 208 (76).

Spectroscopic data are in good agreement with the literature.[55]

**Ethyl (2*E*)-3-iodoprop-2-enoate 159**

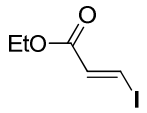

A solution of (*Z*)-alkene **158** (9.12 g, 40.3 mmol) in toluene (20 mL) was treated with hydroiodic acid (0.55 mL, 57 % aq). The resulting mixture was heated at 80 ºC for 6 h, after which, the solution was cooled to rt and diluted with diethyl ether (60 mL). The organic layer was washed with $NaHCO_3$ (30 mL, sat aq), $Na_2S_2O_3$ (30 mL, 10 % aq) and brine (30 mL). The organic phase was dried, filtered and concentrated *in vacuo* to afford (*E*)-alkene **159** as a brown liquid (8.43 g, 92 %).

**$R_f$** (Hexane:EtOAc, 9:1) = 0.28; **IR** (neat, $cm^{-1}$) 1732 (C=O), 1680 (C=C); **$^1$H NMR** δ (360 MHz, $CDCl_3$) 7.86 (1H, d, *J* = 14.8 Hz, C*H*), 6.86 (1H, d, *J* = 14.8 Hz, C*H*), 4.19 (2H, q, *J* = 7.2 Hz, C$H_2$CH$_3$), 1.28 (3H, t, *J* = 7.2 Hz, CH$_2$C$H_3$); **$^{13}$C NMR** δ (62.9 MHz, $CDCl_3$) 164.18 (C), 136.54 (CH), 99.26 (CH), 60.97 ($CH_2$), 14.15 ($CH_3$); ***m/z*** (ESI+, MeOH) 264 ($[M+K]^+$, 100 %), 242 (28), 209 (27), 198 (19).

Spectroscopic data are in good agreement with the literature.[55]

**Ethyl (2*E*)-hex-2-en-4-ynoate 161**

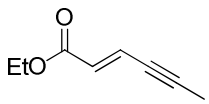

A solution of 1-propynylmagnesium bromide (354 mL, 0.50 M in THF, 177 mmol) was added dropwise to a stirred slurry of dry $ZnCl_2$ (24.1 g, 177 mmol) in THF (70 mL) at 0 °C. After 15 min a solution of (*E*)-vinyl iodide **158** (20.0 g, 88.5 mmol) in THF (10 mL) and $Pd(PPh_3)_2Cl_2$ (3.11 g, 4.43 mmol) were added and the resulting mixture was stirred for ~18 h at rt. The reaction mixture was then poured into $NH_4Cl$ (400 mL, sat aq) and extracted with ether (4 × 200 mL). The combined organic extracts were washed with brine (20 mL), dried, filtered and concentrated *in vacuo*. The residue was passed through a short silica column eluting with hexane to give the alkyne **161** as a yellow oil (10.9 g, 90 %).

**$R_f$** (Hexane:EtOAc, 9:1) = 0.24; **IR** (neat, $cm^{-1}$) 2222 (C≡C), 1714 (C=O), 1621 (C=C); **$^1$H NMR** δ (360 MHz, $CDCl_3$) 6.72 (1H, dq, *J* = 15.8, 2.5 Hz, CH=C*H*C), 6.12 (1H, dq, *J* = 15.8, 0.7 Hz, $CO_2$EtC*H*=CH), 4.19 (2H, q, *J* = 7.2 Hz, C$H_2$$CH_3$), 2.01 (3H, dd, *J* = 2.5, 0.7 Hz, CC$H_3$), 1.28 (3H, t, *J* = 7.2, Hz, $CH_2$C$H_3$); **$^{13}$C NMR** δ (62.9 MHz, $CDCl_3$) 165.00 (C), 129.28 (CH), 125.91 (CH), 96.09 (C), 77.00 (C), 60.48 ($CH_2$), 14.10 ($CH_3$), 4.61 ($CH_3$); ***m/z*** (CI, *i*-butane) 154 ($[M+CH_4]^+$, 80 %), 139 ($[M+H]^+$, 100), 111 (79).

Spectroscopic data are in good agreement with the literature.[159]

**(2*E*)-Hex-2-en-4-yn-1-ol 162**

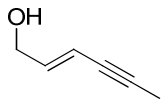


To a solution of ester **161** (1.50 g, 10.8 mmol) in DCM (8 mL) at −78 ºC was added DIBAL (32.5 mL, 1 M in hexanes, 32.5 mmol) dropwise. The reaction mixture was stirred at −78 ºC for 1 h and then warmed to 0 °C and diluted with ether (20 mL). Water (1.25 mL) was added slowly, followed by NaOH (2 mL, 10 % aq) and further water (3 mL), The mixture was then allowed to warm to rt and stirred for 15 min. $MgSO_4$ (~5 g) was added and the mixture stirred for 30 min, after which the suspension was filtered and the filtrate concentrated *in vacuo*. The crude oil was purified by flash chromatography (hexane:EtOAc, 9:1) to give the alcohol **162** as a light yellow oil (0.790 g, 73 %).

**$R_f$** (Hexane:EtOAc, 3:1) = 0.19; **IR** (neat, $cm^{-1}$) 3379 (OH), 2223 (C≡C), 1633 (C=C); **$^1$H NMR** δ (500 MHz, $CDCl_3$) 6.15 (1H, dtq, *J* = 15.8, 5.4, 0.6 Hz, $CH_2CH$=CH), 5.69 (1H, dq, *J* = 15.8, 2.2 Hz, CH=C*H*C), 4.17 (2H, d, *J* = 5.4 Hz, $CH_2$), 1.94 (3H, dd, *J* = 2.2, 0.6 Hz, $CCH_3$); **$^{13}$C NMR** δ (126 MHz, $CDCl_3$) 140.24 (CH), 111.26 (CH), 86.80 (C), 77.50 (C), 63.09 ($CH_2$), 4.26 ($CH_3$); ***m/z*** (CI, *i*-butane) 97 ($[M+H]^+$, 63 %), 79 (94), 71 (100).

Spectroscopic data are in good agreement with the literature.[160]

**(*E*)-Hex-2-en-4-ynal 140**

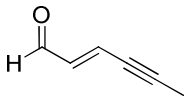

Method A

To a solution of ester **161** (100 mg, 0.72 mmol) in DCM (1 mL) at −78 ºC was added DIBAL (0.80 mL, 1 M in hexanes, 0.80 mmol) dropwise. The reaction mixture was stirred at −78 ºC for 1 h, then quenched with MeOH (0.5 mL) followed by sodium potassium tartrate (2 mL, sat aq). The reaction mixture was warmed to rt, diluted with ether (10 mL), and stirred for 30 min while protected from light, then diluted with further ether (5 mL) and water (5 mL). The organic phase was separated and the aqueous phase was extracted with ether (3 × 15 mL) and the combined organic extracts were washed with brine (1 × 15 mL), dried, filtered and concentrated *in vacuo* to give the highly volatile aldehyde **140** as a pale yellow oil, which was used immediately in subsequent steps without further purification.

Method B

To a solution of the alcohol **162** (230 mg, 2.30 mmol) in DMSO (5 mL) at rt was added 2-iodoxybenzoic acid (3.28 g, 45 wt. %, 5.27 mmol), the solution was stirred at rt for 30 min. The reaction mixture was diluted with ether (20 mL) and water (30 mL), the organic phase was separated and the aqueous phase was extracted with ether (2 × 20 mL), the organic phases were combined, washed with brine (15 mL), dried, filtered and concentrated *in vacuo* to give the highly volatile aldehyde **140** as a pale yellow oil, which was used immediately in subsequent steps without further purification.

Method C[60]

A thoroughly stirred suspension of manganese dioxide (1.03 g, 11.9 mmol) in diethyl ether (10 mL) was treated with ultrasonic vibration for 30 min, then alcohol **162** (57 mg, 0.59 mmol) dissolved in diethyl ether (1 mL) was added. The suspension was stirred for ~18 h at rt and then filtered through celite and the solvent was carefully removed *in vacuo* (no heat) to give the highly volatile aldehyde **140** as a pale yellow

oil, which was used immediately in subsequent steps without further purification.

**$R_f$** (Hexane:EtOAc, 13:1) = 0.51; **$^1$H NMR** δ (360 MHz, $CDCl_3$) 9.54 (1H, d, *J* = 7.9 Hz, C*H*O), 6.56 (1H, dq, *J* = 15.5, 2.3 Hz, CH=C*H*C), 6.40 (1H, dd, *J* = 15.5, 7.9 Hz, CHOC*H*=CH), 2.09 (3H, d, *J* = 2.3 Hz, CC$H_3$); ***m/z*** (CI, *i*-butane) 189 ($[2M+H]^+$, 8 %), 187 (27), 171 (100), 149 (8), 95.0 ($[M+H]^+$, 6 %).

Spectroscopic data are in good agreement with the literature.[58]

**Ethyl (2*E*)-hex-2-en-4-ynethiolate 182**

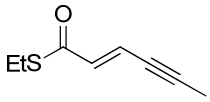


To a solution of ester **161** (317 mg, 2.30 mmol) in THF (8 ml) at rt was added aluminium chloride (368 mg, 2.46 mmol) and (ethylthio)trimethylsilane (0.75 mL, 4.60 mmol). The resulting mixture was stirred at 70 °C for 3 h and then cooled to rt and quenched with $NH_4Cl$ (10 mL, sat aq) and diluted with ether (30 mL). The organic layer was separated and the aqueous phase was extracted with diethyl ether (2 × 25 mL). The organic extracts were combined, dried, filtered and concentrated *in vacuo*. The crude material was purified by flash chromatography (hexane:EtOAc, 3:1) to give the thiol ester **182** as a yellow oil (317 mg, 90 %).

**$R_f$** (Hexane:EtOAc, 9:1) = 0.48; **IR** (neat, $cm^{-1}$) 2220 (C≡C), 1660 (C=O), 1598 (C=C); **$^1$H NMR** δ (250 MHz, $CDCl_3$) 6.63 (1H, dq, *J* = 15.6, 2.4 Hz, CH=C*H*C), 6.37 (1H, dq, *J* = 15.6, 0.7 Hz, COSEtC*H*=CH), 2.94 (2H, q, *J* = 7.4 Hz, C$H_2$CH$_3$), 2.01 (3H, dd, *J* = 2.4, 0.7 Hz, CC$H_3$), 1.27 (3H, t, *J* = 7.4 Hz, CH$_2$C$H_3$); **$^{13}$C NMR** δ (62.9 MHz, $CDCl_3$) 189.63 (C), 136.06 (CH), 122.12 (CH), 97.20 (C), 77.77 (C), 23.77 ($CH_2$), 15.04 ($CH_3$), 5.25 ($CH_3$); ***m/z*** (EI) 154 ($[M]^+$, 16 %), 126 (20), 93 (100); **HRMS** (EI) $[M]^+$ found 154.0446, $C_8H_{10}OS$ requires 154.0447.

**4-(*tert*-Butyldimethylsilyloxymethyl)-2-methyl-1,3-oxazole 212a**

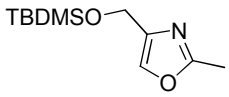


To a solution of the alcohol **141** (1.00 g, 8.84 mmol) in DCM (80 mL) at 0 °C was added *tert*-butyldimethylsilyl trifluoromethanesulfonate (2.13 mL, 9.28 mmol) followed by 2,6-lutidine (1.24 mL, 10.6 mmol). After stirring for 1 h at 0 °C the reaction was quenched by the addition of sodium bicarbonate (20 mL, sat aq) and extracted with DCM (3 × 40 mL). The organic extracts were combined, dried, filtered and concentrated *in vacuo*. The crude material was purified by flash chromatography (hexane:EtOAc, 9:1) to give the silyl ether **212a** as pale yellow oil (1.67 g, 89 %).

**$R_f$** (Hexane:EtOAc, 10:1) = 0.19; **IR** (neat, $cm^{-1}$) 1581 (C=C), 1253 ($SiCH_3$); **$^1$H NMR** δ (360 MHz, $CDCl_3$) 7.41 (1H, s, Ar*H*), 4.60 (2H, s, O$CH_2$), 2.43 (3H, s, Ar$CH_3$), 0.91 (9H, s, C($CH_3$)$_3$), 0.10 (6H, s, 2 × Si$CH_3$) ; **$^{13}$C NMR** δ (126 MHz, $CDCl_3$) 161.31 (C), 141.06 (C), 134.56 (CH), 58.45 ($CH_2$), 25.78 ($CH_3$), 18.25 (C), 13.74 ($CH_3$), −5.49 ($CH_3$); ***m/z*** (ESI+, MeOH) 476 ($[2M+Na]^+$, 100 %), 250 ($[M+Na]^+$, 75), 228 ($[M+H]^+$, 86).

Spectroscopic data are in good agreement with the literature.[84]

**2-Methyl-4-([2-(trimethylsilyl)ethoxy]methoxymethyl)-1,3-oxazole 212b**

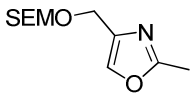


Sodium hydride (97 mg, 60% in mineral oil, 2.43 mmol) was added to a solution of alcohol **141** (250 mg, 2.21 mmol) in THF (4 mL) at 0 °C, and the mixture was stirred at 0 °C for 10 min and at rt for an additional 1 h. The mixture was cooled to 0 °C and 2-(trimethylsilyl)ethoxymethyl chloride (0.469 mL, 2.65 mmol) was added dropwise. The reaction mixture was stirred at 0 °C for 10 min and at rt for an additional 3 h. The mixture was poured into water (15 mL) and extracted with ethyl acetate (2 × 30 mL). The combined organic extracts were washed with brine (20 mL), dried, filtered and concentrated *in vacuo*. The crude material was purified by flash chromatography (hexane:EtOAc, 1:1) to give the ether **212b** as a pale yellow oil (370 mg, 68 %).

**$R_f$** (Hexane:EtOAc, 1:1) = 0.50; **IR** (neat, $cm^{-1}$) 1581 (C=C), 1271 ($SiCH_3$); **$^1$H NMR** δ (400 MHz, $CDCl_3$) δ 7.52 (1H, s, Ar*H*), 4.78 (2H, s, $OCH_2O$), 4.51 (2H, s, $OCH_2Ar$), 3.77 – 3.61 (2H, m, $OCH_2$), 2.47 (3H, s, $ArCH_3$), 1.04 – 0.95 (2H, m, $CH_2Si$), 0.05 (9H, s, $SiCH_3$);**$^{13}$C NMR** δ (101 MHz, $CDCl_3$) 162.03 (C), 137.51 (C), 135.86 (CH), 94.31 ($CH_2$), 65.36 ($CH_2$), 61.07 ($CH_2$), 18.13 ($CH_2$), 13.92 (3 × $CH_3$), −1.39 ($CH_3$); ***m/z*** (CI, *i*-butane) 244 ($[M+H]^+$, 100 %); **HRMS** (CI, *i*-butane) $[M+H]^+$ found 244.1375, $C_{11}H_{22}O_3NSi$ requires 244.1374.

**4-[(Methoxymethoxy)methyl]-2-methyl-1,3-oxazole 212c**

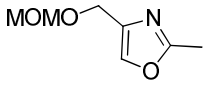


Sodium hydride (0.53 g, 60 % in mineral oil, 13.4 mmol) was added to a solution of alcohol **141** (1.37 g, 12.2 mmol) in THF (25 mL) at 0 °C, and the mixture was stirred at 0 °C for 10 min and at rt for an additional 1 h. The mixture was cooled to 0 °C and chloromethyl methyl ether (1.10 mL, 14.6 mmol) was added dropwise. The reaction mixture was stirred at 0 °C for 10 min and at rt for an additional 3 h. The mixture was poured into water (50 mL) and extracted with EtOAc (2 × 100 mL). The combined organic extracts were washed with brine (50 mL), dried, filtered and concentrated *in vacuo*. The crude material was purified by flash chromatography (hexane:EtOAc, 3:2) to give the ether **212c** as an orange oil (1.41 g, 73 %).

**$R_f$** (Hexane:EtOAc, 1:1) = 0.21; **IR** (neat, $cm^{-1}$) 1581 (C=C); **$^1$H NMR** δ (500 MHz, $CDCl_3$) 7.52 (1H, s, Ar*H*), 4.72 (2H, s, OC$H_2$O), 4.48 (2H, s, OC$H_2$), 3.41 (3H, s, OC$H_3$), 2.46 (3H, s, ArC$H_3$); **$^{13}$C NMR** δ (126 MHz, $CDCl_3$) 162.14 (C), 137.22 (C), 136.03 (CH), 95.79 ($CH_2$), 60.83 ($CH_2$), 55.46 ($CH_3$), 13.99 ($CH_3$); ***m/z*** (EI) 157 ($[M]^+$, 3 %), 127 (8), 97 (31), 45 (100); **HRMS** (EI) $[M]^+$ found 157.0735, $C_7H_{11}NO_3$ requires 157.0733.

**General Procedure A**

Methyl oxazole (1.77 mmol) was dissolved in dry THF (10 mL) and was cooled with stirring to −78 °C. To this solution *n*BuLi (8.85 mmol, 0.83 M in hexanes) was added dropwise and the solution allowed to stir for 1 h, after which diethylamine (10.6 mmol) was added. After a further 45 min the aldehyde (2.55 mmol) was added and the solution was stirred for 45 min at −78 °C. The reaction mixture was quenched with $NH_4Cl$ (10 mL, sat aq) and allowed to warm to rt, the reaction mixture was then extracted with DCM (3 × 20 mL). The organic extracts were combined, dried, filtered and concentrated *in vacuo* to give the alcohol. The crude mixture was purified by column chromatography.

**4-Hydroxymethyl-2-[(3*E*)-pent-3-en-2-ol-1-yl]-1,3-oxazole 194**

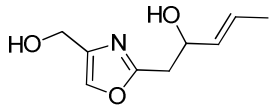


**General procedure A** was followed with methyl oxazole **141** (200 mg, 1.77 mmol). Flash chromatography (1:19 MeOH:DCM) resulted in an inseparable mixture of methyl oxazole starting material (**141**) and product **194**.

**$R_f$** (DCM:MeOH, 9:1) = 0.23; **IR** (neat, $cm^{-1}$) 3349 (OH), 1671 (C=N), 1581 (C=C); **$^1$H NMR** (250 MHz, $CDCl_3$) δ 7.51 (1H, s, Ar*H*), 5.70 (1H, dqd, CH=C*H*$CH_3$, *J* = 15.4, 6.5, 1.1 Hz), 5.55 (1H, ddq, *J* = 15.4, 6.5, 1.4 Hz, CHOHC*H*=CH), 4.58 – 4.55 (3H, m, C$H_2$OH and C*H*OH), 2.95 – 2.92 (2H, m, ArC$H_2$CH), 1.69 (3H, dd, *J* = 6.5, 1.4 Hz, CHC$H_3$); **$^{13}$C NMR** δ (90.6 MHz, $CDCl_3$) 163.03 (C), 139.98 (C), 134.98 (CH), 132.04 (CH), 127.71 (CH), 69.85 (CH), 56.42 ($CH_2$), 35.99 ($CH_2$), 17.65 ($CH_3$); ***m/z*** (EI) 183 ($[M]^+$, 5%), 165 (36), 113 (88), 95 (100); **HRMS** (EI) $[M]^+$ found 183.0890, $C_9H_{13}NO_3$ requires 183.0890.

**4-([2-(Trimethylsilyl)ethoxy]methoxymethyl)-2-[(3*E*)-pent-3-en-2-ol-1-yl]-1,3-oxazole 213b**

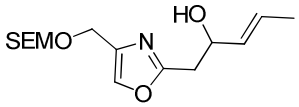


**General procedure A** was followed with SEM protected oxazole **212b** (100 mg, 0.41 mmol). Flash chromatography (1:49 MeOH:DCM) resulted in an inseparable mixture of methyl oxazole starting material (**212b**) and product **213b**.

**$R_f$** (hexane: EtOAc, 1:1) = 0.36; **$^1$H NMR** (500 MHz, $CDCl_3$) δ 7.54 (1H, s, Ar*H*), 5.75 (1H, dq, CH=C*H*$CH_3$, *J* = 15.4, 6.5 Hz), 5.56 (1H, ddq, *J* = 15.4, 6.5, 1.4 Hz, CHC*H*=CH), 4.75 (2H, s, OC$H_2$O), 4.57 - 4.56 (1H, m, C*H*OH), 4.49 (2H, s, ArC$H_2$O), 3.67 – 3.63 (2H, m, OC$H_2$), 3.27 (1H, s, O*H*), 2.94 – 2.88 (2H, m, ArC$H_2$CH), 1.69 (3H dd, *J* = 6.5, 1.4 Hz CHC$H_3$), 0.97 – 0.94 (2H, m, C$H_2$Si), 0.02 (9H, s, Si(C$H_3$)$_3$); ***m/z*** (ESI+, MeOH) 649 ($[2M+Na]^+$, 87 %), 336 ($[M+Na]^+$, 100), 314 ($[M+H]^+$, 31).

**4-[(Methoxymethoxy)methyl]-2-[(3*E*)-pent-3-en-2-ol-1-yl]-1,3-oxazole 213c**

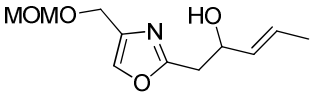


**General procedure A** was followed with MOM protected oxazole **212c** (130 mg, 0.83 mmol). The product was purified by flash chromatography (1:8 MeOH:DCM) to give the alcohol **213c** as an brown gum (94 mg, 50 %).

**$R_f$** (MeOH:DCM, 1:9) = 0.57; **IR** (neat, $cm^{-1}$) 3408 (OH), 1672 (C=N), 1570 (C=C); **$^1$H NMR** δ (500 MHz, $CDCl_3$) 7.52 (1H, s, Ar*H*), 5.72 (1H, dqd, CH=C*H*$CH_3$, *J* = 15.3, 6.5, 1.0 Hz), 5.53 (1H, ddq, *J* = 15.3, 6.5, 1.5 Hz, CHOHC*H*=CH), 4.67 (2H, s, OC$H_2$O), 4.54 - 4.49 (1H, m, C*H*OH), 4.46 (2H, s, ArC$H_2$O), 3.33 (3H, s, $OCH_3$), 2.95 – 2.88 (2H, m, ArC$H_2$CH) 1.66 (3H, dd, *J* = 6.5, 1.5 Hz, CHC$H_3$); **$^{13}$C NMR** δ (126 MHz, $CDCl_3$) 163.03 (C), 137.29 (C), 136.07 (CH), 132.04 (CH), 127.71 (CH), 95.75 ($CH_2$), 69.89 (CH), 60.81 ($CH_2$), 55.41 ($CH_3$), 35.92 ($CH_2$), 17.66 ($CH_3$); ***m/z*** (CI, *i*-butane) 228 ($[M+H]^+$, 47 %), 210 (89), 57 (100); **HRMS** (CI, *i*-butane) $[M+H]^+$ found 228.1225, $C_{11}H_{18}NO_4$ requires 228.1230.

**4-[(Methoxymethoxy)methyl]-2-[(3*E*)-hept-3-en-5-yn-2-ol-1-yl]-1,3-oxazole 214**

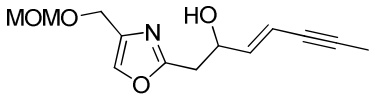


**General procedure A** was followed with MOM protected oxazole **212c** (480 mg, 3.06 mmol). The product was purified by flash chromatography (1:20 MeOH:DCM) twice to give the alcohol **214** as a brown gum (192 mg, 25 % (40 % yield based on recovered starting material from 2nd column)).

**$R_f$** (DCM:MeOH, 11:1) = 0.47; **IR** (neat, $cm^{-1}$) 3383 (OH), 2200 (C≡C), 1610 (C=N), 1570 (C=C), 1149; **$^1$H NMR** (400 MHz, $CDCl_3$) δ 7.55 (1H, s, Ar*H*), 6.08 (1H, dd, *J* = 15.8, 5.7 Hz, CHOHC*H*=CH), 5.78 (1H, dhex, *J* = 15.8, 2.3 Hz, CH=C*H*C), 4.71 (2H, s, OC$H_2$O), 4.66-4.64 (1H, m, C*H*OH), 4.49 (2H, s, ArC$H_2$O), 3.45 (1H, br s, OH), 3.41 (3H, s, $OCH_3$), 2.99 (1H, dd, *J* = 16.0, 4.0 Hz, ArC$H_X$C$H_Y$CH), 2.90 (1H, dd, *J* = 16.0, 8.3 Hz, ArC$H_X$C$H_Y$CH), 1.95 (3H, d, *J* = 2.3 Hz, CC$H_3$); **$^{13}$C NMR** δ (126 MHz, $CDCl_3$) 162.56 (C), 141.56 (CH), 137.30 (C), 136.26 (CH), 111.62 (CH), 95.78 ($CH_2$), 87.50 (C), 77.27 (C), 69.15 (CH), 60.71 ($CH_2$), 55.50 ($CH_3$), 35.35 ($CH_2$), 4.37 ($CH_3$); ***m/z*** (EI) 251 ($[M]^+$, 22 %), 157 (66), 125 (57), 95 (100); **HRMS** (EI) $[M]^+$ found 251.1152, $C_{13}H_{17}NO_4$ requires 251.1152.

**4-[(Methoxymethoxy)methyl]-2-[(3*E*)-2-Methoxyhept-3-en-5-yn-1-yl]-1,3-oxazole 215**

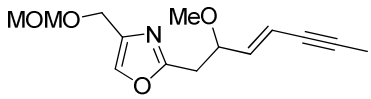


To a solution of alcohol **214** (100 mg, 0.40 mmol) in THF (3 mL) at 0 °C was added NaH (39 mg, 0.99 mmol, 60 % dispersion in mineral oil), and the suspension was stirred for 30 min. Iodomethane (0.05 mL, 0.8 mmol) was then added and the mixture stirred at 0 °C for 40 min and then at rt for ~18 h. The excess NaH was quenched by dropwise addition of $NaHCO_3$ (5 mL, sat aq) and diethyl ether was added (10 mL). The two layers were separated and the organic layer was washed with $Na_2S_2O_3$ (10 mL, 0.1 M), water (10 mL) and brine (10 mL), then dried, filtered and concentrated *in vacuo*. The product was purified by flash chromatography (1:1 EtOAc:hexane) to give the methyl ether **215** as a brown oil (30 mg, 29 %).

**$R_f$** (EtOAc:hexane, 1:3) = 0.28; **IR** (neat, $cm^{-1}$) 2220 (C≡C), 1680 (C=N), 1571 (C=C); **$^1$H NMR** (500 MHz, $CDCl_3$) δ 7.56 (1H, s, Ar*H*), 5.95 (1H, dd, *J* = 15.9, 7.7 Hz, CHC*H*=CH), 5.70 (1H, dd, *J* = 15.9, 2.0 Hz, CH=C*H*C), 4.74 (2H, s, OC$H_2$O ), 4.53 (2H, s, ArC$H_2$O), 4.12 (1H, q, *J* = 7.6 Hz, C*H*OMe), 3.43 (3H, s, OC$H_3$), 3.29 (3H, s, OC$H_3$ ), 3.07 (1H, dd, *J* = 15.0, 7.6 Hz, ArC$H_X$C$H_Y$CH), 2.96 (1H, dd, *J* = 15.0, 5.8 Hz, ArC$H_X$C$H_Y$CH), 1.97 (3H, d, *J* = 2.0 Hz, CC$H_3$). **$^{13}$C NMR** δ (126 MHz, $CDCl_3$) 161.95 (C), 140.07 (CH), 137.57 (C), 136.18 (CH), 113.72 (CH), 95.85 ($CH_2$), 87.52 (C), 79.36 (CH), 77.19 (C), 61.05 ($CH_2$), 56.71 ($CH_3$), 55.45 ($CH_3$), 34.76 ($CH_2$), 4.27 ($CH_3$); ***m/z*** (EI) 265 ($[M]^+$, 4 %), 234 (3), 109 (100), **HRMS** (EI) $[M]^+$ found 265.1318, $C_{14}H_{19}NO_4$ requires 265.1319.

**4-Hydroxymethyl-2-[(3*E*)-2-Methoxyhept-3-en-5-yn-1-yl]-1,3-oxazole 389**

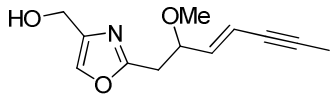


To a solution of MOM protected alcohol **215** in methanol was added HCl (5 drops, conc. aq) and the solution was stirred for ~18 h at rt. The solvent was removed *in vacuo* and the residue was taken into EtOAc, washed with $NaHCO_3$ (10 mL, sat aq). The aqueous phase was extracted with EtOAc (2 × 10 mL). The organic layers were combined, dried, filtered and concentrated *in vacuo*, to give the alcohol **389** as a brown oil 42 mg (74 %).

**$R_f$** (MeOH:DCM, 1:9) = 0.50; **IR** (neat, $cm^{-1}$) 3392 (OH), 2223 (C≡C), 1680 (C=C), 1570 (C=C); **$^1$H NMR** (500 MHz, $CDCl_3$) δ 7.50 (1H, s, Ar*H*), 5.90 (1H, dd, *J* = 15.9, 7.7 Hz, CHC*H*=CH), 5.67 (1H, dq, *J* = 15.9, 2.2 Hz, CH=C*H*C), 4.55 (2H, s, C$H_2$OH ), 4.06 (1H, q, *J* = 7.4 Hz, C*H*OMe), 3.25 (3H, s, OC$H_3$), 3.02 (1H, dd, *J* = 15.1, 7.4 Hz, ArC$H_X$CH$_Y$CH), 2.91 (1H, dd, *J* = 15.1, 5.7 Hz, ArCH$_X$C$H_Y$CH), 1.93 (3H, d, *J* = 2.2 Hz, CC$H_3$). **$^{13}$C NMR** δ (126 MHz, $CDCl_3$) 162.01 (C), 140.26 (C), 139.91 (CH), 135.10 (CH), 113.85 (CH), 87.62 (C), 79.26 (CH), 77.14 (C), 56.68 ($CH_2$), 56.60 ($CH_3$), 34.68 ($CH_2$), 4.26 ($CH_3$); ***m/z*** (EI) 221 ($[M]^+$, 26 %), 167 (27), 149 (34), 139 (44), 109 (100); **HRMS** (EI) $[M]^+$ found 221.1054, $C_{12}H_{15}NO_3$ requires 221.1057.

**2-[(3*E*)-2-Methoxyhept-3-en-5-yn-1-yl]-1,3-oxazole-4-carbaldehyde (±)-131**

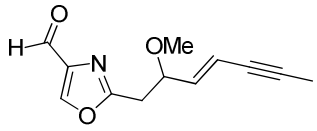


$NaHCO_3$ (201 mg, 2.4 mmol) was suspended in DCM (5 mL) and Dess-Martin periodinane (100 mg, 0.024 mmol) was added and the suspension stirred for 5 min at rt. The mixture was cooled to 0 °C and alcohol **389** (35 mg, 0.16 mmol) was added in DCM (1 mL) and the suspension was stirred at 0 °C for 2 h, after which a 1:1 mixture of $NaHCO_3$ (5 mL, sat aq) and $Na_2S_2O_3$ (5 mL, 0.1 M aq) was added and the mixture stirred for 10 min. The biphasic mixture was separated and the aqueous layer extracted with DCM (2 × 10 mL), the organic layers were combined, dried, filtered and concentrated *in vacuo*. The product was purified by flash chromatography (1:1 EtOAc:hexane) to give the aldehyde **(±)-131** as a brown oil (15 mg, 43 %).

**$R_f$** (EtOAc:hexane, 1:1) = 0.38; **IR** (neat, $cm^{-1}$) 2220 (C≡C), 1699 (C=O), 1583 (C=C); **$^1$H NMR** (500 MHz, $CDCl_3$) δ 9.91 (1H, s, C*H*O) 8.19 (1H, s, Ar*H*), 5.92 (1H, dd, *J* = 15.9, 7.7 Hz, CHC*H*=CH), 5.70 (1H, dqd, *J* = 15.9, 2.1, 0.9 Hz, CH=C*H*C), 4.15-4.11 (1H, m, C*H*OMe), 3.27 (3H, s, OC$H_3$), 3.10 (1H, dd, *J* = 15.2, 7.7 Hz, ArC$H_X$CH$_Y$CH), 3.01 (1H, dd, *J* = 15.2, 5.5 Hz, ArCH$_X$C$H_Y$CH), 1.95 (3H, d, *J* = 2.1 Hz, CC$H_3$). **$^{13}$C NMR** δ (126 MHz, $CDCl_3$) 184.02 (CH), 163.10 (C), 144.43 (CH), 140.94 (C), 139.44 (CH), 113.31 (CH), 87.96 (C), 79.10 (CH), 77.23 (C) 56.74 ($CH_3$), 34.59 ($CH_2$), 4.28 ($CH_3$); ***m/z*** (EI) 219 ($[M]^+$, 23 %), 204 (11), 188 (17), 167 (20), 149 (41), 109 (100), **HRMS** (EI) $[M]^+$ found 219.0898, $C_{12}H_{13}NO_3$ requires 219.0901.

## 6.3 Experimental for Chapter 3

**2-[(4*R*)-2,2-Dimethyl-1,3-dioxolan-4-yl]acetaldehyde 221**

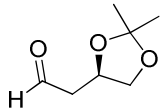

To a stirred solution of oxalyl chloride (4.34 mL, 51.3 mmol) in dry DCM (80 mL), DMSO (8.83 mL, 82.1 mmol) was added at −78 °C and stirred at −78 °C for 30 min. A solution of alcohol **220** (5.00 g, 34.2 mmol) in DCM (10 mL) was added at −78 °C and stirred for 3 h at −78 °C. The reaction mixture was warmed to 0 °C, treated with $Et_3N$ (23.0 mL, 165 mmol) and stirred for 15 min. The reaction mixture was diluted with DCM (300 mL) and washed with water (200 mL). The organic layer was dried, filtered and concentrated *in vacuo* to afford aldehyde **221** as a pale yellow syrup (quant), which was used directly in the next step.

**$^1$H NMR** (400 MHz, $CDCl_3$) δ 9.80 (1H, t, $J$ = 1.6 Hz, C*H*O), 4.53 (1H, quintet, $J$ = 6.4 Hz, $CH_2CHCH_2$), 4.19 (1H, dd, $J$ = 8.3, 6.0 Hz, $CHCH_XCH_Y$), 3.59 (1H, dd, $J$ = 8.3, 6.7 Hz, $CHCH_XCH_Y$), 2.84 (1H, ddd, $J$ = 17.1, 6.6, 1.6 Hz, $CHOCH_ACH_B$), 2.64 (1H, ddd, $J$ = 17.1, 6.5, 1.6 Hz, $CHOCH_ACH_B$), 1.41 (3H, d, $J$ = 0.4 Hz, $CH_3$), 1.36 (3H, d, $J$ = 0.4 Hz, $CH_3$).

Spectroscopic data are in good agreement with the literature.[161]

**2-[(4*R*)-2,2-Dimethyl-1,3-dioxolan-4-yl]acetic acid 26b**

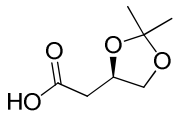

To a stirred solution of aldehyde **221** (assumed 34.2 mmol) in *tert*-butanol/water (7:3, 1000 mL), sodium chlorite (4.64 g, 51.3 mmol), and $H_2O_2$ (25 mL, 6% aq) were added and the mixture was stirred at rt for ~18 h. The reaction mixture was concentrated, the residue dissolved in EtOAc (100 mL), washed with water (20 mL) and brine (20 mL), dried, filtered and concentrated *in vacuo*. The crude product was passed through a silica plug eluting with EtOAc to afford the unstable acid **26b** as a colourless syrup (4.15 g, 76 % over 2 steps).

**$^1$H NMR** (400 MHz, $CDCl_3$) δ 4.47 (1H, quintet, $J$ = 6.5 Hz, $CH_2CHCH_2$), 4.16 (1H, dd, $J$ = 8.4, 6.0 Hz, $CHCH_XCH_YO$), 3.66 (1H, dd, $J$ = 8.4, 6.2 Hz, $CHCH_XCH_YO$), 2.74 (1H, dd, $J$ = 16.2, 6.7 Hz, $CO_2HCH_ACH_B$), 2.57 (1H, dd, $J$ = 16.2, 6.7 Hz, $CO_2HCH_ACH_B$), 1.42 (3H, d, $J$ = 0.5 Hz, $CH_3$), 1.36 (3H, d, $J$ = 0.5 Hz, $CH_3$).

Spectroscopic data are in good agreement with the literature.[162]

**Methyl 2-{2-[(4*R*)-2,2-dimethyl-1,3-dioxolan-4-yl]acetamido}-3-hydroxypropanoate 27b**

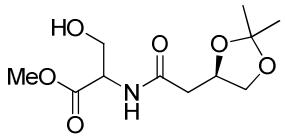

To a solution of acid **26b** (1.20 g, 6.89 mmol) in THF (10 mL) at 0 °C was added 1,1'- carbonyldiimidazole (1.34 g, 6.96 mmol), and the mixture was stirred for 30 min. The cooling bath was removed, serine methyl ester hydrochloride (1.08 g, 6.96 mmol) was added in one portion, and the reaction mixture was stirred for ~18 h at rt. The solvent was removed *in vacuo*, and the crude residue was partitioned between EtOAc/brine (4:1, 25 mL). The resulting biphasic mixture was separated, and the aqueous phase was extracted with EtOAc (4 × 10 mL). The organic extracts were combined, dried, filtered and concentrated *in vacuo*. The crude residue was purified by flash chromatography (1:9, hexane: EtOAc) to provide amide **27b** as a pale orange syrup (0.850 g, 47%).

**$R_f$** (Hexane:EtOAc, 1:9) = 0.20; **$[\alpha]_D$** = +11.6 (c 0.86, $CHCl_3$), lit[25] ent +31.0 (c 0.5, $CHCl_3$) ; **IR** (neat, $cm^{-1}$) 3354 (OH/NH), 1747 (C=O), 1660 (C=O); **$^1$H NMR** δ (400 MHz, $CDCl_3$) 7.01 (0.45 H, d, *J* = 6.5 Hz, N*H*), 6.88 (0.55H, d, *J* = 6.5 Hz, N*H*), 4.69 – 4.64 (1H, m, $CH_2CHCH_2$), 4.46 (1H, m, $CHCH_XCH_YO$), 4.14 (1H, m, $CHCH_XCH_YO$), 3.96 (2H, dd, *J* = 3.4, 2.0 Hz, $CH_2OH$), 3.80 (3H, s, $CO_2CH_3$), 3.66 (1H, dt, *J* = 6.5, 2.0, Hz, COC*H*NH), 2.59 – 2.54 (2H, m, $COCH_2$), 1.47 (1.35H, s, $CH_3$), 1.45 (1.65H, d, *J* = 8.6 Hz, $CH_3$), 1.37 (3H, s, $CH_3$); **$^{13}$C NMR** δ (101 MHz, $CDCl_3$) 170.82*, 170.74 (C), 170.33*, 170.24 (C), 109.56*, 109.52 (C), 72.54*, 72.15 (CH), 69.01*, 68.62 ($CH_2$), 63.36, 63.08* ($CH_2$), 54.97, 54.81* (CH), 52.80 ($CH_3$), 40.57*, 40.20 ($CH_2$), 26.90*, 26.61 ($CH_3$), 25.48*, 25.06 ($CH_3$) (*denotes minor rotamer); ***m/z*** (ESI–, MeOH) 260 ($[M-H]^-$, 100 %), 230 (56).

Spectroscopic data are in good agreement with the literature.[25]

**Methyl 2-{[(4*R*)-2,2-dimethyl-1,3-dioxolan-4-yl]methyl}-2,5-dihydro-1,3-oxazole-4-carboxylate 390**

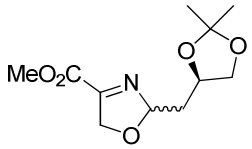

To a solution of amide **27b** (0.800 g, 3.06 mmol) in DCM (8 mL) at −78 °C was added diethylaminosulfur trifluoride (DAST) (0.420 mL, 3.22 mmol), and the reaction was stirred for 45 min. Solid $K_2CO_3$ (0.845 g, 6.12 mmol) was then added, and the reaction was stirred for 1 h and then warmed to rt. The orange slurry was slowly added to saturated aqueous $NaHCO_3$ (10 mL), and the resultant biphasic mixture was separated. The aqueous phase was extracted with DCM (2 × 10 mL), and the combined organics were dried, filtered and concentrated *in vacuo*. The crude oxazoline **390** was taken on without further purification.

**$^1$H NMR** δ (400 MHz, $CDCl_3$) 4.74 (1H, m, $CH_2CHCH_2$), 4.51 – 4.38 (3H, m, NOC*H*$CH_2$and C$H_2$ring), 4.14 (1H, m, $CHCH_XCH_YO$), 3.79 (3H, s, $CO_2CH_3$), 3.70 (1H, m, $CHCH_XCH_YO$), 2.73 (1H, m, $CHCH_ACH_BCH$), 2.52 (1H, m, $CHCH_ACH_BCH$), 1.40 (3H, s, C$H_3$), 1.34 (3H, s, C$H_3$).

**Methyl 2-{[(4*R*)-2,2-dimethyl-1,3-dioxolan-4-yl]methyl}-1,3-oxazole-4-carboxylate 28b**

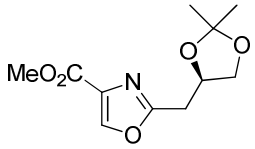

Crude oxazoline **390** (assumed 3.06 mmol) was dissolved in DCM (15 mL), and then cooled to 0 °C. To this solution was added DBU (0.91 mL, 6.12 mmol) followed by $BrCCl_3$ (0.33 mL, 3.40 mmol), and the reaction mixture was stirred for ~18 h without further cooling. $NH_4Cl$ (20 mL, sat aq) was then added, and the biphasic mixture was separated. The aqueous phase was extracted with DCM (3 × 10 mL) and the combined organic extracts were dried, filtered and concentrated *in vacuo*, and the crude residue was purified *via* column chromatography (1:1, hexane:EtOAc) to provide the oxazole **28b** (0.50 g, 68%, over two steps) as a colourless oil.

**$R_f$** (Hexane:EtOAc, 1:1) = 0.24; **$[\alpha]_D$** = +4.8 (c 1.43, $CHCl_3$), lit[25] ent –0.7 (c 1.0, $CHCl_3$); **IR** (neat, $cm^{-1}$) 1743 (C=O), 1587 (C=C); **$^1$H NMR** δ (500 MHz, $CDCl_3$) 8.18 (1H, s, Ar*H*), 4.56 (1H, quintet, *J* = 6.0 Hz, $CH_2CHCH_2$), 4.14 (1H, dd, *J* = 8.5, 6.0 Hz $CHCH_XCH_YO$), 3.90 (3H, s, $CO_2CH_3$), 3.77 (1H, dd, *J* = 8.5, 6.0 Hz, $CHCH_XCH_YO$), 3.15 (1H, dd, *J* = 15.2, 6.5 Hz, $ArCH_ACH_B$), 3.02 (1H, dd, *J* = 15.2, 6.5 Hz, $ArCH_ACH_B$), 1.40 (3H, s, $CH_3$), 1.34 (3H, s, $CH_3$); **$^{13}$C NMR** δ (126 MHz, $CDCl_3$) 162.20 (C), 161.59 (C), 144.15 (CH), 133.39 (C), 109.75 (C), 73.04 (CH), 68.77 ($CH_2$), 52.18 ($CH_3$), 32.94 ($CH_2$), 26.89 ($CH_3$), 25.47 ($CH_3$); ***m/z*** (ESI+, MeOH) 264 ($[M+Na]^+$, 100 %), 242 ($[M+H]^+$, 7), 184 (33).

Spectroscopic data are in good agreement with the literature.[25]

**Methyl 2-[(2*R*)-2,3-dihydroxyprop-1-yl]-1,3-oxazole-4-carboxylate 391**

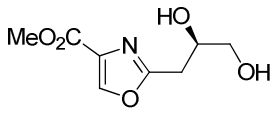


To a solution of acetonide **28b** (0.65 g, 2.69 mmol) in methanol (10 mL) was added DOWEX 50WX8-200 until the solution was acidic (monitored by pH indicator paper) and the reaction mixture was stirred at rt for ~18 h. The solids were removed by filtration through celite and the solvent removed *in vacuo* to give diol **391** as an orange oil (0.54 g, quant).

**$R_f$** (DCM:MeOH, 9:1) = 0.24; **$[\alpha]_D$** = +19.5 (c 0.41, $CHCl_3$), lit[25] ent –21.3 (c 0.4, $CHCl_3$); **IR** (neat, $cm^{-1}$) 3354 (OH), 1737 (C=O), 1587 (C=C); **$^1$H NMR** δ (400 MHz, $CDCl_3$) 8.18 (1H, s, Ar*H*), 4.37 – 4.18 (1H, m, $CH_2CHCH_2$), 3.91 (3H, s, $CO_2CH_3$), 3.77 (1H, dd, *J* = 11.3, 3.7 Hz, $CHCH_XH_YO$), 3.62 (1H, dd, *J* = 11.3, 5.8 Hz $CHCH_XH_YO$), 3.09 (1H, dd, *J* = 16.0, 8.1 Hz, $ArCH_AH_BCH$), 3.02 (1H, dd, *J* = 16.0, 4.6 Hz, $ArCH_AH_BCH$), 2.04 (1H, br s, O*H*); **$^{13}$C NMR** δ (126 MHz, $CDCl_3$) 163.39 (C), 161.50 (C), 144.02 (CH), 133.14 (C), 69.13 (CH), 65.64 ($CH_2$), 52.21 ($CH_3$), 32.01 ($CH_2$); ***m/z*** (ESI+, MeOH/DCM) 425 $[2M+Na]^+$, 100 %), 224 ($[M+Na]^+$, 32), 202 ($[M+H]^+$, 9).

Spectroscopic data are in good agreement with the literature.[25]

**Methyl 2-[(2*R*)-2-hydroxy-3-{[tris(propan-2-yl)silyl]oxy}prop-1-yl]-1,3-oxazole-4-carboxylate 223**

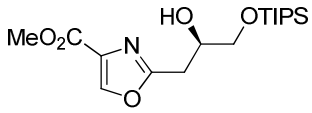


To a solution of diol **391** (0.500 g, 2.49 mmol) in DCM (40 mL) at −78 °C was added 2,6-lutidine (0.320 mL, 2.73 mmol) followed by TIPSOTf (0.800 mL, 2.98 mmol). The solution was stirred at −78 °C for 1 h and allowed to warm to rt over 1 h. Brine (50 mL) was added and the reaction mixture was extracted with DCM (2 × 50 mL), the combined organic layers were dried, filtered and concentrated *in vacuo*. The crude residue was purified by flash chromatography (1:1, hexane: EtOAc) to give the silyl ether **223** as pale yellow oil (0.690 g, 78 %).

**$R_f$** (Hexane:EtOAc, 1:1) = 0.40; **$[\alpha]_D$** = +15.7 (c 1.66, $CHCl_3$), lit[25] ent -13.9 (c 0.9, $CHCl_3$); **IR** (neat, $cm^{-1}$) 3450 (OH), 1741 (C=O), 1587 (C=C); **$^1$H NMR** δ (400 MHz, $CDCl_3$) 8.21 (1H, s, Ar*H*), 4.27– 4.20 (1H, m, $CH_2CHCH_2$), 3.94 (3H, s, $CO_2CH_3$), 3.81 (1H, dd, *J* = 9.9, 4.6 Hz, $CH_XH_YOTIPS$), 3.74 (1H, dd, *J* = 9.9, 5.6 Hz, $CH_XH_YOTIPS$), 3.08 (1H, dd, *J* = 13.2, 3.2 Hz, $ArCH_AH_BCH$ ), 3.04 (1H, dd, *J* = 13.2, 5.0 Hz, $ArCH_AH_BCH$), 2.90 (1H, d, *J* = 5.3 Hz, O*H*), 1.28 - 0.95 (21H, m, $Si(CH(CH_3)_2)_3$); **$^{13}$C NMR** δ (101 MHz, $CDCl_3$) 163.41 (C), 161.65 (C), 143.98 (CH), 133.29 (C), 69.64 (CH), 66.36 ($CH_2$), 52.14 ($CH_3$), 32.27 ($CH_2$), 17.93 ($6CH_3$), 11.89 (3CH); ***m/z*** (ESI+, MeOH/DCM) 737 ($[2M+Na]^+$, 62 %), 380 ($[M+Na]^+$, 100), 358 (($[M+H]^+$, 32).

Spectroscopic data are in good agreement with the literature.[25]

**Methyl 2-[(2*R*)-2-methoxy-3-{[tris(propan-2-yl)silyl]oxy}prop-1-yl]-1,3-oxazole-4-carboxylate 392**

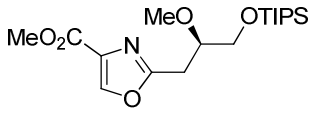


Alcohol **223** (0.350 g, 1.03 mmol), iodomethane (1.16 mL, 18.6 mmol) and silver(I) oxide (0.429 g, 1.85 mmol) in MeCN (20 mL) were heated at 60 °C for ~18 h. The brown suspension was allowed to cool to rt, ether (50 mL) was added and the solids were removed by filtration through celite. The solvent was removed *in vacuo* and the crude residue was purified by flash chromatography (3:1, hexane: EtOAc) to give the methyl ether **392** as a yellow oil (0.240 g, 63 %).

**$R_f$** (Hexane:EtOAc, 3:1) = 0.30; **$[\alpha]_D$** = +24.0 (c 0.25, $CHCl_3$), lit[25] ent −7.8 (c 0.5, $CHCl_3$); **IR** (neat, $cm^{-1}$) 1749 (C=O), 1585 (C=C); **$^1$H NMR** δ (500 MHz, $CDCl_3$) 8.19 (1H, s, Ar*H*), 3.94 (3H, s, $CO_2CH_3$), 3.89 – 3.78 (2H, m, $CH_XCH_YOTIPS$ and $CH_2CHCH_2$), 3.76 - 3.73 (1H, m, $CH_XCH_YOTIPS$), 3.17 (3H, s, $OCH_3$), 3.17 (1H, dd, *J* = 15.3, 4.8 Hz, $ArCH_ACH_B$), 3.03 (1H, dd, *J* = 15.3, 7.7 Hz, $ArCH_ACH_B$), 1.18-0.99 (21H, m, $Si(CH(CH_3)_2)_3$); **$^{13}$C NMR** δ (126 MHz, $CDCl_3$) 163.76 (C), 161.80 (C), 143.85 (CH), 133.32 (C), 79.72 (CH), 64.42 ($CH_2$), 58.06 ($CH_3$), 52.11 ($CH_3$), 30.89 ($CH_2$), 17.95 ($6CH_3$), 11.90 (3CH); ***m/z*** (ESI+, MeOH/DCM) 394 ($[M+Na]^+$, 100 %), 372 ($[M+H]^+$, 75).

Spectroscopic data are in good agreement with the literature.[25]

**Methyl 2-[(2*R*)-2,3-dihydroxyprop-1-yl]-1,3-oxazole-4-carboxylate 29b**

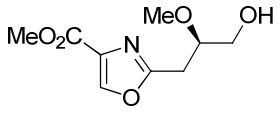


To a solution of silyl ether **392** (95 mg, 0.25 mmol) in THF (5 mL) at 0 °C was added TBAF (0.38 mL, 0.38 mmol, 1 M in THF) dropwise and the solution was stirred for ~18 h at rt. The solvent was removed *in vacuo* and the crude residue was purified by flash chromatography (1:1, hexane: EtOAc) to give the alcohol **29b** as an orange oil (40 mg, 73 %).

**$R_f$** (Hexane:EtOAc, 1:3) = 0.24; **$[\alpha]_D$** = –14.3 (c 0.45, $CHCl_3$), lit[29] -13.89 (c 3.47, $CHCl_3$); **IR** (neat, $cm^{-1}$) 3471 (OH), 1737 (C=O), 1585 (C=C); **$^1$H NMR** δ (500 MHz, $CDCl_3$) 8.20 (1H, s, Ar*H*), 3.94 (3H, s, $CO_2CH_3$), 3.82 – 3.78 (2H, m, $CH_XCH_YOH$ and $CH_2CHCH_2$), 3.63 - 3.58 (1H, m, $CH_XCH_YOH$), 3.43 (3H, s, $OCH_3$), 3.15 (1H, dd, *J* = 15.3, 6.1 Hz, $ArCH_ACH_B$), 3.07 (1H, dd, *J* = 15.3, 6.4 Hz, $ArCH_ACH_B$), 2.06 (1H, t, *J* = 6.1 Hz, O*H*); **$^{13}$C NMR** δ (126 MHz, $CDCl_3$) 162.90 (C), 161.61 (C), 144.01 (CH), 133.39 (C), 78.99 (CH), 63.20 ($CH_2$), 57.58 ($CH_3$), 52.18 ($CH_3$), 30.20 ($CH_2$); ***m/z*** (ESI+, MeOH/DCM) 453 ($[2M+Na]^+$, 100 %), 238 (($[M+Na]^+$, 36), 216 (($[M+H]^+$, 20).

Spectroscopic data are in good agreement with the literature.[29]

**Ethyl 2-amino-1,3-oxazole-4-carboxylate·HCl 240**

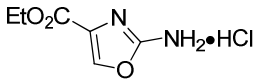


Ethyl bromopyruvate (2.00 mL, 15.9 mmol) and urea (1.44 g, 23.9 mmol) in ethanol (5 mL) were heated under reflux for 2 h. The cooled reaction mixture was concentrated *in vacuo* to give an oil, to this was added water (5 mL) and the mixture adjusted to pH 10 by the addition of NaOH (10 % aq). The mixture was extracted with ether (4 × 30 mL) and the extract treated with HCl in ether (20 mL, 1 M) and the precipitate filtered to give the hydrochloride salt of amino oxazole **240** as colourless solid (2.23 g, 73 %).

**$R_f$** (DCM:MeOH, 9:1) = 0.00 **Mp** = 135-138 °C, lit[163] 133-135 °C ; **IR** (neat, $cm^{-1}$) 3381 ($NH_2$), 1715 (C=O); **$^1$H NMR** δ (500 MHz, DMSO-$d_6$) 8.27 (1H, s, Ar*H*), 5.18 (2H, br s, N$H_2$), 4.23 (2H, q, $J$ = 7.1 Hz, C$H_2$), 1.25 (3H, t, $J$ = 7.1 Hz, C$H_3$); **$^{13}$C NMR** δ (126 MHz, DMSO-$d_6$) 160.82 (C), 160.04 (C), 138.08 (CH), 128.31 (C), 61.31 ($CH_2$), 14.54 ($CH_3$); ***m/z*** (EI) 156 ($[M]^+$, 100 %), 128 (89), 110 (12).
Spectroscopic data are in good agreement with the literature.[163]

**Ethyl 2-chloro-1,3-oxazole-4-carboxylate 230a**

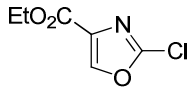


2-Aminooxazole **240** (200 mg, 1.28 mmol) was added in portions to a solution of *tert*-butyl nitrite (0.220 mL, 1.50 mmol) and copper (II) chloride (258 mg, 1.50 mmol) in acetonitrile (6 mL) at 60 °C. The mixture was then heated at 80 °C for 2 h. The mixture was cooled and partitioned between DCM (30 mL), water (15 mL), and HCl (2 mL, conc). The aqueous layer was further extracted with DCM (2 × 20 mL) and the combined organics were washed with brine, dried, filtered and concentrated *in vacuo*. The residue was purified by flash chromatography (3:1 hexane:ether) to give chlorooxazole **230a** (60 mg, 27 %).

**$R_f$** (EtOAc:hexane, 1:3) = 0.42; **IR** (neat, $cm^{-1}$) 1766 (C=N), 1726 (C=O), 1523 (C=C); **Mp** = 75 °C, lit[164] 97-99 °C ; **$^1$H NMR** δ (500 MHz, $CDCl_3$) 8.20 (1H, s, Ar*H*), 4.40 (2H, q, $J$ = 7.1 Hz, C$H_2$), 1.39 (3H, t, $J$ = 7.1 Hz, C$H_3$); **$^{13}$C NMR** δ (126 MHz, $CDCl_3$) 160.04 (C), 148.29 (C), 145.42 (CH), 135.09 (C), 61.74 ($CH_2$), 14.27 ($CH_3$); ***m/z*** (EI) 175 ($[M]^+$, 100 %), 157 (42), 147 (33), 130 (58), 119 (49), 111 (100). Spectroscopic data are in good agreement with the literature.[164]

**Ethyl 1,3-oxazole-4-carboxylate 244**

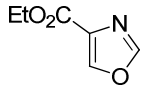

To a solution of formic acid (2.00 mL, 53.0 mmol) in THF (30 mL) at rt was added 1,1-dicarbonyldiimidazole (8.58 g, 53.0 mmol) portionwise. The resulting solution was stirred for 30 min after which, ethyl isocyanoacetate (5.79 mL, 53.0 mmol) was added, followed by triethylamine (14.8 mL, 106mmol). The resulting solution was stirred for 1 h at rt and then heated at reflux for 20 h. The mixture was cooled to rt and concentrated *in vacuo*, the residue was dissolved in ether (50 mL) and washed with water (80 mL). The aqueous layer was extracted with EtOAc (3 × 50 mL), the combined organic layers were washed with brine (50 mL), dried, filtered and concentrated *in vacuo*. The residue was purified by flash chromatography (1:1 hexane:EtOAc) to give oxazole **244** as a brown liquid which solidified on standing (6.0 g, 80 %).

**$R_f$** (EtOAc:hexane, 1:1) = 0.46; **IR** (neat, $cm^{-1}$) 1732 (C=O), 1577 (C=C); **Mp** = 39-41 °C, lit[165] 47-49 ºC; **$^1$H NMR** δ (400 MHz, $CDCl_3$) 8.29 (1H, d, *J* = 1.0 Hz, Ar*H*), 7.95 (1H, d, *J* = 1.0 Hz, Ar*H*), 4.42 (2H, q, *J* = 7.1 Hz, C$H_2$), 1.42 (3H, t, *J* = 7.1 Hz, C$H_3$); **$^{13}$C NMR** δ (101 MHz, $CDCl_3$) 160.99 (C), 151.38 (CH), 144.03 (CH), 133.40 (C), 61.35 ($CH_2$), 14.27 ($CH_3$); ***m/z*** (EI) 141 ($[M]^+$, 73 %), 113 (68), 96 (100).
Spectroscopic data are in good agreement with the literature.[104]

**Pent-3-yn-1-yl 4-methylbenzene-1-sulfonate 264**

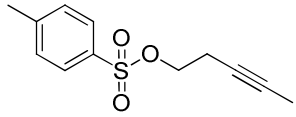

A solution of toluene-*p*-sulfonyl chloride (25.3 g, 132 mmol) in warm pyridine (12.0 mL, 154 mmol) was cooled rapidly in ice to obtain small crystals and pent-3-ynol (10.0 g, 118 mmol) was added slowly to keep the temperature below 25 °C. The reaction mixture was stirred at rt for ~18 h, then cooled to 0 °C and water (20 mL) was added. The mixture was poured into more water (200 mL) and extracted with ether (200 mL). The organic layer was washed with HCl (4 × 200 mL, 1 M aq) and $NaHCO_3$ (100 mL, sat aq), dried, filtered and concentrated *in vacuo* to give the tosylate **264** as a colourless liquid (26.0 g, 92 %).

**$R_f$** (EtOAc:hexane, 1:1) = 0.56; **IR** (neat, $cm^{-1}$) 1597 (C=C), 1359 (S=O), 1174 (S=O); **$^1$H NMR** δ (500 MHz, $CDCl_3$ ) 7.83 (2H, d, *J* = 8.1 Hz, Ar*H*), 7.27 (2H, d, *J* = 8.1 Hz, Ar*H*), 4.08 (2H, t, *J* = 7.2 Hz, TsOC$H_2$), 2.52 - 2.49 (2H, m, C$H_2$C), 2.48 (3H, s, C$H_3$Ar), 1.74 (3H, t, *J* = 2.5 Hz, CC$H_3$); **$^{13}$C NMR** (126 MHz, $CDCl_3$) δ 144.86 (C), 133.01 (C), 129.85 (2 × CH), 127.99 (2 × CH), 78.22 (C), 73.12 (C), 68.26 ($CH_2$), 21.66 ($CH_3$), 19.71 ($CH_2$), 3.40 ($CH_3$); ***m/z*** (CI, *i*-butane) 239.0 ($[M+H]^+$, 100 %), 149 (73), 132 (74).

Spectroscopic data are in good agreement with the literature.[166]

**Pent-1-en-3-yne 248**

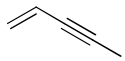

Tosylate **264** (26.0 g, 109 mmol) in ethanol (15 mL) was added dropwise to a solution of potassium hydroxide (7.35 g, 131 mmol) in water (15 mL) and ethanol (10 mL) containing a trace of detergent at 120 °C. Enyne **248** was evolved as a gas which was collected by passage through a fractionating column and condenser. The colourless highly volatile liquid collected (1.20 g) was used immediately in the next step.

**BP** 60 °C, lit[114] 57-59 °C; **$^1$H NMR** δ (400 MHz, $CDCl_3$) 5.78 (1H, ddq, *J* = 17.7, 11.0, 2.3 Hz, $CH_2$=C*H*), 5.57 (1H, dd, *J* = 17.7, 2.3 Hz, C$H_X$H$_Y$=CH), 5.40 (1H, dd, *J* = 11.0, 2.3 Hz, CH$_X$$H_Y$=CH), 1.97 (3H, d, *J* = 2.3, CC$H_3$).

Spectroscopic data are in good agreement with the literature.[114]

**Attempted synthesis of 2-[(1*E*)-pent-1-en-3-yn-1-yl]oxirane 231 Grubbs method**

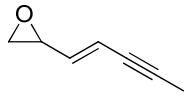

To a solution of enyne **248** (0.08 g, 1.21 mmol) in DCM (12 mL) were added butadiene monoxide (0.2 mL, 2.44 mmol) followed by Grubbs II (18 mg, 20 μmol). The reaction mixture was heated at reflux for 5 h, after which more catalyst was added (18 mg, 20 μmol) and the reaction heated for ~18 h. The solvent was removed *in vacuo* and the crude residue purified by column chromatography (9:1 hexane:EtOAc). The only product isolated was 2-[(*E*)-2-(oxiran-2-yl)ethenyl]oxirane **254** (20 mg).

**2-[(*E*)-2-(oxiran-2-yl)ethenyl]oxirane 254**

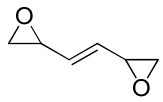

**$R_f$** (EtOAc:hexane, 1:3) = 0.49; **$^1$H NMR** δ (400 MHz, $CDCl_3$) δ 5.72 – 5.60 (2H, m, 2 × C*H*), 3.35 (2H, ddd, *J* = 6.7, 4.3, 2.6 Hz, 2 × C*H*O), 2.96 (2H, dt, *J* = 5.3, 3.8 Hz, 2 × C$H_X$H$_Y$), 2.71 – 2.60 (2H, m, 2 × CH$_X$$H_Y$).

Spectroscopic data are in good agreement with the literature.[116]

**But-2-ynyltriphenylphosphonium bromide 250**

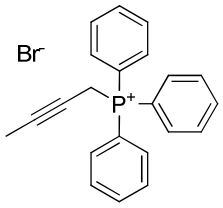


1-Bromo-2-butyne (1.00 mL, 11.4 mmol)and triphenyl phosphine (2.99 g, 11.42 mmol) were stirred at rt for 16 h. The resultant solid was filtered, washed with hexane (20 mL) and dried under vacuum to give phosphonium salt **250** as a yellow solid (3.24 g, 72 %).

**$R_f$** (MeOH:DCM, 1:9) = 0.48; **IR** (neat, $cm^{-1}$) 1585 (C=C), 997 (C=C); **Mp** = 195-197 °C; **$^1$H NMR** δ (500 MHz, $CDCl_3$) 7.82 - 7.74 (9H, m, Ar*H*), 7.66 – 7.62 (6H, m, Ar*H*), 4.87 (2H, dq, *J* = 14.8, 2.5 Hz, C$H_2$), 1.60 (3H, dt, *J* = 6.3, 2.5 Hz, C$H_3$); **$^{13}$C NMR** (126 MHz, $CDCl_3$) δ 135.34 (d, $^4J_{PC}$ = 3.0 Hz, 3 × CH), 133.90 (d, $^3J_{PC}$ = 9.9 Hz, 6 × CH), 130.35 (d, $^2J_{PC}$ = 12.8 Hz, 6 × CH), 117.62 (d, $^1J_{PC}$ = 87.4 Hz, 3 × C), 84.85 (d, $^3J_{PC}$ = 9.5 Hz, C), 66.21 (d, $^2J_{PC}$ = 13.6 Hz, C), 18.21 (d, $^1J_{PC}$ = 55.9 Hz, $CH_2$), 3.72 (d, $^4J_{PC}$ = 3.3 Hz, $CH_3$); ***m/z*** (ESI+, MeOH) 315 ($[M]^+$, 100 %).

Spectroscopic data are in good agreement with the literature.[119]

**Polymer supported But-2-ynyltriphenylphosphonium bromide 271**

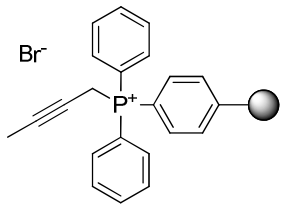


1-Bromo-2-butyne (1.16 mL, 13.2 mmol) was added dropwise to a suspension of polymer bound triphenyl phosphine (4.00 g, 12 mmol, 3mmol/g) in DMF (15 mL). The mixture was heated at 70 °C for 48 h, after cooling the suspension was filtered and washed several times with DCM, then ether over the course of several hours. Phosphine **271** was obtained as a brown solid (6.77 g, quant).

**Attempted synthesis of 2-[(1*E*)-pent-1-en-3-yn-1-yl]oxirane 231 Wittig method**

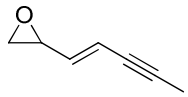

$NaHCO_3$ (1.83 g, 15 mmol) was suspended in DCM (30 mL) and Dess-Martin periodinane (0.925 g, 2.18 mmol) was added at rt. The mixture was stirred for 5 min, then cooled to 0 °C and glycidol (0.096 mL, 1.45 mmol) was added and the mixture was stirred for 2 h.

To a suspension of polymer supported phosphine **271** (0.812 g, 1.74 mmol) in THF (10 mL) was added *n*BuLi (0.91 mL, 1.75 mmol, 1.6 M in hexane) and the reaction was stirred at rt for 1 h. This suspension was added into the Dess-Martin reaction above and the reaction stirred for ~18 h at rt. The reaction mixture was filtered and washed with DCM (30 mL) and the filtrate was then washed with $NaHCO_3$ (30 mL, sat aq) and brine (50 mL). The organic layer was dried, filtered and concentrated *in vacuo* and the crude residue purified by flash chromatography (9:1 hexane:EtOAc) to give the product **277** as a yellow oil (50 mg).

**Possible product 277**

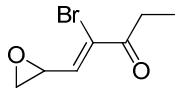

**$R_f$** (EtOAc:hexane, 1:3) = 0.65; **IR** (neat, $cm^{-1}$) 1693 (C=O); **$^1$H NMR** (400 MHz, $CDCl_3$) δ 6.74 (1H, d, *J* = 7.6 Hz), 3.92 (1H, ddd, *J* = 7.6, 4.2, 2.5 Hz), 3.19 (1H, dd, *J* = 5.4, 4.2 Hz), 2.89 (1H, dd, *J* = 5.4, 2.5 Hz), 2.83 (2H, qd, *J* = 7.2, 2.5 Hz), 1.17 (3H, t, *J* = 7.2 Hz); **$^{13}$C NMR** (126 MHz, $CDCl_3$) δ 193.93 (C), 140.42,(CH) 128.89 (C), 51.24 (CH), 48.23 ($CH_2$), 31.95 ($CH_2$), 8.40 ($CH_3$); ***m/z*** (CI, *i*-butane) 176 ([$^{81}$BrM-$CH_2O$]$^+$, 62 %), 174 ([$^{79}$BrM-$CH_2O$]$^+$, 63 %), 161 (99), 159 (100).

**Diethyl (but-2-yn-1-yl)phosphonate 281**

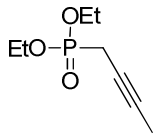

1-bromo-2-butyne (0.50 mL, 5.71 mmol) and triethyl phosphate (1.07 mL, 6.28 mL) were heated at reflux for 3 h. The reaction mixture was allowed to cool to rt and water (20 mL) and EtOAc (30 mL) were added. The layers were separated and the aqueous layer was extracted with EtOAc (3 × 30 mL), the combined organic layers were washed with brine (30 mL), dried, filtered and concentrated *in vacuo*. The residue was passed through a short plug of silica eluting with 1:1 EtOAc:hexane to give the phosphonate **281** as a brown liquid (1.08 g, quant).

**$R_f$** (EtOAc) = 0.30; **IR** (neat, $cm^{-1}$) 1257 (P=O), 1242 (P=O), 1020 (P-OEt); **$^1$H NMR** δ (500 MHz, $CDCl_3$) 4.25 - 4.11 (4H, m, 2 × C$H_2$CH$_3$), 2.69 (2H, dq, *J* = 21.8, 2.7 Hz, C$H_2$), 1.80 (3H, dt, *J* = 6.2, 2.7 Hz, C$H_3$), 1.35 (6H, t, *J* = 7.1 Hz, 2 × CH$_2$C$H_3$); **$^{13}$C NMR** (126 MHz, $CDCl_3$) δ 78.56 (d, $^3J_{PC}$ = 10.1 Hz, C), 68.44 (d, $^2J_{PC}$ = 14.6 Hz, C), 62.78 (d, $^2J_{PC}$ = 6.6 Hz, 2 × CH$_2$), 17.92 (d, $^1J_{PC}$ = 146.6 Hz, CH$_2$), 16.37 (d, $^3J_{PC}$ = 5.9 Hz, 2 × CH$_3$), 3.61 (d, $^4J_{PC}$ = 3.4 Hz, CH$_3$); ***m/z*** (CI, *i*-butane) 191 ($[M+H]^+$, 100 %).

Spectroscopic data are in good agreement with the literature.[167]

## 6.4 Experimental for Chapter 4

**[(4*S*)-2,2-Dimethyl-1,3-dioxolan-4-yl]methyl 4-methylbenzene-1-sulfonate 290**

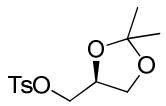


To a solution of (*R*)-2,2-dimethyl-1,3-dioxolane-4-methanol (15.0 g, 113 mmol) in pyridine (50 ml) at 0 °C *p*-toluenesulfonyl chloride (21.9 g, 114 mmol) was added and stirred at rt for ~18 h. Diethyl ether was added (200 mL) and the precipitate was removed by filtration and washed with a small amount of ether. The organic phase was washed with HCl (100 mL, 1 M aq), water (100 mL), $NaHCO_3$ (100 mL, sat aq) and more water (100 mL). The organic layer was dried, filtered and concentrated *in vacuo* giving the tosylate **290** as a colourless oil (32.4 g, quant)

**$R_f$** (Hexane:EtOAc, 1:1) = 0.69; **$[\alpha]_D$** = +7.7 (c 0.65, EtOH), lit[168] +4.3 (c 1.0, EtOH); **IR** (neat, $cm^{-1}$) 1598 (C=C), 1363 (S=O), 1179 (S=O); **$^1$H NMR** (400 MHz, $CDCl_3$) δ 7.78 (2H, d, *J* = 8.2 Hz, Ar*H*), 7.34 (2H, d, *J* = 8.2 Hz, Ar*H*), 4.36 – 4.19 (1H, m, $CH_2CHOCH_2$), 4.01 (1H, dd, *J* = 8.8, 6.3 Hz, $CH_XH_YO$), 4.00 (1H, dd, *J* = 10.1, 5.2 Hz, $TsOCH_AC H_B$), 3.96 (1H, dd, *J* = 10.1, 5.2 Hz, $TsOCH_ACH_B$), 3.74 (1H, dd, *J* = 8.8, 5.2 Hz, $CH_XH_YO$), 2.43 (3H, s, $CH_3Ar$ ), 1.31 (3H, s, $CH_3C$), 1.29 (3H, s, $CH_3C$); **$^{13}$C NMR** (101 MHz, $CDCl_3$) δ 145.10 (C), 132.65 (C), 129.94 (2 × CH), 128.00 (2 × CH), 110.05 (C), 72.92 (CH), 69.52 ($CH_2$), 66.17 ($CH_2$), 26.63 ($CH_3$), 25.15 ($CH_3$), 21.65 ($CH_3$); ***m/z*** (ESI+) 595 ($[2M+Na]^+$, 14 %), 309 ($[M+Na]^+$, 100), 287 ($[M+H]^+$, 10).

The spectroscopic data is in good agreement with the literature.[168]

**(2*S*)-3-{[(4-Methylbenzene)sulfonyl]oxy}propane-1,2-diol 291**

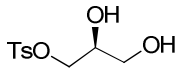


To a solution of acetonide **290** (32.4 g, 113 mmol) in methanol (250 mL) was added DOWEX 50WX8-200 until the solution was acidic (monitored by pH indicator paper) and stirred at rt for ~18 h. The solids were removed by filtration through celite and the solvent removed *in vacuo* to give a pale orange oil. Ether was added to the oil and it was allowed to stand at −18 °C for ~18 h. A colourless solid formed which was collected by filtration to give the diol **291** (34.3 g, 87 %).

**$R_f$** (EtOAc, 1:1) = 0.44; **Mp** = 56-58 °C $Et_2O$, lit[169] 59-60°C $Et_2O$; **$[\alpha]_D$** = +10.2 (c 1.18, EtOH), lit[169] +9.7 (c 1.00, EtOH); **IR** (neat, $cm^{-1}$) 3473 (OH), 1357 (S=O), 1174 (S=O); **$^1$H NMR** (500 MHz, $CDCl_3$) δ 7.83 (2H, d, *J* = 8.2 Hz, Ar*H*), 7.39 (2H, d, *J* = 8.2 Hz, Ar*H*), 4.13 (1H, dd, *J* = 10.0, 4.4 Hz, $TsOCH_ACH_B$), 4.10 (1H, dd, *J* = 10.0, 5.5 Hz, $TsOCH_ACH_B$), 4.02-3.95 (1H, m, $CH_2CHOCH_2O$), 3.74 (1H, ddd, *J* = 10.0, 5.6, 4.3 Hz, $CH_XH_YOH$), 3.67-3.63 (1H, m, $CH_XH_YOH$), 2.60 (1H, d, *J* = 5.3 Hz, CHO*H*) 2.49 (3H, s, $CH_3Ar$ ), 2.03 (1H, t, *J* = 6.0 Hz, $CH_2OH$); **$^{13}$C NMR** (126 MHz, $CDCl_3$) δ 145.29 (C), 132.44 (C), 130.04 (2 × CH), 128.01 (2 × CH), 70.63 ($CH_2$), 69.63 (CH), 66.70 ($CH_2$), 21.70 ($CH_3$); ***m/z*** (ESI+) 269 ($[M+Na]^+$, 100 %).

The spectroscopic data is in good agreement with the literature.[169]

**(2*S*)-1-{[tris(propan-2-yl)silyl]oxy}-3-{[(4-methylbenzene)sulfonyl]oxy}propan-2-ol 393**

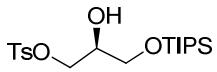


To a solution of diol **291** (5.00 g, 20.3 mmol) in DCM (300 mL) at −78 °C was added 2,6-lutidine (2.59 mL, 22.3 mmol) followed by TIPSOTf (6.55 mL, 24.4 mmol). The solution was stirred at −78 °C for 1 h and then allowed to warm to rt over 1 h. Brine (200 mL) was added, the layers were separated and the aqueous layer was extracted with DCM (2 × 200 mL). The combined organic layers were dried, filtered and concentrated *in vacuo*. The crude residue was purified by flash chromatography (1:1 hexane: EtOAc) to give the silyl ether **393** as colourless liquid (8.17 g, quant).

**$R_f$** (Hexane:EtOAc, 1:1) = 0.75; **$[\alpha]_D$** = +16.4 (c 0.67, EtOH); **IR** (neat, $cm^{-1}$) 3541 (OH), 1598 (C=C), 1361 (S=O), 1176 (S=O); **$^1$H NMR** (500 MHz, $CDCl_3$) δ 7.83 (2H, d, *J* = 8.2 Hz, Ar*H*), 7.37 (2H, d, *J* = 8.2 Hz, Ar*H*), 4.13 (1H, dd, *J* = 10.1, 5.5 Hz TsOC$H_X$H$_Y$), 4.07 (1H, dd, *J* = 10.1, 5.6 Hz, TsOCH$_X$$H_Y$), 3.94 - 3.86 (1H, m, C*H*OH), 3.74 (2H, d, *J* = 5.0 Hz, C$H_2$OTIPS) 2.48 (3H, s, C$H_3$Ar ), 1.10 - 1.01 (21H, m, Si(C*H*(C$H_3$)$_2$)$_3$); **$^{13}$C NMR** (101 MHz, $CDCl_3$) δ 144.99 (C), 132.69 (C), 129.90 (2 × CH), 128.04 (2 × CH), 70.12 ($CH_2$), 69.44 (CH), 63.26 ($CH_2$), 21.66 ($CH_3$), 17.88 (6 × $CH_3$), 11.80 (3 × CH); ***m/z*** (ESI+) 827 ($[2M+Na]^+$, 15 %), 425 ($[M+Na]^+$, 100), 403 ($[M+H]^+$, 7); **HRMS** (ESI) $[M+Na]^+$ found 425.1807, $C_{19}H_{34}O_5NaSSi$ requires 425.1788.

**(2*S*)-2-Methoxy-3-{[tris(propan-2-yl)silyl]oxy}propyl 4-methylbenzene-1-sulfonate 294**

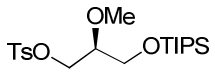


Alcohol **393** (7.00 g, 17.4 mmol), iodomethane (19.4 mL, 313 mmol) and silver (I) oxide (7.25 g, 31.3 mmol) in acetonitrile (100 mL) were heated at 60 °C for ~18 h. The brown suspension was allowed to cool to rt, ether (200 mL) was added and the suspension filtered through celite. The solvent was removed *in vacuo* and the crude residue was purified by flash chromatography (19:1 hexane: EtOAc) to give the methoxy ether **294** as a colourless oil (3.98 g, 55 %).

**$R_f$** (Hexane:EtOAc, 9:1) = 0.64; **$[\alpha]_D$** = +15.1 (c 1.52, DCM); **IR** (neat, $cm^{-1}$) 1598 (C=C), 1363 (S=O), 1178 (S=O); **$^1$H NMR** (400 MHz, $CDCl_3$) δ 7.82 (2H, d, *J* = 8.2 Hz, Ar*H*), 7.35 (2H, d, *J* = 8.2 Hz, Ar*H*), 4.26 (1H, dd, *J* = 10.4, 3.6 Hz TsOC$H_XH_Y$), 4.07 (1H, dd, *J* = 10.4, 5.9 Hz, TsOC$H_XH_Y$), 3.75 (1H, dd, *J* = 10.3, 5.0 Hz, C$H_AH_B$OTIPS) 3.63 (1H, dd, *J* = 10.3, 6.6 Hz, C$H_AH_B$OTIPS), 3.47 - 3.43 (1H, m, C*H*OH), 3.38 (3H, s, OC$H_3$), 2.46 (3H, s, C$H_3$Ar), 1.18-0.77 (21H, m, Si(C*H*(C$H_3$)$_2$)$_3$; **$^{13}$C NMR** (101 MHz, $CDCl_3$) δ 144.73 (C), 132.94 (C), 129.78 (2 × CH), 128.01 (2 × CH), 79.49 (CH), 69.38 ($CH_2$), 61.66 ($CH_2$), 58.17 ($CH_3$), 21.62 ($CH_3$), 17.88 (6 × $CH_3$), 11.80 (3 × CH); ***m/z*** (ESI+) 439 ($[M+Na]^+$, 100 %), 417 ($[M+H]^+$, 10); **HRMS** (ESI) ($[M+Na]^+$ found 439.1951, $C_{20}H_{36}O_5NaSSi$ requires 439.1945.

**[(2,4*S*)-2-(4-Methoxyphenyl)-1,3-dioxolan-4-yl]methyl 4-methylbenzene-1-sulfonate 296**

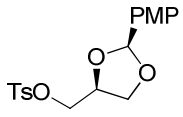


To a solution of diol **291** (10.0 g, 40.6 mmol) in DMF (100 mL) was added *p*-methoxy benzaldehyde dimethyl acetal (13.8 mL, 81.3 mmol) and *p*-toluene sulfonic acid monohydrate (0.770 g, 4.06 mmol), the solution was stirred at rt for ~18 h. The reaction mixture was diluted with DCM (200 mL) and washed with $NaHCO_3$ (200 mL, sat aq) and water (2 × 250 mL). The organic layer was dried, filtered and concentrated *in vacuo*. Ether was added to the crude residue, it was cooled to 0 °C and a colourless solid precipitated. The solid was removed by filtration to give the acetal **296** (11.8 g, 80 %).

**$R_f$** (Hexane:EtOAc, 3:1) = 0.16; **Mp** = 121-123 °C, EtOAc; **$[\alpha]_D$** = –3.3 (c 1.51, DCM); **IR** (neat, $cm^{-1}$) 1614 (C=C),1598 (C=C), 1516 (C=C), 1363 (S=O), 1180 (S=O); **$^1$H NMR** (400 MHz, $CDCl_3$) δ 7.82 (2H, d, *J* = 8.2 Hz, Ar*H*), 7.36 (2H, d, *J* = 8.2 Hz, Ar*H*), 7.34 (2H, d, *J* = 8.7 Hz, Ar*H*), 6.89 (2H, d, *J* = 8.7 Hz, Ar*H*), 5.74 (1H, s, C*H*PMP), 4.47 – 4.39 (1H, m, $CH_2CHCH_2$), 4.14 (1H, dd, *J* = 10.2, 5.0 Hz, $TsOCH_XH_Y$), 4.08 (1H, dd, *J* = 10.2, 6.3 Hz, $TsOCH_XH_Y$), 4.08 (1H, dd, *J* = 8.6, 6.8 Hz, $CHCH_AH_BO$), 4.04 (1H, dd, *J* = 8.6, 4.2 Hz, $CHCH_AH_BO$), 3.84 (3H, s, $OCH_3$), 2.48 (3H, s, $CH_3Ar$); **$^{13}$C NMR** (101 MHz, $CDCl_3$) δ 160.64 (C), 145.12 (C), 132.60 (C), 129.96 (2 × CH), 128.58 (C), 128.04 (2 × CH), 113.78 (2 × CH), 104.71 (2 × CH), 73.09 (CH), 69.43 ($CH_2$), 67.49 ($CH_2$), 55.33 ($CH_3$), 21.69 ($CH_3$); ***m/z*** (EI+) 364 ($[M]^+$, 100 %), 193 (76), 179 (28); **HRMS** (EI) $[M]^+$ found 364.0975, $C_{18}H_{20}O_6S$ requires 364.0975.

**(2*S*)-1-[(4-Methoxyphenyl)methoxy]-3-{[(4-methylbenzene)sulfonyl]oxy}propan-2-ol 299**

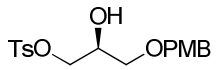


To a solution of acetal **296** (5.00 g, 13.7 mmol) in DCM (100 mL) at −78 °C was added DIBAL (31.1 mL, 1 M in hexanes, 30.2 mmol) and the solution was stirred at −78 °C for 45 min. The ice bath was removed and the excess DIBAL was quenched slowly with MeOH until the effervescence ceased, Rochelle's salt (20 mL, sat aq) and DCM (20 mL) were added and the reaction mixture allowed to warm to rt. Water (100 mL) was added and the aqueous layer was extracted with DCM (3 × 70 mL). The organic layers were combined, dried, filtered and concentrated *in vacuo* to give alcohol **299** as a colourless liquid (5.02 g, quant).

**$R_f$** (Hexane:EtOAc, 1:1) = 0.35; **$[\alpha]_D$** = +5.9 (c 1.33, $CHCl_3$); **IR** (neat, $cm^{-1}$) 3549 (OH), 1612 (C=C), 1512 (C=C), 1361 (S=O), 1176 (S=O); **$^1$H NMR** (500 MHz, $CDCl_3$) δ 7.81 (2H, d, *J* = 8.2 Hz, Ar*H*), 7.37 (2H, d, *J* = 8.2 Hz, Ar*H*), 7.22 (2H, d, *J* = 8.7 Hz, Ar*H*), 6.90 (2H, d, *J* = 8.7 Hz, Ar*H*), 4.46 (2H, s, OC$H_2$PMP), 4.12 (1H, dd, *J* = 10.1, 4.9 Hz, TsOC$H_X$H$_Y$), 4.07 (1H, dd, *J* = 10.1, 5.7 Hz, TsOCH$_X$$H_Y$), 4.04 - 3.98 (1H, m, C*H*OH), 3.84 (3H, s, ArOC$H_3$), 3.53 (1H, dd, *J* = 9.7, 4.6 Hz, C$H_A$H$_B$OPMB), 3.49 (1H, dd, *J* = 9.7, 5.4 Hz, CH$_A$$H_B$OPMB), 2.47 (3H, s, C$H_3$Ar), 2.43 (1H, d, *J* = 5.6 Hz, O*H*); **$^{13}$C NMR** (126 MHz, $CDCl_3$) δ 159.44 (C), 145.04 (C), 132.65 (C), 129.93 (2 × CH), 129.56 (C), 129.45 (2 × CH), 128.02 (2 × CH), 113.91 (2 × CH), 73.22 ($CH_2$), 70.56 ($CH_2$), 69.70 ($CH_2$), 68.38 (CH), 55.31 ($CH_3$), 21.68 ($CH_3$); ***m/z*** (EI+) 366 ($[M]^+$, 44 %), 216 (26), 173 (41), 155 (67), 137 (100); **HRMS** (EI) $[M]^+$ found 366.1133, $C_{18}H_{22}O_6S$ requires 366.1132.

**1-[(4-Methoxyphenyl)methoxy]-3-{[(4-methylbenzene)sulfonyl]oxy}propan-2-one 300**

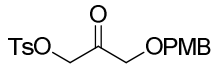


To a stirred solution of oxalyl chloride (0.080 mL, 1.02 mmol) in dry DCM (10 mL), DMSO (0.120 mL, 1.63 mmol) was added at −78 °C and the reaction mixture was stirred −78 °C for 30 min. A solution of alcohol **299** (0.250g, 0.680 mmol) in DCM (5 mL) was added at −78 °C and stirred for 3 h at −78 °C. The reaction mixture was treated with $Et_3N$ (0.450 mL, 3.26 mmol) and stirred for 15 min. The reaction mixture was diluted with DCM (30 mL) and washed with water (20 mL). The layers were separated and the organic layer was dried, filtered and concentrated *in vacuo*. The crude residue was passed through a plug of silica eluting with DCM to afford ketone **300** as an orange syrup (0.21 g, 91 %).

**$R_f$** (Hexane:EtOAc, 1:1) = 0.42; **IR** (neat, $cm^{-1}$) 1749 (C=O), 1612 (C=C), 1597 (C=C), 1514 (C=C), 1359 (S=O), 1174 (S=O); **$^1$H NMR** (500 MHz, $CDCl_3$) δ 7.83 (2H, d, *J* = 8.2 Hz, Ar*H*), 7.38 (2H, d, *J* = 8.2 Hz, Ar*H*), 7.26 (2H, d, *J* = 8.7 Hz, Ar*H*), 6.92 (2H, d, *J* = 8.7 Hz, Ar*H*), 4.79 (2H, s, TsOC$H_2$) 4.52 (2H, s, OC$H_2$PMP), 4.17 (2H, s, C$H_2$OPMB), 3.85 (3H, s, ArOC$H_3$), 2.48 (3H, s, C$H_3$Ar); **$^{13}$C NMR** (126 MHz, $CDCl_3$) δ 200.19 (C), 159.72 (C), 145.44 (C), 132.41 (C), 129.99 (2 × CH), 129.77 (2 × CH), 128.53 (C), 128.10 (2 × CH), 114.05 (2 × CH), 73.40 ($CH_2$), 73.08 ($CH_2$), 70.86 ($CH_2$), 55.33 ($CH_3$), 21.71 ($CH_3$); ***m/z*** (EI+) 364 ($[M]^+$, 5%), 155 (11), 137 (100); **HRMS** (EI) $[M]^+$ found 364.0979, $C_{18}H_{20}O_6S$ requires 364.0975.

**(2*S*)-2-Methoxy-3-[(4-methoxyphenyl)methoxy]propyl 4-methylbenzene-1-sulfonate 303**

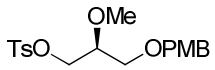


Alcohol **299** (4.71 g, 12.8 mmol), iodomethane (14.4 mL, 321 mmol) and silver (I) oxide (5.36 g, 23.1 mmol) in acetonitrile (100 mL) were heated at 60 °C for ~18 h. The brown suspension was allowed to cool to rt, ether (100 mL) was added and the suspension filtered through celite. The solvent was removed *in vacuo* and the crude residue was purified by flash chromatography (4:1 hexane: EtOAc) to give the methoxy ether **303** as a colourless oil (4.18 g, 85 %).

**$R_f$** (Hexane:EtOAc, 3:1) = 0.24; **$[\alpha]_D$** = +8.6 (c 1.39, $CHCl_3$ ); **IR** (neat, $cm^{-1}$) 1612 (C=C), 1514 (C=C), 1359 (S=O), 1176 (S=O); **$^1$H NMR** (400 MHz, $CDCl_3$) δ 7.81 (2H, d, *J* = 8.2 Hz, Ar*H*), 7.35 (2H, d, *J* = 8.2 Hz, Ar*H*), 7.22 (2H, d, *J* = 8.7 Hz, Ar*H*), 6.89 (2H, d, *J* = 8.7 Hz, Ar*H*), 4.43 (2H, s, OC$H_2$PMP), 4.20 (1H, dd, *J* = 10.5, 4.1 Hz, TsOCH$_X$$H_Y$), 4.10 (1H, dd, *J* = 10.5, 5.6 Hz, TsOC$H_X$H$_Y$), 3.83 (3H, s, ArOC$H_3$), 3.61 - 3.54 (1H, m, C*H*OMe), 3.49 (2H, d, *J* = 5.0 Hz, C$H_2$OPMB), 3.49 (3H, s, OC$H_3$), 2.47 (3H, s, C$H_3$Ar); **$^{13}$C NMR** (101 MHz, $CDCl_3$) δ 159.31 (C), 144.84 (C), 132.89 (C), 129.84 (2 × CH), 129.46 (C), 129.33 (2 × CH), 128.00 (2 × CH), 113.82 (2 × CH), 77.75 (CH), 73.16 ($CH_2$), 69.13 ($CH_2$), 67.93 ($CH_2$), 58.08 ($CH_3$), 55.30 ($CH_3$), 21.66 ($CH_3$); ***m/z*** (EI+) 380 ($[M]^+$, 21 %), 155 (29), 137 (71), 121 (100); **HRMS** (EI) $[M]^+$ found 380.1291, $C_{19}H_{24}O_6S$ requires 380.1288.

**(2*S*)-2-Methoxy-3-{[(4-methylbenzene)sulfonyl]oxy}propan-1-ol 295**

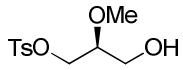


To a solution of PMB ether **303** (3.80 g, 10.0 mmol) in DCM:water (80 mL:8 mL) was added DDQ (2.72 g, 12.0 mmol) and the green/brown suspension was stirred at rt for 30 min. The reaction mixture was diluted with DCM (100 mL) and washed with $NaHCO_3$ (2 × 100 mL, sat aq) and brine (100 mL). The organic layer was dried, filtered and concentrated *in vacuo* and the crude residue was purified by flash chromatography (3:1 hexane: EtOAc) to give the alcohol **295** as a colourless oil (2.06 g, 79 %).

**$R_f$** (Hexane:EtOAc, 1:1) = 0.19; **$[\alpha]_D$** = –21.4 (c 3.31, $CHCl_3$ ); **IR** (neat, $cm^{-1}$) 3516 (OH), 1597 (C=C), 1354 (S=O), 1174 (S=O); **$^1$H NMR** (400 MHz, $CDCl_3$) δ 7.81 (2H, d, *J* = 8.2 Hz, Ar*H*), 7.37 (2H, d, *J* = 8.2 Hz, Ar*H*), 4.15 (1H, dd, *J* = 9.0, 3.5 Hz, $CH_XH_YOTs$), 4.12 (1H, dd, *J* = 9.0, 3.5 Hz, $CH_XH_YOTs$), 3.70 (1H, dd, *J* = 11.8, 4.2 Hz, $CH_AH_BOH$), 3.58 (1H, dd, *J* = 11.8, 5.1 Hz, $CH_AH_BOH$), 3.52 - 3.47 (1H, m, C*H*OMe), 3.40 (3H, s, $OCH_3$), 2.46 (3H, s, $CH_3Ar$), 2.14 (1H, br s, O*H*); **$^{13}$C NMR** (101 MHz, $CDCl_3$) δ 145.09 (C), 132.65 (C), 129.94 (2 × CH), 127.96 (2 × CH), 78.93 (CH), 68.31 ($CH_2$), 60.99 ($CH_2$), 58.10 ($CH_3$), 21.66 ($CH_3$); ***m/z*** (EI+) 261 ($[M]^+$, 100%); **HRMS** (EI) $[M]^+$ found 261.0794, $C_{11}H_{17}O_5S$ requires 261.0791.

**(2*S*,3*E*)-4-Iodo-2-methoxybut-3-en-1-yl 4-methylbenzene-1-sulfonate 305**

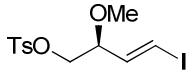


$NaHCO_3$ (970 mg, 11.6 mmol) was suspended in DCM (3 mL) and Dess-Martin periodinane (489 mg, 1.15 mmol) was added and the suspension stirred for 5 min at rt. The mixture was cooled to 0 °C and the alcohol **295** (200 mg, 0.77 mmol) was added in DCM (3 mL) and the suspension was stirred at 0 °C for 2 h, after which a 1:1 mixture of $NaHCO_3$ (5 mL, sat aq) and $Na_2S_2O_3$ (5 mL, 0.1 M aq) was added and the mixture stirred for 10 min. The biphasic mixture was separated and the aqueous layer extracted with DCM (2 × 20 mL), the organic layers were combined, washed with water (30 mL), dried, filtered and evaporated *in vacuo*. The crude mixture was used directly in the next step.

To a suspension of dry $CrCl_2$ (946 mg, 7.70 mmol) in THF (1 mL) was added the aldehyde (assumed 0.77 mmol) and iodoform (827 mg, 2.10 mmol) in 1,4-dioxane (6 mL), the suspension was stirred at rt for ~18 h. The reaction mixture was diluted with ether (15 mL) and washed with water (2 × 20 mL). The organic layer was dried, filtered and concentrated *in vacuo* and the crude residue was purified by flash chromatography (3:1 hexane: EtOAc) to give the vinyl iodide **305** (*E*:*Z* = 5:1) as a yellow oil (134 mg, 45 % over 2 steps).

**$R_f$** (Hexane:EtOAc, 3:1) = 0.44; **$[\alpha]_D$** = +50.0 (c 0.62, $CHCl_3$ ); **IR** (neat, $cm^{-1}$) 1598 (C=C), 1361 (S=O), 1176 (S=O); ***m/z*** (CI+) 383 ($[M+H]^+$, 5%), 351 (39), 255 (16), 211 (22), 197 (100); **HRMS** (CI+) $[M+H]^+$ found 382.9805, $C_{12}H_{16}O_4IS$ requires 382.9808.

***E*-isomer $^1$H NMR** (400 MHz, $CDCl_3$) δ 7.81 (2H, d, *J* = 8.2 Hz, Ar*H*), 7.38 (2H, d, *J* = 8.2 Hz, Ar*H*), 6.51 (1H, dd, *J* = 14.6, 0.9 Hz, CH=C*H*I), 6.33 (1H, dd, *J* = 14.6, 7.1 Hz, C*H*=CHI), 4.00 (2H, d, *J* = 5.3 Hz, TsOC$H_2$), 3.86 - 3.81 (1H, m, C*H*OMe), 3.30 (3H, s, OC$H_3$), 2.48 (3H, s, C$H_3$Ar); **$^{13}$C NMR** (101 MHz, $CDCl_3$) δ 145.02 (C), 141.11 (CH), 132.78 (C), 129.92 (2 × CH), 128.02 (2 × CH), 81.72 (CH), 81.02 (CH), 70.05 ($CH_2$), 57.24 ($CH_3$), 21.70 ($CH_3$).

**Z-isomer diagnostic peaks $^1$H NMR** (400 MHz, $CDCl_3$) δ 6.63 (1H, dd, *J* = 7.9, 1.1 Hz, CH=C*H*I), 6.12 (1H, t, *J* = 7.9 Hz, C*H*=CHI), 3.31 (3H, s, OC$H_3$), 2.47 (3H, s,

C*H*$_3$Ar); **$^{13}$C NMR** (101 MHz, $CDCl_3$) δ 144.88 (C), 136.92 (CH), 132.96 (C), 129.84 (2 × CH), 128.08 (2 × CH), 87.40 (CH), 80.85 (CH), 69.86 ($CH_2$), 57.05 ($CH_3$), 21.68 ($CH_3$).

**(2*S*,3*E*)-2-Methoxyhept-3-en-5-yn-1-yl 4-methylbenzene-1-sulfonate 306**

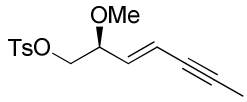


A solution of 1-propynylmagnesium bromide (1.82 mL, 0.50 M in THF, 0.910 mmol) was added dropwise to a stirred slurry of dry $ZnCl_2$ (0.124 g, 0.910 mmol) in THF (5 mL) at 0 °C. After 15 min a solution of iodide **305** (0.175 g, 0.450 mmol) in THF (2 mL) and $Pd(PPh_3)_2Cl_2$ (16 mg, 0.022 mmol) were added and the resulting mixture was stirred at rt for ~18 h. The reaction mixture was then poured into $NH_4Cl$ (10 mL, sat aq) and extracted with ether (4 × 20 mL). The combined organic layers were washed with brine (10 mL), dried, filtered and concentrated *in vacuo*. The residue was passed through a short silica column eluting with hexane to give the enyne **306** (*E*:*Z* = 5:1) as a brown oil (0.114 g, 86 %).

**$R_f$** (Hexane:EtOAc, 3:1) = 0.42; **$[\alpha]_D$** = +65.3 (c 0.26, $CHCl_3$ ); **IR** (neat, $cm^{-1}$) 2220 (C≡C), 1598 (C=C), 1359 (S=O), 1176 (S=O); ***m/z*** (ESI+) 317 ($[M+Na]^+$, 100 %); **HRMS** (ESI+) $[M+Na]^+$ found 317.0816, $C_{15}H_{18}O_4NaS$ requires 317.0818.

***E*-isomer $^1$H NMR** (500 MHz, $CDCl_3$) δ 7.81 (2H, d, *J* = 8.2 Hz, Ar*H*), 7.36 (2H, d, *J* = 8.2 Hz, Ar*H*), 5.78 - 5.70 (2H, m, C*H*=C*H*), 4.04 - 3.95 (2H, m, TsOC$H_2$), 3.88-3.85 (1H, m, C*H*OMe), 3.27 (3H, s, OC$H_3$), 2.47 (3H, s, C$H_3$Ar), 1.97 (3H, d, *J* = 1.6 Hz, CC$H_3$); **$^{13}$C NMR** (126 MHz, $CDCl_3$) δ 144.86 (C), 136.02 (CH), 132.93 (C), 129.83 (2 × CH), 128.02 (2 × CH), 115.41 (CH), 88.31 (C), 79.12 (CH), 76.96 (C), 71.03 ($CH_2$), 57.00 ($CH_3$), 21.67 ($CH_3$), 4.27 ($CH_3$).

***Z*-isomer diagnostic peaks $^{1}$H NMR** (500 MHz, $CDCl_3$) δ 5.71 – 5.69 (1H, m, CH=C*H*I), 5.62 – 5.80 (1H, m, C*H*=CHI), 4.47 (1H, td, *J* = 7.8, 3.3 Hz, C*H*OMe), 4.12 (1H, dd, *J* = 10.4, 3.3 Hz, TsOC$H_A$C$H_B$), 3.29 (3H, s, OC$H_3$), 2.00 (3H, d, J = 2.3 Hz, CC$H_3$); **$^{13}$C NMR** (101 MHz, $CDCl_3$) δ 144.70 (C), 136.20 (CH), 133.15 (C), 129.75 (2 × CH), 115.54 (CH), 93.47 (CH), 76.48 (CH), 56.87 ($CH_3$), 4.43 ($CH_3$).

**1-Iodo-2-methoxyhexane 322**

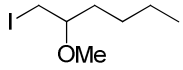


To a stirred mixture of hex-1-ene (1.24 mL, 10.0 mmol), silver oxide (2.66 g, 11.5 mmol), and methanol (50 mL) cooled to 0 °C, iodine (3.01 g, 11.9 mmol) was added portionwise. The resulting mixture was stirred for 6 h at rt and then filtered. The methanolic solution was diluted with water (50 mL) and extracted with diethyl ether (2 × 30 mL). The combined organic layers were washed with sodium thiosulfate (50 mL, sat aq) and brine (50 mL), dried, filtered and concentrated *in vacuo* to give iodide **322** as a colourless liquid (2.17 g, 90 %).

**$R_f$** (hexane:EtOAc, 3:1) = 0.62; **IR** (neat, $cm^{-1}$) 1458, 1093; **$^{1}$H NMR** δ (500 MHz, $CDCl_3$) 3.36 (3H, s, OC$H_3$), 3.28 (1H, dd, *J* = 10.6, 5.0 Hz, IC$H_X$H$_Y$), 3.24 (1H, dd, *J* = 10.6, 5.0 Hz, I CH$_X$$H_Y$), 3.05-2.97 (1H, m, C*H*OCH$_3$), 1.56 (2H, q, *J* = 7.0 Hz, CHC$H_2$), 1.40 – 1.25 (4H, m, C$H_2$C$H_2$), 0.93 – 0.88 (3H, m, CH$_2$C$H_3$); **$^{13}$C NMR** (126 MHz, $CDCl_3$) δ 79.78 (CH), 57.01 ($CH_3$), 34.02 ($CH_2$), 27.34 ($CH_2$), 22.64 ($CH_2$), 14.02 ($CH_3$), 9.89 ($CH_2$); ***m/z*** (EI) 242 ([M]$^+$, 12 %), 185 (52), 101 (100); **HRMS** (EI) [M]$^+$ found 242.0162, $C_7H_{15}IO$ requires 242.0162.

**Attempted Oxazole C-H Activation 312**

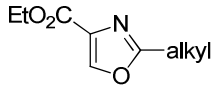


General Procedure: To a solution of ethyl oxazole-4-carboxylate **244** (100 mg, 0.71 mmol) in dioxane (2 mL) was added the alkyl halide (1.42 mmol), palladium acetate (8.0 mg, 0.034 mmol), caesium carbonate (0.460 g, 1.42 mmol) and (2-biphenyl)dicyclohexylphosphine (21.0 mg, 0.071 mmol) and the reaction was stirred at 110 °C for ~18 h. The reaction mixture was allowed to cool to rt, filtered through Celite and concentrated *in vacuo*. The residue was purified by flash chromatography (3:1 hexane:EtOAc to 1:3 hexane:EtOAc).

**Ethyl 2-[4-(ethoxycarbonyl)-1,3-oxazol-2-yl]-1,3-oxazole-4-carboxylate 320**

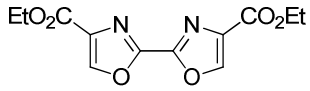


**$R_f$** (EtOAc:hexane, 1:1) = 0.34; **IR** (neat, $cm^{-1}$) 1720 (C=O); **Mp** = 191-193 °C; **$^1$H NMR** δ (400 MHz, $CDCl_3$) 8.39 (2H, s, 2 × Ar*H*), 4.44 (4H, q, *J* = 7.1 Hz, 2 × C*H*$_2$CH$_3$), 1.14 (6H, t, *J* = 7.1 Hz, 2 × CH$_2$C*H*$_3$); **$^{13}$C NMR** (101 MHz, $CDCl_3$) δ 160.16 (2 × C), 145.35 (2 × CH), 135.48 (2 × C), 110.00 (2 × C), 61.80 (2 × $CH_2$), 14.28 (2 × $CH_3$); ***m/z*** (EI) 280 ($[M]^+$, 66 %), 253 (56), 141 (100); **HRMS** (EI) $[M]^+$ found 280.0686, $C_{12}H_{12}N_2O_6$ requires 280.0690.

**(4*E*,6*S*)-7-Azido-6-methoxyhept-4-en-2-yne 394**

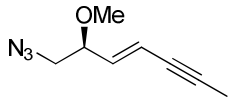


To a solution of tosylate **306** (50 mg, 0.170 mmol) in DMSO (2 mL) was added sodium azide (110 mg, 1.70 mmol) and the solution was heated at reflux for 2 h. The solution was cooled to rt and diluted with $CHCl_3$ (20 mL) and washed with water (3 ×15 mL). The aqueous phase was extracted with $CHCl_3$ (20 mL) and the combined organic phases were dried, filtered and concentrated *in vacuo*. The crude residue was purified by flash chromatography (3:1 hexane: EtOAc) to give the azide **394** (*E*:*Z* = 10:1) as a colourless volatile liquid (29 mg, quant).

**$R_f$** (Hexane:EtOAc, 3:1) = 0.58; **$[\alpha]_D$** = +74.2 (c 0.31, $CHCl_3$); **IR** (neat, $cm^{-1}$) 2220 (C≡C), 2100 (N=N), 1632 (C=C); **$^1$H NMR** (500 MHz, $CDCl_3$) δ 5.89 (1H, ddq, *J* = 15.9, 7.3, 0.5 Hz, CHC*H*=CH), 5.77 (1H, dq *J* = 15.0, 2.2 Hz, CHCH=C*H*C), 3.89 - 3.74 (1H, m, C*H*OMe), 3.37 (3H, s, OC$H_3$), 3.33 (1H, dd, *J* = 12.9, 7.5 Hz, $N_3CH_XH_Y$), 3.20 (1H, dd, *J* = 12.9, 3.8 Hz, $N_3CH_XH_Y$), 1.98 (3H, d, *J* = 2.2 Hz, CC$H_3$); **$^{13}$C NMR** (126 MHz, $CDCl_3$) δ 137.90 (CH), 114.63 (CH), 88.05 (C), 81.06 (CH), 77.23 (C), 56.85 ($CH_3$), 54.50 ($CH_2$), 4.27 ($CH_3$).

***Z*-isomer diagnostic peaks $^1$H NMR** (500 MHz, $CDCl_3$) 2.02 (3H, d, *J* = 2.2 Hz, CC$H_3$); **$^{13}$C NMR** (126 MHz, $CDCl_3$) δ 138.16 (CH), 114.76 (CH), 92.98 (C), 78.14 (CH), 56.79 ($CH_3$), 54.14 ($CH_2$), 4.44 ($CH_3$).

**Methyl 1-[(2*S*,3*E*)-2-methoxyhept-3-en-5-yn-1-yl]-1*H*-1,2,3-triazole-4-carboxylate 359**

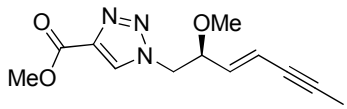

To a solution of azide **394** (8.0 mg, 50 μmmol) in *tert*-butanol (2 mL) and water (1 mL), copper sulfate pentahydrate (2.0 mg, 5 μmmol) and sodium ascorbate (2.0 mg, 10 μmmol) were added and the mixture was stirred at rt for 10 min. After this time methyl propiolate (12 μL, 60 μmmol) and TBTA (3.0 mg, 5 μmmol) were added and the reaction was stirred at rt for ~18 h. The solution was diluted with EtOAc (10 mL) and washed with water (10 mL), the organic layer was dried, filtered and concentrated *in vacuo*. The crude residue was purified by flash chromatography (1:1 hexane: EtOAc) to give the triazole **359** (*E*:*Z* = 11:1) as a colourless solid (7.2 mg, 58 %).

**$R_f$** (Hexane:EtOAc, 1:1) = 0.31; **Mp** = 97-99 °C; **$[\alpha]_D$** = +39.1 (c 0.25, $CHCl_3$); **IR** (neat, $cm^{-1}$) 2223 (C≡C), 1728 (C=O), 1634 (C=C), 1543 (C=C); **$^1$H NMR** (500 MHz, $CDCl_3$) δ 8.22 (1H, s, Ar*H*), 5.81 - 5.76 (2H, m, C*H*=C*H*), 4.60 (1H, dd, *J* = 14.1, 3.3 Hz, ArC$H_X$H$_Y$), 4.34 (1H, dd, *J* = 14.1, 8.2 Hz, ArCH$_X$$H_Y$), 4.04 - 4.00 (1H, m, C*H*OMe), 3.99 (3H, s, $CO_2CH_3$), 3.26 (3H, s, OC$H_3$), 1.98 (3H, d, *J* = 1.6 Hz, CC$H_3$); **$^{13}$C NMR** (126 MHz, $CDCl_3$) δ 161.27 (C), 139.85 (C), 135.96 (CH), 129.00 (CH), 116.08 (CH), 89.00 (C), 79.85 (CH), 76.70 (C), 56.89 ($CH_3$), 54.32 ($CH_2$) 52.21 ($CH_3$), 4.29 ($CH_3$); ***m/z*** (ESI+) 272 ($[M+Na]^+$, 53 %), 250 ($[M+H]^+$, 5); **HRMS** (ESI+) $[M+Na]^+$ found 272.0998, $C_{12}H_{15}N_3O_3Na$ requires 272.1006.

***Z*-isomer diagnostic peak $^1$H NMR** (500 MHz, $CDCl_3$) 2.01 (3H, d, *J* = 2.3 Hz, CC$H_3$).

**Ethyl 1*H*-pyrrole-3-carboxylate 364**

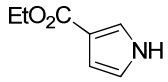


Ethylacrylate (1.00 g, 9.99 mmol) and TosMIC (1.93 g, 9.89 mmol) in diethyl ether/DMSO (42 mL, 2:1) were slowly added *via* an addition funnel to a suspension of NaH (0.816 g, 60% dispersion in mineral oil, 19.58 mmol) in diethyl ether (30 mL). The reaction was stirred at rt for 3 h. Water (50 mL) was added carefully and the layers were separated. The aqueous phase was extracted with diethyl ether (3 × 20 mL) and the combined organic layers were dried, filtered and concentrated *in vacuo*. The crude residue was purified by flash chromatography (3:1 hexane: EtOAc) to give the pyrrole **364** as a yellow liquid (0.60 g, 43 %).

**$R_f$** (Hexane:EtOAc, 1:1) = 0.50; **IR** (neat, $cm^{-1}$) 3327 (NH), 1697 (C=O), 1554 (C=C), 1504 (C=C); **$^1$H NMR** (400 MHz, $CDCl_3$) δ 8.58 (1H, br s, N*H*), 7.46 (1H, dt, *J* = 3.2, 1.8 Hz, Ar*H*), 6.78 (1H, br q, *J* = 3.2 Hz, Ar*H*), 6.69 (1H, td, *J* = 2.8, 1.5 Hz, ArH), 4.31 (2H, q, *J* = 7.1 Hz, C*H*$_2$CH$_3$), 1.37 (3H, t, *J* = 7.1 Hz, CH$_2$C*H*$_3$); **$^{13}$C NMR** (101 MHz, $CDCl_3$) δ 165.10 (C), 123.41 (CH), 118.72 (CH), 116.76 (C), 109.81 (CH), 59.76 ($CH_2$), 14.49 ($CH_3$); ***m/z*** (EI) 139 ($[M]^+$, 91 %), 94 (100).

Spectroscopic data are in good agreement with the literature.[147]

**Ethyl 1-[(2*S*,3*E*)-2-methoxyhept-3-en-5-yn-1-yl]-1*H*-pyrazole-4-carboxylate 358**

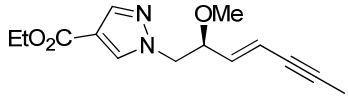

To a solution of tosylate **306** (30 mg, 0.1 mmol) in DMF (2 mL) was added ethyl 1*H*-pyrazole-4-carboxylate (16 mg, 0.11 mmol) and $K_2CO_3$ (21 mg, 0.15 mmol) and the mixture was stirred for 48 h at rt. The reaction mixture was diluted with EtOAc (10 mL) and washed with water (3 × 20 mL) and brine (20 mL). The organic layer was dried, filtered and concentrated *in vacuo*. The crude residue was purified by flash chromatography (3:1 hexane: EtOAc) to give the pyrazole **358** (*E*:*Z* = 5:1) as a yellow oil (15 mg, 58 %).

**$R_f$** (Hexane:EtOAc, 3:1) = 0.22; **$[\alpha]_D$** = +28.2 (c 0.43, $CHCl_3$); **IR** (neat, $cm^{-1}$) 2223 (C≡C), 1712 (C=O), 1554 (C=C); **$^1$H NMR** (500 MHz, $CDCl_3$) δ 7.96 (1H, s, Ar*H*), 7.93 (1H, s, Ar*H*), 5.85 (1H, ddq, *J* = 16.0, 7.3, 0.5 Hz, CHC*H*=CH), 5.75 (1H, dq *J* = 16.0, 2.2 Hz, CHCH=C*H*C), 4.31 (2H, q, *J* = 7.1 Hz, C$H_2$CH$_3$), 4.21 (1H, dd, *J* = 13.9, 3.9 Hz, ArC$H_X$H$_Y$), 4.11 (1H, dd, *J* = 13.9, 8.0 Hz, ArCH$_X$$H_Y$), 4.04 (1H, td, *J* = 7.3, 3.8 Hz C*H*OMe), 3.24 (3H, s, OC$H_3$), 1.97 (3H, d, *J* = 2.2 Hz, CC$H_3$), 1.37 (3H, t, *J* = 7.1 Hz, CH$_2$C$H_3$); **$^{13}$C NMR** (126 MHz, $CDCl_3$) δ 163.08 (C), 141.18 (CH), 137.21 (CH), 133.99 (CH), 115.10 (C), 115.07 (CH), 88.26 (C), 80.13 (CH), 76.98 (C), 60.16 ($CH_2$), 57.02 ($CH_3$), 56.56 ($CH_2$), 14.40 ($CH_3$), 4.28 ($CH_3$); ***m/z*** (EI) 262 ($[M]^+$, 11 %), 217 (7), 204 (13), 109 (100); **HRMS** (EI) $[M]^+$ found 262.1310, $C_{14}H_{18}O_3N_2$ requires 262.1312.

***Z*-isomer diagnostic peaks $^1$H NMR** (500 MHz, $CDCl_3$) 7.99 (1H, s, Ar*H*), 5.66 – 5.60 (1H, m, CHCH=C*H*C), 3.30 (3H, s, C$H_3$), 2.01 (3H, d, *J* = 2.4 Hz, CC$H_3$); **$^{13}$C NMR** (126 MHz, $CDCl_3$) δ 163.18 (C), 140.90 (CH), 137.31 (CH), 133.92 (CH), 115.43 (CH), 115.15 (C), 93.24 (C), 77.21 (CH), 60.12 ($CH_2$), 56.82 ($CH_3$), 55.94 ($CH_2$), 14.41 ($CH_3$), 4.47 ($CH_3$).

**(4*E*)-7-Iodo-6-methoxyhept-4-en-2-yne 341**

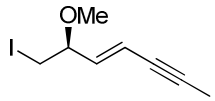


Tosylate **306** (25 mg, 0.085 mmol) and NaI (50 mg, 0.340 mmol) in acetone were heated at 60 °C for ~18 h. The reaction mixture was cooled and the solvent removed *in vacuo*. The residue was dissolved in ether (10 mL) and washed with water (10 mL) and brine (10 mL), the organic layer was dried, filtered and concentrated *in vacuo* to give iodide **341** (*E*:*Z* = 10:1) as a yellow oil (13 mg, 62 %).

**$R_f$** (Hexane:EtOAc, 9:1) = 0.67; **$[\alpha]_D$** = –3.5 (c 0.23, $CHCl_3$); **IR** (neat, $cm^{-1}$) 2223 (C≡C); **$^1$H NMR** (500 MHz, $CDCl_3$) δ 5.88 (1H dd, *J* = 15.9, 7.5 Hz, CHC*H*=CH), 5.75 (1H, dq *J* = 16.0, 2.2 Hz, CHCH=C*H*C), 3.70 (1H, m, C*H*OMe), 3.36 (3H, s, OC$H_3$), 3.22 (1H, dd, *J* = 9.0, 3.8 Hz, IC$H_X$C$H_Y$), 3.19 (1H, dd, *J* = 9.0, 5.1 Hz, IC$H_X$C$H_Y$), 1.99 (3H, d, *J* = 2.2 Hz, CC$H_3$); **$^{13}$C NMR** (126 MHz, $CDCl_3$) δ 139.34 (CH), 114.52 (CH), 88.12 (C), 80.99 (CH), 77.23 (C), 56.99 ($CH_3$), 8.19 ($CH_2$), 4.27 ($CH_3$). ***m/z***; (CI, *i*-butane) 251 ($[M]^+$, 3 %), 196 (100), 165 (24). **HRMS** (CI, *i*-butane) $[M+H]^+$ found 250.9928, $C_8H_{12}OI$ requires 250.9927.

***Z*-isomer diagnostic peak $^1$H NMR** (500 MHz, $CDCl_3$) δ 2.03 (3H, d, *J* = 2.3 Hz, CC$H_3$);

**4-[(Methoxymethoxy)methyl]-1,3-oxazole 340**

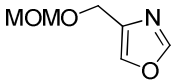


Sodium hydride (0.088 g, 60 % in mineral oil, 2.20 mmol) was added to a solution of alcohol **245** (0.200 g, 2.02 mmol) in THF (5 mL) at 0 °C, and the mixture was stirred at 0 °C for 10 min and at rt for an additional 1 h. The mixture was cooled to 0 °C and chloromethyl methyl ether (0.182 mL, 2.40 mmol) was added dropwise. The reaction mixture was stirred at 0 °C for 10 min and at rt for an additional 3 h. The mixture was poured into water (10 mL) and extracted with EtOAc (2 × 20 mL). The combined organic extracts were washed with brine (20 mL), dried, filtered and concentrated *in vacuo*. The crude material was purified by flash chromatography (3:1, hexane:EtOAc) to give the ether **340** as an orange oil (1.41 g, 73 %).

**$R_f$** (Hexane:EtOAc, 1:1) = 0.29; **IR** (neat, $cm^{-1}$) 1514 (C=C); **$^1$H NMR** δ (500 MHz, $CDCl_3$) 7.90 (1H, s, Ar*H*), 7.68 (1H, q, *J* = 0.7 Hz, Ar*H*), 4.74 (2H, s, OC$H_2$O), 4.58 (2H, d, *J* = 0.7 Hz, C$H_2$Ar), 3.43 (3H, s, OC$H_3$); **$^{13}$C NMR** δ (126 MHz, $CDCl_3$) 151.38 (CH), 137.35 (C), 136.45 (CH), 95.86 ($CH_2$), 60.87 ($CH_2$), 55.44 ($CH_3$); ***m/z*** (EI) 143 ($[M]^+$, 2 %), 113 (20), 83 (100); **HRMS** (EI) $[M]^+$ found 143.0576, $C_6H_9NO_3$ requires 143.0577.

**4-(*tert*-Butyldimethylsilyloxymethyl)-1,3-oxazole 246**

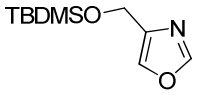


To a solution of alcohol **245** (50.0 mg, 0.05 mmol) in DCM (2 mL) at 0 °C was added *tert*-butyldimethylsilyl trifluoromethanesulfonate (0.122 mL, 0.53 mmol) followed by 2,6-lutidine (0.070 mL, 0.60 mmol). After stirring for 1 h at 0 °C the reaction was quenched by the addition of sodium bicarbonate (5 mL, sat. aq.) and extracted with DCM (3 × 10 mL). The organic extracts were combined, dried, filtered and concentrated *in vacuo*. The crude material was purified by flash chromatography (hexane:EtOAc, 9:1) to give the silyl ether **246** as pale yellow oil (91.0 mg, 86 %).

**$R_f$** (Hexane:EtOAc, 10:1) = 0.24; **IR** (neat, $cm^{-1}$) 1516 (C=C), 1256 ($SiCH_3$); **$^1$H NMR** δ (400 MHz, $CDCl_3$) 7.86, (1H, s, Ar*H*), 7.60 (1H, s, Ar*H*), 4.72 (2H, s, $OCH_2$), 0.96 (9H, s, $C(CH_3)_3$), 0.14 (6H, s, 2 × $SiCH_3$) ; **$^{13}$C NMR** δ (101 MHz, $CDCl_3$) 151.05 (CH), 141.01 (C), 135.35 (CH), 58.57 ($CH_2$), 25.88 ($3CH_3$), 18.38 (C), −5.34 ($2CH_3$); ***m/z*** (ESI+, MeOH) 237 ($[M+Na]^+$, 100 %), 214 ($[M+H]^+$, 7); **HRMS** (ESI) $[M+Na]^+$ found 236.1071, $C_{10}H_{19}NO_2NaSi$ requires 236.1077.

# 7 References


(1) Butler, M. S. *Nat. Prod. Rep.* **2008**, *25*, 475–516.
(2) Jansen, R.; Irschik, H.; Reichenbach, H.; Wray, V.; Hofle, G. *Liebigs Ann. Chem.* **1994**, 759–773.
(3) Carvalho, R.; Reid, R.; Viswanathan, N.; Gramajo, H.; Julien, B. *Gene* **2005**, *359*, 91–98.
(4) Kopp, M.; Irschik, H.; Pradella, S.; Müller, R. *ChemBioChem* **2005**, *6*, 1277–1286.
(5) Floss, H. G.; Beale, J. M. *Angew. Chem. Int. Ed.* **1989**, *28*, 146–177.
(6) Reid, R.; Piagentini, M.; Rodriguez, E.; Ashley, G.; Viswanathan, N.; Carney, J.; Santi, D. V.; Hutchinson, C. R.; McDaniel, R. *Biochemistry* **2003**, *42*, 72–79.
(7) Caffrey, P. *ChemBioChem* **2003**, *4*, 654–657.
(8) Irschik, H.; Jansen, R.; Gerth, K.; Hofle, G.; Reichenbach, H. *The Journal of Antibiotics* **1995**, *48*, 31–35.
(9) Darling, D. *The Encyclopedia of Science*, http://www.daviddarling.info/encyclopedia/C/cell_cycle.html (accessed 26/02/11)
(10) Elnakady, Y. A.; Sasse, F.; Lunsdorf, H.; Reichenbach, H. *Biochem. Pharmacol.* **2004**, *67*, 927–935.
(11) Jordan, M. A. *Curr. Med. Chem. Anticancer Agents* **2002**, *2*, 1–17.
(12) Kingston, D. G. I. *J. Nat. Prod.* **2009**, *72*, 507–515.
(13) Hopkins, C. D.; Wipf, P. *Nat. Prod. Rep.* **2009**, *26*, 585–601.
(14) Wipf, P.; Graham, T. H.; Vogt, A.; Sikorski, R. P.; Ducruet, A. P.; Lazo, J. S. *Chem. Biol. Drug Des.* **2006**, *67*, 66–73.
(15) Wipf, P.; Graham, T. H. *J. Am. Chem. Soc.* **2004**, *126*, 15346–15347.
(16) Brisson Tierno, M.; Kitchens, C. A.; Petrik, B.; Graham, T. H.; Wipf, P.; Xu, F. L.; Saunders, W. S.; Raccor, B. S.; Balachandran, R.; Day, B. W.; Stout, J. R.; Walczak, C. E.; Ducruet, A. P.; Reese, C. E.; Lazo, J. S. *J. Pharmacol. Exp. Ther.* **2008**, *328*, 715–722.
(17) Hearn, B. R.; Arslanian, R. L.; Fu, H.; Liu, F.; Gramajo, H.; Myles, D. C. *J. Nat. Prod.* **2006**, *69*, 148–150.
(18) Wipf, P.; Graham, T. H.; Xiao, J. *Pure Appl. Chem.* **2007**, *79*, 753–761.
(19) Graham, T. H. The Synthesis of Oxazole-containing Natural Products, University of Pittsburgh, **2006**.
(20) Hopkins, C. D.; Schmitz, J. C.; Chu, E.; Wipf, P. *Org. Lett.* **2011**, *13*, 4088–4091.
(21) Mohamadi, F.; Richards, N. G. J.; Guida, W. C.; Liskamp, R.; Lipton, M.; Caufield, C.; Chang, G.; Hendrickson, T.; Still, W. C. *Journal of Computational Chemistry* **1990**, *11*, 440–467.
(22) Irschik, H.; Jansen, R.; Sasse, F. Biologically active compounds obtainable from Sorangium cellulosum; EP1743897A1 **2007**.
(23) Schäckel, R.; Hinkelmann, B.; Sasse, F.; Kalesse, M. *Angew. Chem. Int. Ed.* **2010**, *49*, 1619–1622.
(24) Hillier, M. C.; Park, D. H.; Price, A. T.; Ng, R.; Meyers, A. I. *Tetrahedron Lett.* **2000**, *41*, 2821–2824.
(25) Hillier, M. C.; Price, A. T.; Meyers, A. I. *J. Org. Chem.* **2001**, *66*, 6037–6045.

(26) Parikh, J. R.; Doering, W. v. E. *J. Am. Chem. Soc.* **1967**, *89*, 5505–5507.
(27) Stork, G.; Zhao, K. *Tetrahedron Lett.* **1989**, *30*, 2173–2174.
(28) Hofle, G. *GBF Annual Report* **1999**, 102–103.
(29) Hartung, I. V.; Niess, B.; Haustedt, L. O.; Hoffmann, H. M. R. *Org. Lett.* **2002**, *4*, 3239–3242.
(30) Niess, B.; Hartung, I. V.; Haustedt, L. O.; Hoffmann, H. M. R. *Eur. J. Org. Chem.* **2006**, 1132–1143.
(31) Bode, J. W.; Jr, D. R. G.; Carreira, E. M. *Chem. Comm.* **2001**, 2560–2561.
(32) Furukawa, J.; Kawabata, N.; Nishimura, J. *Tetrahedron Lett.* **1966**, *7*, 3353–3354.
(33) Salit, A.-F.; Meyer, C.; Cossy, J.; Delouvrié, B.; Hennequin, L. *Tetrahedron* **2008**, *64*, 6684–6697.
(34) Haustedt, L. O.; Panicker, S. B.; Kleinert, M.; Hartung, I. V.; Eggert, U.; Niess, B.; Hoffmann, H. M. . *Tetrahedron* **2003**, *59*, 6967–6977.
(35) Kiyooka, S.; Kaneko, Y.; Komura, M.; Matsuo, H.; Nakano, M. *J. Org. Chem.* **1991**, *56*, 2276–2278.
(36) Hafner, A.; Duthaler, R. O.; Marti, R.; Rihs, G.; Rothe-Streit, P.; Schwarzenbach, F. *J. Am. Chem. Soc.* **1992**, *114*, 2321–2336.
(37) Shiina, I.; Kubota, M.; Oshiumi, H.; Hashizume, M. *J. Org. Chem.* **2004**, *69*, 1822–1830.
(38) Bluet, G.; Bazán-Tejeda, B.; Campagne, J.-M. *Org. Lett.* **2001**, *3*, 3807–3810.
(39) Pagenkopf, B. L.; Krüger, J.; Stojanovic, A.; Carreira, E. M. *Angew. Chem. Int. Ed.* **1998**, *37*, 3124–3126.
(40) Shiina, I.; Kubota, M.; Ibuka, R. *Tetrahedron Lett.* **2002**, *43*, 7535–7539.
(41) Evans, D. A.; Hoveyda, A. H. *J. Am. Chem. Soc.* **1990**, *112*, 6447–6449.
(42) Aird, J. I.; Hulme, A. N.; White, J. W. *Org. Lett.* **2007**, *9*, 631–634.
(43) Roy, R. S.; Gehring, A. M.; Milne, J. C.; Belshaw, P. J.; Walsh, C. T. *Nat. Prod. Rep.* **1999**, *16*, 249–263.
(44) Ichiba, T.; Yoshida, W. Y.; Scheuer, P. J.; Higa, T.; Gravalos, D. G. *J. Am. Chem. Soc.* **1991**, *113*, 3173–3174.
(45) Cocito, C. *Microbiol. Rev.* **1979**, *43*, 145–192.
(46) Searle, P. A.; Molinski, T. F.; Brzezinski, L. J.; Leahy, J. W. *J. Am. Chem. Soc.* **1996**, *118*, 9422–9423.
(47) Williams, D. R.; Berliner, M. A.; Stroup, B. W.; Nag, P. P.; Clark, M. P. *Org. Lett.* **2005**, *7*, 4099–4102.
(48) Connell, R. D.; Tebbe, M.; Gangloff, A. R.; Helquist, P. *Tetrahedron* **1993**, *49*, 5445–5459.
(49) Hallinan, E. A.; Hagen, T. J.; Tsymbalov, S.; Stapelfeld, A.; Savage, M. A. *Bioorg. Med. Chem.* **2001**, *9*, 1–6.
(50) Stojanovic, F. M.; Arnold, Z. *Collect. Czech. Chem. Commun.* **1967**, 2155–2160.
(51) Wilt, J. W. *J. Org. Chem.* **1956**, *21*, 920–921.
(52) Benoit, G.-E.; Carey, J. S.; Chapman, A. M.; Chima, R.; Hussain, N.; Popkin, M. E.; Roux, G.; Tavassoli, B.; Vaxelaire, C.; Webb, M. R.; Whatrup, D. *Org. Process Res. Dev.* **2008**, *12*, 88–95.
(53) Lafontaine, J. A.; Provencal, D. P.; Gardelli, C.; Leahy, J. W. *J. Org. Chem.* **2003**, *68*, 4215–4234.

(54) Bagley, M. C.; Dale, J. W.; Xiong, X.; Bower, J. *Org. Lett.* **2003**, *5*, 4421–4424.
(55) Trost, B. M.; Papillon, J. P. N.; Nussbaumer, T. *J. Am. Chem. Soc.* **2005**, *127*, 17921–17937.
(56) King, A. O.; Negishi, E.; Villani Jr., F. J.; Silveira Jr., A. *J. Org. Chem.* **1978**, *43*, 358–360.
(57) Bellina, F.; Biagetti, M.; Carpita, A.; Rossi, R. *Tetrahedron* **2001**, *57*, 2857–2870.
(58) Boland, W.; Schroer, N.; Sieler, C.; Feigel, M. *Helv. Chim. Acta* **1987**, *70*, 1025–1040.
(59) Dhulut, S.; Bourin, A.; Lannou, M.-I.; Fleury, E.; Lensen, N.; Chelain, E.; Pancrazi, A.; Ardisson, J.; Fahy, J. *Eur. J. Org. Chem.* **2007**, 5235–5243.
(60) Koop, U.; Handke, G.; Krause, N. *Liebigs Ann. Chem.* **1996**, 1487–1499.
(61) Wang, J.-X.; Jia, X.; Meng, T.; Xin, L. *Synthesis* **2005**, *17*, 2838–2844.
(62) Concellón, J. M.; Concellón, C. *J. Org. Chem.* **2006**, *71*, 4428–4432.
(63) Haddad, T. D.; Hirayama, L. C.; Singaram, B. *J. Org. Chem.* **2010**, *75*, 642–649.
(64) Wessjohann, L. A.; Schmidt, G.; Schrekker, H. S. *Synlett* **2007**, *13*, 2139–2141.
(65) Guimarães, R. L.; Lima, D. J. P.; Barros, M. E. S. B.; Cavalcanti, L. N.; Hallwass, F.; Navarro, M.; Bieber, L. W.; Malvestiti, I. *Molecules* **2007**, *12*, 2089–2105.
(66) Sain, B.; Prajapati, D.; Sandhu, J. S. *Tetrahedron Lett.* **1992**, *33*, 4795–4798.
(67) Gangloff, A. R.; Aakermark, B.; Helquist, P. *J. Org. Chem.* **1992**, *57*, 4797–4799.
(68) Bergdahl, M.; Hett, R.; Friebe, T. L.; Gangloff, A. R.; Iqbal, J.; Wu, Y.; Helquist, P. *Tetrahedron Lett.* **1993**, *34*, 7371–7374.
(69) Schlessinger, R. H.; Li, Y.-J. *J. Am. Chem. Soc.* **1996**, *118*, 3301–3302.
(70) Linder, J.; Blake, A. J.; Moody, C. J. *Org. Biomol. Chem.* **2008**, *6*, 3908–3916.
(71) Girard, P.; Namy, J. L.; Kagan, H. B. *J. Am. Chem. Soc.* **1980**, *102*, 2693–2698.
(72) Williams, D. R.; Kiryanov, A. A.; Emde, U.; Clark, M. P.; Berliner, M. A.; Reeves, J. T. *Angew. Chem. Int. Ed.* **2003**, *42*, 1258–1262.
(73) Wu, J.; Panek, J. S. *Angew. Chem. Int. Ed.* **2010**, *49*, 6165–6168.
(74) Breuilles, P.; Uguen, D. *Tetrahedron Lett.* **1998**, *39*, 3149–3152.
(75) Smith, A. B.; Minbiole, K. P.; Verhoest, P. R.; Schelhaas, M. *J. Am. Chem. Soc.* **2001**, *123*, 10942–10953.
(76) Breton, G. W.; Shugart, J. H.; Hughey, C. A.; Conrad, B. P.; Perala, S. *Molecules* **2001**, *6*, 655–662.
(77) Berk, S. C.; Knochel, P.; Yeh, M. C. P. *J. Org. Chem.* **1988**, *53*, 5789–5791.
(78) Metzger, A.; Schade, M. A.; Knochel, P. *Org. Lett.* **2008**, *10*, 1107–1110.
(79) Metzger, A.; Piller, F. M.; Knochel, P. *Chem. Comm.* **2008**, 5824–5826.
(80) Tokuyama, H.; Yokoshima, S.; Yamashita, T.; Lin, S.-C.; Li, L.; Fukuyama, T. *J. Braz. Chem. Soc.* **1998**, *9*, 381–387.
(81) Des Mazery, R.; Pullez, M.; López, F.; Harutyunyan, S. R.; Minnaard, A. J.; Feringa, B. L. *J. Am. Chem. Soc.* **2005**, *127*, 9966–9967.
(82) Lipshutz, B. H.; Hungate, R. W. *J. Org. Chem.* **1981**, *46*, 1410–1413.
(83) Turchi, I. J.; Dewar, M. J. S. *Chem. Rev.* **1975**, *75*, 389–437.

(84) Zhang, X.; Hinkle, B.; Ballantyne, L.; Gonzales, S.; Pena, M. *J. Het. Chem.* **1997**, *34*, 1061–1065.
(85) Entwistle, D. A.; Jordan, S. I.; Montgomery, J.; Pattenden, G. *J. Chem. Soc. Perkin Trans. 1* **1996**, 1315–1317.
(86) Hamana, H.; Sugasawa, T. *Chem. Lett.* **1983**, 333–336.
(87) Evans, D. A.; Cee, V. J.; Smith, T. E.; Santiago, K. J. *Org. Lett.* **1999**, *1*, 87–90.
(88) Knaus, G.; Meyers, A. I. *J. Org. Chem.* **1974**, *39*, 1192–1195.
(89) Smith, T. E.; Mourad, M. S.; Velander, A. J. *Heterocycles* **2002**, *57*, 1211–1217.
(90) Dess, D. B.; Martin, J. C. *J. Org. Chem.* **1983**, *48*, 4155–4156.
(91) Ghosh, A. K.; Lei, H. *J. Org. Chem.* **2002**, *67*, 8783–8788.
(92) Deng, Y.; Salomon, R. G. *J. Org. Chem.* **1998**, *63*, 7789–7794.
(93) Wender, P. A.; Verma, V. A. *Org. Lett.* **2006**, *8*, 1893–1896.
(94) Omura, K.; Swern, D. *Tetrahedron* **1978**, *34*, 1651–1660.
(95) Sharma, G. V. M.; Cherukupalli, G. R. *Tetrahedron: Asymm.* **2006**, *17*, 1081–1088.
(96) Takai, K.; Nitta, K.; Utimoto, K. *J. Am. Chem. Soc.* **1986**, *108*, 7408–7410.
(97) Allan, G. R.; Carnell, A. J. *J. Org. Chem.* **2001**, *66*, 6495–6497.
(98) Cao, J.; Kopajtic, T.; Katz, J. L.; Newman, A. H. *Bioorg. & Med. Chem. Lett.* **2008**, *18*, 5238–5241.
(99) Ng, J. S.; Behling, J. R.; Campbell, A. L.; Nguyen, D.; Lipshutz, B. *Tetrahedron Lett.* **1988**, *29*, 3045–3048.
(100) Hodgetts, K. J.; Kershaw, M. T. *Org. Lett.* **2002**, *4*, 2905–2907.
(101) Young, G. L.; Smith, S. A.; Taylor, R. J. K. *Tetrahedron Lett.* **2004**, *45*, 3797–3801.
(102) Watterson, S. H.; Xiao, Z.; Dodd, D. S.; Tortolani, D. R.; Vaccaro, W.; Potin, D.; Launay, M.; Stetsko, D. K.; Skala, S.; Davis, P. M.; Lee, D.; Yang, X.; McIntyre, K. W.; Balimane, P.; Patel, K.; Yang, Z.; Marathe, P.; Kadiyala, P.; Tebben, A. J.; Sheriff, S.; Chang, C. Y.; Ziemba, T.; Zhang, H.; Chen, B.-C.; DelMonte, A. J.; Aranibar, N.; McKinnon, M.; Barrish, J. C.; Suchard, S. J.; Murali Dhar, T. G. *J. Med. Chem.* **2010**, *53*, 3814–3830.
(103) Skepper, C. K.; Quach, T.; Molinski, T. F. *J. Am. Chem. Soc.* **2010**, *132*, 10286–10292.
(104) Turnbull, P. S.; Cadilla, R.; Larkin, A. L.; Stewart, E. L.; Stetson, K. 4-Substituted Arylamine Derivatives and Their Use in Pharmaceutical Compositions; WO2006/133216.
(105) Zhou, Jiacheng; Bhattacharjee, A.; Chen, S.; Chen, Y.; Farmer, J.; Goldberg, J.; Hanselmann, R.; Lou, R.; Orbin, A.; Oyelere, A., K.; Salvino, J., M.; Springer, D.; Tran, J.; Wang, D.; Wu, Y. The Biaryl Heterocyclic Compounds and Methods of Making and Using the Same; WO2005/019211.
(106) Kajino, M.; Hird, N.; Tarui, N.; Banno, H.; Kawano, Y.; Inatomi, N. Fused Quinoline Derivative and Use Thereof; WO2005/105802.
(107) Bezencon, O.; Boss, C.; Bur, D.; Cormin-Boeuf, O.; Fischli, W.; Grisostomi, C.; Remen, L.; Richard, S.; Sifferlen, T.; Weller, T. Bicyclononene Derivatives as Renin Inhibitors; WO 2006/021402.
(108) Chatterjee, A. K.; Morgan, J. P.; Scholl, M.; Grubbs, R. H. *J. Am. Chem. Soc.* **2000**, *122*, 3783–3784.

(109) Kumar, P.; Pandey, M.; Gupta, P.; Naidu, S. V.; Dhavale, D. D. *Eur. J. Org. Chem.* **2010**, *2010*, 6993–7004.
(110) Kang, B.; Kim, D.-H.; Do, Y.; Chang, S. *Org. Lett.* **2003**, *5*, 3041–3043.
(111) Love, J. A.; Morgan, J. P.; Trnka, T. M.; Grubbs, R. H. *Angew. Chem. Int. Ed.* **2002**, *41*, 4035–4037.
(112) Hansen, E. C.; Lee, D. *Org. Lett.* **2004**, *6*, 2035–2038.
(113) Kang, B.; Lee, J. M.; Kwak, J.; Lee, Y. S.; Chang, S. *J. Org. Chem.* **2004**, *69*, 7661–7664.
(114) Collins, C. J.; Hanack, M.; Stutz, H.; Auchter, G.; Schoberth, W. *J. Org. Chem.* **1983**, *48*, 5260–5268.
(115) Eglinton, G.; Whiting, M. C. *J. Chem. Soc.* **1950**, 3650–3656.
(116) Kuszmann, J.; Sohár, P. *Carb. Res.* **1980**, *83*, 63–72.
(117) Khrimyan, A. P.; Makaryan, G. M.; Ovanisyan, A. L.; Wimmer, Z.; Romanyuk, M.; Streinz, L.; Badanyan, S. O. *Chem. Nat. Comp.* **1991**, *27*, 103–108.
(118) Ray, P. C.; Roberts, S. M. *J. Chem. Soc., Perkin Trans. 1* **2001**, 149–153.
(119) Navarro, I.; Mas, E.; Fabriàs, G.; Camps, F. *Bioorg. & Med. Chem. Lett.* **1997**, *5*, 1267–1274.
(120) Praveen, C.; Perumal, P. T. *Synlett* **2011**, 521–524.
(121) Marotta, E.; Micheloni, L. M.; Scardovi, N.; Righi, P. *Org. Lett.* **2001**, *3*, 727–729.
(122) Claffey, D. J.; Ruth, J. A. *Tetrahedron: Asymm.* **1997**, *8*, 3715–3716.
(123) Brown, P.; Djerassi, C. *Angew. Chem. Int. Ed.* **1967**, *6*, 477–496.
(124) Gawdzik, B.; Saletra, A.; Wawrzenczyk, C. *Phosphorus, Sulfur and Silicon* **1998**, *134/135*, 321–329.
(125) Corey, E. J.; Chaykovsky, M. *J. Am. Chem. Soc.* **1965**, *87*, 1353–1364.
(126) Purpura, M.; Krause, N. *Eur. J. Org. Chem.* **1999**, 267–275.
(127) Sakai, D.; Watanabe, K. 3-Methyl-2- ( (2S) -2- (4- (3-Methyl-1, 2, 4-oxadiazol-5-yl) phenyl) morpholino) -6- (pyrimidin-4-yl) pyrimidin-4 (3H) -one as Tau Protein Kinase Inhibitor; WO2009/035159.
(128) Aggarwal, V. K.; Charmant, J.; Dudin, L.; Porcelloni, M.; Richardson, J. *PNAS* **2004**, *101*, 5467 –5471.
(129) Aggarwal, V. K.; Angelaud, R.; Bihan, D.; Blackburn, P.; Fieldhouse, R.; Fonquerna, S. J.; Ford, G. D.; Hynd, G.; Jones, E.; Jones, R. V. H.; Jubault, P.; Palmer, M. J.; Ratcliffe, P. D.; Adams, H. *J. Chem. Soc., Perkin Trans. 1* **2001**, 2604–2622.
(130) Soulé, J.-F.; Mathieu, A.; Norsikian, S.; Beau, J.-M. *Org. Lett.* **2010**, *12*, 5322–5325.
(131) Takano, S.; Akiyama, M.; Sato, S.; Ogasawara, K. *Chem. Lett.* **1983**, 1593–1596.
(132) Trygstad, T. M.; Pang, Y.; Forsyth, C. J. *J. Org. Chem.* **2009**, *74*, 910–913.
(133) Evans, D. A.; Ng, H. P. *Tetrahedron Lett.* **1993**, *34*, 2229.
(134) Verrier, C.; Hoarau, C.; Marsais, F. *Org. Biomol. Chem.* **2009**, *7*, 647–650.
(135) Hoarau, C.; Du Fou de Kerdaniel, A.; Bracq, N.; Grandclaudon, P.; Couture, A.; Marsais, F. *Tetrahedron Lett.* **2005**, *46*, 8573–8577.
(136) Sezen, B.; Sames, D. *Org. Lett.* **2003**, *5*, 3607–3610.
(137) Yao, T.; Hirano, K.; Satoh, T.; Miura, M. *Chem. Eur. J.* **2010**, *16*, 12307–12311.

(138) Vechorkin, O.; Proust, V.; Hu, X. *Angew. Chem. Int. Ed.* **2010**, *49*, 3061–3064.
(139) Whitney, S. E.; Rickborn, B. *J. Org. Chem.* **1991**, *56*, 3058–3063.
(140) Brown, D. J.; Ghosh, P. B. *J. Chem. Soc. B* **1969**, 270–276.
(141) Hodges, J. C.; Patt, W. C.; Connolly, C. J. *J. Org. Chem.* **1991**, *56*, 449–452.
(142) Jacobi, P. A.; Ueng, S.-N.; Carr, D. *J. Org. Chem.* **1979**, *44*, 2042–2044.
(143) Vedejs, E.; Monahan, S. D. *J. Org. Chem.* **1996**, *61*, 5192–5193.
(144) Chittari, P.; Hamada, Y.; Shioiri, T. *Synlett* **1988**, 1022–1024.
(145) Dorgan, P. D.; Durrani, J.; Cases-Thomas, M. J.; Hulme, A. N. *J. Org. Chem.* **2010**, *75*, 7475–7478.
(146) Dorgan, P. D. An Evans-Tishchenko/Ring-Closing Alkyne Metathesis Approach Towards the Synthesis of Disorazole C1, University of Edinburgh, **2010**.
(147) Krayer, M.; Ptaszek, M.; Kim, H.-J.; Meneely, K. R.; Fan, D.; Secor, K.; Lindsey, J. S. *J. Org. Chem.* **2010**, *75*, 1016–1039.
(148) van Leusen, A. M.; Siderius, H.; Hoogenboom, B. E.; van Leusen, D. *Tetrahedron Lett.* **1972**, *13*, 5337–5340.
(149) Kolb, H. C.; Finn, M. G.; Sharpless, K. B. *Angew. Chem. Int. Ed.* **2001**, *40*, 2004–2021.
(150) Trinh, M.-C.; Florent, J.-C.; Monneret, C. *Tetrahedron* **1988**, *44*, 6633–6644.
(151) Ralston, K. *Unpublished results*.
(152) Fürstner, A.; Mathes, C.; Lehmann, C. W. *Chem. Eur. J.* **2001**, *7*, 5299–5317.
(153) Fürstner, A.; Flugge, S.; Larionov, O.; Takahashi, Y.; Kubota, T.; Kobayashi, J. *Chem. Eur. J.* **2009**, *15*, 4011 – 4029.
(154) Mortreux, A.; Blanchard, M. *J. Chem. Soc., Chem. Commun.* **1974**, 786–787.
(155) Hellbach, B.; Gleiter, R.; Rominger, F. *Synthesis* **2003**, 2535–2541.
(156) Beer, S.; Hrib, C. G.; Jones, P. G.; Brandhorst, K.; Grunenberg, J.; Tamm, M. *Angew. Chem. Int. Ed.* **2007**, *46*, 8890–8894.
(157) Beer, S.; Brandhorst, K.; Grunenberg, J.; Hrib, C. G.; Jones, P. G.; Tamm, M. *Org. Lett.* **2008**, *10*, 981–984.
(158) Smith, A. B.; Adams, C. M.; Kozmin, S. A.; Paone, D. V. *J. Am. Chem. Soc.* **2001**, *123*, 5925–5937.
(159) Miura, T.; Shimada, M.; de Mendoza, P.; Deutsch, C.; Krause, N.; Murakami, M. *J. Org. Chem.* **2009**, *74*, 6050–6054.
(160) Pavlakos, E.; Georgiou, T.; Tofi, M.; Montagnon, T.; Vassilikogiannakis, G. *Org. Lett.* **2009**, *11*, 4556–4559.
(161) Lebar, M. D.; Baker, B. J. *Tetrahedron Lett.* **2007**, *48*, 8009–8010.
(162) Schmidt, A.-K. C.; Stark, C. B. W. *Org. Lett.* **2011**, *13*, 4164–4167.
(163) Crank, G.; Foulis, M. J. *J. Med. Chem.* **1971**, *14*, 1075–1077.
(164) Hodgetts, K. J.; Kershaw, M. T. *Org. Lett.* **2003**, *5*, 2911–2914.
(165) Cornforth, J. W.; Cornforth, R. H. *J. Chem. Soc.* **1947**, 96–102.
(166) Ren, X.-F.; Turos, E.; Lake, C. H.; Churchill, M. R. *J. Org. Chem.* **1995**, *60*, 6468–6483.
(167) Khachatryan, R. A.; Ovsepyan, S. A.; Indzhikyan, M. G. *J. Gen. Chem. USSR (Engl. Transl.)* **1987**, *57*, 1709–1711,1524–1525.
(168) Danielmeier, K.; Steckhan, E. *Tetrahedron: Asymm.* **1995**, *6*, 1181–1190.
(169) Wirz, B.; Schmid, R.; Foricher, J. *Tetrahedron: Asymm.* **1992**, *3*, 137–142.

# 8 Abbreviations

| | |
|---|---|
| Ac | Acetyl |
| AIBN | Azo*bis*isobutyronitrile |
| BAIB | *bis*(Acetoxy)iodobenzene |
| 9-BBN | 9-Borabicyclo[3.3.1]nonane |
| Binap | 2,2'-*bis*(Diphenylphosphino)-1,1'-binaphthyl |
| BOP | (Benzotriazol-1-yloxy)*tris*(dimethylamino)phosphonium hexafluorophosphate |
| Bu | Butyl |
| Bz | Benzyl |
| CDI | 1,1'-Carbonyldiimidazole |
| CM | Cross metathesis |
| COSY | Homonuclear correlation spectroscopy |
| DAST | Diethylaminosulfur trifluoride |
| DBU | 1,8-Diazabicyclo[5.4.0]undec-7-ene |
| DCC | N,N'-Dicyclohexylcarbodiimide |
| DCM | Dichloromethane |
| DDQ | 2,3-Dichloro-5,6-dicyano-1,4-benzoquinone |
| DFT | Discrete Fourier transform |
| DIBAL | Diisobutylaluminium hydride |
| DIPEA | *N*,*N*-Diisopropylethylamine |
| DIPT | Diisopropyl tartarate |
| DMAP | 4-Dimethylaminopyridine |
| DMB | Dimethoxybenzyl |
| DMF | Dimethylformamide |
| DMP | Dess–Martin periodinane |
| DMSO | Dimethyl sulfoxide |
| DPTC | *O*,*O*'-Di(2-pyridyl) thiocarbonate |
| EDC | 1-Ethyl-3-(3-dimethylaminopropyl) carbodiimide |
| ee | Enantiomeric excess |
| EI | Electron ionisation |

| | |
|---|---|
| Et | Ethyl |
| ET | Evans-Tishchenko |
| FAB | Fast aton bombardment |
| HMBC | Heteronuclear Multiple Bond Correlation |
| HMPA | Hexamethylphosphoramide |
| HMTA | Hexamethylenetetramine |
| HOBT | Hydroxybenzotriazole |
| HPLC | High-performance liquid chromatography |
| HRMS | High resolution mass spectrometry |
| HSQC | Heteronuclear Single Quantum Coherence |
| HWE | Horner-waddsworth-Emmons |
| IBCF | Isobutyl chloroformate |
| IBX | 2-iodoxybenzoic acid |
| $IC_{50}$ | Half maximal inhibitory concentration |
| Imid | Imidazole |
| IR | Infra Red |
| KHMDS | Potassium *bis*(trimethylsilyl)amide |
| LCMS | Liqiud chromatography mass spectrometry |
| LDA | Lithium diisopropylamide |
| LG | Leaving group |
| LHMDS | Lithium *bis*(trimethylsilyl)amide |
| Lys | Lysine |
| MDR | Multiple drug resistance |
| Me | Methyl |
| Mes | Mesityl (2,4,6-trimethylphenyl) |
| MMFF | Merck molecular forc field |
| MIC | Minimum inhibitory concentration |
| MNBA | 2-Methyl-6-nitrobenzoic anhydride |
| MOM | Methoxymethyl |
| MS | Molecular sieves |
| MTT | 3-(4,5-Dimethylthiazol-2-yl)-2,5-diphenyltetrazolium bromide |
| NADP | Nicotinamide adenine dinucleotide phosphate |

| | |
|---|---|
| NBS | *N*-Bromosuccinimide |
| NMM | *N*-Methylmorpholine |
| NMO | *N*-Methylmorpholine-N-oxide |
| NMR | Nuclear magnetic resonance |
| NRPS | Non-robosomal polyketide synthase |
| OD | Optical density |
| PDC | Pyridinium dichromate |
| Pgp | P-glycoprotein 1 |
| Ph | Phenyl |
| PLE | Pig liver esterase |
| PMB | *Para*methoxybenzyl |
| PMP | *Para*methoxyphenyl |
| PPTs | Pyridinium *p*-toluenesulfonate |
| Pr | Propyl |
| Py | Pyridine |
| RCAM | Ring-closing alkyne metathesis |
| RCM | Ring-closing matathesis |
| Red-Al | Sodium bis(2-methoxyethoxy)aluminium hydride |
| RORCM | Ring-opening/ring-closing metathesis |
| Rt | Room temperature |
| SEM | 2-(Trimethylsilyl)ethoxymethyl |
| Ser | Serine |
| TBAF | Tetra-*n*-butylammonium fluoride |
| TBDMS/TBS | *tert*-Butyldimethylsilyl chloride |
| $^{t}$Bu | *tert*-Butyl |
| TEMPO | (2,2,6,6-Tetramethylpiperidin-1-yl)oxyl |
| TES | Triethylsilyl |
| Tf | Triflate |
| TFA | Trifluoroacetic acid |
| THF | Tetrahydrofuran |
| TIPS | Triisopropylsilyl |
| TLC | Thin layer chromatography |

| | |
|---|---|
| TMP | 2,2,6,6-Tetramethylpiperidine |
| TMS | Trimethylsilyl |
| TOCSY | Total Correlation Spectroscopy |
| Ts | Tosyl |
| Tyr | Tyrosine |
| Val | Valine |

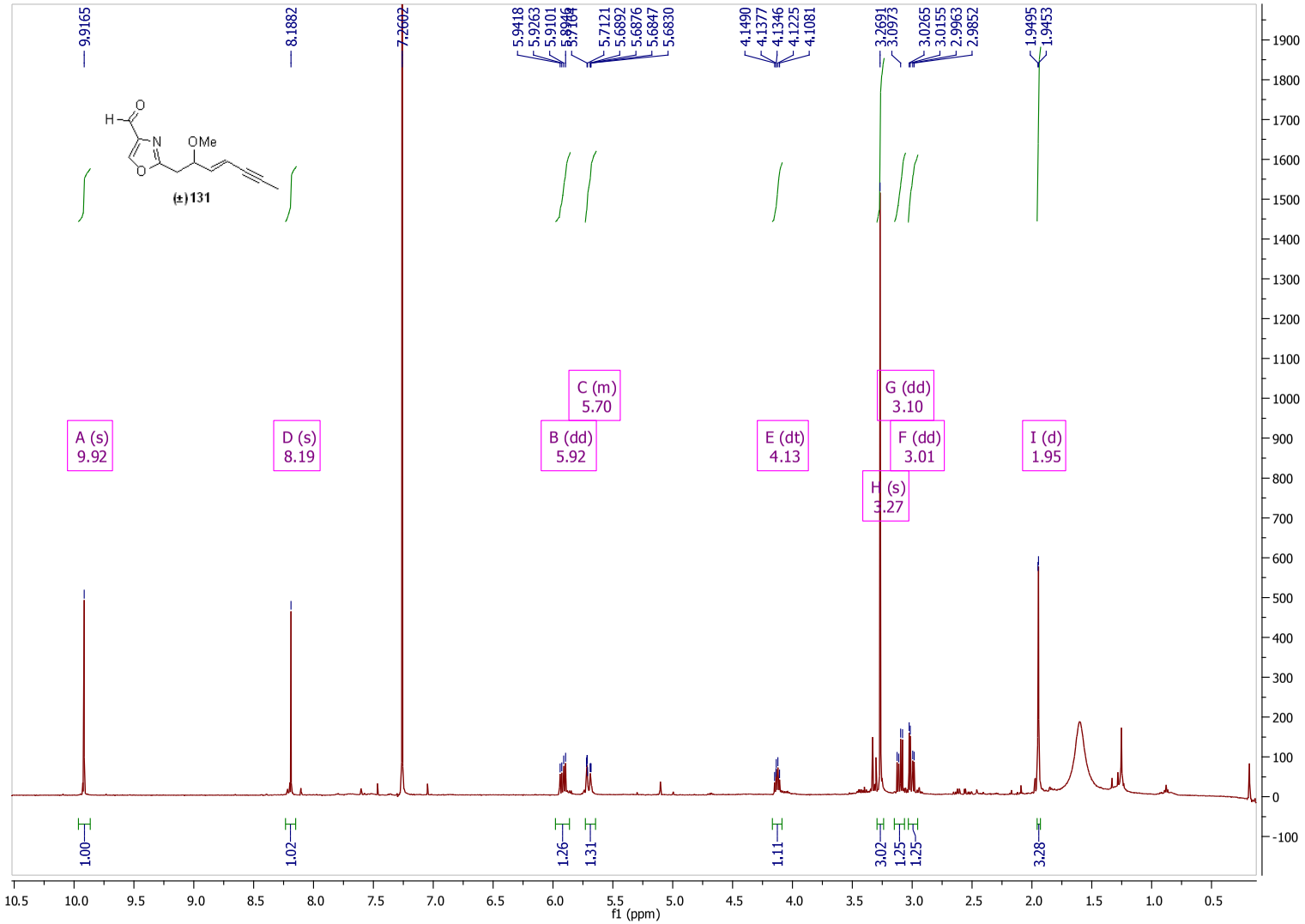
9.9165
8.1882
7.2602
5.9418
5.9263
5.9101
5.8946
5.8784
5.7121
5.6892
5.6876
5.6847
5.6830
4.1490
4.1377
4.1346
4.1225
4.1081
3.2691
3.0973
3.0265
3.0155
2.9963
2.9852
1.9495
1.9453
(±)131
A (s) 9.92
D (s) 8.19
C (m) 5.70
B (dd) 5.92
E (dt) 4.13
G (dd) 3.10
F (dd) 3.01
H (s) 3.27
I (d) 1.95
1.00
1.02
1.26
1.31
1.11
3.02
1.25
1.25
3.28
f1 (ppm)

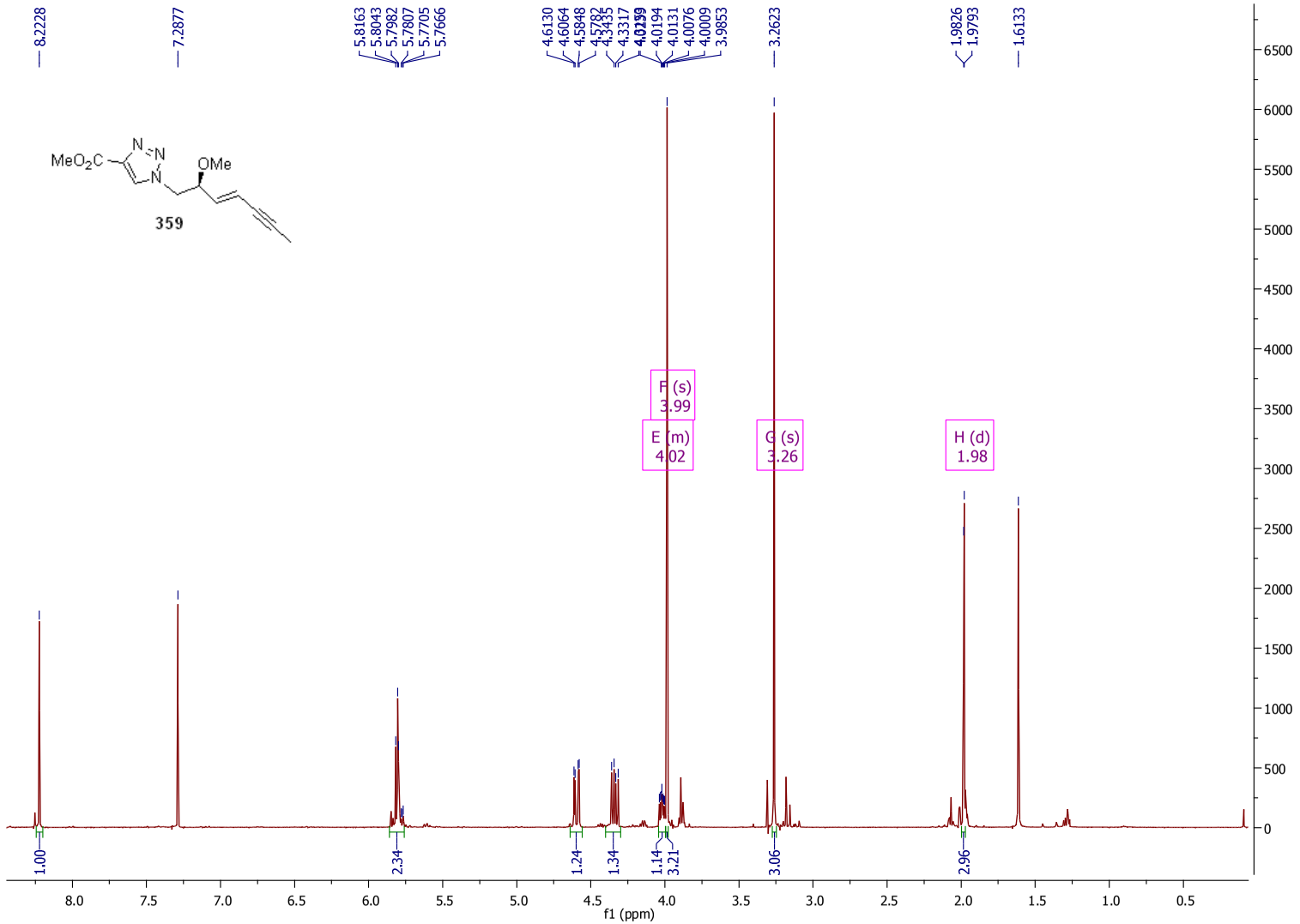
8.2228
7.2877
5.8163
5.8043
5.7982
5.7807
5.7705
5.7666
4.6130
4.6064
4.5848
4.5782
4.3435
4.3317
4.0194
4.0131
4.0076
4.0009
3.9853
3.2623
1.9826
1.9793
1.6133
MeO2C
OMe
359
F (s)
3.99
E (m)
4.02
G (s)
3.26
H (d)
1.98
1.00
2.34
1.24
1.34
1.14
3.21
3.06
2.96
f1 (ppm)

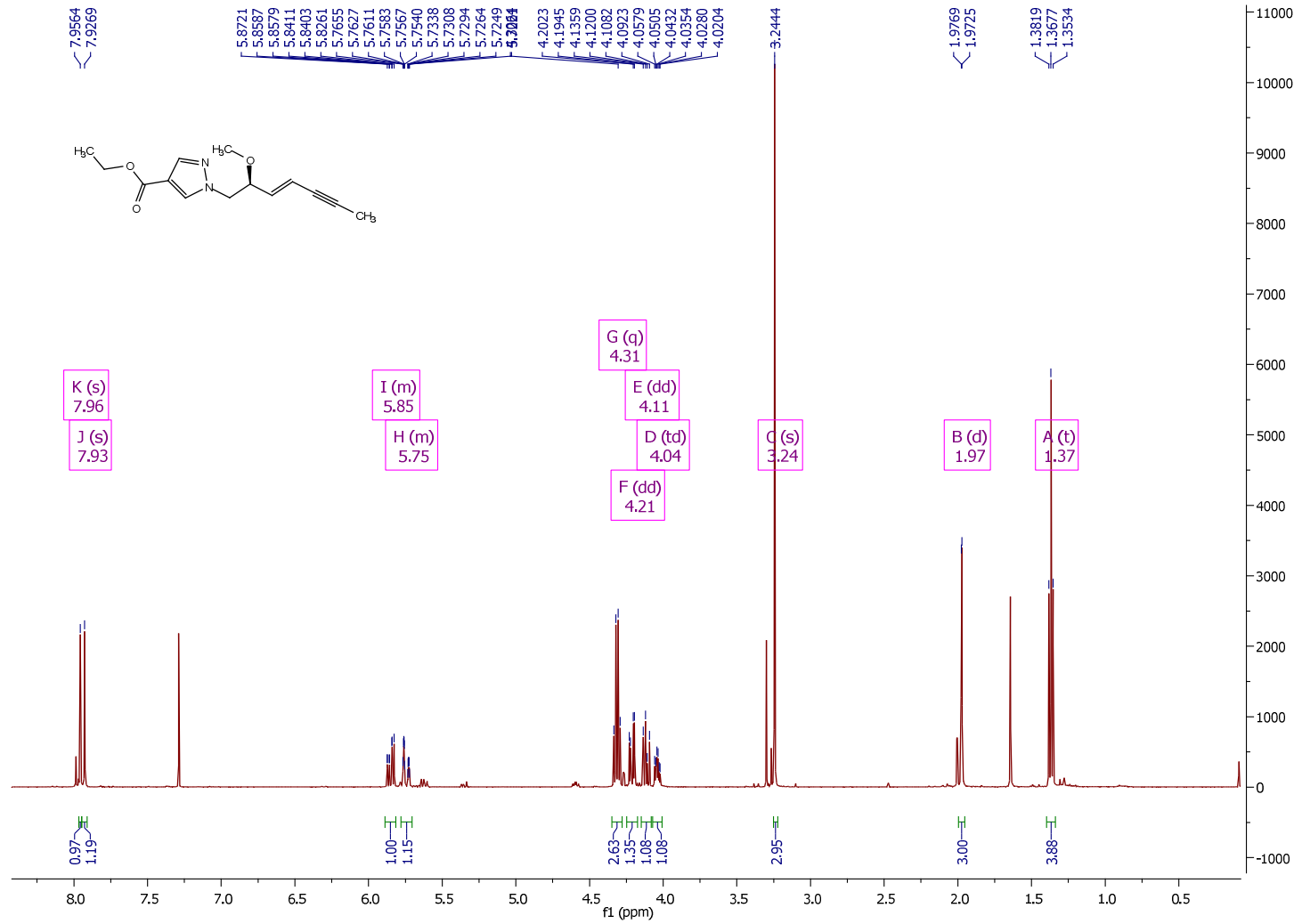
7.9564
7.9269
5.8721
5.8587
5.8579
5.8411
5.8403
5.8261
5.7655
5.7627
5.7611
5.7583
5.7567
5.7540
5.7338
5.7308
5.7294
5.7264
5.7249
4.2023
4.1945
4.1359
4.1200
4.1082
4.0923
4.0579
4.0505
4.0432
4.0354
4.0280
4.0204
3.2444
1.9769
1.9725
1.3819
1.3677
1.3534
K (s)
7.96
J (s)
7.93
I (m)
5.85
H (m)
5.75
G (q)
4.31
E (dd)
4.11
D (td)
4.04
F (dd)
4.21
C (s)
3.24
B (d)
1.97
A (t)
1.37
0.97
1.19
1.00
1.15
2.63
1.35
1.08
1.08
2.95
3.00
3.88
f1 (ppm)